

Climate change projections for the Canterbury Region

Prepared for Environment Canterbury

February 2020

Prepared by:

Gregor Macara, John-Mark Woolley, Petra Pearce, Sanjay Wadhwa, Christian Zammit, Abha Sood, Scott Stephens

For any information regarding this report please contact:

Gregor Macara
Climate Scientist
Climate Data and Applications
+64-4-386 0509
gregor.macara@niwa.co.nz

National Institute of Water & Atmospheric Research Ltd
Private Bag 14901
Kilbirnie
Wellington 6241

Phone +64 4 386 0300

NIWA CLIENT REPORT No: 2019339WN
Report date: February 2020
NIWA Project: ECA20301

Quality Assurance Statement		
	Reviewed by:	Petra Pearce Manager – Climate, Atmosphere and Hazards NIWA Auckland
	Formatting checked by:	Victoria McIntyre
	Approved for release by:	Andrew Tait Chief Scientist – Climate, Atmosphere and Hazards NIWA Wellington

© All rights reserved. This publication may not be reproduced or copied in any form without the permission of the copyright owner(s). Such permission is only to be given in accordance with the terms of the client's contract with NIWA. This copyright extends to all forms of copying and any storage of material in any kind of information retrieval system.

Whilst NIWA has used all reasonable endeavours to ensure that the information contained in this document is accurate, NIWA does not give any express or implied warranty as to the completeness of the information contained herein, or that it will be suitable for any purpose(s) other than those specifically contemplated during the Project or agreed by NIWA and the Client.

Contents

- Executive summary 9**

- 1 Introduction 10**
 - 1.1 Global and New Zealand climate change..... 12
 - 1.2 Year to year climate variability and climate change..... 14

- 2 Methodology..... 19**
 - 2.1 Representative Concentration Pathways 19
 - 2.2 Climate modelling 21
 - 2.3 Hydrological modelling 22
 - 2.4 Limitations 23

- 3 Current and future climate of the Canterbury Region..... 24**

- 4 Temperature 25**
 - 4.1 Mean temperature 25
 - 4.2 Maximum temperature 36
 - 4.3 Minimum temperature..... 44
 - 4.4 Hot days 52
 - 4.5 Frost days..... 60

- 5 Precipitation..... 68**
 - 5.1 Rainfall 68
 - 5.2 Dry days 79
 - 5.3 Snow days 87
 - 5.4 Potential evapotranspiration deficit..... 90
 - 5.5 Soil moisture deficit 93

- 6 Other climate variables 101**
 - 6.1 Mean wind speed 101
 - 6.2 Surface solar radiation..... 107
 - 6.3 Relative humidity..... 113
 - 6.4 Air pressure..... 119

- 7 Hydrological impacts of climate change 121**
 - 7.1 Mean annual discharge..... 121

7.2	Mean annual low flow	123
7.3	High flow	125
7.4	Mean annual flood.....	127
8	Sea-level rise and coastal impacts	129
8.1	Impacts of sea-level rise	129
8.2	Projections for New Zealand sea-level rise.....	130
8.3	Tides and the effect of rising sea level	132
9	Summary and conclusions.....	135
10	Glossary of abbreviations and terms	138
Appendix A	Climate modelling methodology	149
Appendix B	Hydrological modelling methodology.....	151
11	References.....	153

Tables

Table 2-1:	Projected change in global mean surface air temperature for the mid- and late-21st century relative to the reference period of 1986-2005 for different RCPs.	20
Table 4-1:	Projected changes in seasonal and annual mean temperature (°C) between 1986-2005 and two climate change scenarios (RCP4.5 and RCP8.5) at two future time periods for Canterbury.	34
Table 5-1:	Projected changes in seasonal and annual rainfall (%) between 1986-2005 and two climate change scenarios (RCP4.5 and RCP8.5) at two future time periods.	77
Table 8-1:	Approximate years, from possible earliest to latest, when specific sea-level rise increments (metres above 1986–2005 baseline) could be reached for various projection scenarios of SLR for the wider New Zealand region.	131

Figures

Figure 1-1:	The Canterbury region administered by Environment Canterbury.	11
Figure 1-2:	New Zealand national temperature series, 1909-2019.	13
Figure 1-3:	The 5-month running mean Southern Oscillation Index (SOI), from January 1950 (i.e. Nov 1949 – Mar 1950) to January 2014 (Nov 2013 – Mar 2014).	15
Figure 1-4:	Average summer percentage of normal rainfall during El Niño (left) and La Niña (right).	15
Figure 1-5:	Annual average Interdecadal Pacific Oscillation (IPO) index, 1871-2016.	16
Figure 1-6:	Daily Southern Annular Mode (SAM), January 2017 - December 2019.	17
Figure 1-7:	New Zealand Temperature - historical record and an illustrative schematic projection illustrating future year-to-year variability.	18

Figure 2-1:	CMIP5 multi-model simulated time series from 1950-2100 for change in global annual mean surface temperature relative to 1986-2005.	20
Figure 4-1:	Modelled annual mean temperature, average over 1986-2005.	26
Figure 4-2:	Projected annual mean temperature changes by 2040 and 2090, under RCP4.5 and RCP8.5.	27
Figure 4-3:	Modelled seasonal mean temperature, average over 1986-2005.	28
Figure 4-4:	Projected seasonal mean temperature changes by 2040 for RCP4.5.	29
Figure 4-5:	Projected seasonal mean temperature changes by 2040 for RCP8.5.	30
Figure 4-6:	Projected seasonal mean temperature changes by 2090 for RCP4.5.	31
Figure 4-7:	Projected seasonal mean temperature changes by 2090 for RCP8.5.	32
Figure 4-8:	Projected seasonal and annual mean temperature change for Canterbury by 2040 (2031-2050).	35
Figure 4-9:	Projected seasonal and annual mean temperature change for Canterbury by 2090 (2081-2100).	35
Figure 4-10:	Modelled annual mean maximum temperature, average over 1986-2005.	37
Figure 4-11:	Projected annual mean maximum temperature changes by 2040 and 2090, under RCP4.5 and RCP8.5.	38
Figure 4-12:	Modelled seasonal mean maximum temperature, average over 1986-2005.	39
Figure 4-13:	Projected seasonal mean maximum temperature changes by 2040 for RCP4.5.	40
Figure 4-14:	Projected seasonal mean maximum temperature changes by 2040 for RCP8.5.	41
Figure 4-15:	Projected seasonal mean maximum temperature changes by 2090 for RCP4.5.	42
Figure 4-16:	Projected seasonal mean maximum temperature changes by 2090 for RCP8.5.	43
Figure 4-17:	Modelled annual mean minimum temperature, average over 1986-2005.	45
Figure 4-18:	Projected annual mean minimum temperature changes by 2040 and 2090, under RCP4.5 and RCP8.5.	46
Figure 4-19:	Modelled seasonal mean minimum temperature, average over 1986-2005.	47
Figure 4-20:	Projected seasonal mean minimum temperature changes by 2040 for RCP4.5.	48
Figure 4-21:	Projected seasonal mean minimum temperature changes by 2040 for RCP8.5.	49
Figure 4-22:	Projected seasonal mean minimum temperature changes by 2090 for RCP4.5.	50
Figure 4-23:	Projected seasonal mean minimum temperature changes by 2090 for RCP8.5.	51
Figure 4-24:	Modelled annual number of hot days (days with maximum temperature $\geq 25^{\circ}\text{C}$), average over 1986-2005.	53
Figure 4-25:	Projected annual hot day (days with maximum temperature $\geq 25^{\circ}\text{C}$) changes by 2040 and 2090, under RCP4.5 and RCP8.5.	54
Figure 4-26:	Modelled seasonal number of hot days (days with maximum temperature $\geq 25^{\circ}\text{C}$), average over 1986-2005.	55
Figure 4-27:	Projected seasonal hot day (days with maximum temperature $\geq 25^{\circ}\text{C}$) changes by 2040 for RCP4.5.	56

Figure 4-28:	Projected seasonal hot day (days with maximum temperature $\geq 25^{\circ}\text{C}$) changes by 2040 for RCP8.5.	57
Figure 4-29:	Projected seasonal hot day (days with maximum temperature $\geq 25^{\circ}\text{C}$) changes by 2090 for RCP4.5.	58
Figure 4-30:	Projected seasonal hot day (days with maximum temperature $\geq 25^{\circ}\text{C}$) changes by 2090 for RCP8.5.	59
Figure 4-31:	Modelled annual number of frost days (days with minimum temperature $\leq 0^{\circ}\text{C}$), average over 1986-2005.	61
Figure 4-32:	Projected annual frost day (days with minimum temperature $\leq 0^{\circ}\text{C}$) changes by 2040 and 2090, under RCP4.5 and RCP8.5.	62
Figure 4-33:	Modelled seasonal number of frost days (days with minimum temperature $\leq 0^{\circ}\text{C}$), average over 1986-2005.	63
Figure 4-34:	Projected seasonal frost day (days with minimum temperature $\leq 0^{\circ}\text{C}$) changes by 2040 for RCP4.5.	64
Figure 4-35:	Projected seasonal frost day (days with minimum temperature $\leq 0^{\circ}\text{C}$) changes by 2040 for RCP8.5.	65
Figure 4-36:	Projected seasonal frost day (days with minimum temperature $\leq 0^{\circ}\text{C}$) changes by 2090 for RCP4.5.	66
Figure 4-37:	Projected seasonal frost day (days with minimum temperature $\leq 0^{\circ}\text{C}$) changes by 2090 for RCP8.5.	67
Figure 5-1:	Modelled annual mean rainfall (mm), average over 1986-2005.	69
Figure 5-2:	Projected annual mean rainfall changes by 2040 and 2090, under RCP4.5 and RCP8.5.	70
Figure 5-3:	Modelled seasonal mean rainfall, average over 1986-2005.	71
Figure 5-4:	Projected seasonal mean rainfall changes by 2040 for RCP4.5.	72
Figure 5-5:	Projected seasonal mean rainfall changes by 2040 for RCP8.5.	73
Figure 5-6:	Projected seasonal mean rainfall changes by 2090 for RCP4.5.	74
Figure 5-7:	Projected seasonal mean rainfall changes by 2090 for RCP8.5.	75
Figure 5-8:	Projected seasonal and annual rainfall change for Christchurch by 2040 (2031-2050).	78
Figure 5-9:	Projected seasonal and annual rainfall change for Christchurch by 2090 (2081-2100).	78
Figure 5-10:	Modelled annual number of dry days (daily rainfall $< 1\text{mm}$), average over 1986-2005.	80
Figure 5-11:	Projected annual number of dry day (daily rainfall $< 1\text{mm}$) changes by 2040 and 2090, under RCP4.5 and RCP8.5.	81
Figure 5-12:	Modelled seasonal number of dry days (daily rainfall $< 1\text{mm}$), average over 1986-2005.	82
Figure 5-13:	Projected seasonal number of dry day (daily rainfall $< 1\text{mm}$) changes by 2040 for RCP4.5.	83
Figure 5-14:	Projected seasonal number of dry day (daily rainfall $< 1\text{mm}$) changes by 2040 for RCP8.5.	84
Figure 5-15:	Projected seasonal number of dry day (daily rainfall $< 1\text{mm}$) changes by 2090 for RCP4.5.	85
Figure 5-16:	Projected seasonal number of dry day (daily rainfall $< 1\text{mm}$) changes by 2090 for RCP8.5.	86
Figure 5-17:	Modelled annual number of snow days, average over 1986-2005.	88

Figure 5-18:	Projected change in the number of annual snow days by 2040 and 2090, under RCP4.5 and RCP8.5.	89
Figure 5-19:	Modelled annual potential evapotranspiration deficit accumulation (mm), average over 1986-2005.	91
Figure 5-20:	Projected annual potential evapotranspiration deficit (PED) accumulation changes for RCP4.5 and RCP8.5, by 2040 and 2090.	92
Figure 5-21:	Modelled annual number of days of soil moisture deficit, average over 1986-2005.	94
Figure 5-22:	Projected change in the annual number of soil moisture deficit days by 2040 and 2090, under RCP4.5 and RCP8.5.	95
Figure 5-23:	Modelled seasonal number of days of soil moisture deficit, average over 1986-2005.	96
Figure 5-24:	Projected change in the number of seasonal soil moisture deficit days by 2040 for RCP4.5.	97
Figure 5-25:	Projected change in the number of seasonal soil moisture deficit days by 2040 for RCP8.5.	98
Figure 5-26:	Projected change in the number of seasonal soil moisture deficit days by 2090 for RCP4.5.	99
Figure 5-27:	Projected change in the number of seasonal soil moisture deficit days by 2090 for RCP8.5.	100
Figure 6-1:	Projected annual mean wind speed changes by 2040 and 2090, under RCP4.5 and RCP8.5.	102
Figure 6-2:	Projected seasonal mean wind speed changes by 2040 for RCP4.5.	103
Figure 6-3:	Projected seasonal mean wind speed changes by 2040 for RCP8.5.	104
Figure 6-4:	Projected seasonal mean wind speed changes by 2090 for RCP4.5.	105
Figure 6-5:	Projected seasonal mean wind speed changes by 2090 for RCP8.5.	106
Figure 6-6:	Projected annual mean surface solar radiation changes by 2040 and 2090, under RCP4.5 and RCP8.5.	108
Figure 6-7:	Projected seasonal mean surface solar radiation changes by 2040 for RCP4.5.	109
Figure 6-8:	Projected seasonal mean surface solar radiation changes by 2040 for RCP8.5.	110
Figure 6-9:	Projected seasonal mean surface solar radiation changes by 2090 for RCP4.5.	111
Figure 6-10:	Projected seasonal mean surface solar radiation changes by 2090 for RCP8.5.	112
Figure 6-11:	Projected annual mean relative humidity changes by 2040 and 2090, under RCP4.5 and RCP8.5.	114
Figure 6-12:	Projected seasonal mean relative humidity changes by 2040 for RCP4.5.	115
Figure 6-13:	Projected seasonal mean relative humidity changes by 2040 for RCP8.5.	116
Figure 6-14:	Projected seasonal mean relative humidity changes by 2090 for RCP4.5.	117
Figure 6-15:	Projected seasonal mean relative humidity changes by 2090 for RCP8.5.	118
Figure 6-16:	Average seasonal mean sea level pressure over the Southwest Pacific, 1981-2010.	119
Figure 7-1:	Percent changes in multi-model median of the mean discharge across Canterbury for mid (top) and late-century (bottom).	122

Figure 7-2:	Percent changes in multi-model median of the mean annual low flow across Canterbury for mid (top) and late-century (bottom).	124
Figure 7-3:	Percent changes in multi-model median Q5% across Canterbury for mid (top) and end of century (bottom).	126
Figure 7-4:	Percent changes in multi-model median of MAF across Canterbury for mid (top) and end of century (bottom).	128
Figure 8-1:	Four scenarios of New Zealand-wide regional SLR projections for use with this guidance, with extensions to 2150 based on Kopp et al. (2014)–K14.	132
Figure 8-2:	High-tide exceedance curve for all predicted high tides at Lyttelton (excluding effects of weather, climate and SLR).	134
Figure 10-1:	Schematic showing dynamical downscaling method used in this report.	150

Executive summary

Canterbury's climate is changing, and these changes are highly likely to continue for the foreseeable future. It is internationally accepted that human greenhouse gas emissions are the dominant cause of recent global climate change, and that further changes will result from increasing amounts of greenhouse gases in the atmosphere. The rate of future climate change depends on how fast greenhouse gas concentrations increase.

Environment Canterbury commissioned NIWA to analyse projected climate changes for the Canterbury Region. This report addresses expected changes for various climate variables out to 2100, drawing heavily on climate model simulations from the Intergovernmental Panel on Climate Change (IPCC) Fifth Assessment Report. In addition, hydrological and sea-level rise impacts of climate change were assessed. The following bullet points outline some key findings of this report:

- The projected Canterbury temperature changes increase with time and increasing greenhouse gas concentrations. Future annual average warming spans a wide range: 0.5-1.5°C by 2040, and 0.5-3.5°C by 2090. Diurnal temperature range (i.e., difference between minimum and maximum temperature of a given day) is expected to increase with time and increasing greenhouse gas concentrations.
- The average number of hot days (days $\geq 25^{\circ}\text{C}$) is expected to increase with time and emission scenario. The number of hot days in some inland areas of Canterbury (particularly the southern Mackenzie Basin) are projected to increase by 60-85 days per year by 2090 under RCP8.5. The number of frost days (days $< 0^{\circ}\text{C}$) is expected to decrease throughout the region. Largest decreases are expected in inland areas; 10-30 fewer frost days per year by 2040, and 20-50 fewer frost days per year by 2090.
- Projected changes in rainfall show variability across the Canterbury region. Small changes to annual rainfall of $\pm 5\%$ are projected for most of the region by 2040 and 2090. Seasonally the largest increases are projected during winter, with 15-40% more rainfall projected in many eastern, western and southern parts (by 2090 under RCP8.5).
- The future amount of accumulated PED (Potential Evapotranspiration Deficit) is projected to increase across most of Canterbury, therefore drought potential is projected to increase.
- Mean annual low flow generally decreases by late century, with decreases exceeding 20% in many areas of the region.
- Floods (characterised by the Mean Annual Flood; MAF) are expected to become larger for many parts of Canterbury, with some increases exceeding 100%. However, there are some pockets of little change or decreasing Mean Annual Flood. Note, MAF should not be considered a comprehensive metric for the possible impact of climate change on New Zealand flooding.
- Sea-level rise will continually lift the base mean sea level on which the tide rides, which means there will be an increasing percentage of normal high tides which exceed a given present-day elevation e.g., street level, berm or stopbank crest. The present-day Highest Astronomical Tide would be exceeded by approximately 82% of all high tides under 0.65 m sea-level rise.

1 Introduction

Climate change is already affecting New Zealand and Canterbury with downstream effects on our natural environment, the economy, and communities. In the coming decades, climate change is highly likely to increasingly pose challenges to New Zealanders' way of life.

Environment Canterbury commissioned the National Institute of Water and Atmospheric Research (NIWA) to undertake a review of climate change projections for the Canterbury region (Figure 1-1). This work follows the publication of the Intergovernmental Panel on Climate Change (IPCC) Fifth Assessment Report in 2013 and 2014, the New Zealand climate change projections report published by the Ministry for the Environment; updated 2018 (Ministry for the Environment, 2018), and New Zealand hydrological projections under climate change (Collins & Zammit, 2016; Collins et al., 2018). The contents of this technical report include analysis of climate projections for the Canterbury region in greater detail than the national-scale analysis. Regional-scale climate projection maps have been provided for various climate variables.

This technical report describes changes which may occur over the 21st century to the climate and river flows of the Canterbury region. Consideration about future change incorporates knowledge of both natural variations in the climate and changes that may result from increasing global concentrations of greenhouse gases that are contributed to by human activities. Climatic variables discussed in this report include temperature, precipitation (rainfall, dry days and potential evapotranspiration deficit), and wind. Projections for hydrological variables and sea-level rise are also discussed.

Some of the information that underpins portions of this report resulted from academic studies based on the latest assessments of the Intergovernmental Panel on Climate Change (IPCC, 2013; 2014a; 2014b; 2014c). Details specific to Canterbury were based on scenarios for New Zealand that were generated by NIWA from downscaling of global climate model simulations. This effort utilised several IPCC representative concentration pathways for the future and this was achieved through NIWA's core-funded Regional Modelling Programme. The climate change information presented in this report is consistent with recently-updated national-scale climate change guidance produced for the Ministry for the Environment (2018).

The remainder of this chapter includes a brief introduction of global and New Zealand climate change, based on the IPCC Fifth Assessment Report. Chapter 2 includes an introduction to the climate change scenarios used in this report, and the methodology that explains the modelling approach for the climate change projections that are presented for Canterbury.

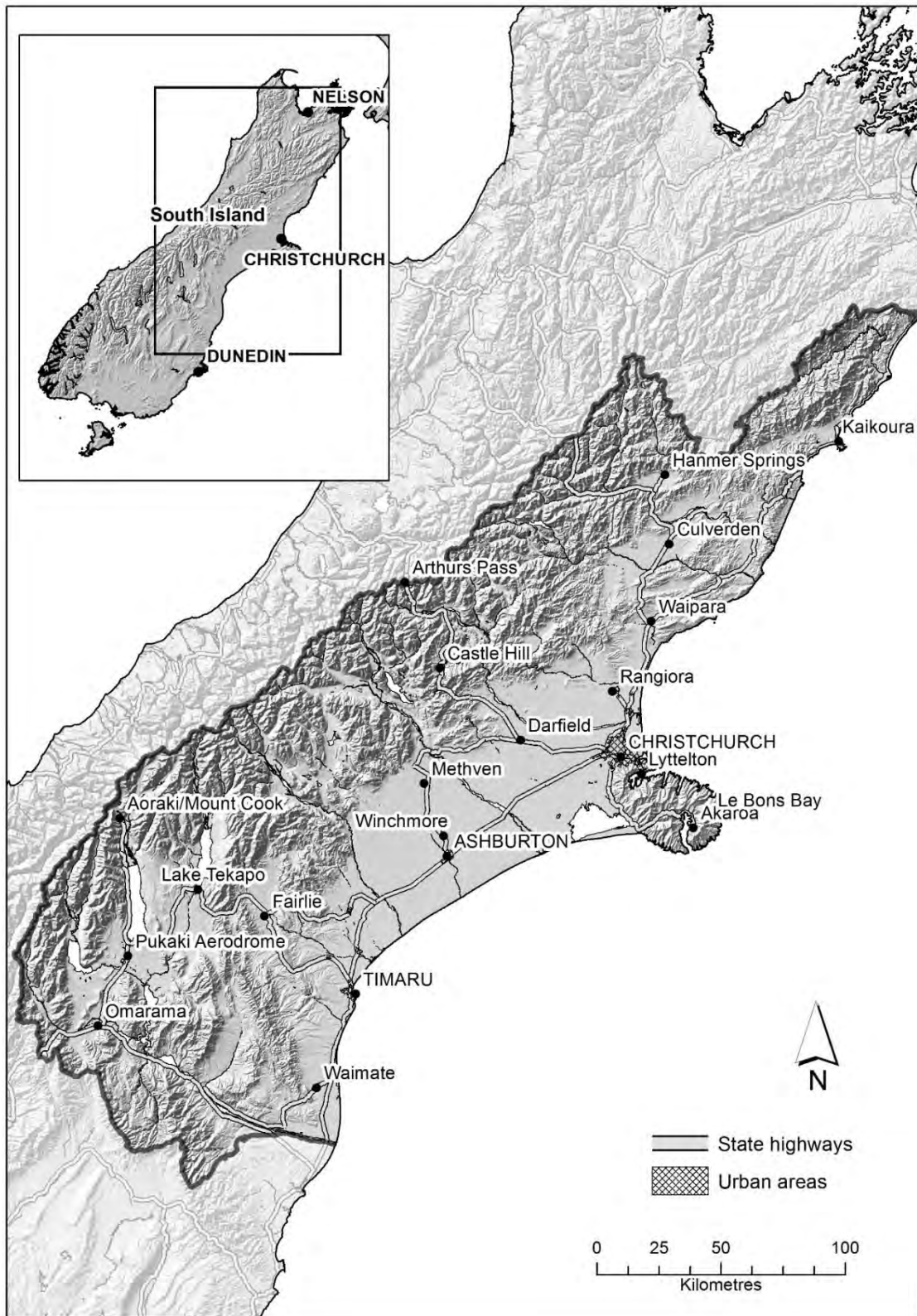


Figure 1-1: The Canterbury region administered by Environment Canterbury.

1.1 Global and New Zealand climate change

Key messages

- The global climate system is warming and many of the recently observed climate changes are unprecedented.
- Global mean sea level has risen over the past century at a rate of about 1.7 mm/year, and has very likely accelerated to 3.2 mm/year since 1993.
- Human activities (and associated greenhouse gas emissions) are estimated to have caused approximately 1.0°C of global warming above pre-industrial levels.
- Estimated human-induced global warming is currently increasing at 0.2°C per decade due to past and ongoing emissions of greenhouse gases.
- Continued increases in greenhouse gas emissions will cause further warming and impacts on all parts of the global climate system. Thus, it is important for relevant authorities to plan with both natural and climate change induced variability in mind.

Warming of the global climate system is unequivocal, and since the 1950s, many of the observed climate changes are unprecedented over short and long timescales (decades to millennia) (IPCC, 2013). These changes include warming of the atmosphere and ocean, diminishing of ice and snow, sea-level rise, and increases in the concentration of greenhouse gases in the atmosphere. Climate change is already influencing the intensity and frequency of many extreme weather and climate events globally. Shifts in average temperatures will result in proportionally large increases in the occurrence of extreme temperatures. The Earth's global temperature has warmed by 1.14°C over the period 1880-2019 (NASA/GISS, 2019). The rate of sea-level rise since the mid-19th century has been larger than the mean rate of change during the previous two millennia. Over the period 1880-2018, global mean sea level has risen about 0.21-0.24 m (Lindsey, 2019).

The atmospheric concentrations of carbon dioxide have increased to levels unprecedented in at least the last 3 million years (Willeit et al., 2019). Carbon dioxide concentrations have increased by at least 40% since pre-industrial times, primarily from fossil fuel emissions and secondarily from net land use change emissions (IPCC, 2013). In May 2019, the carbon dioxide concentration of the atmosphere reached 415 parts per million. The ocean has absorbed about 30% of the emitted anthropogenic carbon dioxide, causing ocean acidification. Due to the influence of greenhouse gases on the global climate system, it is extremely likely that human influence has been the dominant cause of the observed warming since the mid-20th century (IPCC, 2013; IPCC, 2018).

Published information about the expected impacts of climate change on New Zealand is summarised and assessed in the Australasia chapter of the IPCC Working Group II assessment report (Reisinger et al., 2014) as well as a report published by the Royal Society of New Zealand (Royal Society of New Zealand, 2016). Key findings from these publications include:

The regional climate is changing. The Australasia region continues to demonstrate long-term trends toward higher surface air and sea surface temperatures, more hot extremes and fewer cold extremes, and changed rainfall patterns. Over the past 50 years, increasing greenhouse gas concentrations have contributed to rising average temperatures in New Zealand. Changing

precipitation patterns have resulted in increases in rainfall for the south and west of the South Island and west of the North Island and decreases in the northeast of the South Island and the east and north of the North Island. Some heavy rainfall events already carry the fingerprint of a changed climate, in that they have become more intense due to higher temperatures allowing the atmosphere to carry more moisture (Dean et al., 2013). Cold extremes have become rarer and hot extremes have become more common.

The region has already exhibited warming and is virtually certain to continue to do so. New Zealand’s mean annual temperature has increased, on average, by 1.02°C (± 0.25°C) per century since 1909 (Figure 1-2).

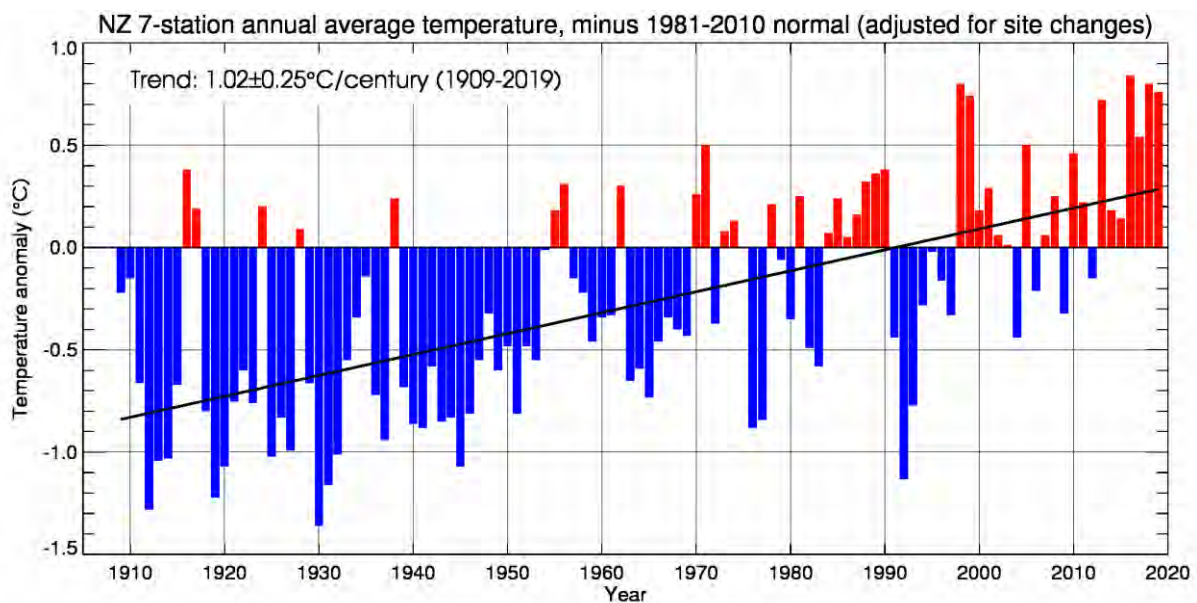


Figure 1-2: New Zealand national temperature series, 1909-2019. More information about the New Zealand seven-station temperature series can be found at <https://www.niwa.co.nz/our-science/climate/information-and-resources/nz-temp-record/seven-station-series-temperature-data>.

Warming is projected to continue through the 21st century along with other changes in climate.

Warming is expected to be associated with rising snow lines, more frequent hot extremes, less frequent cold extremes, and increasing extreme rainfall related to flood risk in many locations. Annual average rainfall is expected to decrease in the northeast South Island and north and east of the North Island, and to increase in other parts of New Zealand. Fire hazard is projected to increase in many parts of New Zealand. Regional sea-level rise will very likely exceed the historical rate, consistent with global mean trends.

Impacts and vulnerability: Without adaptation, further climate-related changes are projected to have substantial impacts on water resources, coastal ecosystems, infrastructure, health, agriculture, and biodiversity. However, uncertainty in projected rainfall changes and other climate-related changes remains large for many parts of New Zealand, which creates significant challenges for adaptation.

Additional information about recent New Zealand climate change can be found in Ministry for the Environment (2018).

1.2 Year to year climate variability and climate change

Key messages

- Natural variability is an important consideration in addition to the underlying climate change signal.
- El Niño-Southern Oscillation is the most dominant mode of inter-annual climate variability and it impacts New Zealand primarily through changing wind, temperature and rainfall patterns.
- The Interdecadal Pacific Oscillation affects New Zealand through drier conditions in the east and wetter conditions in the west during the positive phase the opposite in the negative phase.
- The Southern Annular Mode affects New Zealand through higher temperatures and settled weather during the positive phase and lower temperatures and unsettled weather during the negative phase.
- Natural variability will continue to affect the year-to-year climate of New Zealand into the future.

Much of the material in this report focuses on the projected impact on the climate of Canterbury over the coming century due to increases in global anthropogenic greenhouse gas concentrations. However, natural variations will also continue to occur. Much of the variation in New Zealand's climate is random and lasts for only a short period, but longer term, quasi-cyclic variations in climate can be attributed to different factors. Three large-scale oscillations that influence climate in New Zealand are the El Niño-Southern Oscillation, the Interdecadal Pacific Oscillation, and the Southern Annular Mode (Ministry for the Environment, 2008). Those involved in (or planning for) climate-sensitive activities in the Canterbury region will need to cope with the sum of both anthropogenic change and natural variability.

1.2.1 The effect of El Niño and La Niña

El Niño-Southern Oscillation (ENSO) is a natural mode of climate variability that has wide-ranging impacts around the Pacific Basin (Ministry for the Environment, 2008). ENSO involves a movement of warm ocean water from one side of the equatorial Pacific to the other, changing atmospheric circulation patterns in the tropics and subtropics, with corresponding shifts for rainfall across the Pacific.

During El Niño, easterly trade winds weaken and warm water 'spills' eastward across the equatorial Pacific, accompanied by higher rainfall than normal in the central-east Pacific. La Niña produces opposite effects and is typified by an intensification of easterly trade winds, and retention of warm ocean waters over the western Pacific. ENSO events occur on average three to seven years apart, typically becoming established in April or May and persisting for about a year thereafter (Figure 1-3).

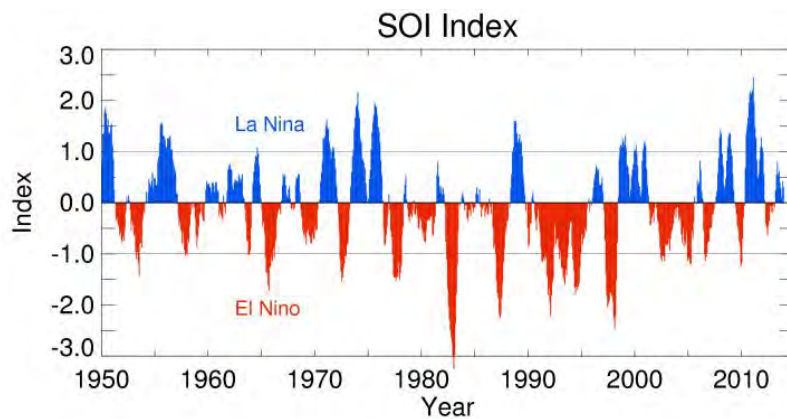


Figure 1-3: The 5-month running mean Southern Oscillation Index (SOI), from January 1950 (i.e. Nov 1949 – Mar 1950) to January 2014 (Nov 2013 – Mar 2014). The most recent 3 years of SOI data can be viewed at <https://niwa.co.nz/climate/information-and-resources/elnino>.

During El Niño events, the weakened trade winds cause New Zealand to experience a stronger than normal south-westerly airflow. This generally brings lower seasonal temperatures to the country and drier than normal conditions to the north and east of New Zealand, including Canterbury (Salinger and Mullan, 1999). During La Niña conditions, the strengthened trade winds cause New Zealand to experience more north-easterly airflow than normal, higher-than-normal temperatures (especially during summer), and generally drier conditions in the west and south of the South Island (Figure 1-4).

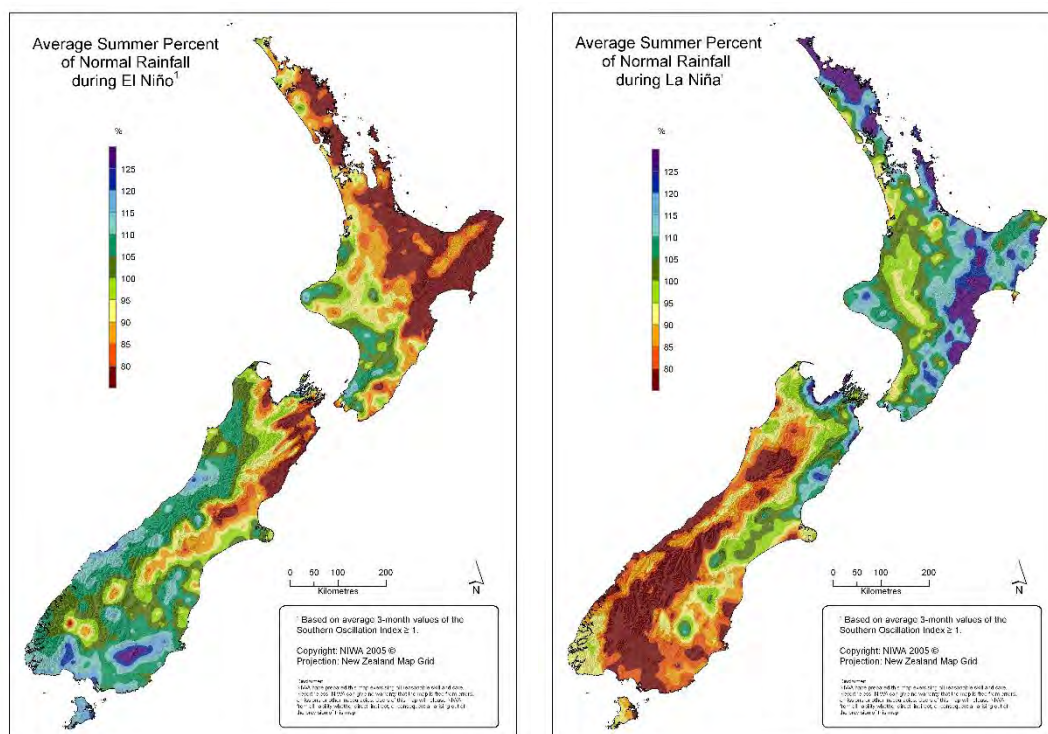


Figure 1-4: Average summer percentage of normal rainfall during El Niño (left) and La Niña (right). El Niño composite uses the following summers: 1963/64, 1965/66, 1968/69, 1969/70, 1972/73, 1976/77, 1977/78, 1982/83, 1986/87, 1987/88, 1991/92, 1994/95, 1997/98, 2002/03. La Niña composite uses the following summers: 1964/65, 1970/71, 1973/74, 1975/76, 1983/84, 1984/85, 1988/89, 1995/96, 1998/99, 1999/2000, 2000/01. This figure was last updated in 2005. © NIWA.

According to IPCC (2013), ENSO is highly likely to remain the dominant mode of natural climate variability in the 21st century, and that rainfall variability relating to ENSO is likely to increase. However, there is uncertainty about future changes to the amplitude and spatial pattern of ENSO.

1.2.2 The effect of the Interdecadal Pacific Oscillation

The Interdecadal Pacific Oscillation (IPO) is a large-scale, long-period oscillation that influences climate variability over the Pacific Basin including New Zealand (Salinger et al., 2001). The IPO operates at a multi-decadal scale, with phases lasting around 20 to 30 years (Figure 1-5). During the positive phase of the IPO, sea surface temperatures around New Zealand tend to be lower, and westerly winds stronger, resulting in drier conditions for eastern areas of both North and South Islands. The opposite occurs in the negative phase. The IPO can modify New Zealand’s connection to ENSO, and it also positively reinforces the impacts of El Niño (during IPO+ phases) and La Niña (during IPO- phases).

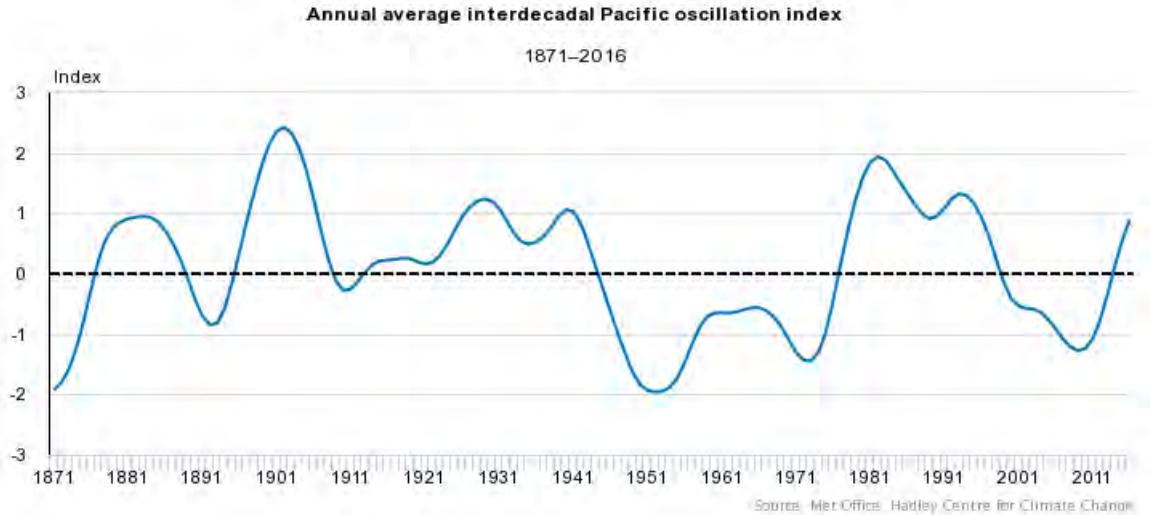


Figure 1-5: Annual average Interdecadal Pacific Oscillation (IPO) index, 1871-2016. The IPO was positive from 1913-44 and 1977-98, and negative from 1945-76. Source: Stats NZ (2020).

1.2.3 The effect of the Southern Annular Mode

The Southern Annular Mode (SAM) represents the variability of circumpolar atmospheric jets that encircle the Southern Hemisphere that extend out to the latitudes of New Zealand. The SAM is often coupled with ENSO, and both phenomena affect New Zealand’s climate in terms of westerly wind strength and storm occurrence (Renwick and Thompson, 2006). In its positive phase, the SAM is associated with relatively light winds and more settled weather over New Zealand, with stronger westerly winds further south towards Antarctica. In contrast, the negative phase of the SAM is associated with unsettled weather and stronger westerly winds over New Zealand, whereas wind and storms decrease towards Antarctica. The SAM tends to operate at a weekly scale, and positive or negative phases may persist for several weeks. During the summer of 2017-18 (i.e. December 2017 – February 2018), the SAM was positive for 86 days, and negative for just four days (Figure 1-6). This was associated with New Zealand’s hottest summer on record, as well as New Zealand’s hottest month on record (January 2018).

The phase and strength of the SAM is influenced by the size of the ozone hole, giving rise to positive trends in the past during spring and summer. In the future other drivers are likely to have an impact on SAM behaviour, for example changing temperature gradients between the equator and the high southern latitudes would have an impact on westerly wind strength in the mid-high latitudes.

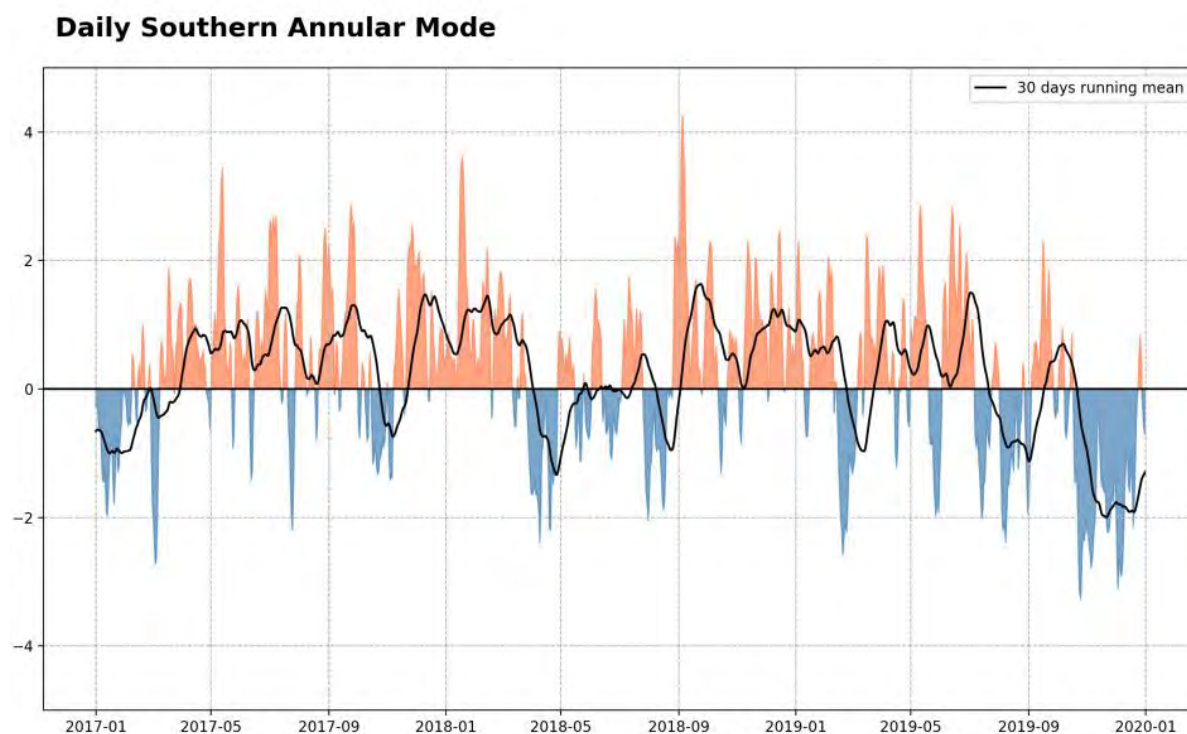


Figure 1-6: Daily Southern Annular Mode (SAM), January 2017 - December 2019. The solid black line represents the 30-day running mean SAM. Image sourced from: NIWA (2020).

1.2.4 The influence of natural variability on climate change projections

It is important to consider human-induced climate change in the context of natural climate variability. An example of this for temperature is shown in Figure 1-7. The solid black line on the left-hand side represents the observed annual average temperature for New Zealand¹, and the dashed black line represents the 1909-2014 trend of 0.92 °C/century extrapolated to 2100. All the other line plots and shading refer to the modelled air temperature averaged over the New Zealand region. Post-2014, the two line plots show the annual temperature changes for the New Zealand region under RCP8.5 (orange) and RCP2.6 (blue); a single model is selected to illustrate the inter-annual variability. The shading shows the range across all IPCC AR5 models for both historical and future periods.

Over the 1900-2014 historical period, the New Zealand observed temperature curve lies within the simulations of all models (purple shading). For the future 2015-2100 period, the RCP2.6 models (blue shading) show very little warming trend after about 2030, whereas the RCP8.5 models (orange shading) 'take off' to be anywhere between +2°C and +5°C by 2100.

¹ <https://www.niwa.co.nz/our-science/climate/information-and-resources/nz-temp-record/seven-station-series-temperature-data>

Figure 1-7 should not be interpreted as a set of specific predictions for individual years. However, it illustrates that although we expect a long term overall upward trend in temperatures (at least for RCP8.5), there will still be some relatively cool years. For this example, a year which is unusually warm under our present climate could become the norm by about 2050, and an “unusually warm” year in 30-50 years’ time (under the higher emission scenarios) is likely to be warmer than anything we currently experience.

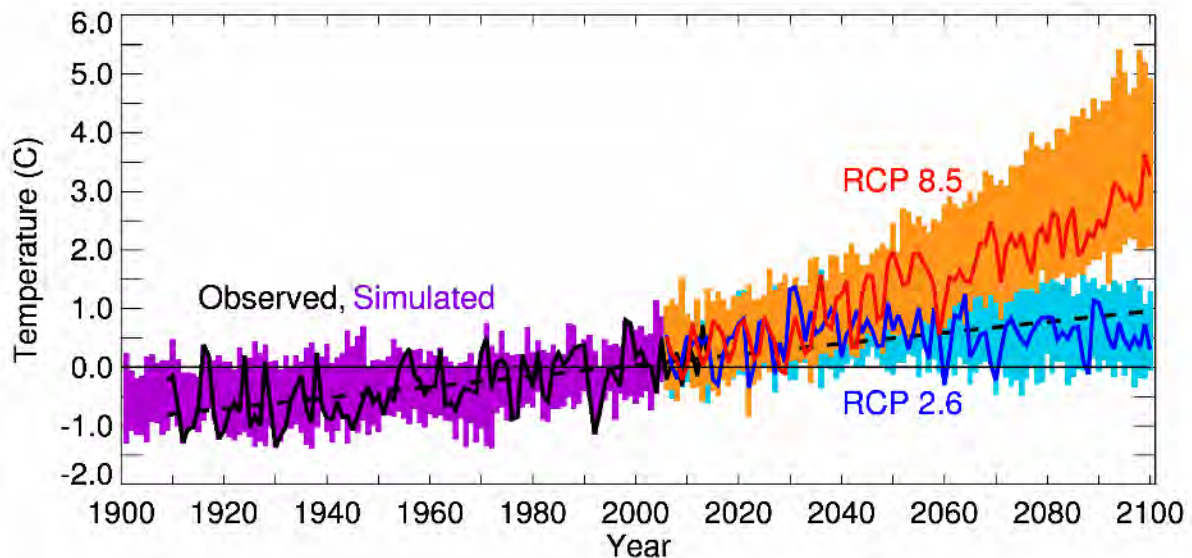


Figure 1-7: New Zealand Temperature - historical record and an illustrative schematic projection illustrating future year-to-year variability. (See text for full explanation). From Ministry for the Environment (2018).

For rainfall, multi-decadal variability associated with the IPO can enhance or counter the impacts of anthropogenic climate change. This influence may generate either slightly above normal or below normal rainfall for parts of New Zealand during summer. IPO-negative conditions coupled with more frequent La Niña episodes could increase rainfall during spring and summer, essentially in the opposite direction as expected from anthropogenic factors (i.e. a potential reduction in spring and summer rainfall). A subsequent further reversal of the IPO in 10-20 years’ time could have the opposite effect, enhancing part of the anthropogenic (drying) trend in rainfall projected for parts of New Zealand for a few decades. The message from this section is *not* that anthropogenic trends in climate can be ignored because of natural variability. In the projections, we have discussed these anthropogenic trends because they become the dominant factor locally as the century progresses. Nevertheless, we need to bear in mind that at some times natural variability will be adding to the human-induced trends, while at others it may be offsetting part of the anthropogenic effect.

2 Methodology

2.1 Representative Concentration Pathways

Key messages

- Future climate change projections are considered under four scenarios of future greenhouse gas concentrations, called Representative Concentration Pathways (RCPs) by the IPCC.
- The four RCPs project different climate futures based on future greenhouse gas concentrations, determined by economic, political and social developments during the 21st century.
- RCP2.6 is a mitigation scenario requiring significant reduction in greenhouse gas emissions, RCP4.5 and RCP6.0 are mid-range scenarios where greenhouse gas concentrations stabilise by 2100, and RCP8.5 is a 'business as usual' scenario with greenhouse gas concentrations continuing to increase at current rates.
- Projections for the future climate in Canterbury are presented for RCP4.5 and RCP8.5 in this report.

Assessing possible changes for our future climate due to human activity is difficult because climate projections depend strongly on estimates for future greenhouse gas concentrations. Those concentrations depend on global greenhouse gas emissions that are driven by factors such as economic activity, population changes, technological advances and policies for sustainable resource use. In addition, for a specific future trajectory of global greenhouse gas concentrations, different climate model simulations produced somewhat different results for future climate change.

This range of uncertainty has been dealt with by the IPCC through consideration of 'scenarios' that describe concentrations of greenhouse gases in the atmosphere. The wide range of scenarios are associated with possible economic, political, and social developments during the 21st century, and via consideration of results from several different climate models for any given scenario. In the 2013 IPCC Fifth Assessment Report, the atmospheric greenhouse gas concentration components of these scenarios are called Representative Concentration Pathways (RCPs). These are abbreviated as RCP2.6, RCP4.5, RCP6.0, and RCP8.5, in order of increasing radiative forcing by greenhouse gases (i.e. the change in energy in the atmosphere due to greenhouse gas emissions). RCP2.6 leads to low anthropogenic greenhouse gas concentrations (requiring removal of CO₂ from the atmosphere, also called the 'mitigation' scenario), RCP4.5 and RCP6.0 are two 'stabilisation' scenarios (where greenhouse gas concentrations and therefore radiative forcing stabilises by 2100) and RCP8.5 has very high greenhouse gas concentrations (the 'business as usual' scenario). Therefore, the RCPs represent a range of 21st century climate policies. Table 2-1 shows the projected global mean surface air temperature for each RCP.

Table 2-1: Projected change in global mean surface air temperature for the mid- and late- 21st century relative to the reference period of 1986-2005 for different RCPs. After IPCC (2013).

Scenario	Alternative name	2046-2065 (mid-century)		2081-2100 (end-century)	
		Mean	Likely range	Mean	Likely range
RCP2.6	Mitigation scenario	1.0	0.4 to 1.6	1.0	0.3 to 1.7
RCP4.5	Stabilisation scenario	1.4	0.9 to 2.0	1.8	1.1 to 2.6
RCP6.0	Stabilisation scenario	1.3	0.8 to 1.8	2.2	1.4 to 3.1
RCP8.5	Business as usual scenario	2.0	1.4 to 2.6	3.7	2.6 to 4.8

The full range of projected globally-averaged temperature increases for all scenarios for 2081-2100 (relative to 1986-2005) is 0.3 to 4.8°C (Figure 2-1). Warming will continue beyond 2100 under all RCP scenarios except RCP2.6. Warming will continue to exhibit inter-annual-to-decadal variability and will not be regionally uniform.

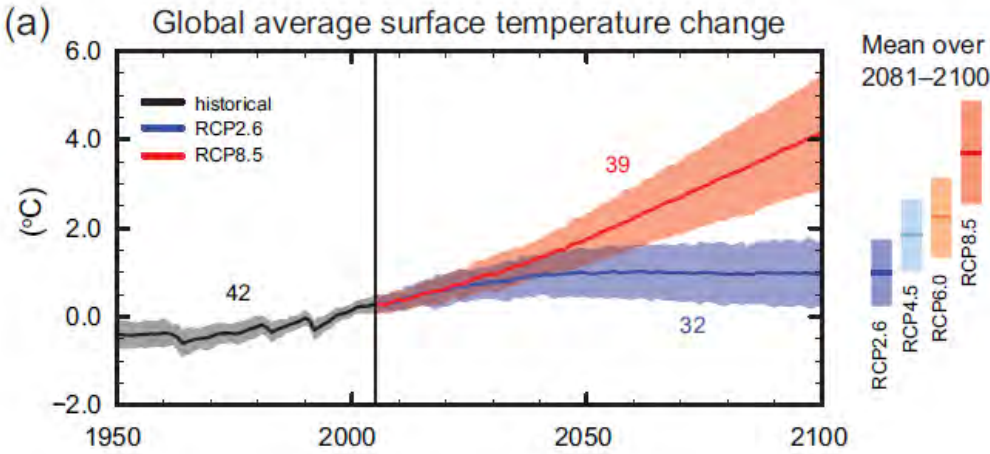


Figure 2-1: CMIP5 multi-model simulated time series from 1950-2100 for change in global annual mean surface temperature relative to 1986-2005. Time series of projections and a measure of uncertainty (shading) are shown for scenarios RCP2.6 (blue) and RCP8.5 (red). Black (grey shading) is the modelled historical evolution using historical reconstructed forcings. The mean and associated uncertainties averaged over 2081–2100 are given for all RCP scenarios as coloured vertical bars to the right of the graph (the mean projection is the solid line in the middle of the bars). The numbers of CMIP5 models used to calculate the multi-model mean is indicated on the graph. From IPCC (2013).

As global temperatures increase, it is virtually certain that there will be more hot and fewer cold temperature extremes over most land areas. It is very likely that heat waves will occur with a higher frequency and duration. Furthermore, the contrast in rainfall between wet and dry regions and wet and dry seasons will increase. Along with increases in global mean temperature, mid-latitude and wet tropical regions will experience more intense and more frequent extreme rainfall events by the end of the 21st century. The global ocean will continue to warm during the 21st century, influencing ocean circulation and sea ice extent.

Cumulative CO₂ emissions will largely determine global mean surface warming by the late 21st century and beyond. Even if emissions are stopped, the inertia of many global climate changes will continue for many centuries to come. This represents a substantial multi-century climate change commitment created by past, present, and future emissions of CO₂.

In this report, global climate model outputs based on two RCPs (RCP4.5 and RCP8.5) have been downscaled to produce future climate projections for the Canterbury Region. The rationale for choosing these two scenarios was to present a 'business-as-usual' scenario if greenhouse gas emissions continue at current rates (RCP8.5) and a scenario which could be realistic if global action is taken towards mitigating climate change, for example the Paris climate change agreement (RCP4.5). In addition, the global model outputs based on RCP4.5 and RCP8.5 have been utilised for the hydrological modelling component of this report.

2.2 Climate modelling

Key messages

- Climate model simulation data from the IPCC Fifth Assessment has been used to produce climate projections for New Zealand.
- Six climate models were chosen by NIWA for dynamical downscaling. These models were chosen because they produced the most accurate results when compared to historical climate and circulation patterns in the New Zealand and southwest Pacific region.
- Downscaled climate change projections are at a 5 km x 5 km resolution over New Zealand.
- Climate projection and historic baseline maps and tables present the average of the six downscaled models.
- Climate projections are presented as a 20-year average for two future periods: 2031-2050 (termed '2040') and 2081-2100 (termed '2090'). All maps show changes relative to the baseline climate of 1986-2005 (termed '1995').
- More details about the methods used in climate change modelling are found in Appendix A.

2.3 Hydrological modelling

Key messages

- NIWA's TopNet model used in this study. TopNet is a spatially semi-distributed, time-stepping model of water balance. The model is driven by time-series of precipitation and temperature, and additional weather elements where available.
- TopNet was run continuously from 1971 to 2100, with the spin-up period 1971 excluded from the analysis. The climate inputs were stochastically disaggregated from daily to hourly time steps.
- The simulation results comprise time-series of modelled river flow for each computational sub-catchment, and for each of the six GCMs and two RCPs considered.
- Hydrological projections are presented as the average for two future periods: 2036-2056 (termed 'mid-century') and 2086-2099 (termed 'late-century'). All maps show changes relative to the baseline climate (1986-2005 average).
- More details about the methods used in hydrological modelling are found in Appendix B

2.4 Limitations

As with any modelling exercise, there are limitations on the results and use of the data. This section outlines some of these limitations and caveats that should be considered when using the results in this report.

- The maps and tables presented in this report (except the model confidence sections 4.1.1 and 5.1.1) show the average of six dynamically downscaled global climate models. This is a relatively small number of models and a clear shift in the distribution of potential future outcomes is not available. This is particularly important when considering extremes (e.g. extreme hot days - not presented in this report) where the models considered here may not accurately capture how rare events are changing.
- The average of six models is used in this report, which gives no indication of the range of results that the models project (note the model confidence sections 4.1.1 and 5.1.1 do indicate the range of temperature and rainfall results projected). However, the six models chosen represented historic climate conditions in New Zealand well, and span a range of future outcomes. Using the average balances out the errors that may be apparent in each model.
- The time periods chosen for historic and future projection span 20-year periods. This is seen as a relatively short timeframe to understand average conditions in the historic period and in the future, as there is likely an influence of underlying climate variability (e.g. decadal signals from climate drivers like the El Niño-Southern Oscillation etc.). However, the IPCC uses 20-year periods, so we have followed that approach for consistency.
- Care needs to be taken when interpreting grid-point-scale projections such as those presented in the tables in this report. The underlying climate data are Virtual Climate Station data, which are interpolated from physical climate stations. Therefore, the data from these grid points may be slightly different to on-the-ground observations, due to the interpolation procedure (particularly if the grid point is surrounded by multiple different stations or if there are no stations nearby). It is useful to look at broader patterns between grid points, e.g. coast vs. inland, and the magnitude of change at different time periods and scenarios, when considering the values.

Although there are limitations and caveats to the approach used here, these climate change projections are the best currently available for New Zealand. A considerable amount of research time has been dedicated to undertaking the modelling and validation of the results, and the projections provide context to base risk assessments and adaptation plans on.

3 Current and future climate of the Canterbury Region

All aspects of the climate of Canterbury are dominated by the influence of the Southern Alps on the prevailing westerly airflows. These prevailing westerlies result in a steep precipitation gradient eastward from the western ranges. Five main climate zones can be distinguished in Canterbury:

- The plains, with prevailing winds from the north-east and south-west, low rainfall, and a relatively large annual temperature range by New Zealand standards.
- The eastern foothills and southern Kaikoura Ranges, with cooler and wetter weather, and a high frequency of north-west winds.
- The high country near the main divide, with prevailing north-west winds, abundant precipitation, winter snow and some glaciers particularly towards the south.
- Banks Peninsula and the coastal strip north of Amberley, with relatively mild winters, and rather high annual rainfall with a winter maximum.
- The inland basins and some sheltered valleys, where rainfall is low with a summer maximum, and diurnal and annual temperature ranges are large.

Although north-west winds are not frequent on the plains they are an important consideration, due to the exceptional evaporation that occurs on north-westerly days. Irrigation is necessary in most parts of the plains during the growing season due to the relatively low rainfall received there. More information about the present climate of Canterbury, outside of the information in this report, can be found in Macara (2016).

The following sections (4-8) present climate change projections for the Canterbury Region.

4 Temperature

4.1 Mean temperature

Key messages

- Projected Canterbury temperature changes increase with time and greenhouse gas concentrations. Future annual average warming spans a wide range: 0.5-1.5°C by 2040, and 0.5-3.5°C by 2090.
- Seasonal mean temperatures are projected to increase by 0.5-1.5°C across much of Canterbury (by 2040 under RCP4.5). By 2090 under RCP8.5, projected increases of 1.5-3.0°C for most of Canterbury, with increases of 3.0-4.0°C for western-most parts of the region.

Historic (average over 1986-2005) and future (average over 2031-2050 and 2081-2100) maps for mean temperature are shown in this section. The historic maps show annual and seasonal mean temperature in units of degrees Celsius (°C) and the future projection maps show the change in mean temperature compared with the historic period, in units of °C. Note that the historic maps are on a different colour scale to the future projection maps.

For the historic period, annual mean temperatures range between 10-14°C for most coastal and inland low-elevation locations of Canterbury (Figure 4-1). Seasonal mean temperatures are shown in Figure 4-3. For coastal and inland low-elevation areas of Canterbury, summer mean temperatures range between 14-18°C, and winter mean temperatures range between 4-8°C. Mean temperatures at high-elevation mountainous areas of Canterbury remain several degrees Celsius lower than the remainder of the region throughout the year.

Annual mean temperature is projected to increase by 0.5-1.5°C by 2040 under RCP4.5 and RCP8.5 (Figure 4-2). By 2090, annual mean temperature increases of 0.5-2.0°C (RCP4.5) and 1.5-3.5°C (RCP8.5) are projected for most of the region. Seasonal projections of mean temperature change are shown for RCP4.5 by 2040 (Figure 4-4) and 2090 (Figure 4-6), and RCP8.5 by 2040 (Figure 4-5) and 2090 (Figure 4-7). By 2040 under RCP4.5, seasonal mean temperatures are projected to increase by 0.5-1.5°C across much of Canterbury. By 2090 under RCP8.5, seasonal mean temperatures are projected to increase by 1.5-3.0°C for most of Canterbury, with increases of 3.0-4.0°C projected for western-most parts of the region in summer, autumn and spring.

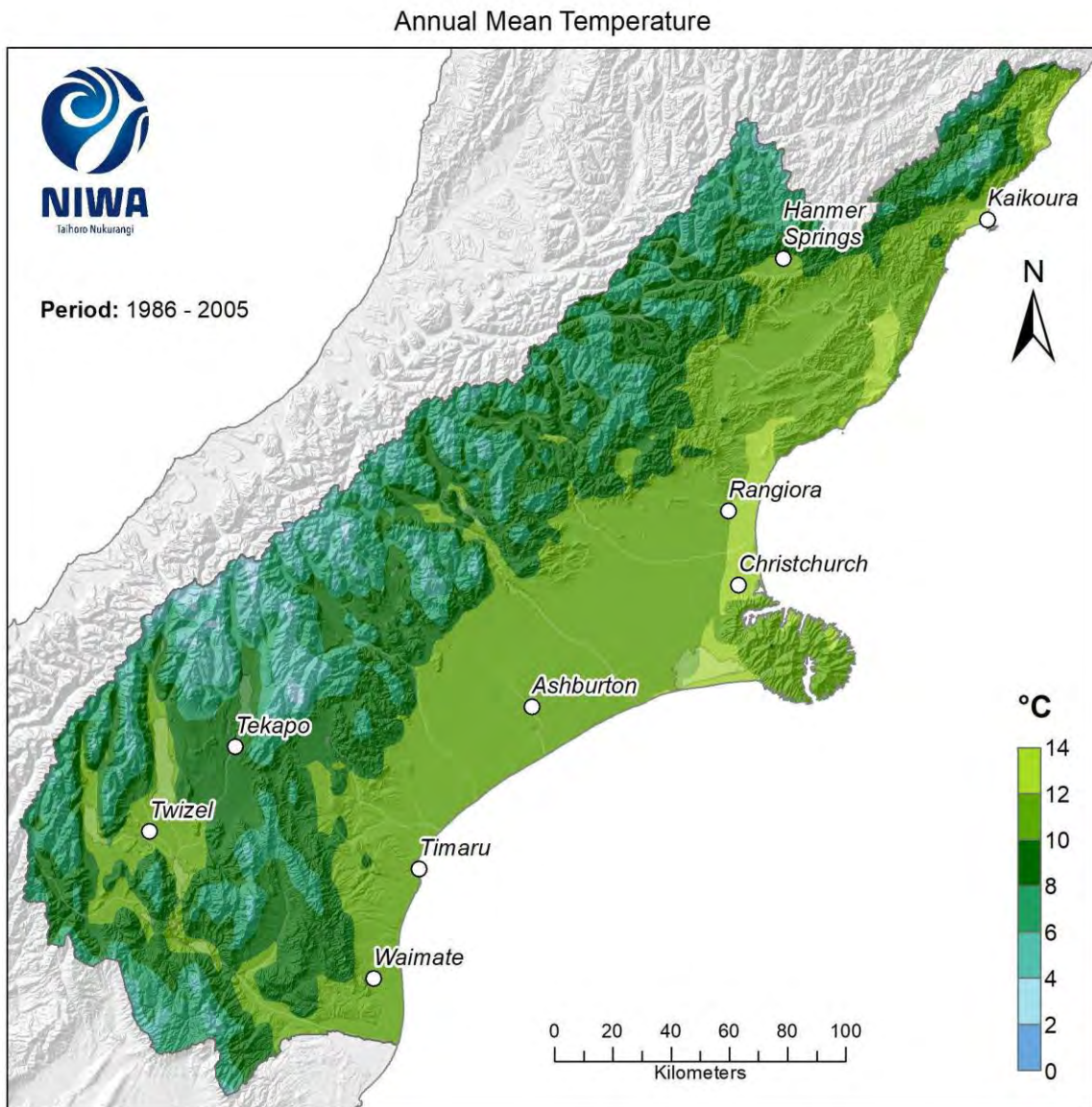


Figure 4-1: Modelled annual mean temperature, average over 1986-2005. Results are based on dynamical downscaled projections using NIWA's Regional Climate Model. Resolution of projection is 5km x 5km.

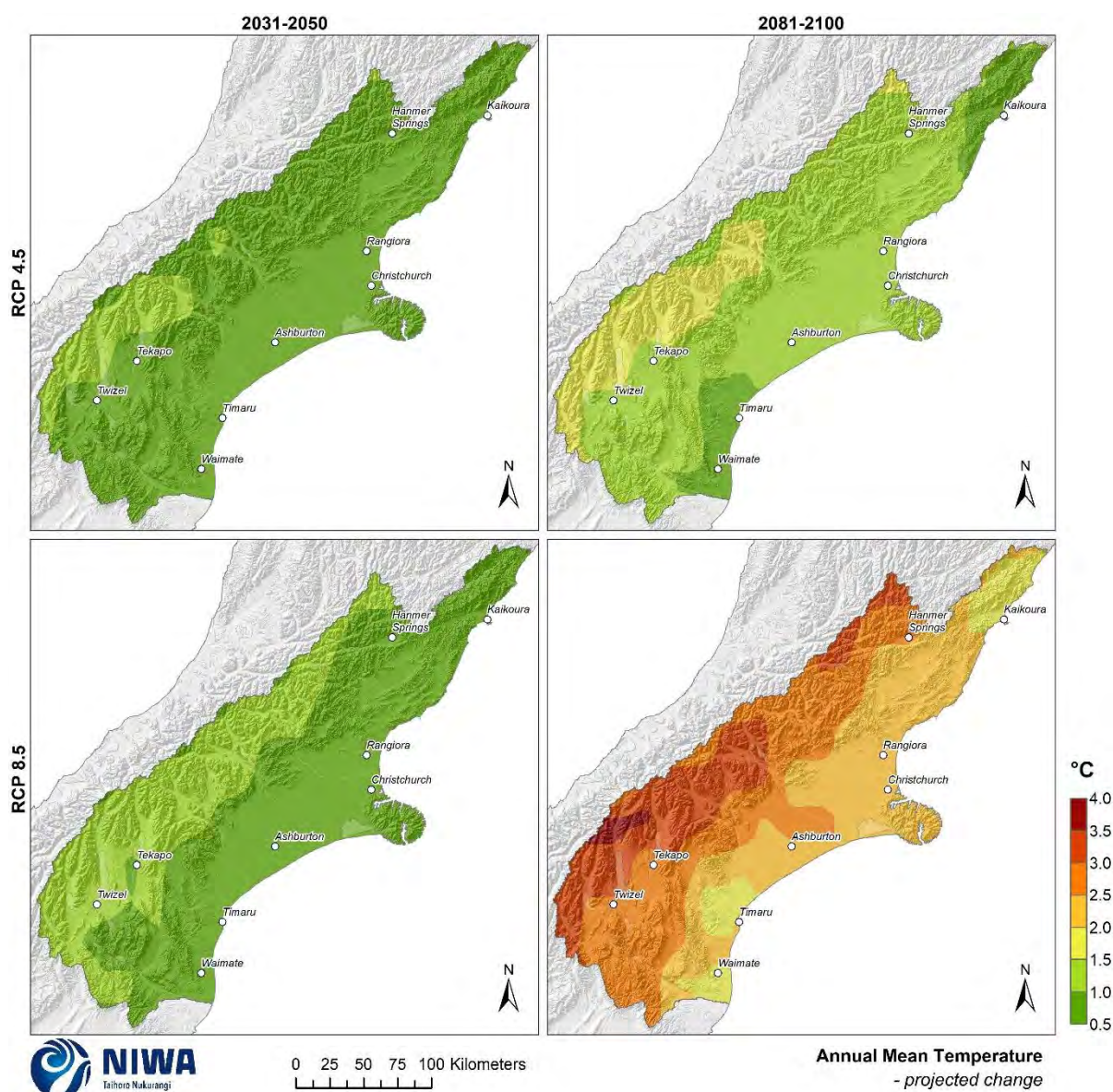


Figure 4-2: Projected annual mean temperature changes by 2040 and 2090, under RCP4.5 and RCP8.5. Climate change scenarios: RCP4.5 (top panels) and RCP8.5 (bottom panels). Time periods: mid-century (2031-2050; “2040” – panels on left) and end-century (2081-2100; “2090” – panels on right). Changes relative to 1986-2005 average, based on the average of six global climate models. Results are based on dynamical downscaled projections using NIWA's Regional Climate Model. Resolution of projection is 5km x 5km.

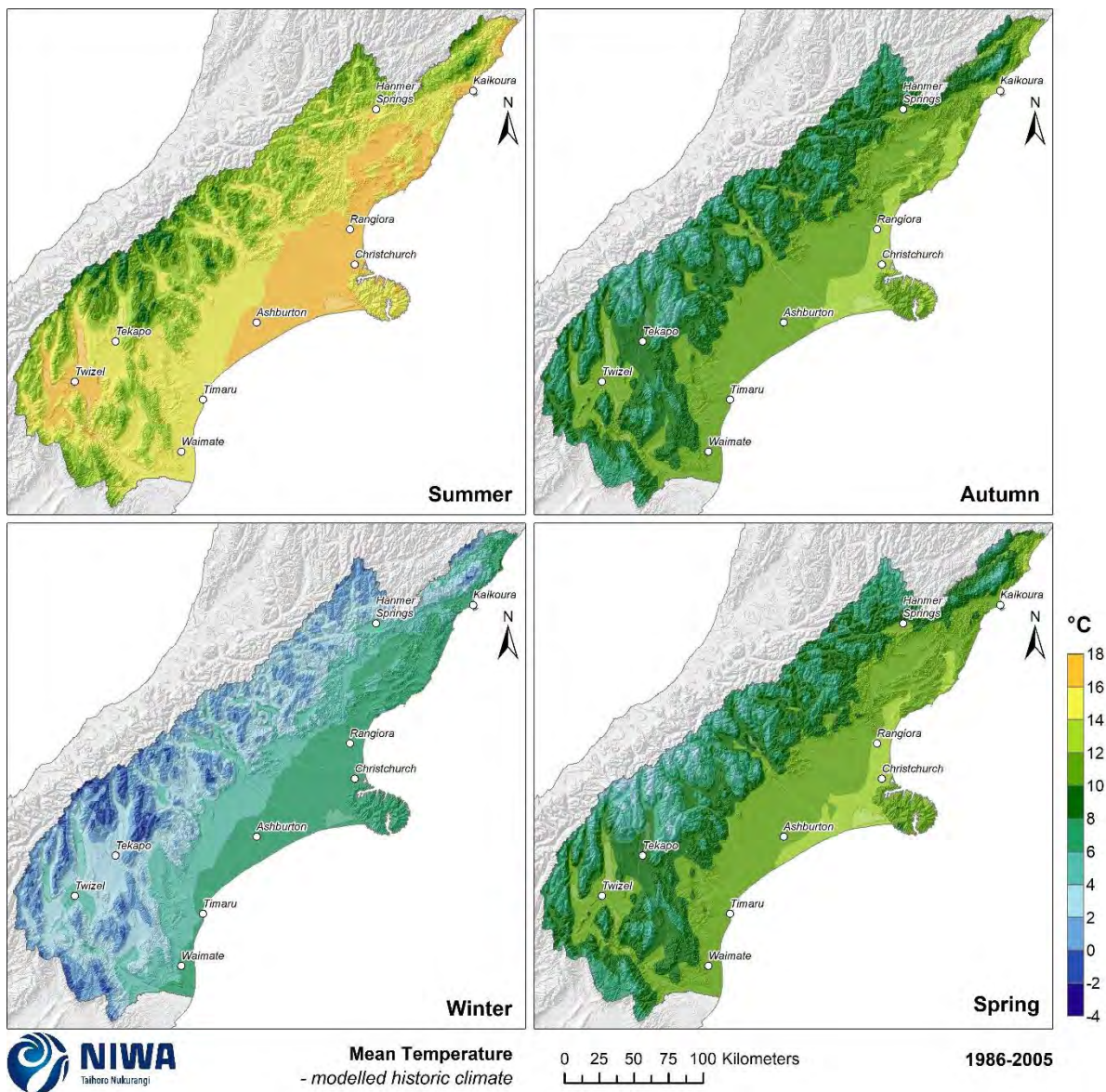


Figure 4-3: Modelled seasonal mean temperature, average over 1986-2005. Results are based on dynamical downscaled projections using NIWA's Regional Climate Model. Resolution of projection is 5km x 5km.

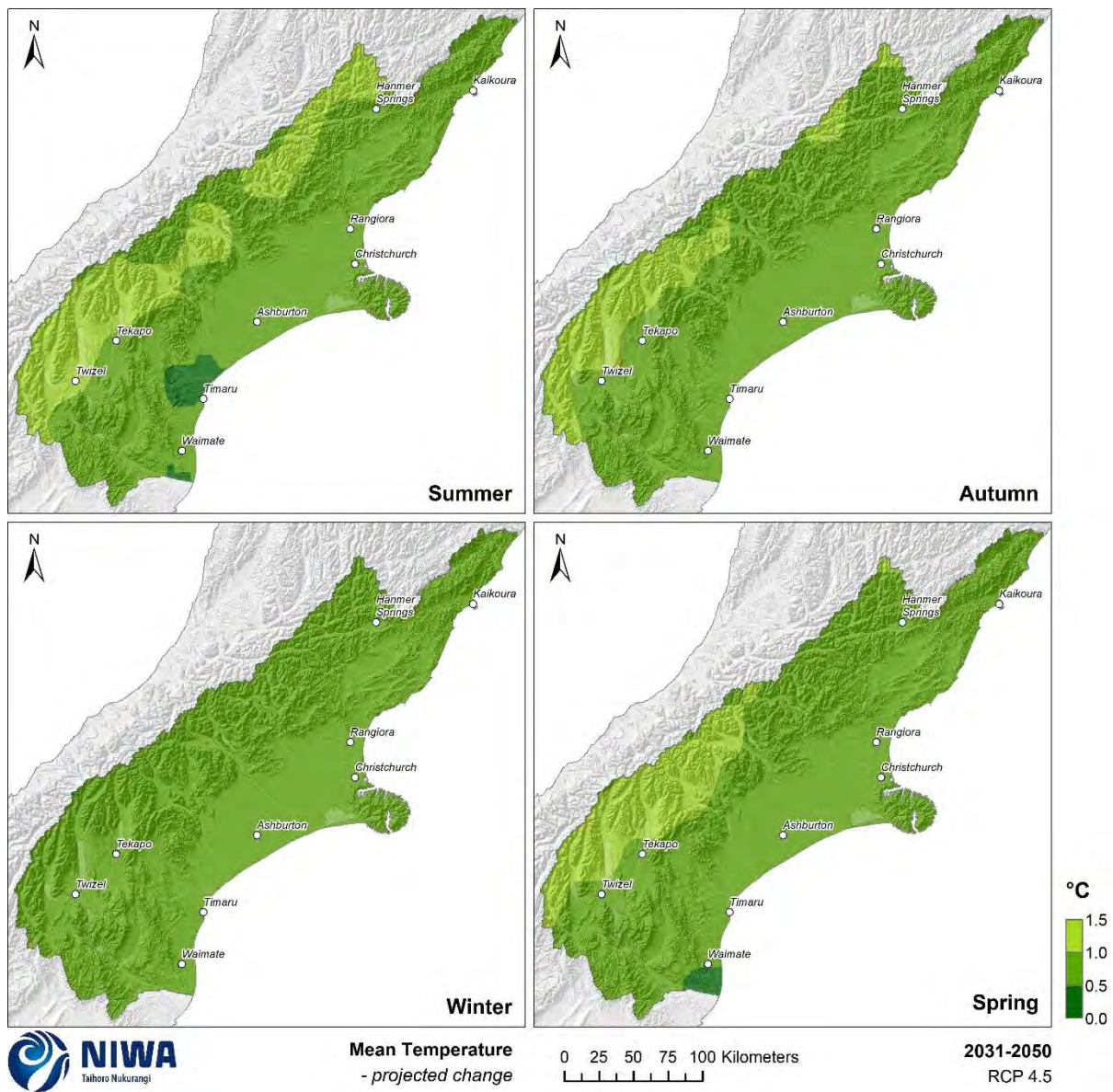


Figure 4-4: Projected seasonal mean temperature changes by 2040 for RCP4.5. Relative to 1986-2005 average, based on the average of six global climate models. Results are based on dynamical downscaled projections using NIWA's Regional Climate Model. Resolution of projection is 5km x 5km.

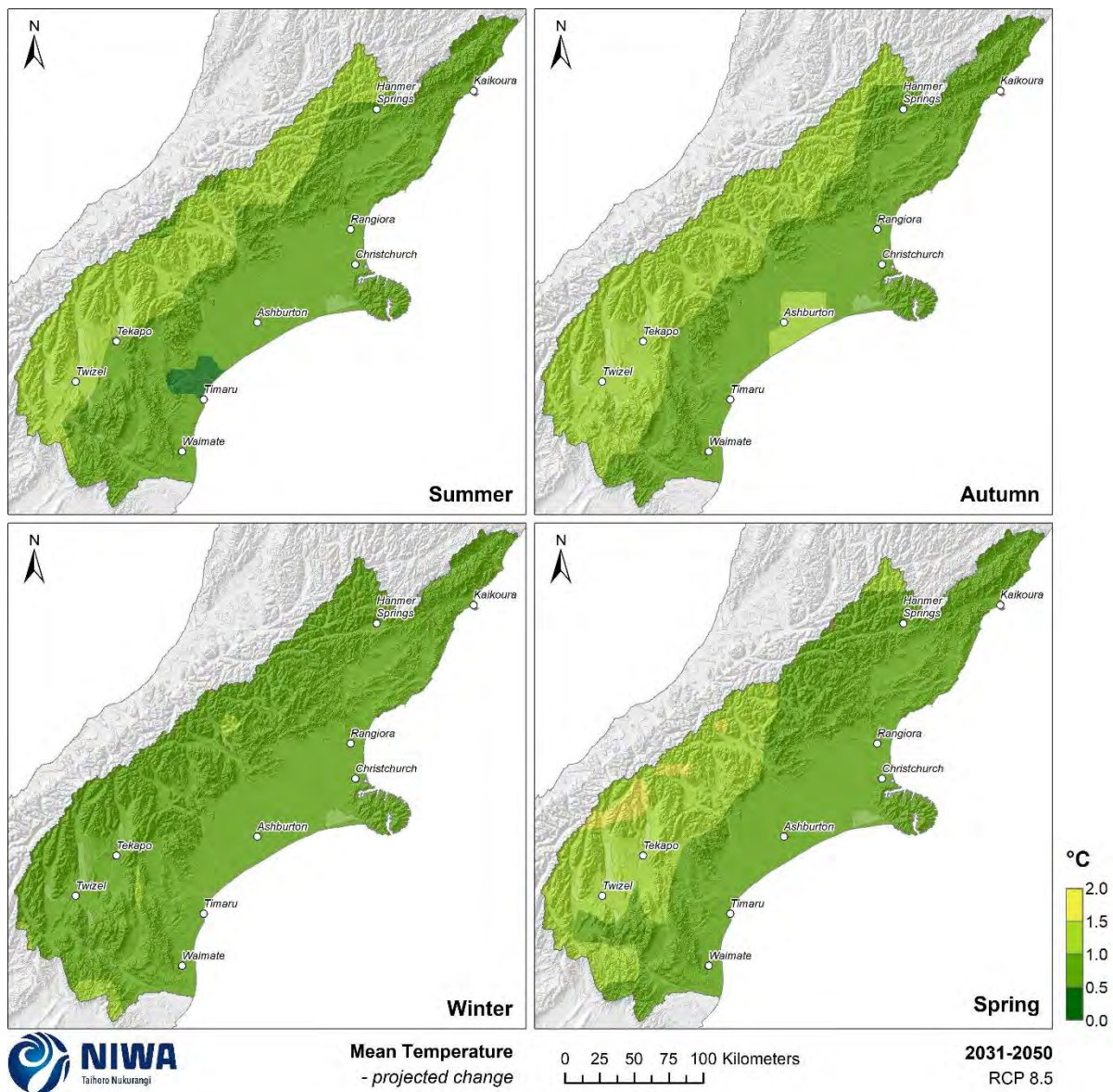


Figure 4-5: Projected seasonal mean temperature changes by 2040 for RCP8.5. Relative to 1986-2005 average, based on the average of six global climate models. Results are based on dynamical downscaled projections using NIWA's Regional Climate Model. Resolution of projection is 5km x 5km.

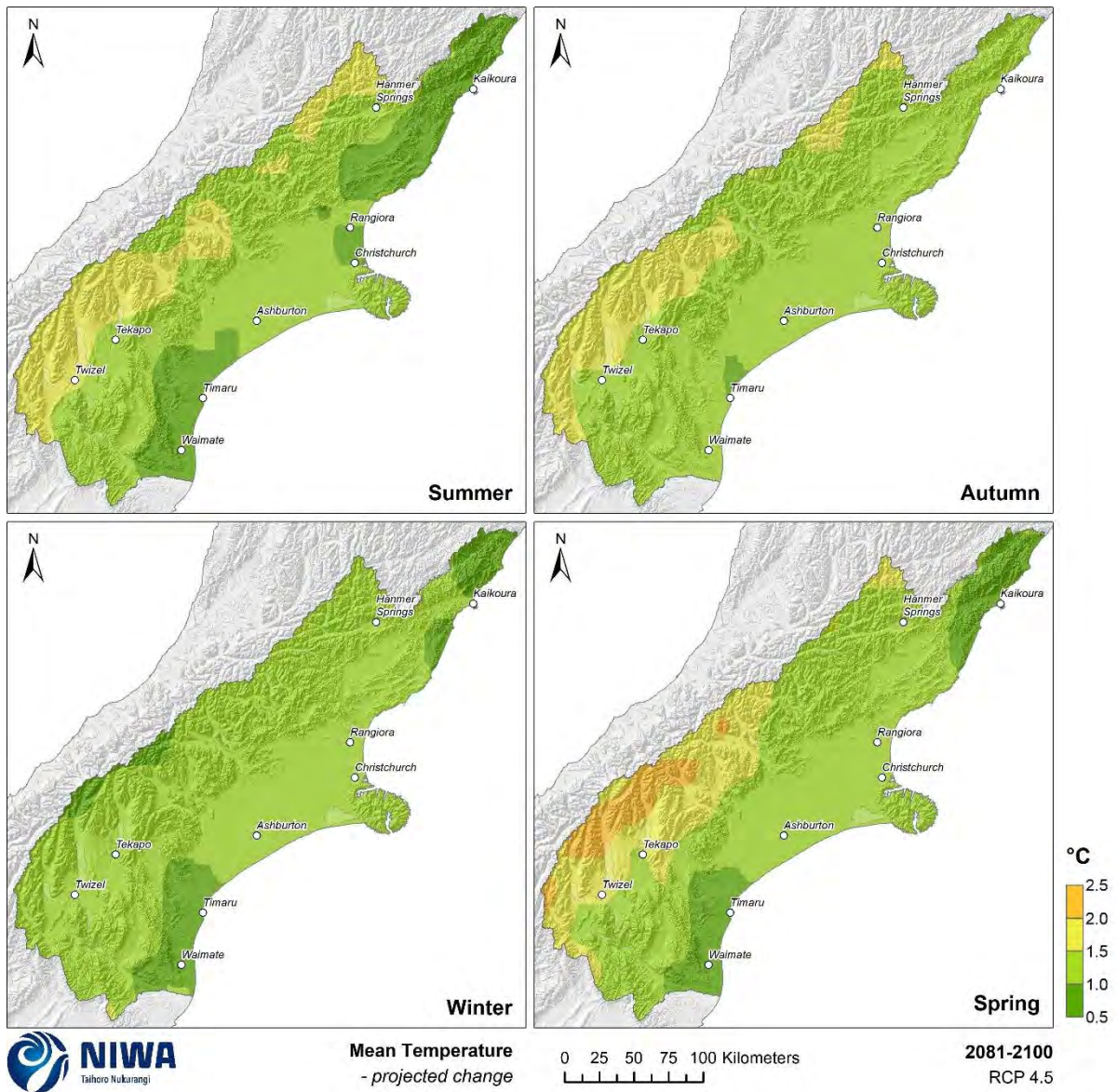


Figure 4-6: Projected seasonal mean temperature changes by 2090 for RCP4.5. Relative to 1986-2005 average, based on the average of six global climate models. Results are based on dynamical downscaled projections using NIWA's Regional Climate Model. Resolution of projection is 5km x 5km.

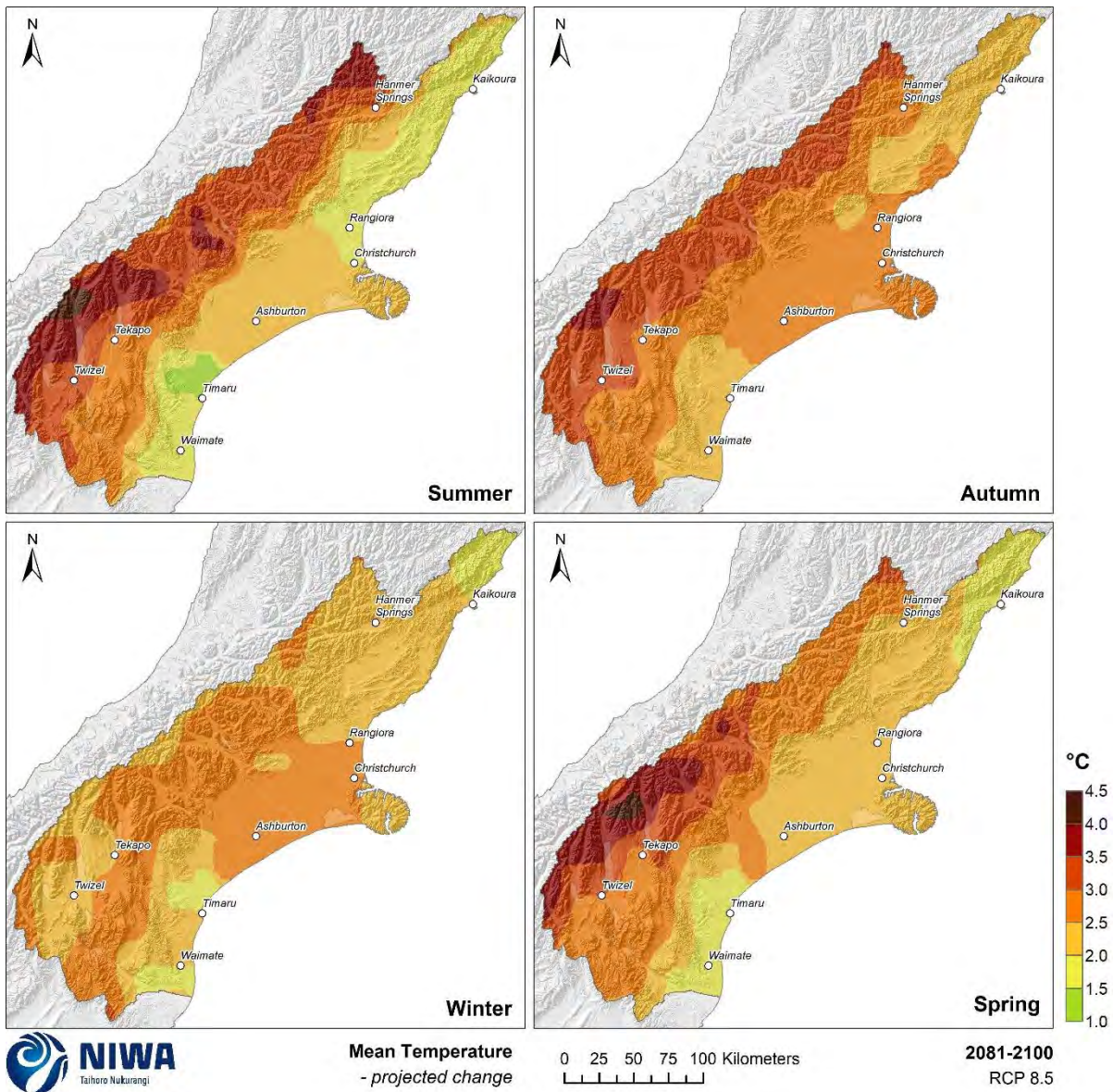


Figure 4-7: Projected seasonal mean temperature changes by 2090 for RCP8.5. Relative to 1986-2005 average, based on the average of six global climate models. Results are based on dynamical downscaled projections using NIWA's Regional Climate Model. Resolution of projection is 5km x 5km.

4.1.1 Model confidence

Key message

- The complete range of model projections (as shown in this section) demonstrate the difference with season and RCP, allowing interpretation of the range of model uncertainty.
- For mean temperature, all models at 2040 project warming, so this direction of change has high certainty.
- By 2090, the model spread is quite large within the scenarios, so the actual value of temperature change is less certain. However, all models for RCP4.5, 6.0 and 8.5 project warming, with higher greenhouse gas concentrations generally projecting more warming.

The climate change projections in other sections of this report show the average of six dynamically downscaled climate models. This is useful as the average is the ‘best estimate’ of future conditions, but these results taken alone do not allow for communication of uncertainty or range in potential future outcomes within the different scenarios and time periods. This section presents the full range of model results for mean temperature, to help the reader understand that there is no ‘single answer’ in terms of future projections.

Projected changes in seasonal and annual mean temperature are shown for the Canterbury region overall in Table 4-1 (i.e. the average of all grid points within Canterbury). Note that data in this table was derived from additional IPCC Fifth Assessment Report models than are presented in the maps in this report (the maps are the average of six dynamically downscaled models, whereas the data here are from ~40 statistically downscaled models), in order to enable an assessment of the range of temperature change projected for Canterbury by 2040 and 2090 under RCP4.5 and RCP8.5. The difference between dynamical and statistical downscaling is explained in Appendix A.

Figure 4-8 and Figure 4-9 illustrate the seasonal and annual temperature projections for each RCP, for the two time periods of 2040 and 2090, respectively. The temperature changes are averaged over all grid-points within the Canterbury region. The coloured vertical bars, and inset stars, show all the individual models, so the complete range is displayed (unlike Table 4-1 where the 5th to 95th percentile range has been calculated). These figures are an excellent way of not only demonstrating the difference between the models for each season and RCP, but also the range of model sensitivity (i.e. how the different models predict future conditions under the same scenarios/greenhouse gas concentrations). The closer together the model outcomes are, it can be inferred that these projections have more certainty. The black stars within each vertical bar represent the results of the six RCM simulations selected for presentation in this report.

For 2040 projections (Figure 4-8 and Table 4-1), the average of all the models is similar between the different scenarios, indicated in the table and by the horizontal black line on each bar in the figure (averages between 0.6 and 1.2°C). The average projection for RCP8.5 is higher than the other RCPs. However, the range of model results for each scenario is quite different as seen by the size of the coloured bars and the numbers inside the parentheses in the table – some models project close to 0°C change under RCP2.6 and others approximately 2°C increase under RCP8.5. Although the models project a range of different outcomes, all the projections are for increases in temperature (i.e. >0°C) so there is high confidence that ongoing warming will be observed to the mid-century period.

For 2090 projections (Figure 4-9 and Table 4-1), there is a much larger range of model results within and between scenarios, indicated by the length of the coloured bars in the figure and the numbers in parentheses in the table. The average mean temperature of all the models (seasonal and annual), indicated by the horizontal black line, is also quite different between the scenarios (around 0.6°C for RCP2.6 for all seasons and annual, and around 2.6-3.3°C for RCP8.5 for all seasons and annual). This is a response of the models to the different greenhouse gas concentrations under each scenario by 2090 compared with similar concentrations between scenarios at 2040. The differences between the model results in the same scenario by 2090 indicates that there is less certainty about the actual value of projected temperatures by this time period. However, for RCP4.5, 6.0 and 8.5, all models project warming, so there is a high degree of certainty that warming will continue under those scenarios, and that higher greenhouse gas concentrations will result in more warming. For RCP2.6, one or two models project cooling by 2090, indicating that 2090 temperatures under this scenario are less certain whether it will be warmer or cooler than the historic period, or about the same.

Table 4-1: Projected changes in seasonal and annual mean temperature (°C) between 1986-2005 and two climate change scenarios (RCP4.5 and RCP8.5) at two future time periods for Canterbury. Time periods: mid-century (2031-2050; “2040”) and end-century (2081-2100; “2090”). The values in each column represent the ensemble average, taken over 41 models (RCP8.5) and 37 models (RCP4.5). Bracketed values represent the range (5th percentile to 95th percentile) over all models within that ensemble. Changes averaged over the Canterbury region. [Source: MFE 2018].

		Summer	Autumn	Winter	Spring	Annual
2040	RCP8.5	1.0 (0.4, 1.6)	1.0 (0.6, 1.5)	1.2 (0.7, 1.6)	0.9 (0.3, 1.3)	1.0 (0.6, 1.6)
	RCP4.5	0.8 (0.3, 1.5)	0.8 (0.4, 1.3)	1.0 (0.6, 1.4)	0.7 (0.3, 1.1)	0.8 (0.5, 1.2)
2090	RCP8.5	3.0 (2.0, 4.9)	3.0 (2.2, 4.5)	3.3 (2.5, 4.4)	2.6 (1.9, 3.6)	3.0 (2.2, 4.3)
	RCP4.5	1.3 (0.6, 2.6)	1.4 (0.8, 2.2)	1.6 (0.9, 2.2)	1.2 (0.6, 1.8)	1.4 (0.8, 2.2)

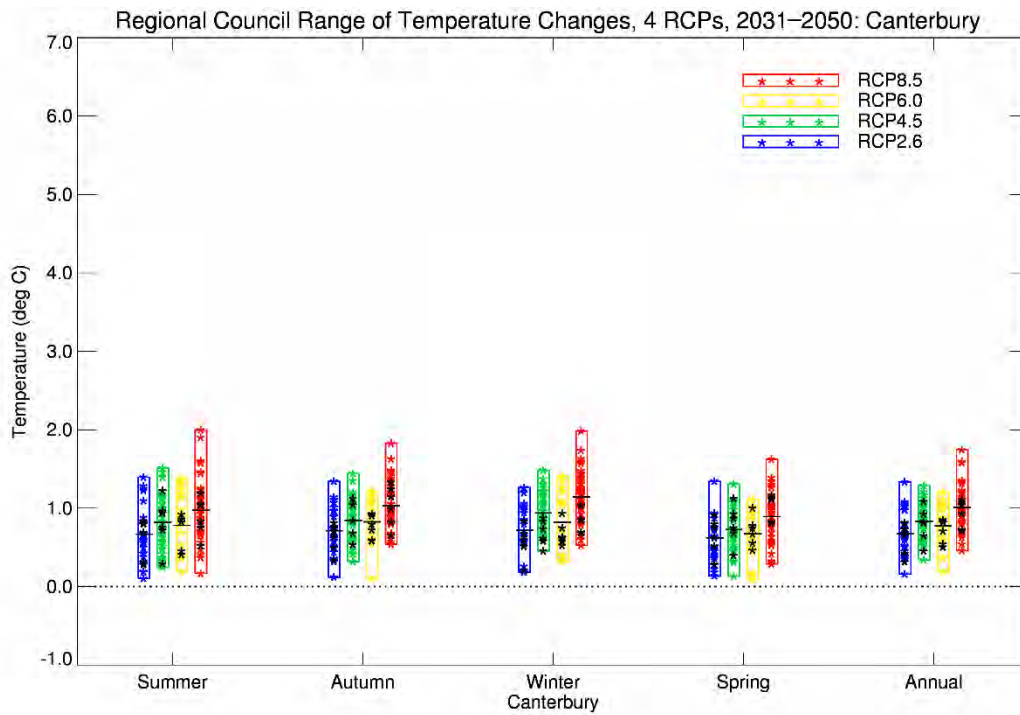


Figure 4-8: Projected seasonal and annual mean temperature change for Canterbury by 2040 (2031-2050). Coloured stars represent all models as derived by statistical downscaling. Black stars correspond to the six-model RCM-downscaling, and the horizontal bars are the average over all downscaled results (statistical and RCM).

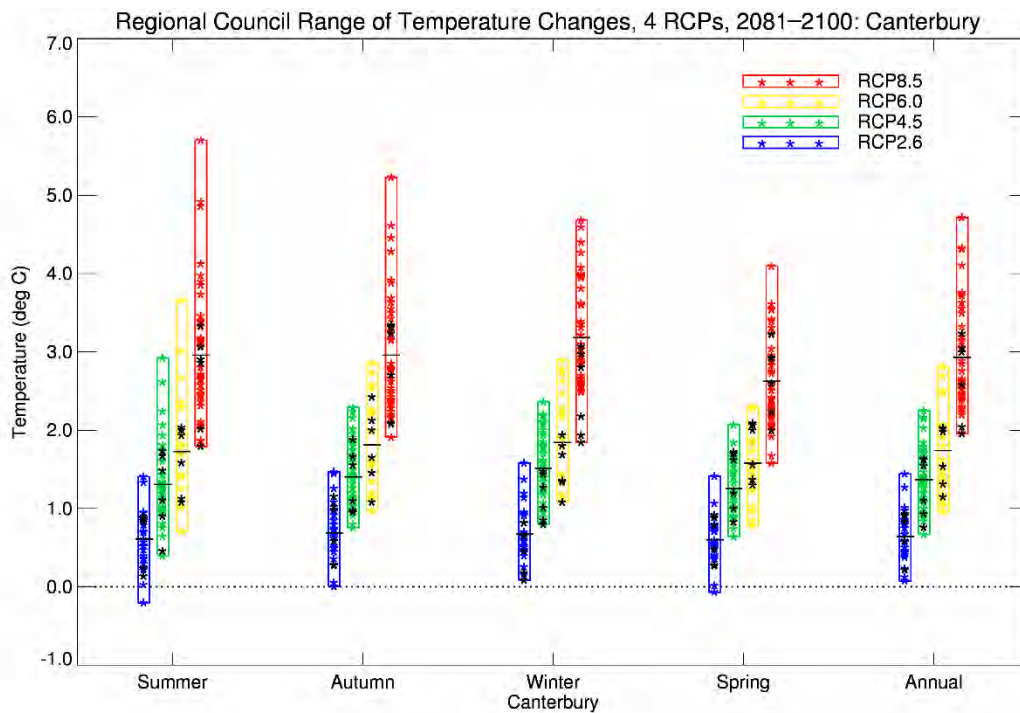


Figure 4-9: Projected seasonal and annual mean temperature change for Canterbury by 2090 (2081-2100). Coloured stars represent all models as derived by statistical downscaling. Black stars correspond to the six-model RCM-downscaling, and the horizontal bars are the average over all downscaled results (statistical and RCM).

4.2 Maximum temperature

Key messages

- Annual mean maximum temperature is projected to increase by 0.5-2.0°C by 2040 under RCP4.5 and RCP8.5.
- By 2090, annual mean maximum temperature increases of 1.0-3.0°C (RCP4.5) and 2.0-5.0°C (RCP8.5) are projected.
- Parts of western Canterbury are projected to observe a 5.0-6.0°C increase in spring and summer mean maximum temperatures by 2090 under RCP8.5.

Maximum temperatures are generally recorded in the afternoon, and therefore are known as daytime temperatures. Historic (average over 1986-2005) and future (average over 2031-2050 and 2081-2100) maps for mean maximum temperature are shown in this section. The historic maps show annual and seasonal mean maximum temperature in units of degrees Celsius (°C) and the future projection maps show the change in mean temperature compared with the historic period, in units of °C. Note that the historic maps are on a different colour scale to the future projection maps.

Annual mean maximum temperatures range between 16-18°C for most low elevation locations of Canterbury (Figure 4-10). Summer mean maximum temperatures range between 20-24°C for most of the region, and winter mean maximum temperatures range between 8-12°C (Figure 4-12). Autumn and spring mean maximum temperatures share similar spatial patterns, and range between 16-18°C for most low elevation areas.

Annual mean maximum temperature is projected to increase by 0.5-2.0°C by 2040 under RCP4.5 and RCP8.5 (Figure 4-11). By 2090, annual mean maximum temperature increases of 1.0-3.0°C (RCP4.5) and 2.0-5.0°C (RCP8.5) are projected. Seasonal projections of mean maximum temperature change are shown for RCP4.5 by 2040 (Figure 4-13) and 2090 (Figure 4-15), and RCP8.5 by 2040 (Figure 4-14) and 2090 (Figure 4-16). By 2040 under RCP4.5, seasonal mean maximum temperatures are projected to increase by 0.5-2.0°C across much of Canterbury. By 2090 under RCP8.5, seasonal mean maximum temperatures are projected to increase by 2.0-5.0°C for much of Canterbury. Notably, some western alpine parts of the region are projected to observe a 5.0-6.0°C increase in spring and summer mean maximum temperatures by 2090 under RCP8.5.

Annual Mean Maximum Temperature

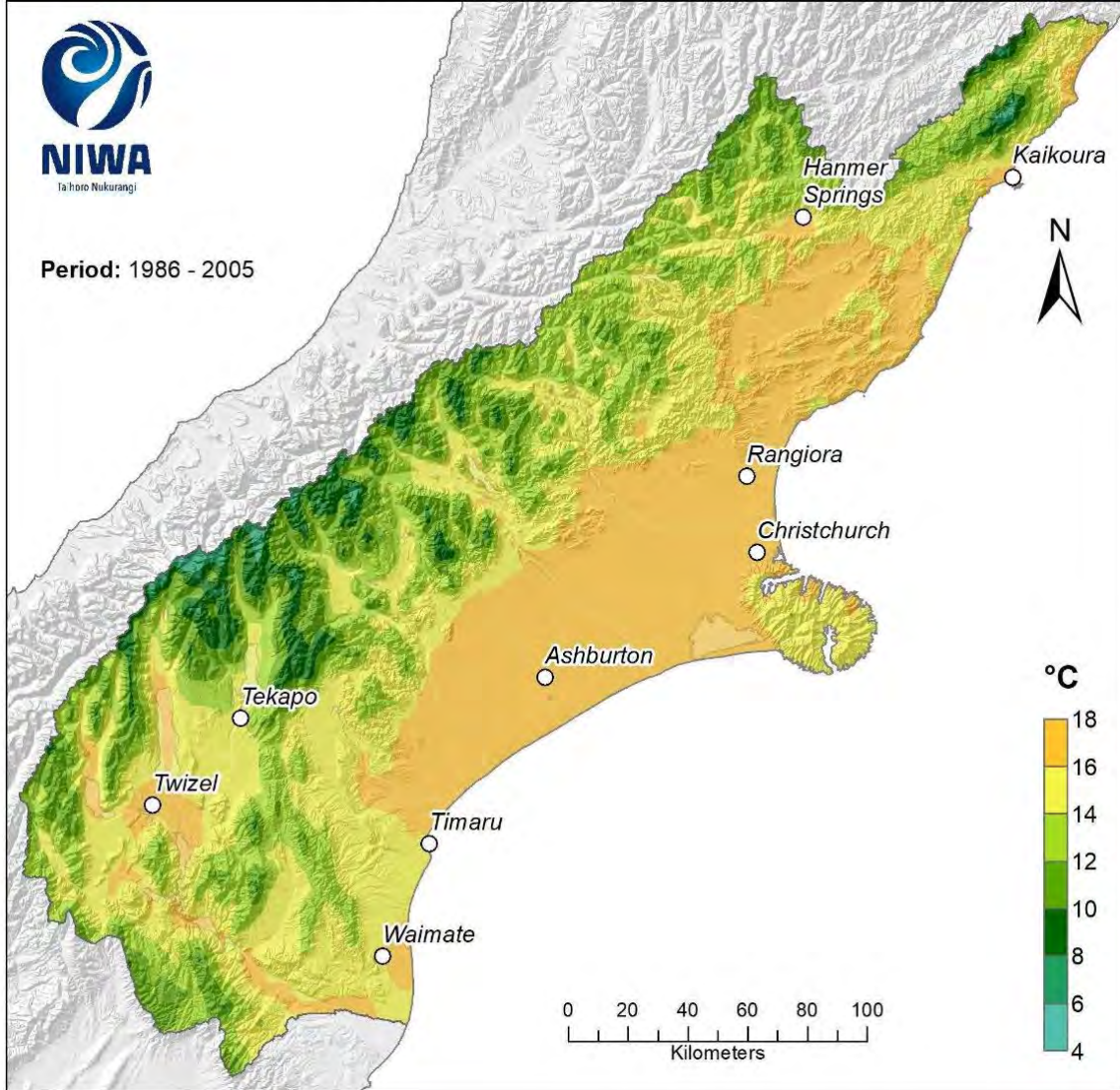


Figure 4-10: Modelled annual mean maximum temperature, average over 1986-2005. Results are based on dynamical downscaled projections using NIWA's Regional Climate Model. Resolution of projection is 5km x 5km.

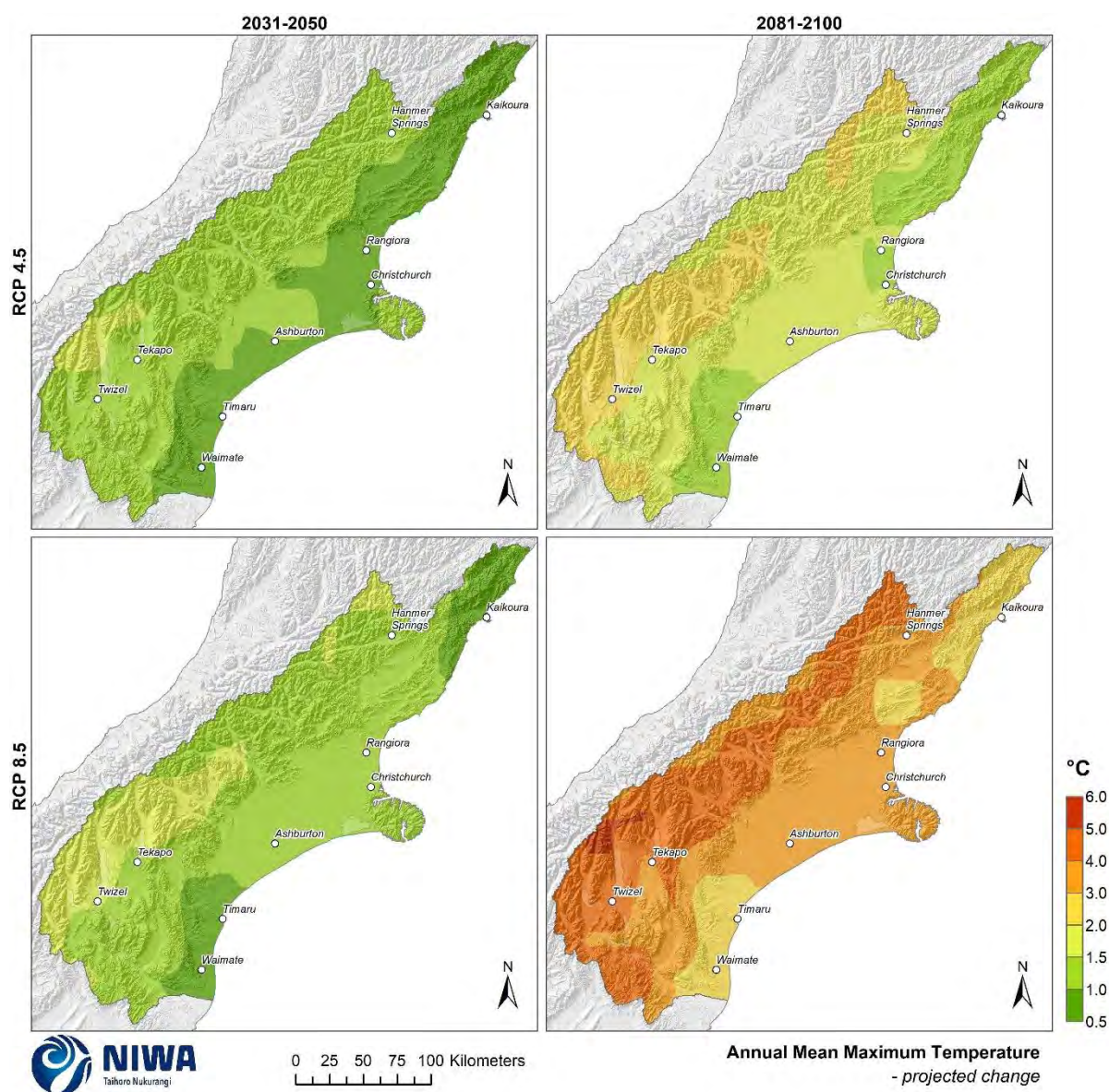


Figure 4-11: Projected annual mean maximum temperature changes by 2040 and 2090, under RCP4.5 and RCP8.5. Climate change scenarios: RCP4.5 (top panels) and RCP8.5 (bottom panels). Time periods: mid-century (2031-2050; “2040” – panels on left) and end-century (2081-2100; “2090” – panels on right). Changes relative to 1986-2005 average, based on the average of six global climate models. Results are based on dynamical downscaled projections using NIWA’s Regional Climate Model. Resolution of projection is 5km x 5km.

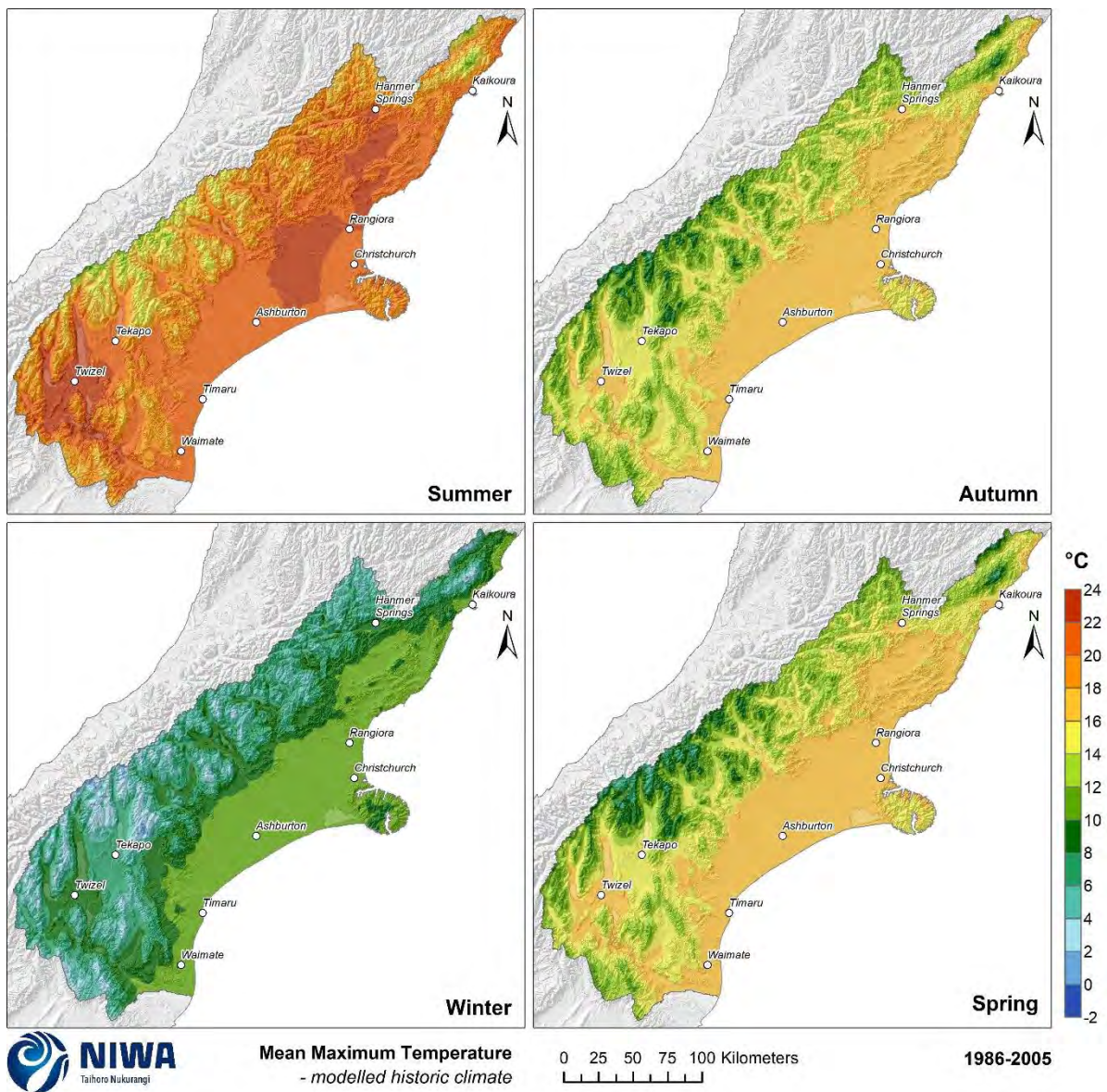


Figure 4-12: Modelled seasonal mean maximum temperature, average over 1986-2005. Results are based on dynamical downscaled projections using NIWA's Regional Climate Model. Resolution of projection is 5km x 5km.

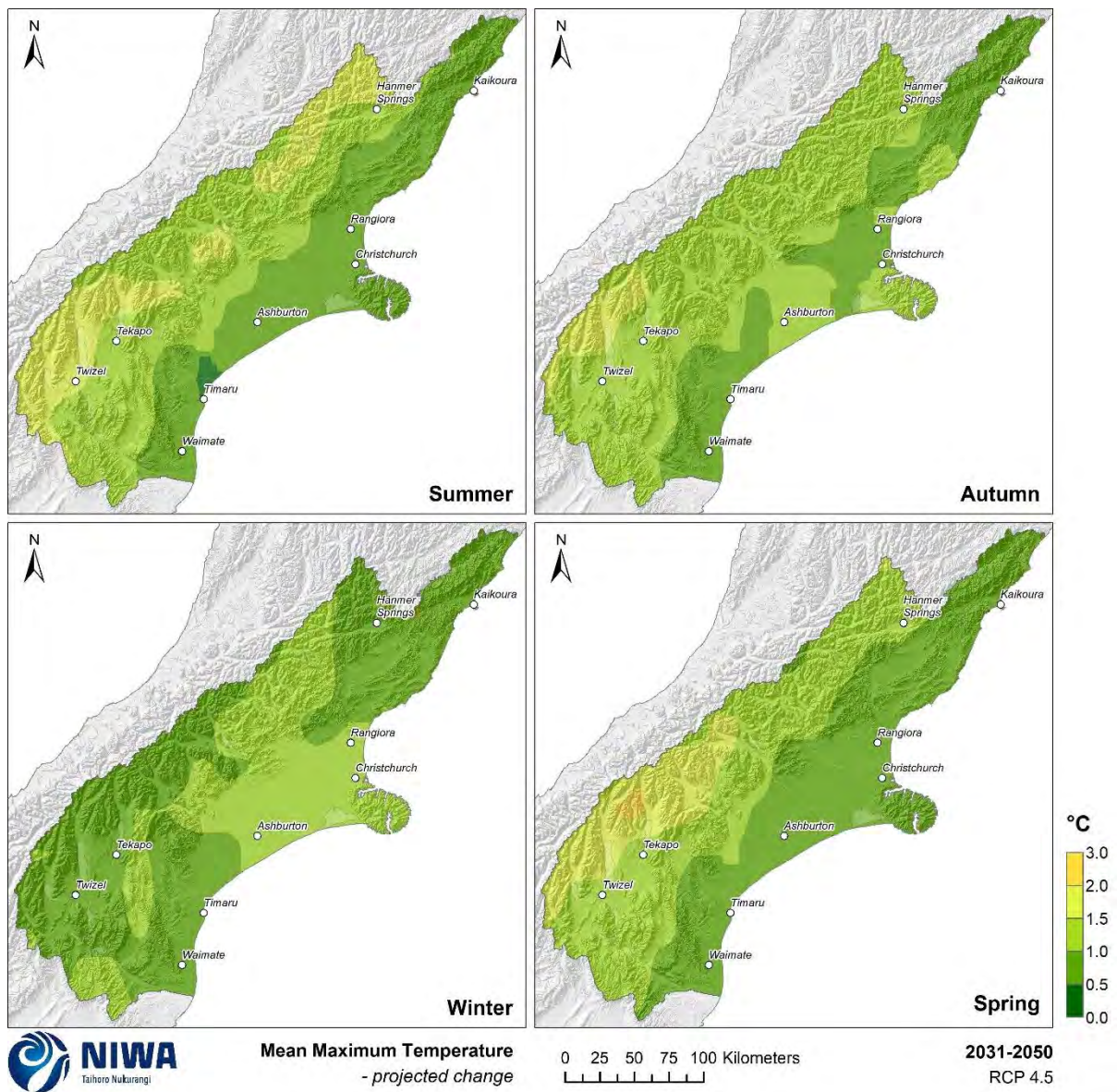


Figure 4-13: Projected seasonal mean maximum temperature changes by 2040 for RCP4.5. Relative to 1986-2005 average, based on the average of six global climate models. Results are based on dynamical downscaled projections using NIWA's Regional Climate Model. Resolution of projection is 5km x 5km.

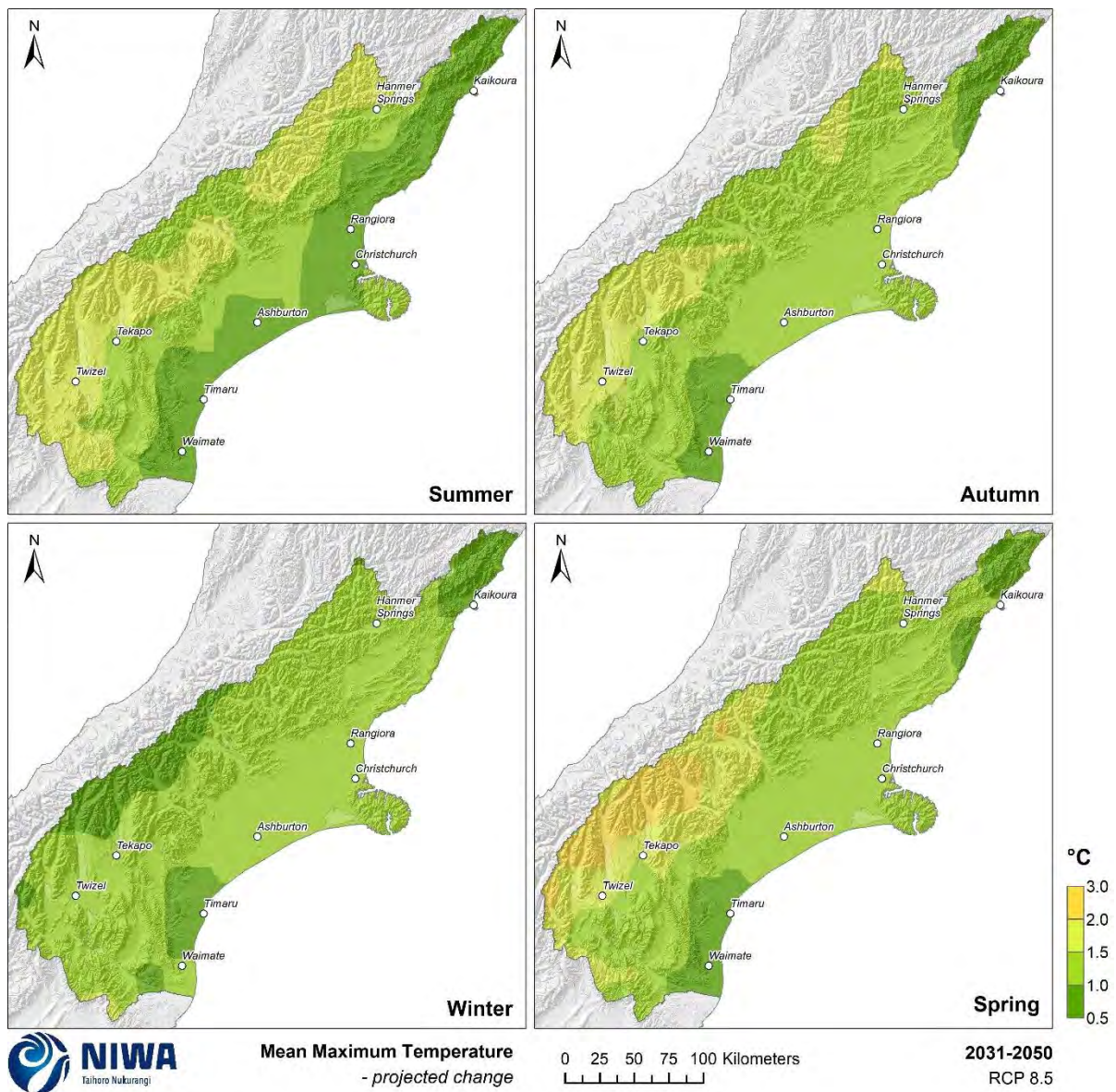


Figure 4-14: Projected seasonal mean maximum temperature changes by 2040 for RCP8.5. Relative to 1986-2005 average, based on the average of six global climate models. Results are based on dynamical downscaled projections using NIWA's Regional Climate Model. Resolution of projection is 5km x 5km.

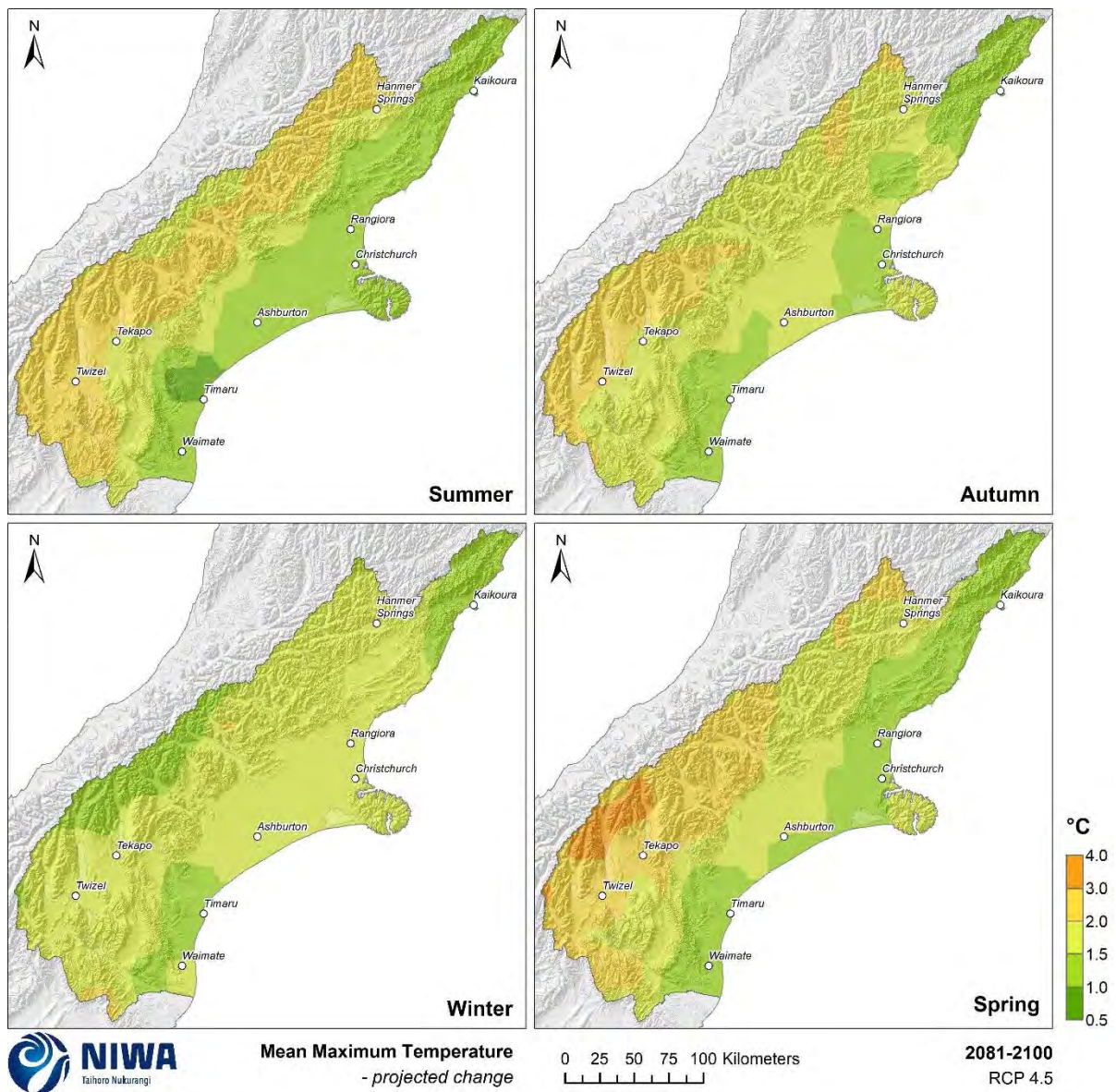


Figure 4-15: Projected seasonal mean maximum temperature changes by 2090 for RCP4.5. Relative to 1986-2005 average, based on the average of six global climate models. Results are based on dynamical downscaled projections using NIWA's Regional Climate Model. Resolution of projection is 5km x 5km.

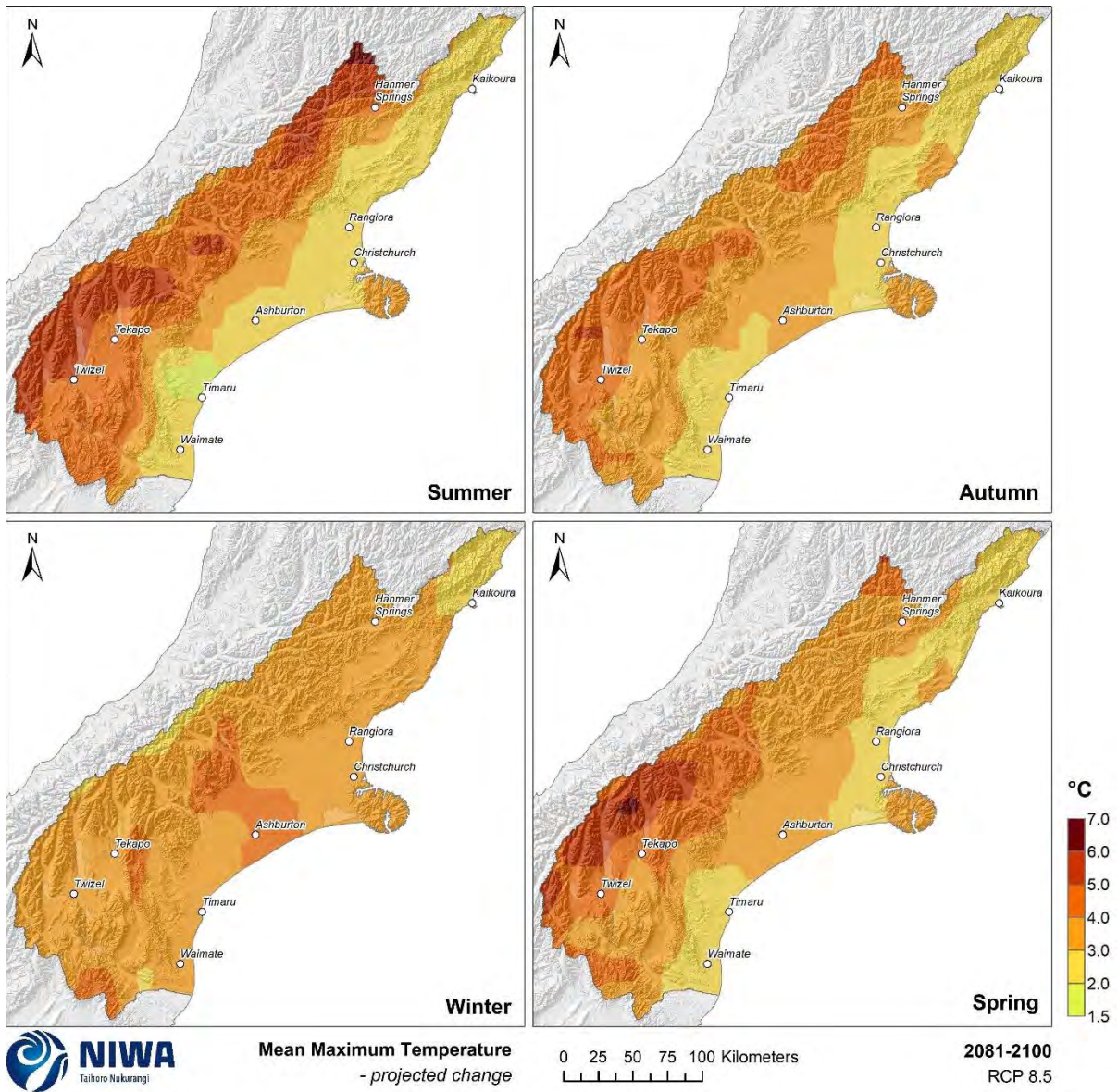


Figure 4-16: Projected seasonal mean maximum temperature changes by 2090 for RCP8.5. Relative to 1986-2005 average, based on the average of six global climate models. Results are based on dynamical downscaled projections using NIWA's Regional Climate Model. Resolution of projection is 5km x 5km.

4.3 Minimum temperature

Key messages

- Annual mean minimum temperature is projected to increase by between 0-1.0°C by 2040 under RCP4.5 and RCP8.5.
- By 2090, annual mean minimum temperature increases of 0.5-1.5°C (RCP4.5) and 1.0-2.5°C (RCP8.5) are projected.
- Seasonal mean minimum temperatures are projected to increase by 0.5-2.5°C for much of Canterbury (by 2090 under RCP8.5).
- Projected increases in mean minimum temperatures are not as high as increases in mean maximum temperatures, leading to a projected increase in the diurnal temperature range.

Minimum temperatures are generally recorded in the early hours of the morning, and therefore are known as night time temperatures. Historic (average over 1986-2005) and future (average over 2031-2050 and 2081-2100) maps for mean minimum temperature are shown in this section. The historic maps show annual and seasonal mean minimum temperature in units of degrees Celsius (°C) and the future projection maps show the change in mean minimum temperature compared with the historic period, in units of °C. Note that the historic maps are on a different colour scale to the future projection maps.

Annual mean minimum temperatures range between 4-8°C for most low-elevation locations of Canterbury, with lowest annual mean minimum temperatures observed in mountainous terrain (Figure 4-17). For eastern areas of Canterbury, summer mean minimum temperatures range between 10-12°C, and winter mean minimum temperatures range between 0-4°C (Figure 4-19). For inland low-elevation locations, summer mean minimum temperatures range between 6-10°C, and winter mean minimum temperatures range from just below freezing (-2°C) to just above freezing (2°C).

Annual mean minimum temperature is projected to increase by between 0-1.0°C by 2040 under RCP4.5 and RCP8.5 (Figure 4-18). By 2090, annual mean minimum temperature increases of 0.5-1.5°C (RCP4.5) and 1.0-2.5°C (RCP8.5) are projected. Seasonal projections of mean minimum temperature change are shown for RCP4.5 by 2040 (Figure 4-20) and 2090 (Figure 4-22), and RCP8.5 by 2040 (Figure 4-21) and 2090 (Figure 4-23). By 2040 under RCP4.5, seasonal mean minimum temperatures are projected to increase by between 0-1.0°C across Canterbury. By 2090 under RCP8.5, seasonal mean minimum temperatures are projected to increase by 0.5-2.5°C for much of Canterbury. Notably, increases in mean minimum temperatures are not projected to be as high as increases in mean maximum temperatures, leading to a projected increase in the diurnal temperature range (i.e. the difference in temperature between daytime and night time temperature).

Annual Mean Minimum Temperature

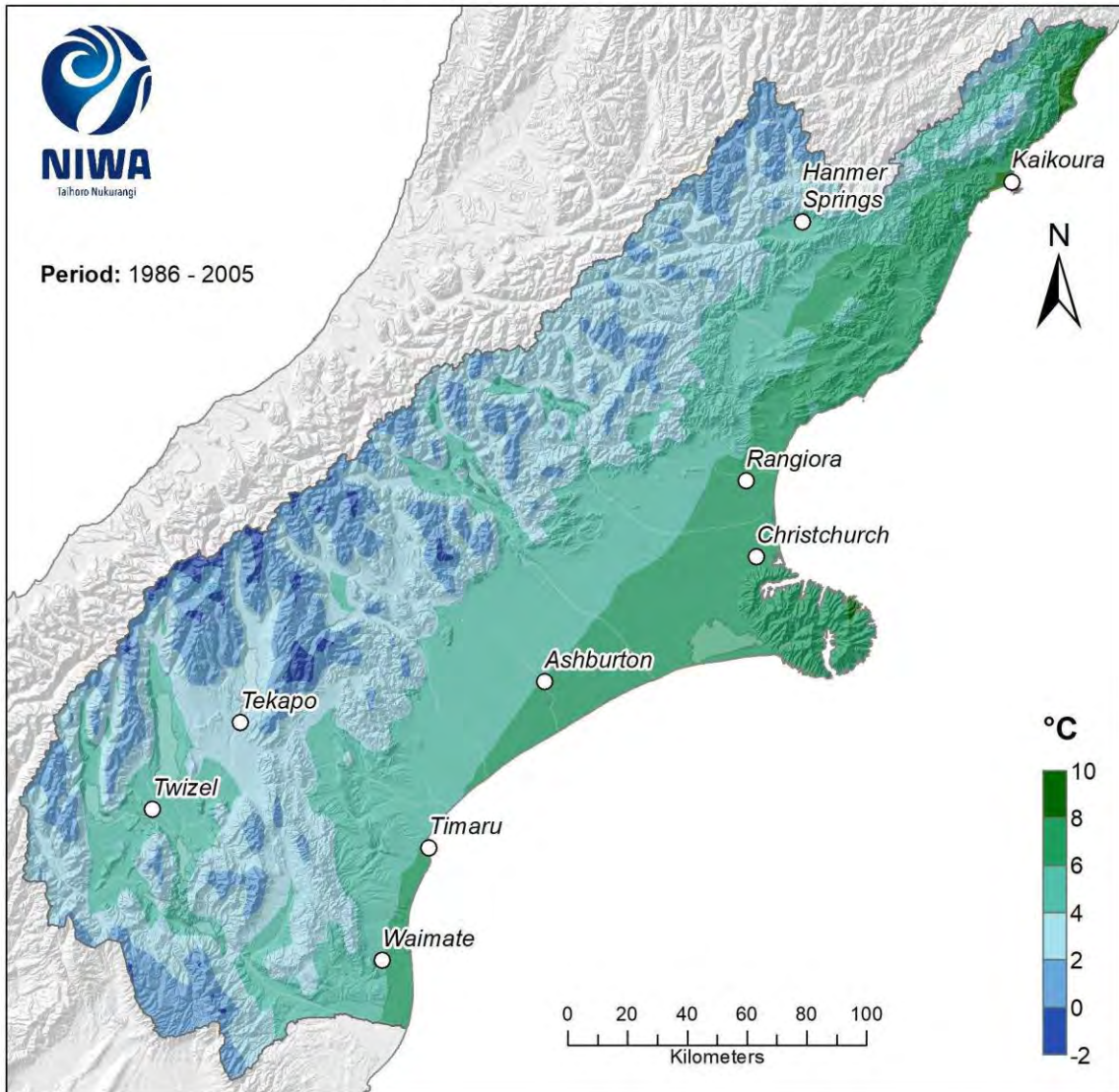


Figure 4-17: Modelled annual mean minimum temperature, average over 1986-2005. Results are based on dynamical downscaled projections using NIWA's Regional Climate Model. Resolution of projection is 5km x 5km.

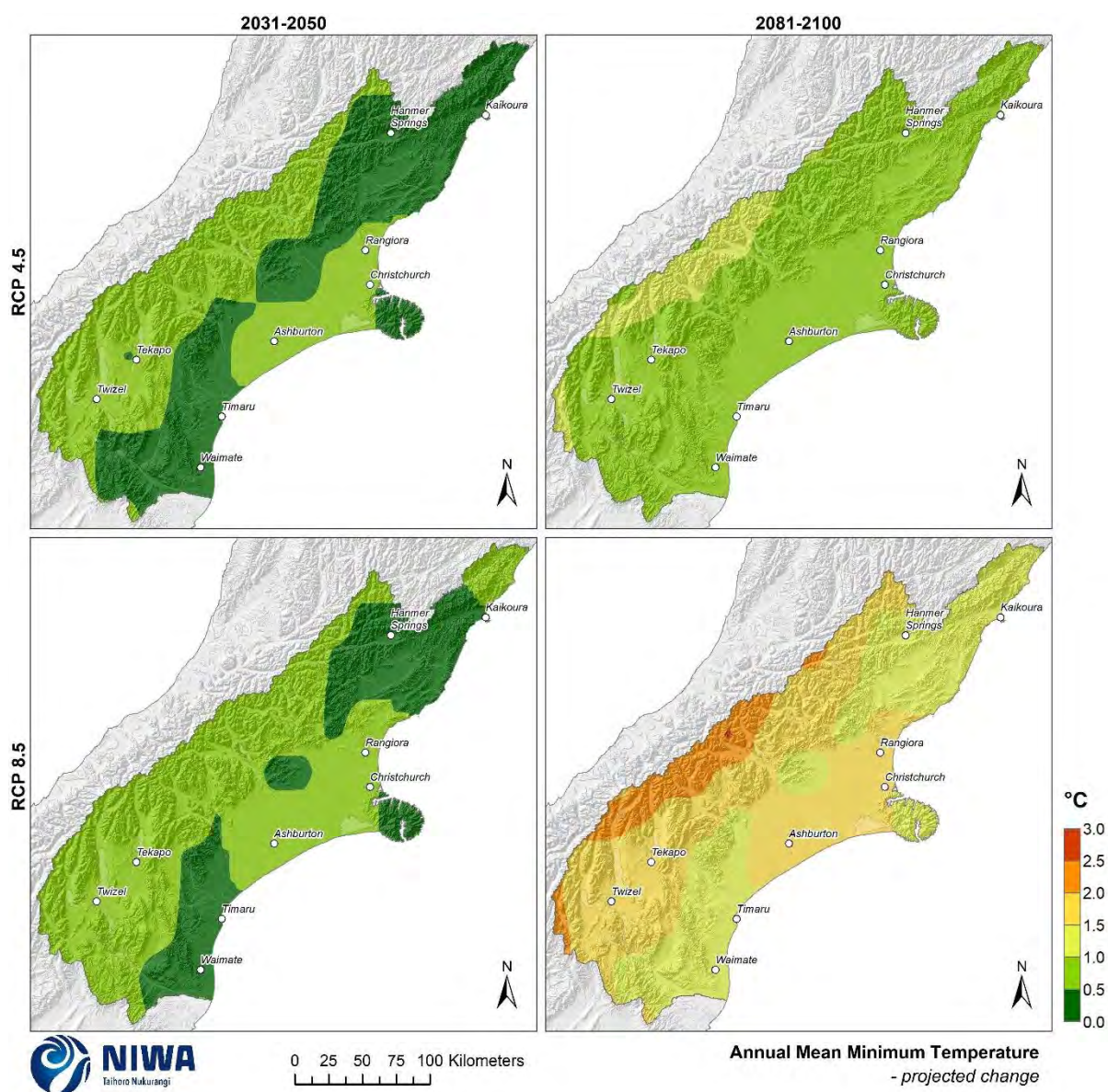


Figure 4-18: Projected annual mean minimum temperature changes by 2040 and 2090, under RCP4.5 and RCP8.5. Climate change scenarios: RCP4.5 (top panels) and RCP8.5 (bottom panels). Time periods: mid-century (2031-2050; “2040” – panels on left) and end-century (2081-2100; “2090” – panels on right). Changes relative to 1986-2005 average, based on the average of six global climate models. Results are based on dynamical downscaled projections using NIWA’s Regional Climate Model. Resolution of projection is 5km x 5km.

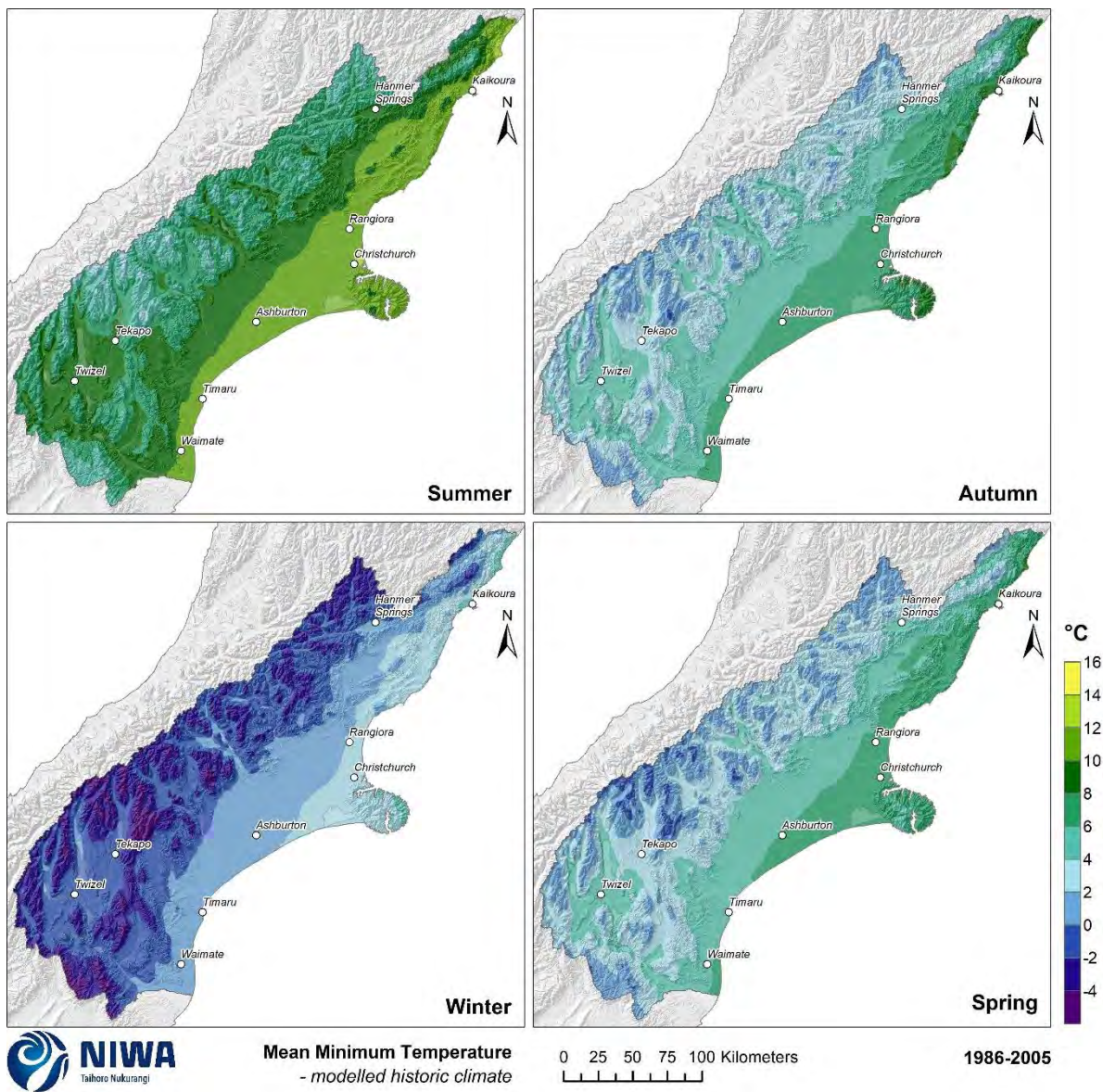


Figure 4-19: Modelled seasonal mean minimum temperature, average over 1986-2005. Results are based on dynamical downscaled projections using NIWA's Regional Climate Model. Resolution of projection is 5km x 5km.

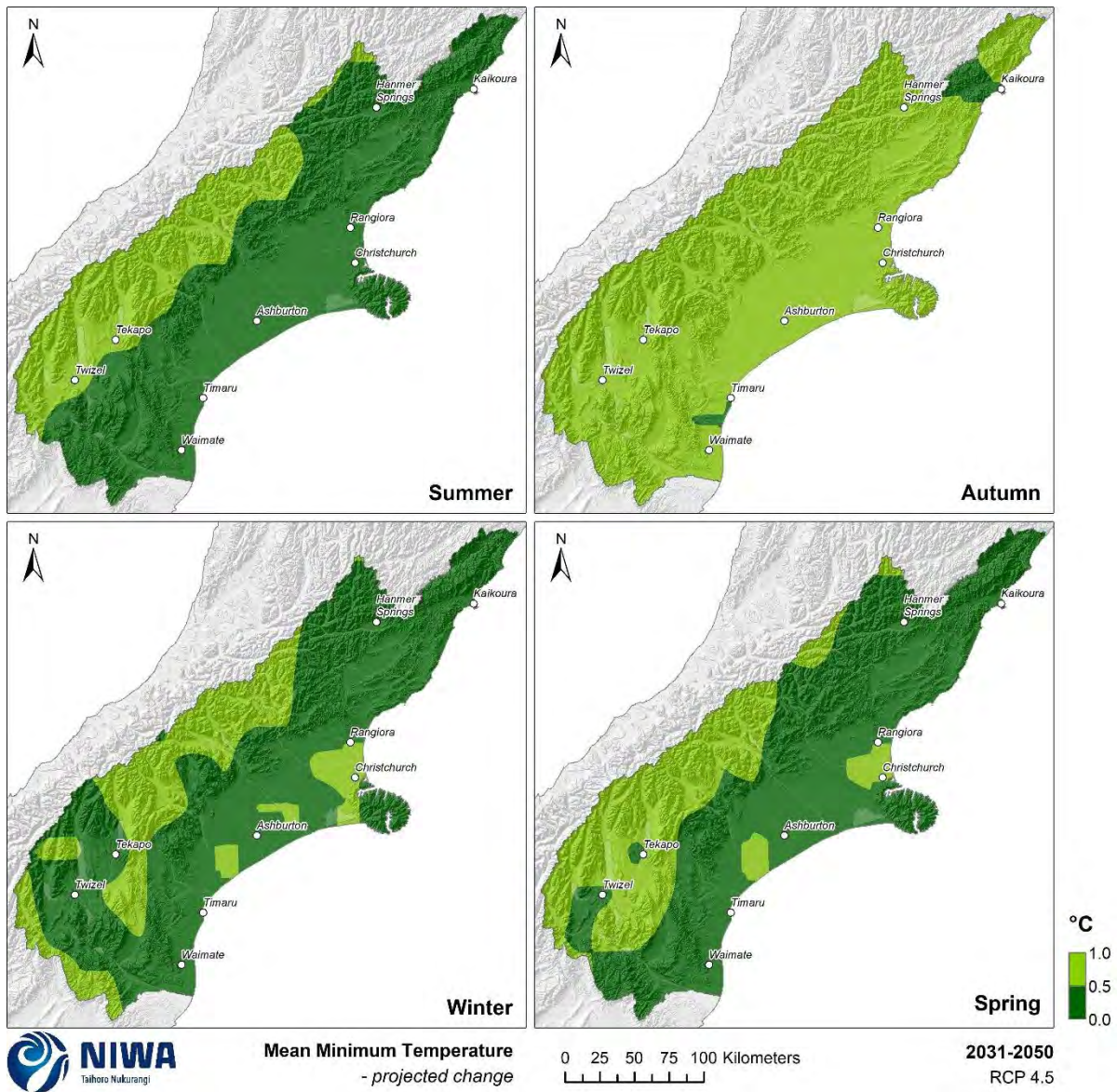


Figure 4-20: Projected seasonal mean minimum temperature changes by 2040 for RCP4.5. Relative to 1986-2005 average, based on the average of six global climate models. Results are based on dynamical downscaled projections using NIWA's Regional Climate Model. Resolution of projection is 5km x 5km.

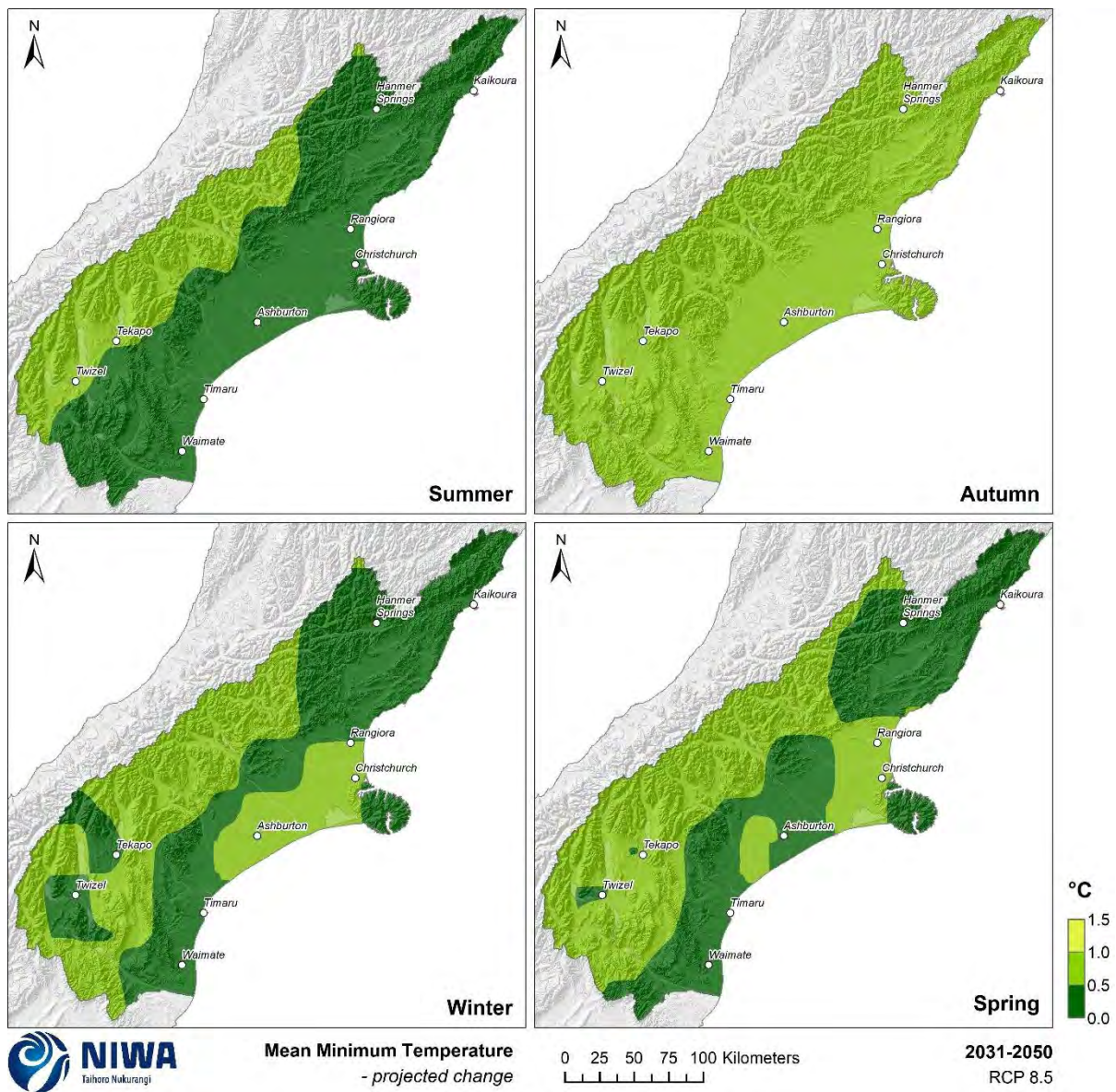


Figure 4-21: Projected seasonal mean minimum temperature changes by 2040 for RCP8.5. Relative to 1986-2005 average, based on the average of six global climate models. Results are based on dynamical downscaled projections using NIWA's Regional Climate Model. Resolution of projection is 5km x 5km.

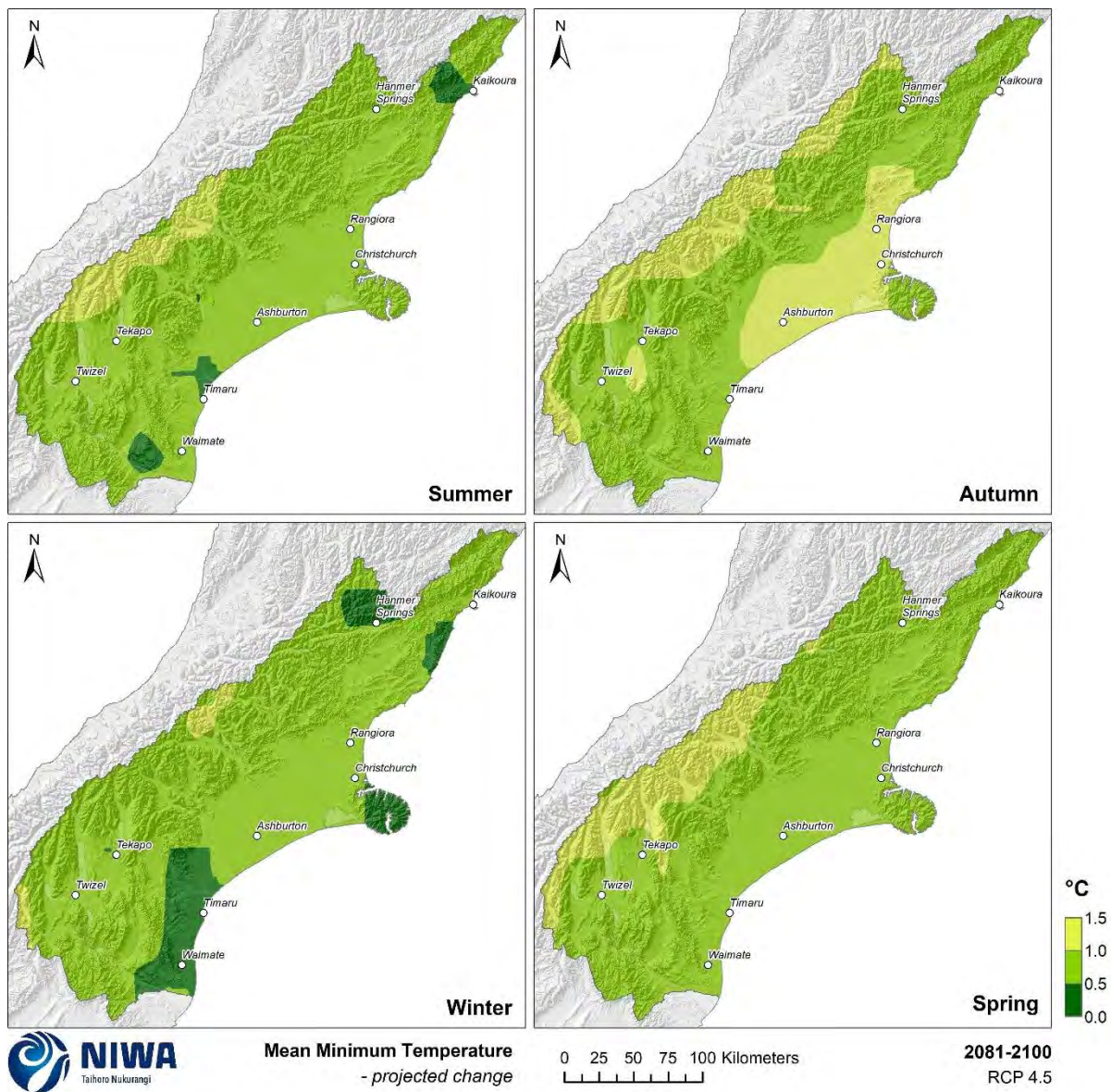


Figure 4-22: Projected seasonal mean minimum temperature changes by 2090 for RCP4.5. Relative to 1986-2005 average, based on the average of six global climate models. Results are based on dynamical downscaled projections using NIWA's Regional Climate Model. Resolution of projection is 5km x 5km.

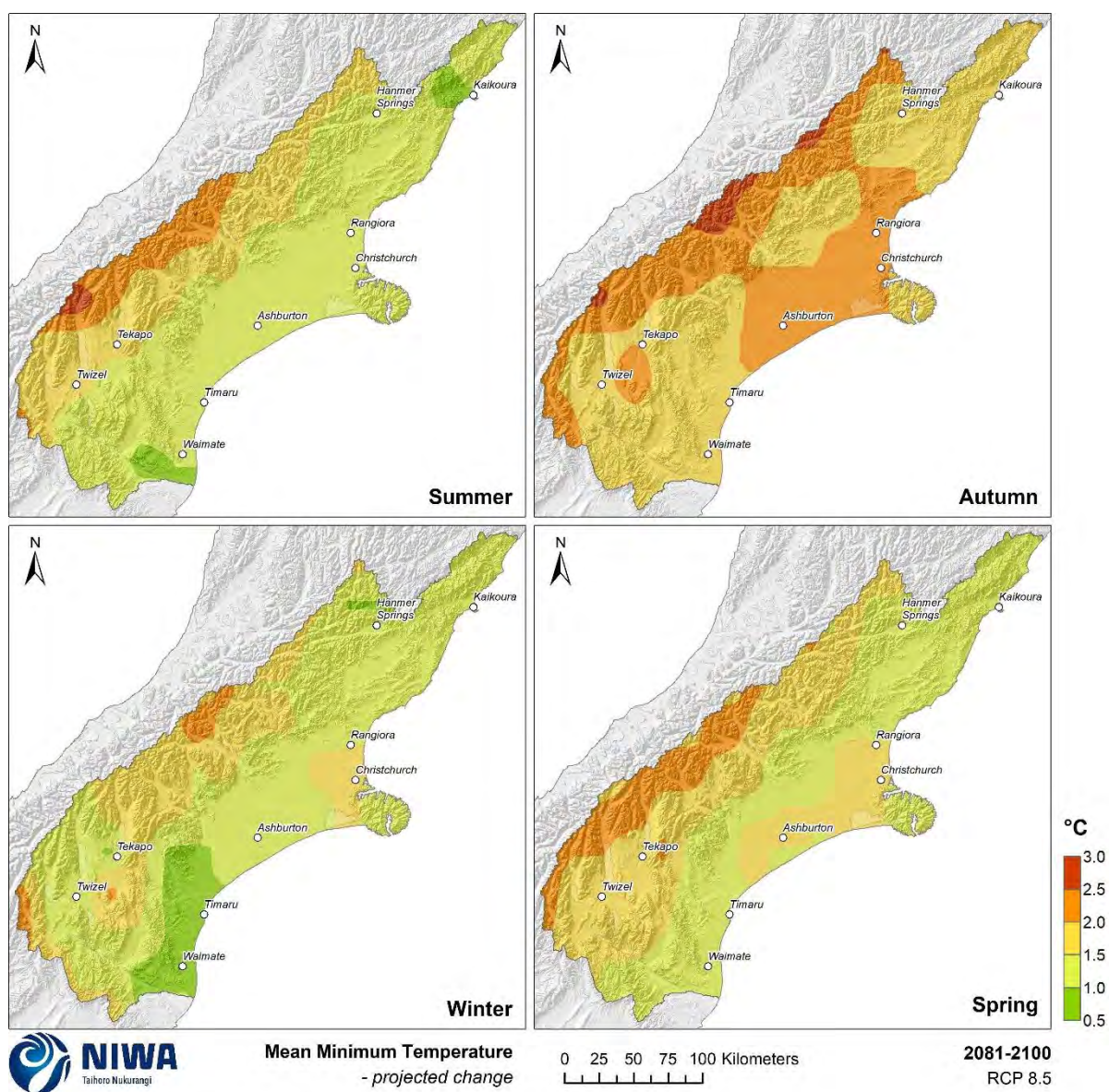


Figure 4-23: Projected seasonal mean minimum temperature changes by 2090 for RCP8.5. Relative to 1986-2005 average, based on the average of six global climate models. Results are based on dynamical downscaled projections using NIWA's Regional Climate Model. Resolution of projection is 5km x 5km.

4.4 Hot days

Key messages

- Much of Canterbury is projected to observe a considerable increase in annual hot days of 20-60 days per year (by 2090 under RCP8.5).
- Some inland areas of Canterbury (particularly the southern Mackenzie Basin) are projected to observe an increase of 60-85 hot days per year (by 2090 under RCP8.5).
- Seasonally, greatest projected increases in hot days occur in summer. Relatively low elevation areas of Canterbury are projected to observe an increase of 5-20 hot days in autumn and spring, respectively (by 2090 under RCP8.5)

In this report, a hot day is considered to occur when the maximum temperature is 25°C or higher. Present-day (average over 1986-2005) and future (average over 2031-2050 and 2081-2100) maps for hot days are shown in this section. The present-day maps show annual and seasonal average numbers of hot days and the future projection maps show the change in the number of hot days compared with present. Note that the present-day maps are on a different colour scale to the future projection maps.

At present, hot days occur most regularly about Twizel. Here, the annual number of hot days averages 40-50 days per year (Figure 4-24). Hot days occur most frequently in summer (Figure 4-26), with most low elevation areas of Canterbury observing between 10-30 hot days during this season.

The annual number of hot days are projected to increase by 10-40 days by 2040 under RCP4.5 and RCP8.5 (Figure 4-25) for many parts of Canterbury. By 2090, annual increases in hot days of 10-20 days (RCP4.5) and 20-60 days (RCP8.5) are projected for much of Canterbury. Annual increases of 60-85 hot days are projected for some inland areas of Canterbury, especially southern parts of the Mackenzie Basin. Seasonal projections of hot day changes are shown for RCP4.5 by 2040 (Figure 4-27) and 2090 (Figure 4-29), and RCP8.5 by 2040 (Figure 4-28) and 2090 (Figure 4-30). By 2040 under RCP4.5, summer hot days are projected to increase by 5-20 days across much of Canterbury. By 2090 under RCP8.5, autumn and spring hot days are projected to increase by 5-20 days for relatively low elevation areas of Canterbury.

Number of Annual Hot Days ($\geq 25^{\circ}\text{C}$)

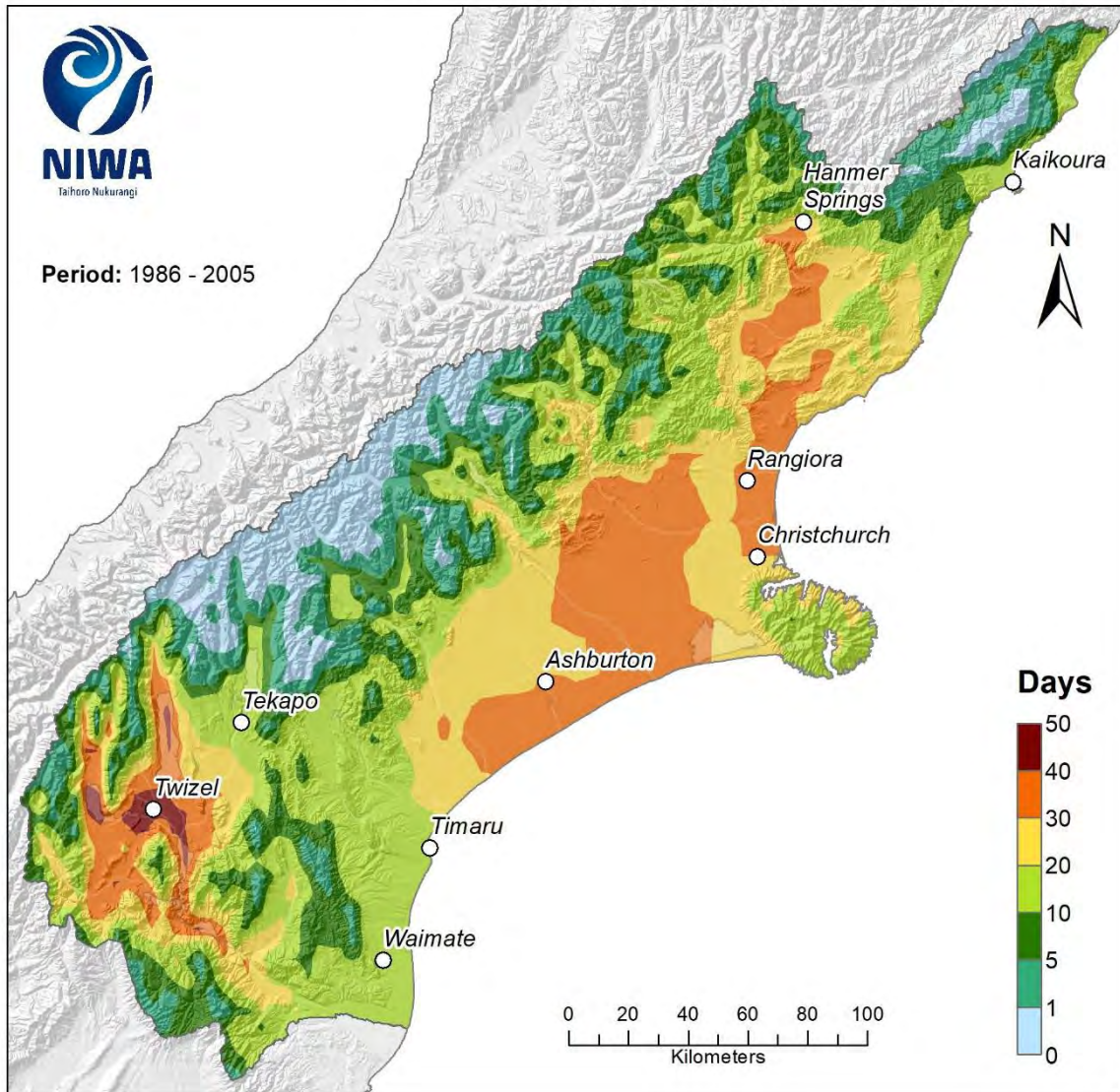


Figure 4-24: Modelled annual number of hot days (days with maximum temperature $\geq 25^{\circ}\text{C}$), average over 1986-2005. Results are based on dynamical downscaled projections using NIWA's Regional Climate Model. Resolution of projection is 5km x 5km.

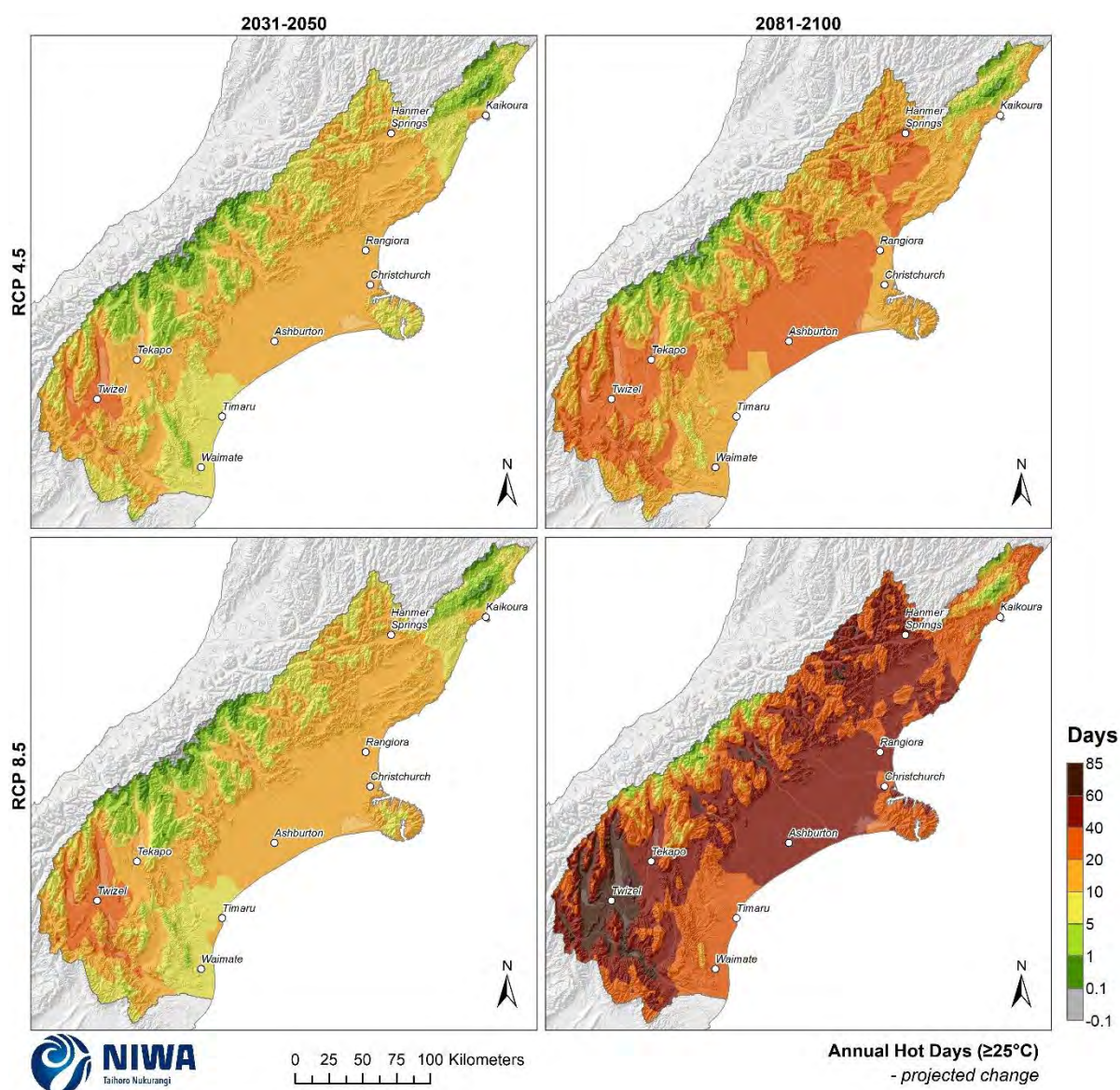


Figure 4-25: Projected annual hot day (days with maximum temperature $\geq 25^{\circ}\text{C}$) changes by 2040 and 2090, under RCP4.5 and RCP8.5. Climate change scenarios: RCP4.5 (top panels) and RCP8.5 (bottom panels). Time periods: mid-century (2031-2050; “2040” – panels on left) and end-century (2081-2100; “2090” – panels on right). Changes relative to 1986-2005 average, based on the average of six global climate models. Results are based on dynamical downscaled projections using NIWA's Regional Climate Model. Resolution of projection is 5km x 5km.

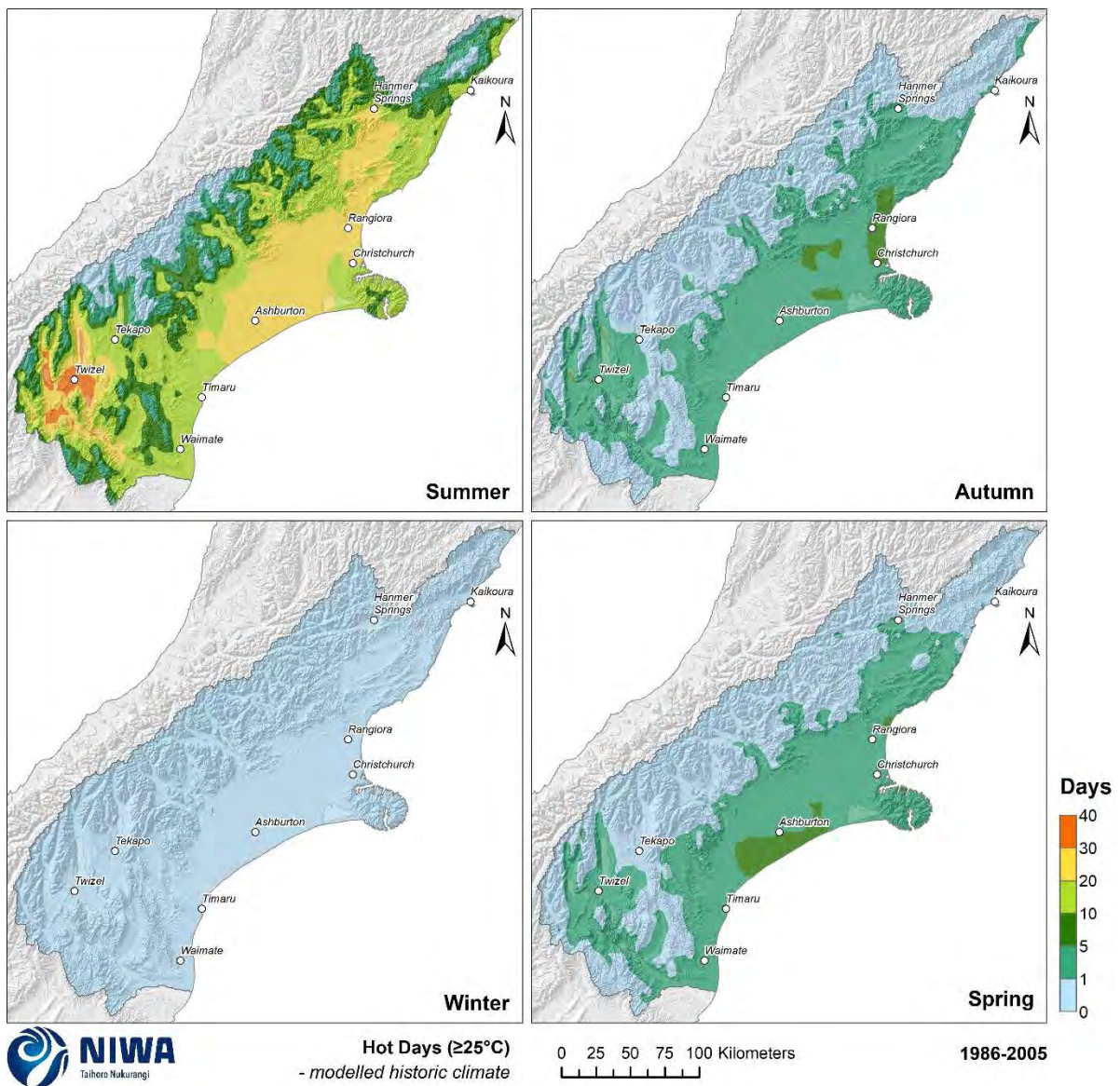


Figure 4-26: Modelled seasonal number of hot days (days with maximum temperature $\geq 25^{\circ}\text{C}$), average over 1986-2005. Results are based on dynamical downscaled projections using NIWA's Regional Climate Model. Resolution of projection is 5km x 5km.

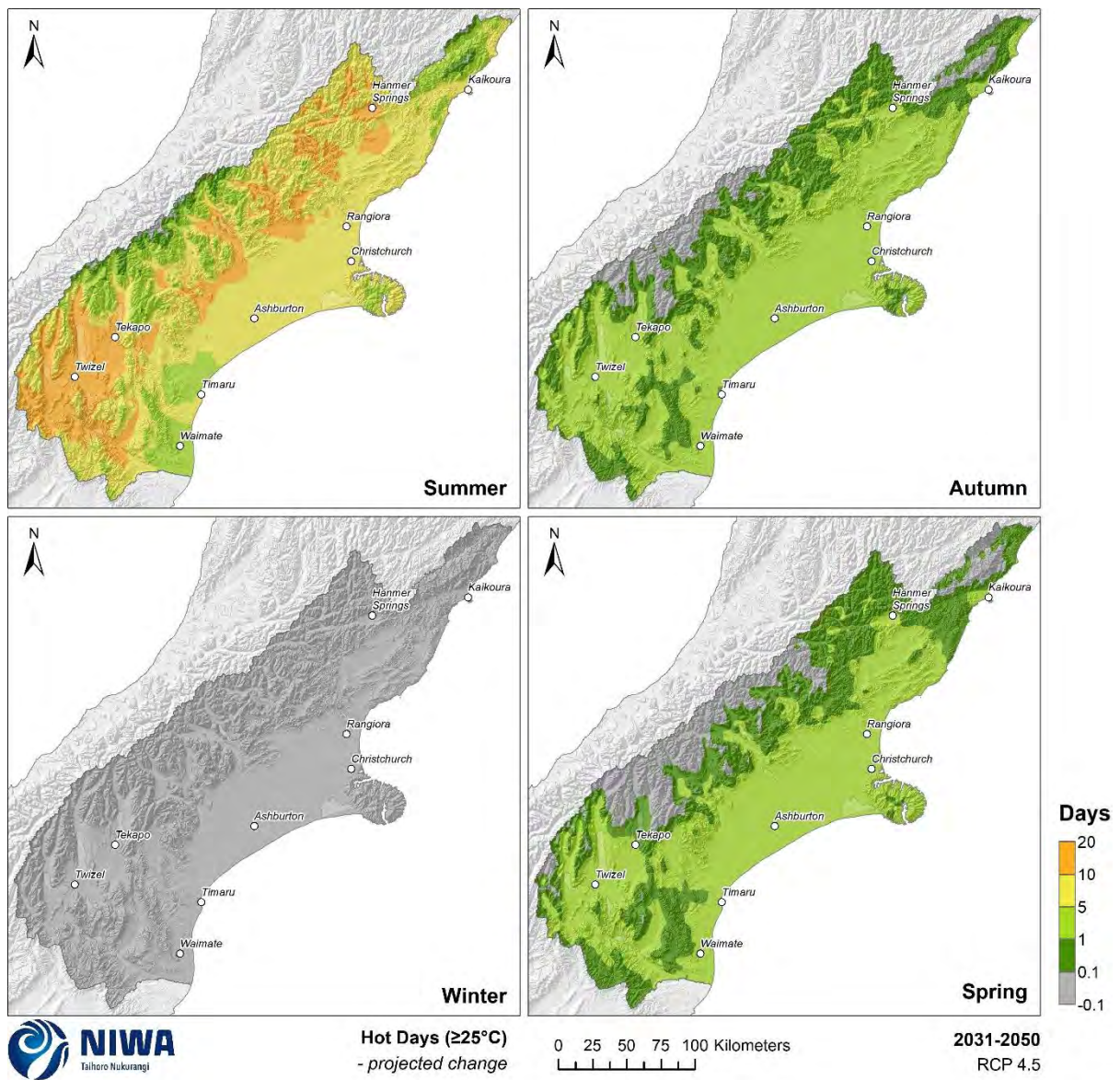


Figure 4-27: Projected seasonal hot day (days with maximum temperature $\geq 25^{\circ}\text{C}$) changes by 2040 for RCP4.5. Relative to 1986-2005 average, based on the average of six global climate models. Results are based on dynamical downscaled projections using NIWA's Regional Climate Model. Resolution of projection is 5km x 5km.

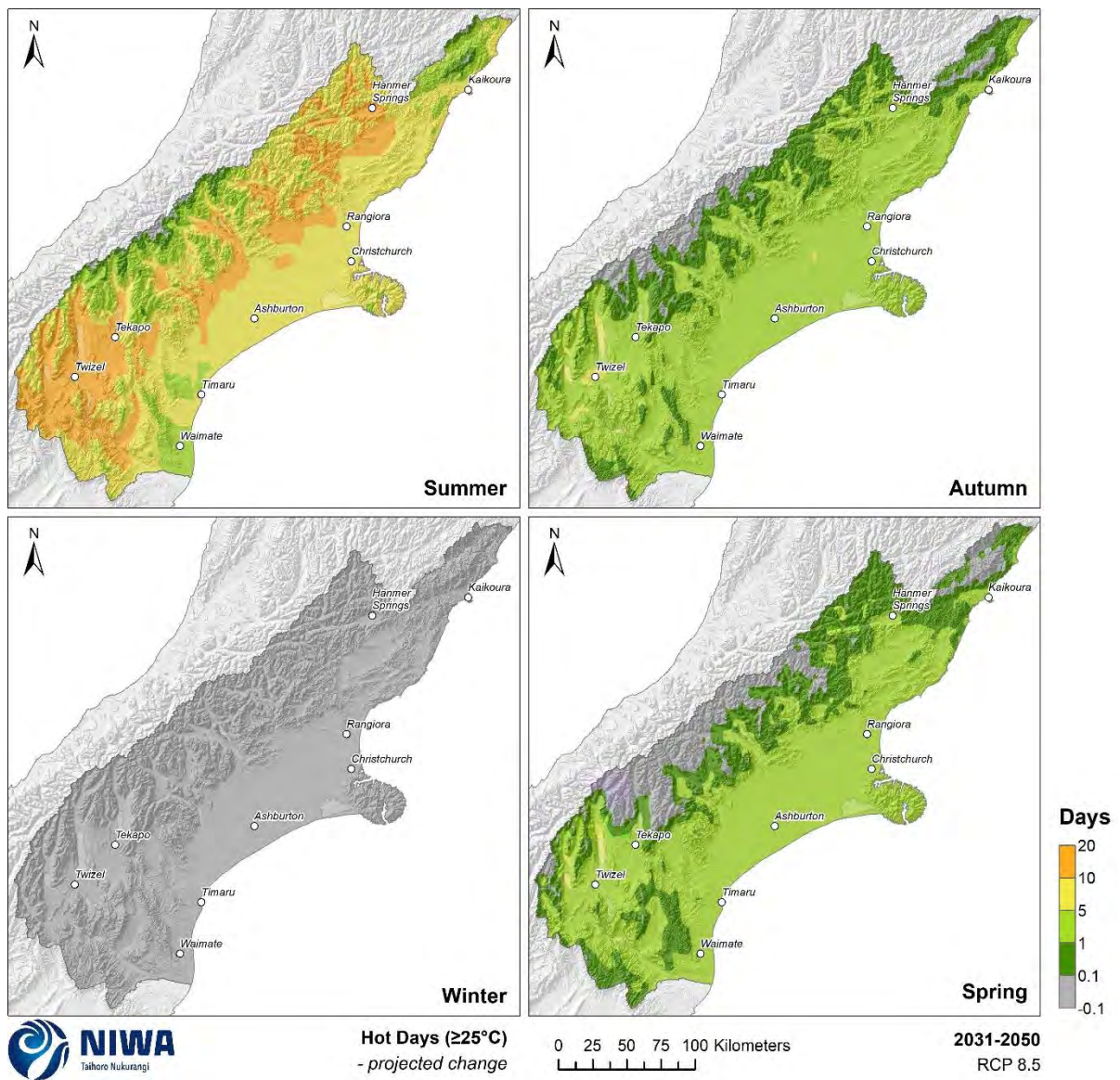


Figure 4-28: Projected seasonal hot day (days with maximum temperature $\geq 25^{\circ}\text{C}$) changes by 2040 for RCP8.5. Relative to 1986-2005 average, based on the average of six global climate models. Results are based on dynamical downscaled projections using NIWA's Regional Climate Model. Resolution of projection is 5km x 5km.

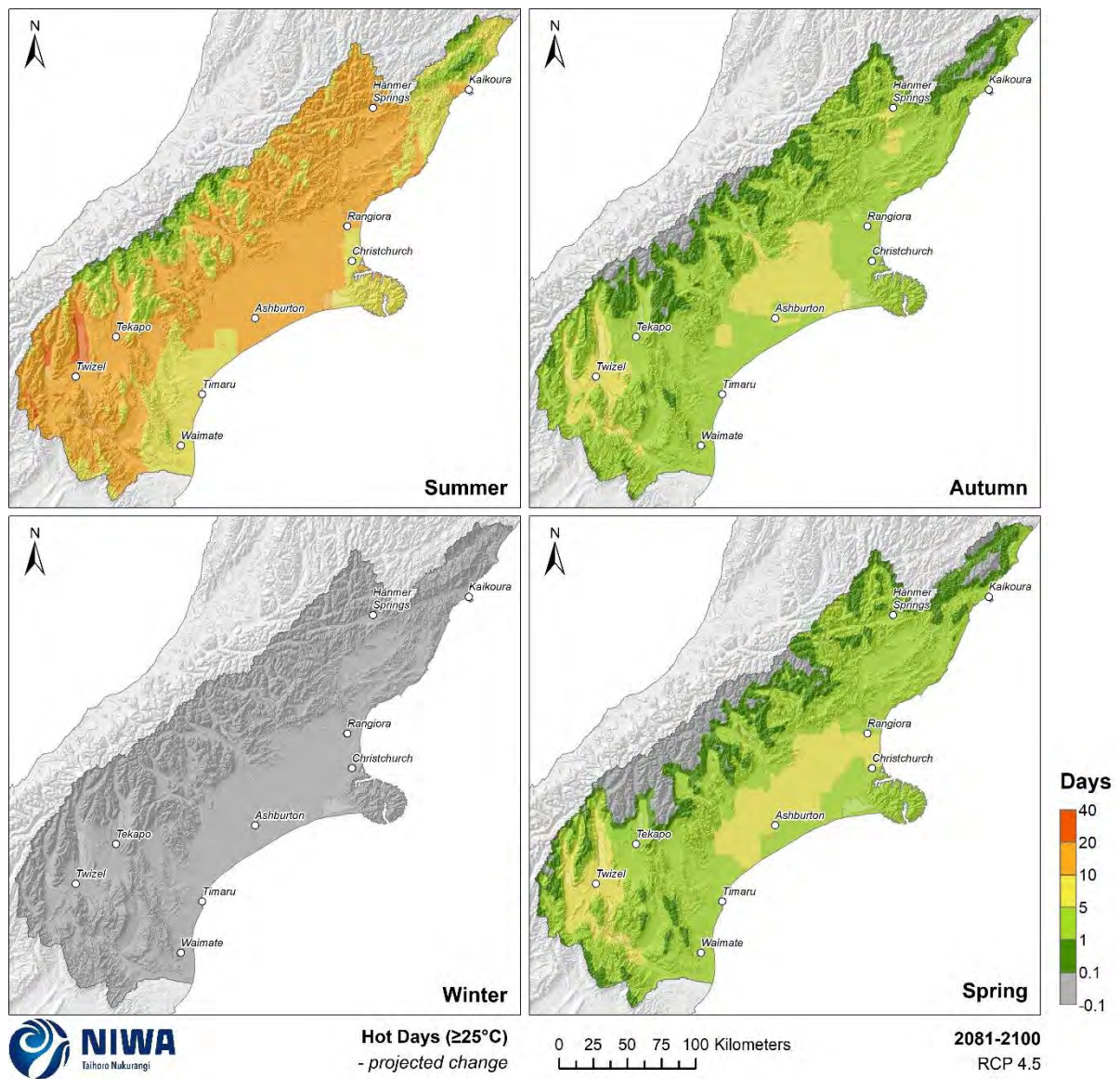


Figure 4-29: Projected seasonal hot day (days with maximum temperature $\geq 25^{\circ}\text{C}$) changes by 2090 for RCP4.5. Relative to 1986-2005 average, based on the average of six global climate models. Results are based on dynamical downscaled projections using NIWA's Regional Climate Model. Resolution of projection is 5km x 5km.

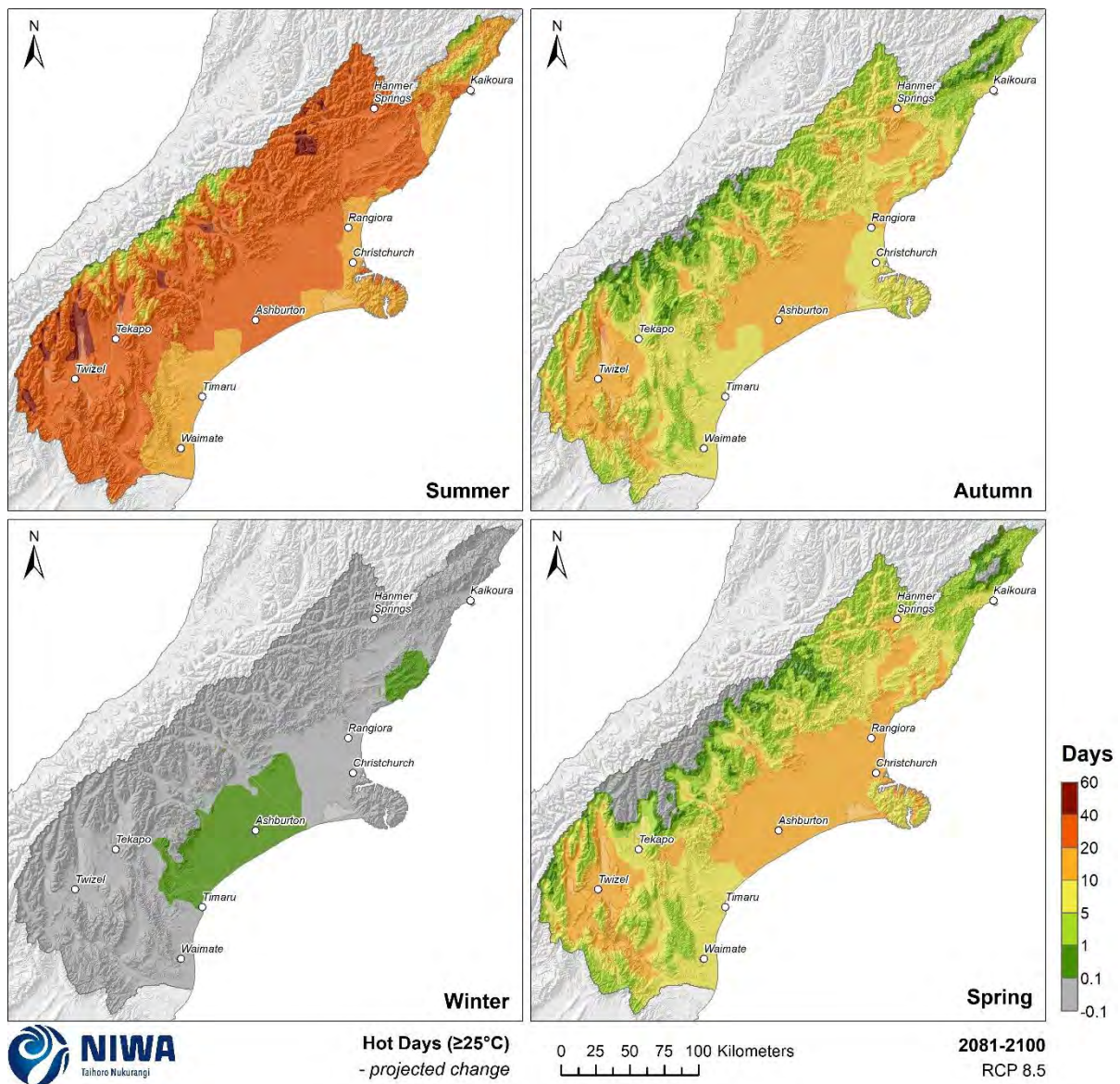


Figure 4-30: Projected seasonal hot day (days with maximum temperature $\geq 25^{\circ}\text{C}$) changes by 2090 for RCP8.5. Relative to 1986-2005 average, based on the average of six global climate models. Results are based on dynamical downscaled projections using NIWA's Regional Climate Model. Resolution of projection is 5km x 5km.

4.5 Frost days

Key messages

- Future annual numbers of frost days are projected to decline throughout the region; larger reductions in frost days are projected inland and at higher elevations (due to more frosts currently being experienced there).
- By 2040, reductions of 10-30 frost days per year are projected for inland parts of the region.
- By 2090, considerable reductions in frost days are projected throughout Canterbury, with 20-50 fewer frost days per year for inland areas (under RCP8.5).
- It is likely that future frost season length will reduce (i.e. the time between the first and last frost in a given year).

In this report, a frost day is considered to occur when the minimum temperature is 0°C or lower. This is purely a temperature-driven metric for assessing the potential for frosts over the 5 km x 5 km climate model grid. Frost conditions are influenced at the local scale (i.e. finer scale than 5 km x 5 km) by temperature, topography, wind, and humidity, so the results presented in this section can be considered as the large-scale *temperature* conditions conducive to frosts.

Present-day (average over 1986-2005) and future (average over 2031-2050 and 2081-2100) maps for frost days are shown in this section. The present-day maps show annual and seasonal average numbers of frost days and the future projection maps show the change in the number of frost days compared with present. Note that the present-day maps are on a different colour scale to the future projection maps.

At present, frost days occur most regularly at inland and high elevation locations. Here, the annual number of frost days averages 50-150 days per year, with up to 250 frost days per year in high alpine terrain (Figure 4-31). Frost days occur most frequently in winter (Figure 4-33), with many low elevation areas of Canterbury observing between 10-50 frost days during this season.

The annual number of frost days are projected to decline throughout the region. Larger reductions in frost days are projected further inland and at higher elevations, due to more frosts currently being experienced there (Figure 4-32). By 2090, annual decreases in frost days of 5-20 days (RCP4.5) and 10-50 days (RCP8.5) are projected for much of Canterbury. Seasonal projections of frost day changes are shown for RCP4.5 by 2040 (Figure 4-34) and 2090 (Figure 4-36), and RCP8.5 by 2040 (Figure 4-35) and 2090 (Figure 4-37). By 2040 under RCP4.5, winter frost days are projected to decrease by 1-10 days across much of Canterbury. By 2090 under RCP8.5, winter frost days are projected to decrease by 10-30 days for many areas of Canterbury.

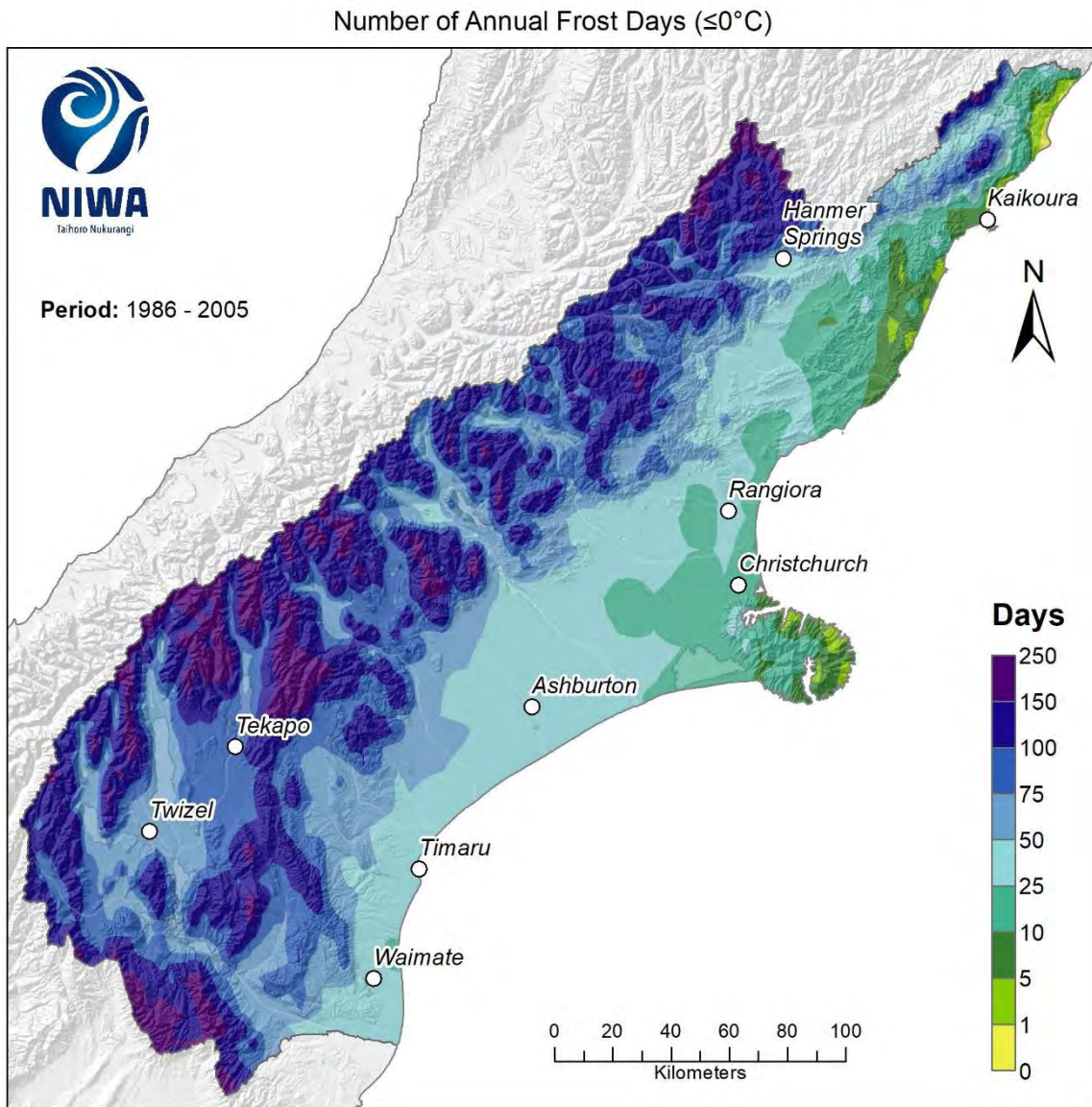


Figure 4-31: Modelled annual number of frost days (days with minimum temperature $\leq 0^{\circ}\text{C}$), average over 1986-2005. Results are based on dynamical downscaled projections using NIWA's Regional Climate Model. Resolution of projection is 5km x 5km.

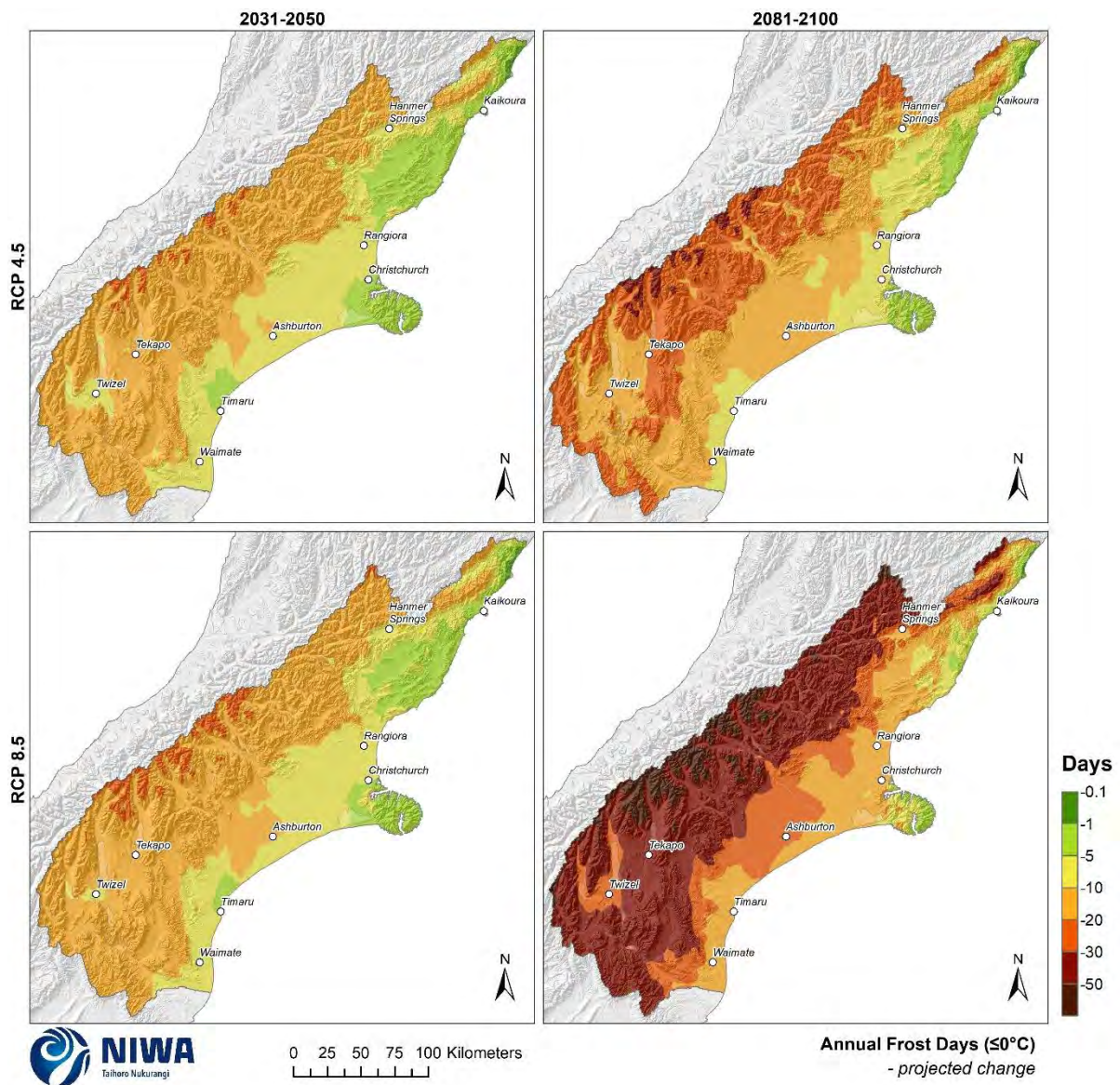


Figure 4-32: Projected annual frost day (days with minimum temperature $\leq 0^{\circ}\text{C}$) changes by 2040 and 2090, under RCP4.5 and RCP8.5. Climate change scenarios: RCP4.5 (top panels) and RCP8.5 (bottom panels). Time periods: mid-century (2031-2050; “2040” – panels on left) and end-century (2081-2100; “2090” – panels on right). Changes relative to 1986-2005 average, based on the average of six global climate models. Results are based on dynamical downscaled projections using NIWA's Regional Climate Model. Resolution of projection is 5km x 5km.

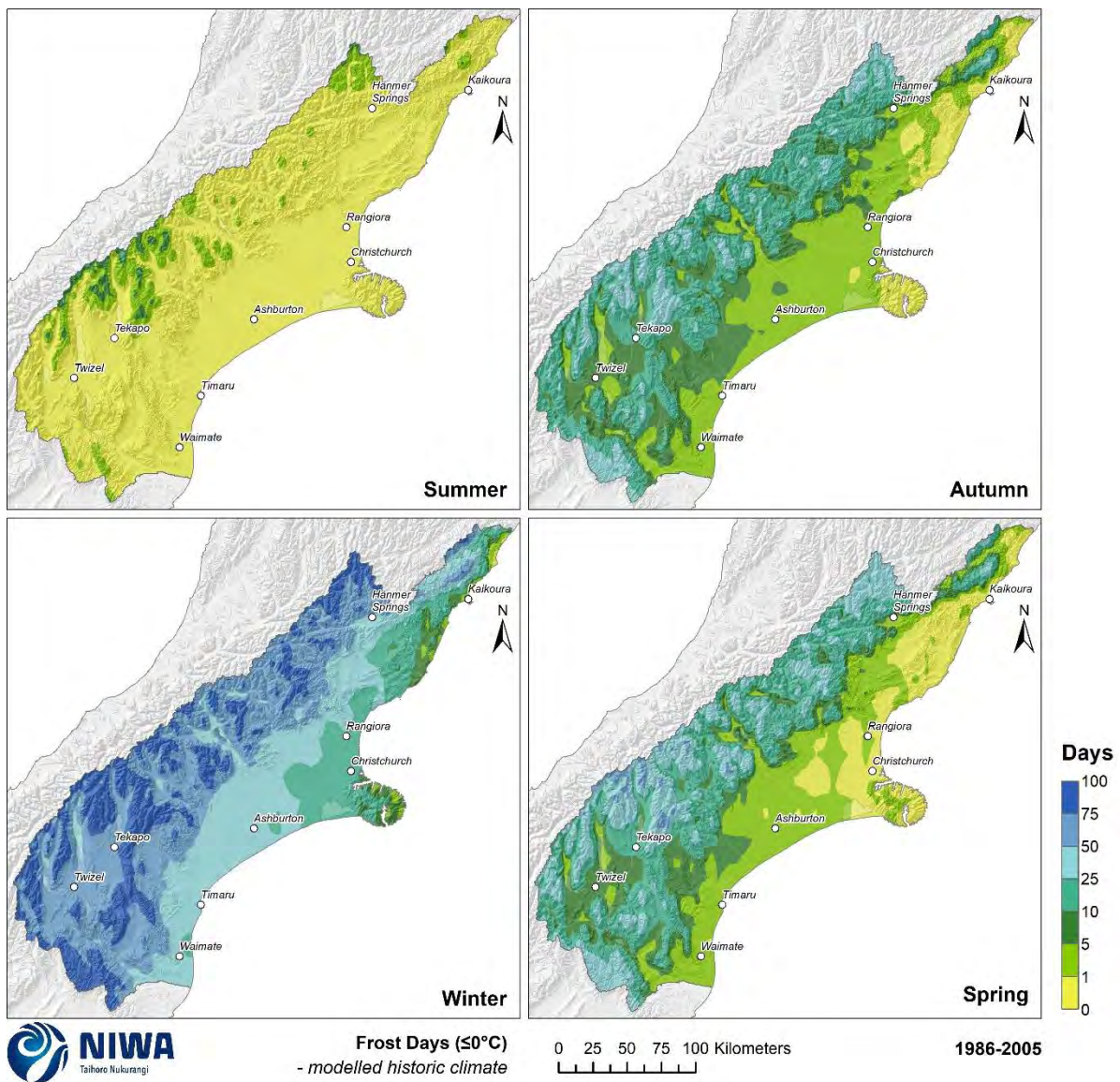


Figure 4-33: Modelled seasonal number of frost days (days with minimum temperature $\leq 0^{\circ}\text{C}$), average over 1986-2005. Results are based on dynamical downscaled projections using NIWA's Regional Climate Model. Resolution of projection is 5km x 5km.

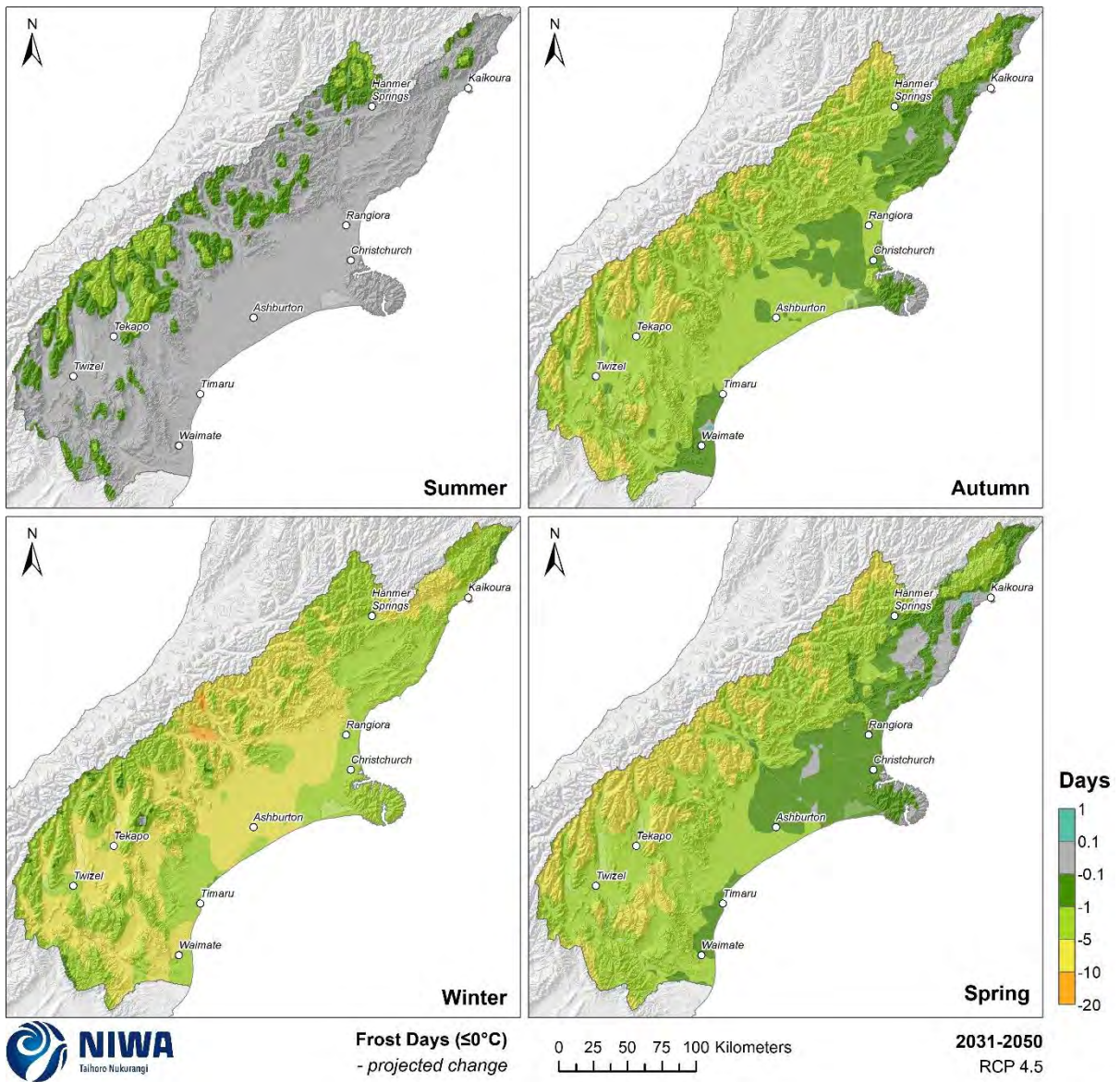


Figure 4-34: Projected seasonal frost day (days with minimum temperature $\leq 0^{\circ}\text{C}$) changes by 2040 for RCP4.5. Relative to 1986-2005 average, based on the average of six global climate models. Results are based on dynamical downscaled projections using NIWA's Regional Climate Model. Resolution of projection is 5km x 5km.

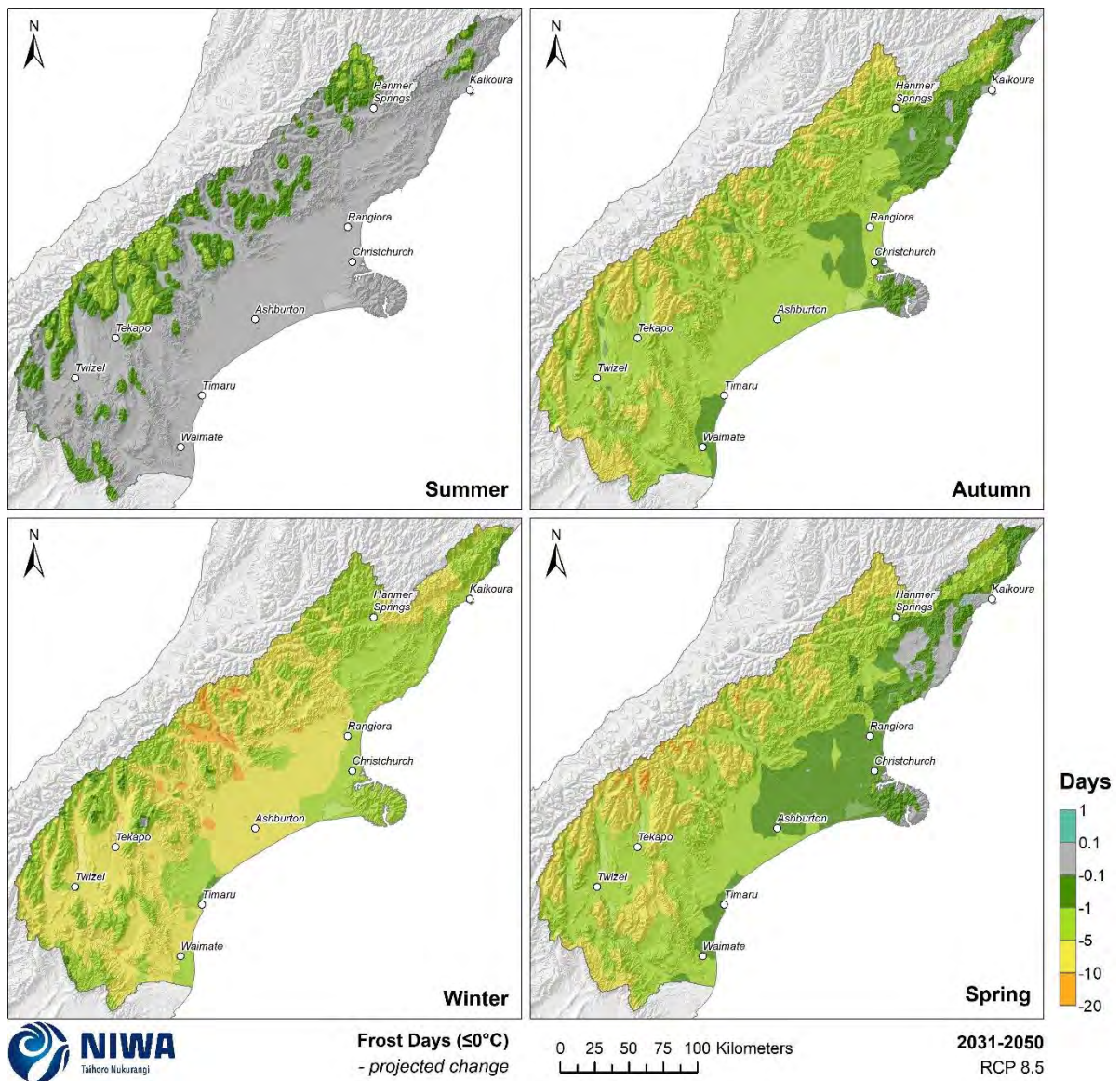


Figure 4-35: Projected seasonal frost day (days with minimum temperature $\leq 0^{\circ}\text{C}$) changes by 2040 for RCP8.5. Relative to 1986-2005 average, based on the average of six global climate models. Results are based on dynamical downscaled projections using NIWA's Regional Climate Model. Resolution of projection is 5km x 5km.

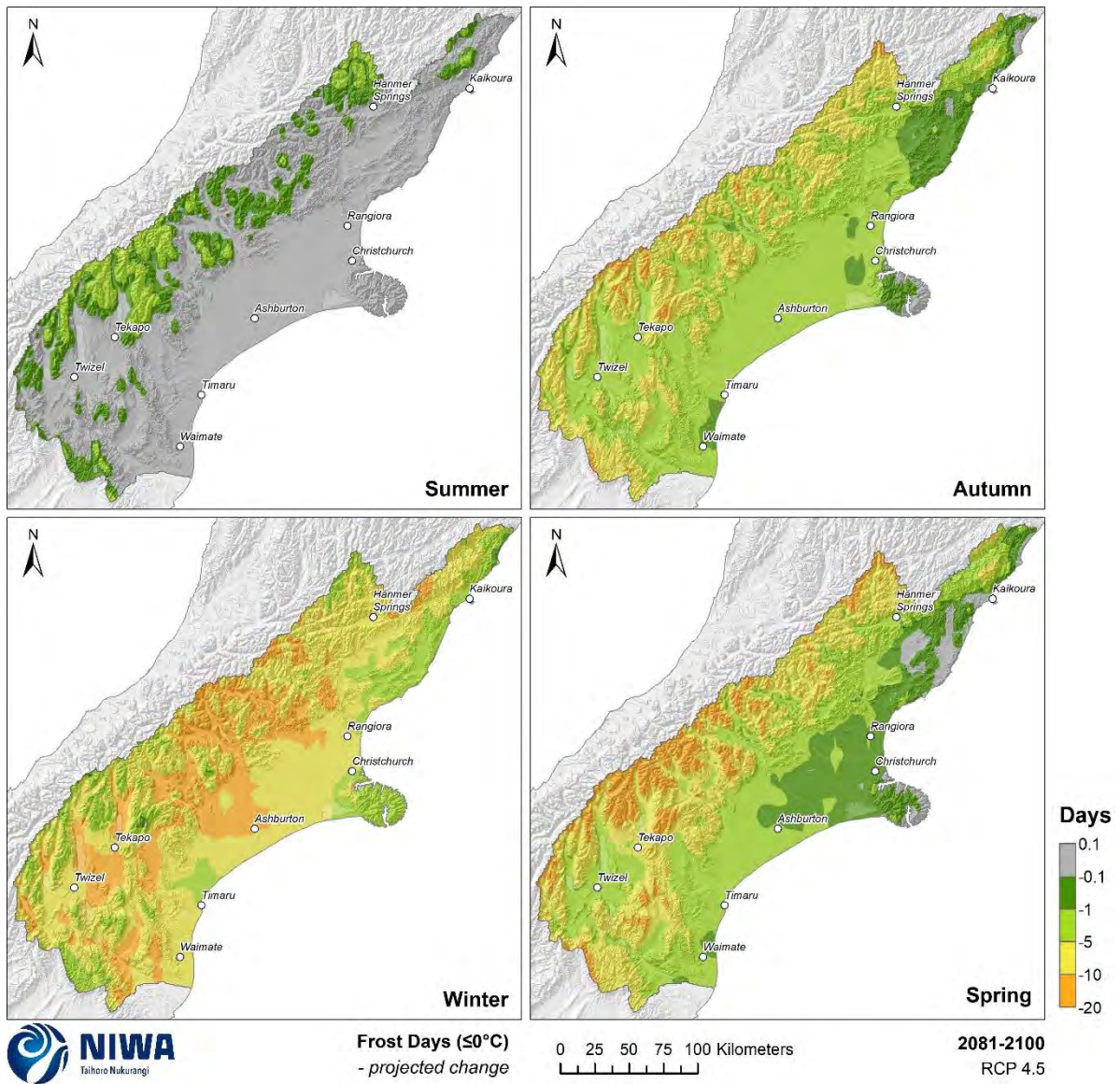


Figure 4-36: Projected seasonal frost day (days with minimum temperature $\leq 0^{\circ}\text{C}$) changes by 2090 for RCP4.5. Relative to 1986-2005 average, based on the average of six global climate models. Results are based on dynamical downscaled projections using NIWA's Regional Climate Model. Resolution of projection is 5km x 5km.

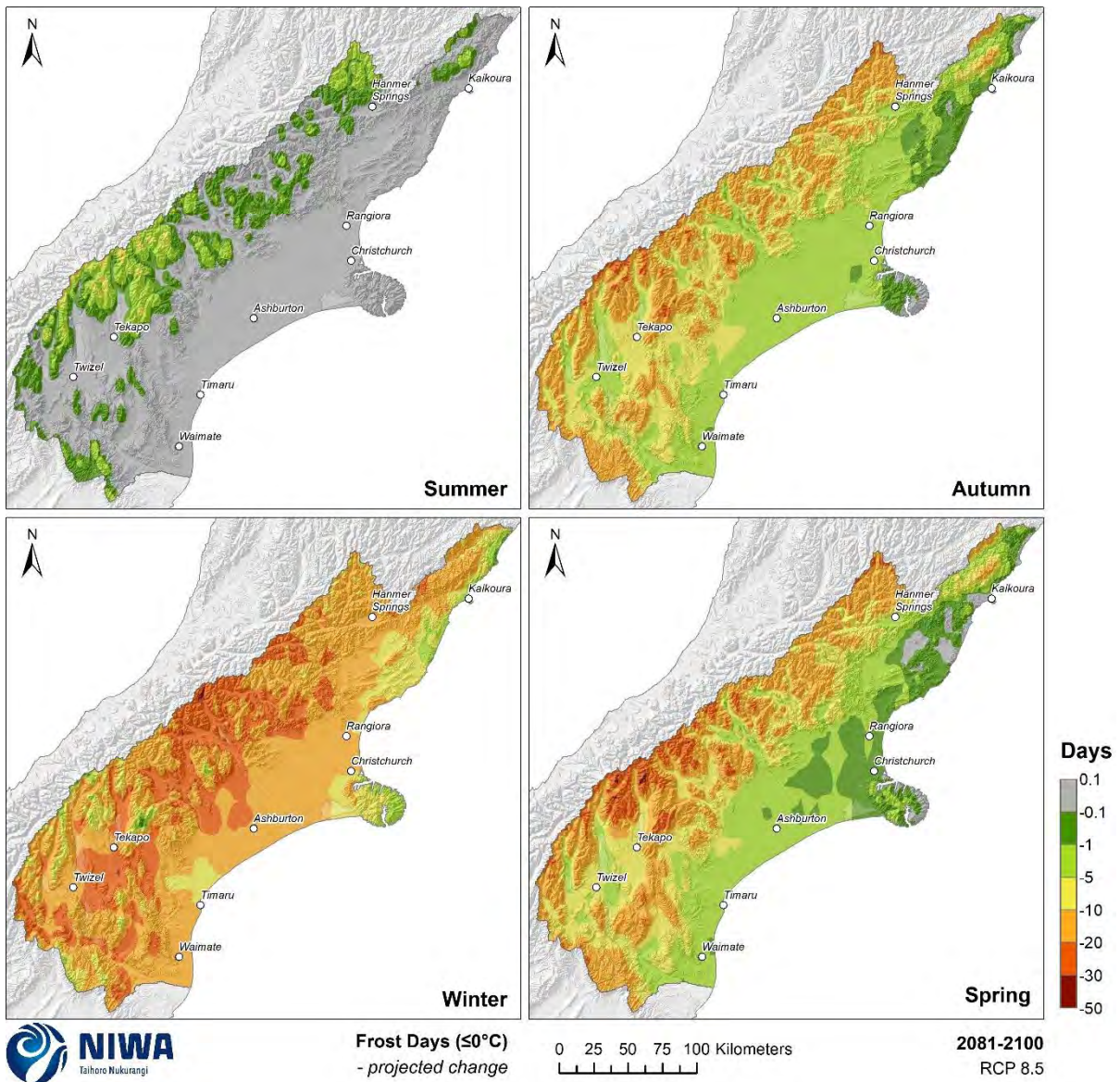


Figure 4-37: Projected seasonal frost day (days with minimum temperature $\leq 0^{\circ}\text{C}$) changes by 2090 for RCP8.5. Relative to 1986-2005 average, based on the average of six global climate models. Results are based on dynamical downscaled projections using NIWA's Regional Climate Model. Resolution of projection is 5km x 5km.

5 Precipitation

5.1 Rainfall

Key messages

- Annual rainfall is projected to change by between $\pm 5\%$ for most of the region by 2040 and 2090.
- Decreases in autumn rainfall of between 0-10% are projected for the Mackenzie Basin by 2040.
- Winter rainfall is projected to increase considerably by 2090 under RCP8.5 in many eastern, western and southern parts, with 15-40% more rainfall projected.
- Decreases in summer rainfall of 5-15% are projected around Banks Peninsula and many inland areas by 2090 under RCP8.5.

This section contains maps showing historic total rainfall and the future projected change in total rainfall. Historic rainfall maps are in units of mm per year or season (average over 1986-2005) and future (average over 2031-2050 and 2081-2100) maps show the percentage change in rainfall compared with the historic total. Note that the historic maps are on a different colour scale to the future projection maps.

Historically, the highest annual rainfall totals are recorded in the high elevations of the western ranges, with lowest annual rainfall totals in inland areas south of Twizel (Figure 5-1). For eastern parts of Canterbury, annual average rainfall typically ranges from 500-800 mm. Winter is typically the driest season of the year for much of Canterbury (Figure 5-3), although the inter-seasonal variability of average rainfall totals is not considerable.

Canterbury is generally projected to observe moderate changes in future annual rainfall (Figure 5-2). By 2040 under RCP4.5 and RCP8.5, annual rainfall is projected to change by between $\pm 5\%$ for most of the region. At the seasonal scale, decreases in autumn rainfall of between 0-10% are projected for the Mackenzie Basin by 2040 under RCP4.5 (Figure 5-4) and RCP8.5 (Figure 5-5). For remaining parts of Canterbury, increases in seasonal rainfall of between 0-10% are typically projected by 2040 under both RCP4.5 and RCP8.5.

By 2090 under RCP4.5 and RCP8.5, annual rainfall is projected to change by between $\pm 5\%$ for most of the region (Figure 5-2). However, by 2090 under RCP8.5, annual rainfall is projected to increase by 20-25% in eastern parts of south Canterbury near Timaru. Seasonal rainfall changes by 2090 are typically less pronounced under RCP4.5 (Figure 5-6) compared to RCP8.5 (Figure 5-7). Winter rainfall is projected to increase considerably by 2090 under RCP8.5 in many eastern, western and southern parts of Canterbury, with 15-40% more rainfall projected. Decreases in summer rainfall of 5-15% are projected around Banks Peninsula and many inland areas by 2090 under RCP8.5.

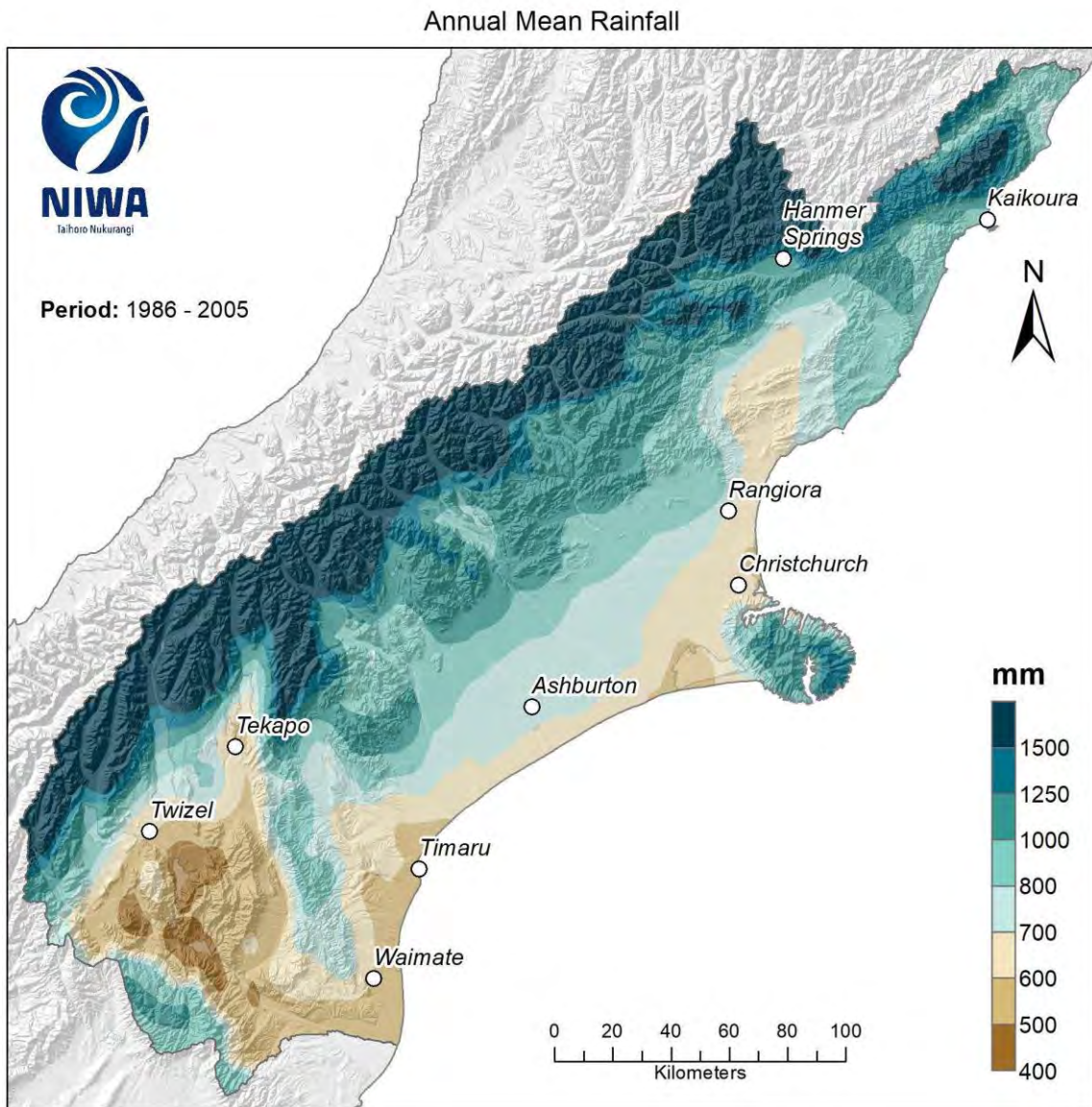


Figure 5-1: Modelled annual mean rainfall (mm), average over 1986-2005. Results are based on dynamical downscaled projections using NIWA's Regional Climate Model. Resolution of projection is 5km x 5km.

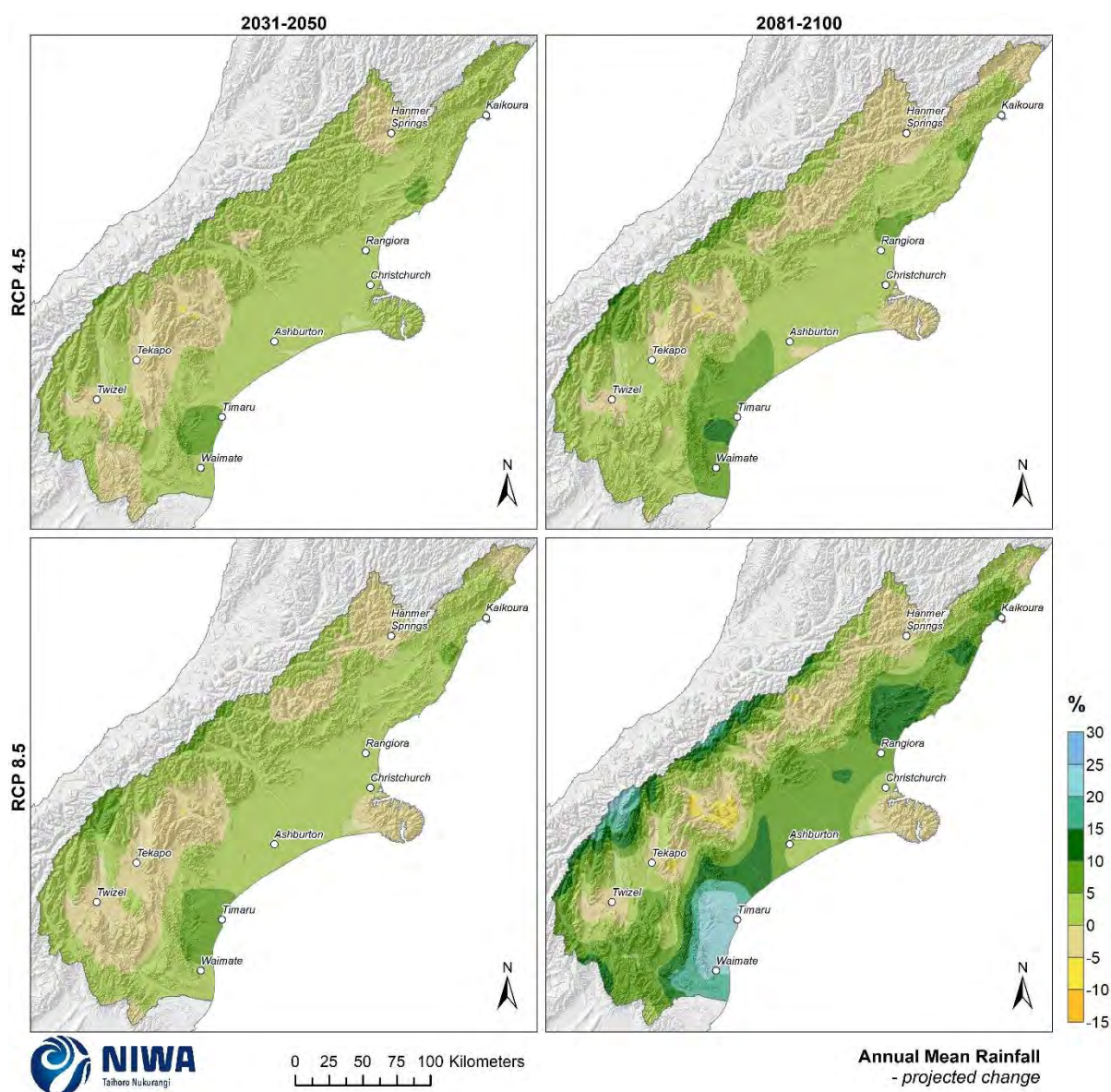


Figure 5-2: Projected annual mean rainfall changes by 2040 and 2090, under RCP4.5 and RCP8.5. Climate change scenarios: RCP4.5 (top panels) and RCP8.5 (bottom panels). Time periods: mid-century (2031-2050; “2040” – panels on left) and end-century (2081-2100; “2090” – panels on right). Changes relative to 1986-2005 average, based on the average of six global climate models. Results are based on dynamical downscaled projections using NIWA’s Regional Climate Model. Resolution of projection is 5km x 5km.

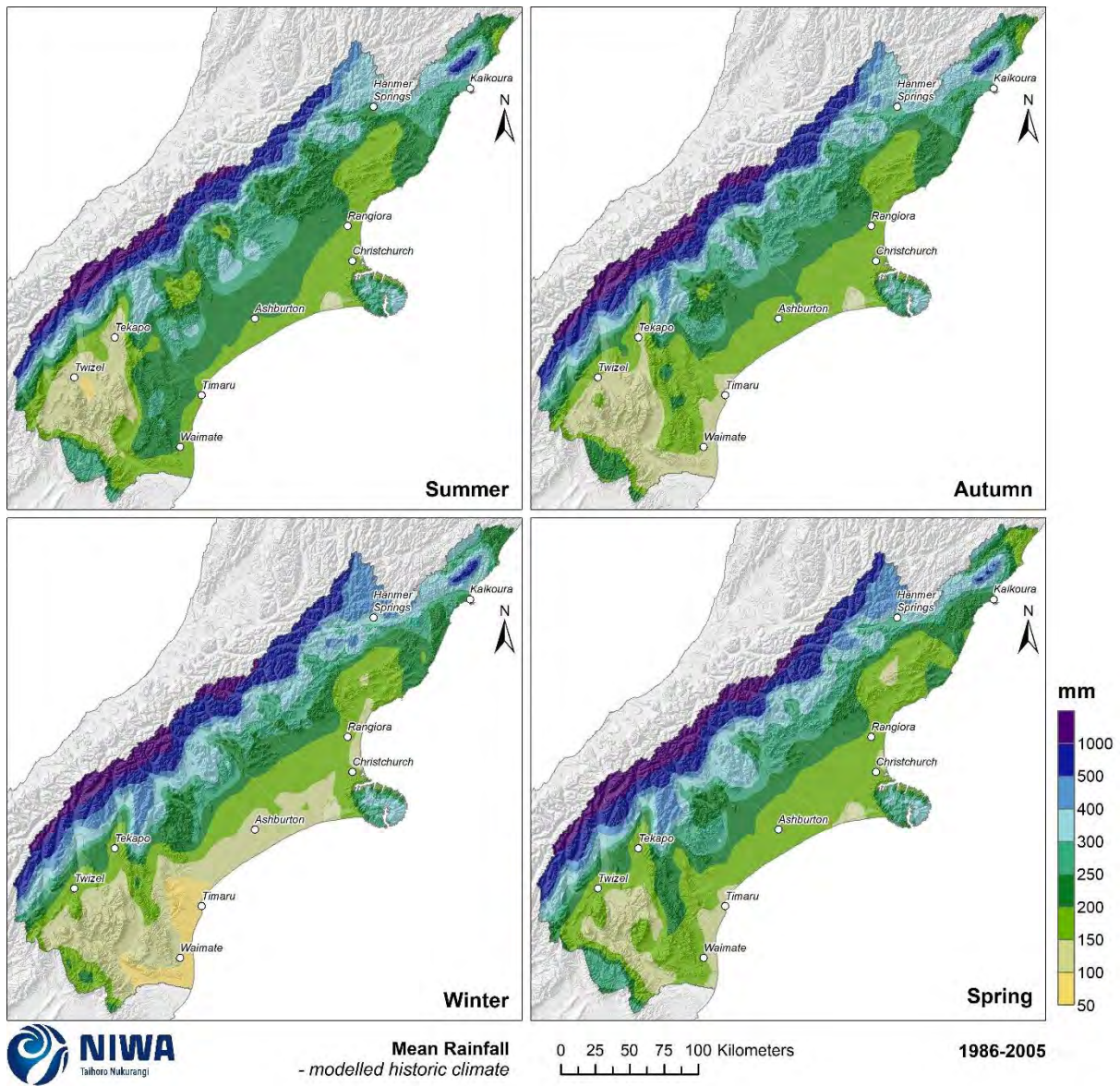


Figure 5-3: Modelled seasonal mean rainfall, average over 1986-2005. Results are based on dynamical downscaled projections using NIWA's Regional Climate Model. Resolution of projection is 5km x 5km.

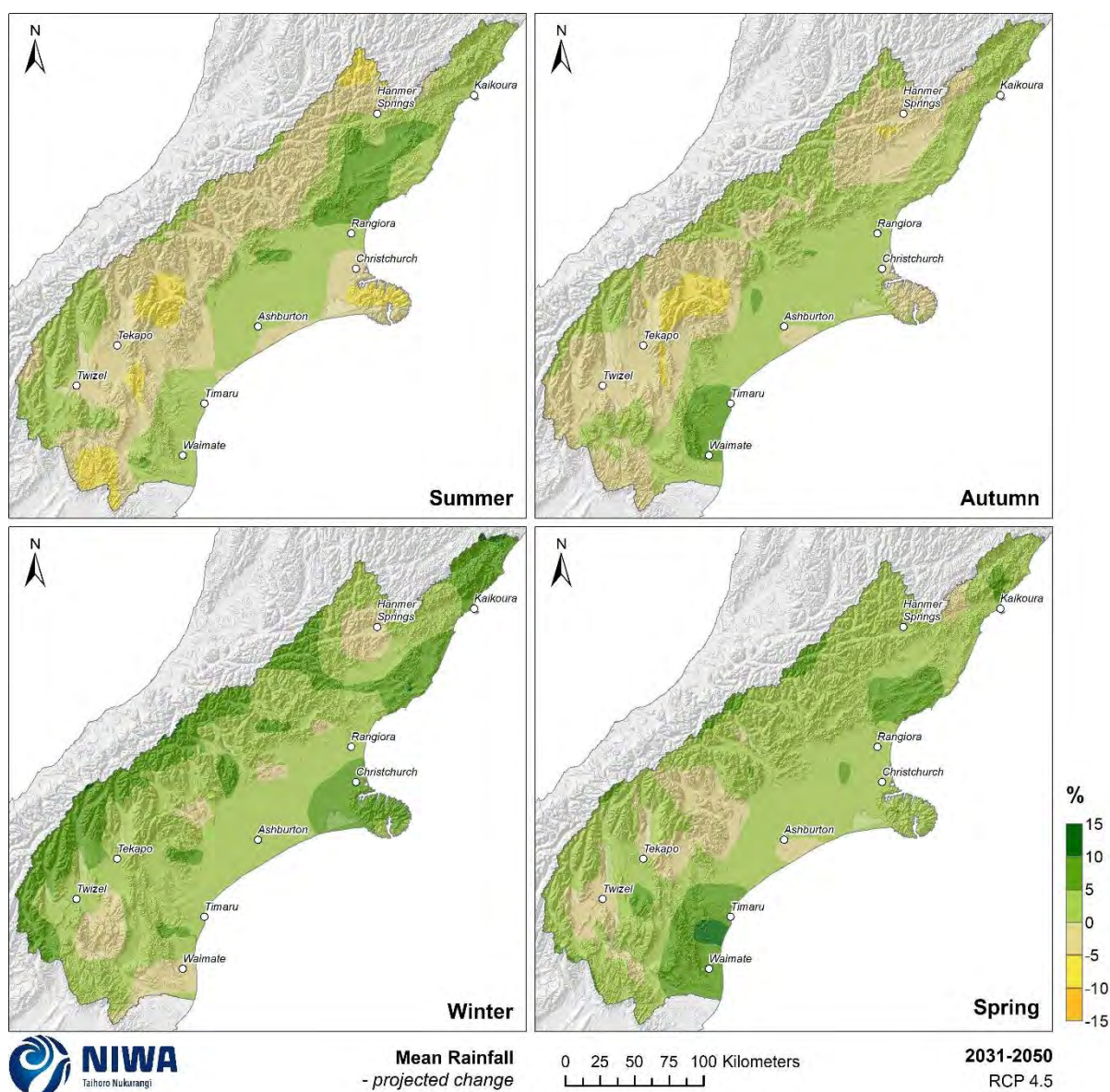


Figure 5-4: Projected seasonal mean rainfall changes by 2040 for RCP4.5. Relative to 1986-2005 average, based on the average of six global climate models. Results are based on dynamical downscaled projections using NIWA's Regional Climate Model. Resolution of projection is 5km x 5km.

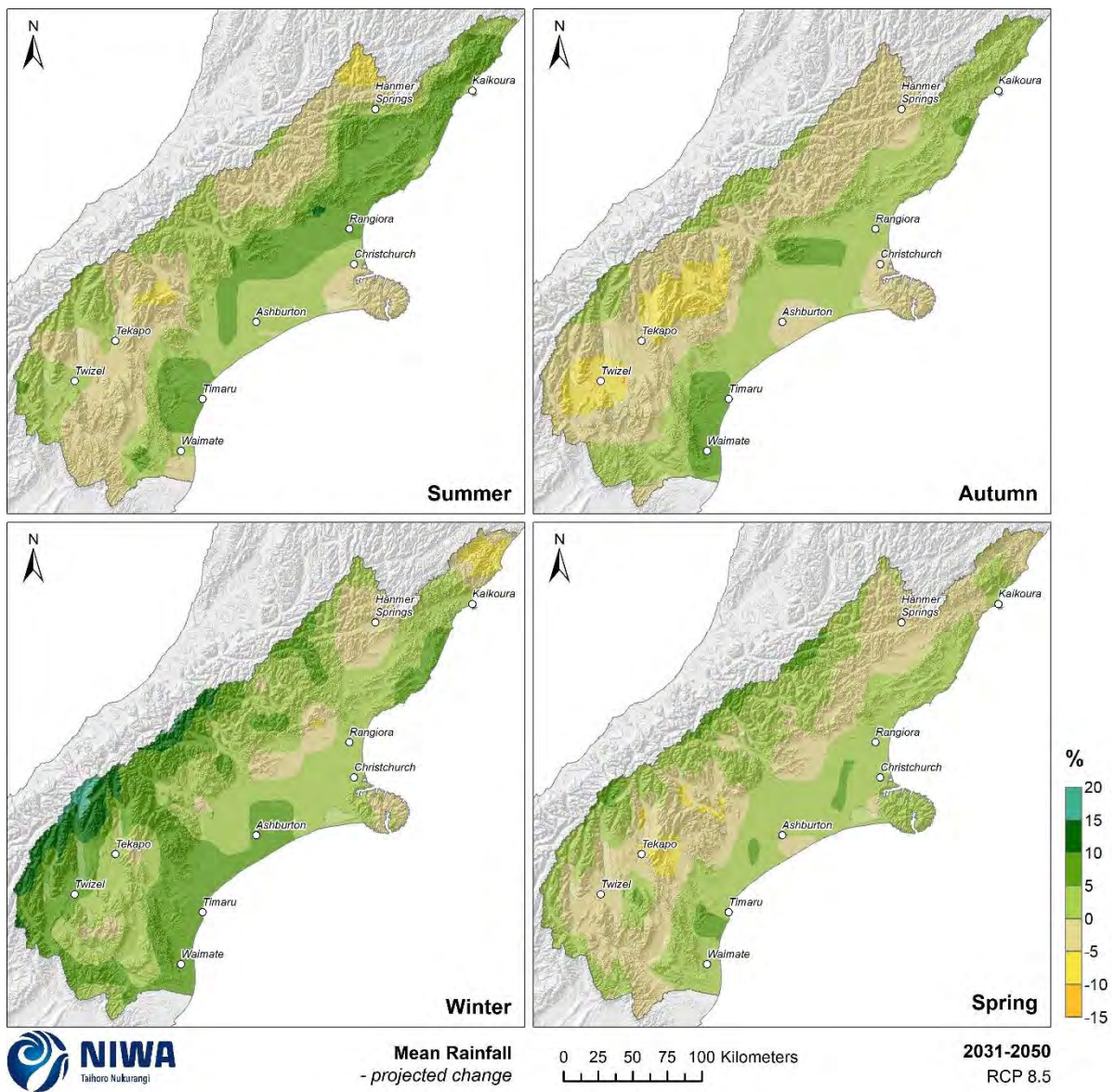


Figure 5-5: Projected seasonal mean rainfall changes by 2040 for RCP8.5. Relative to 1986-2005 average, based on the average of six global climate models. Results are based on dynamical downscaled projections using NIWA's Regional Climate Model. Resolution of projection is 5km x 5km.

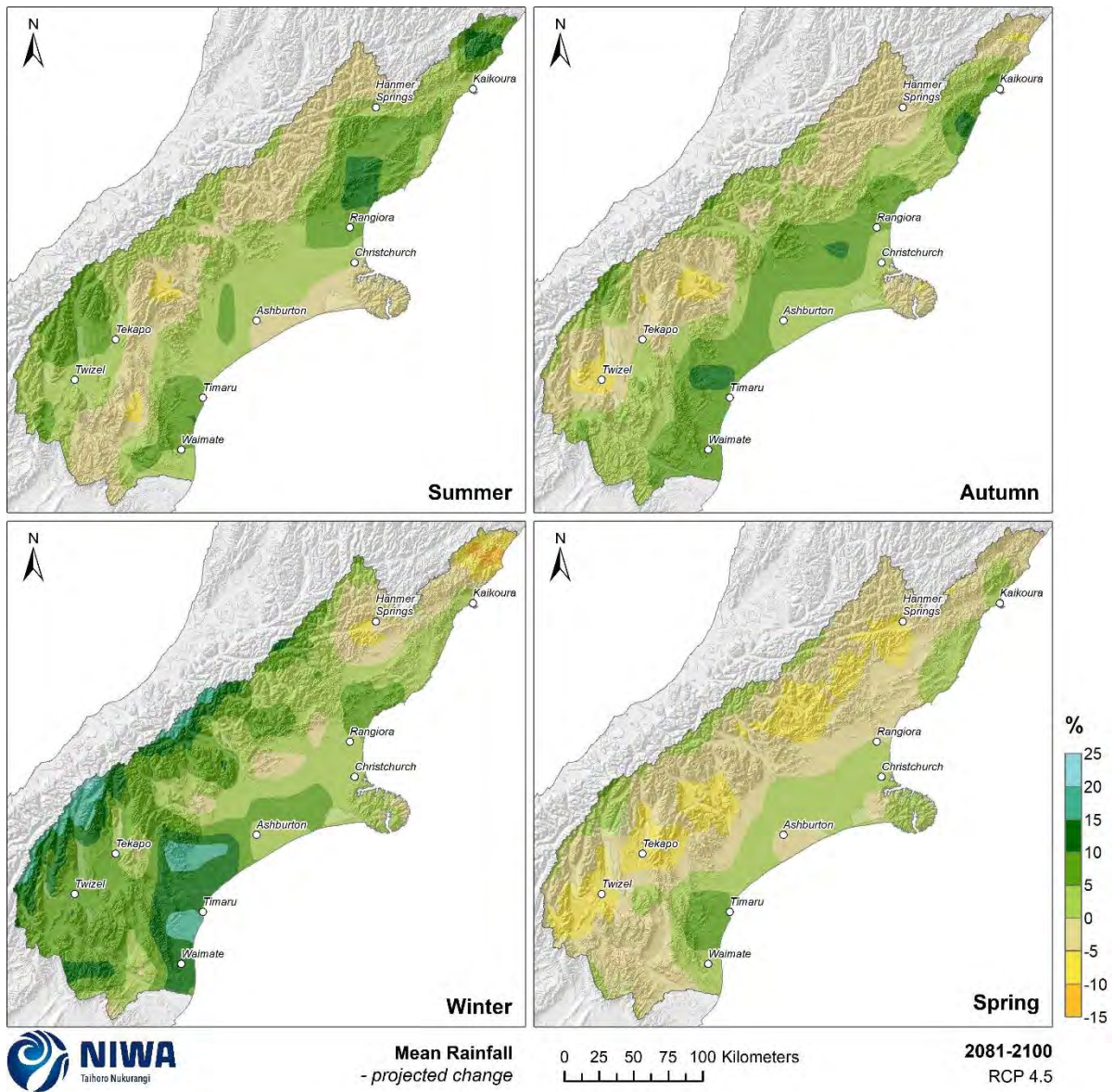


Figure 5-6: Projected seasonal mean rainfall changes by 2090 for RCP4.5. Relative to 1986-2005 average, based on the average of six global climate models. Results are based on dynamical downscaled projections using NIWA's Regional Climate Model. Resolution of projection is 5km x 5km.

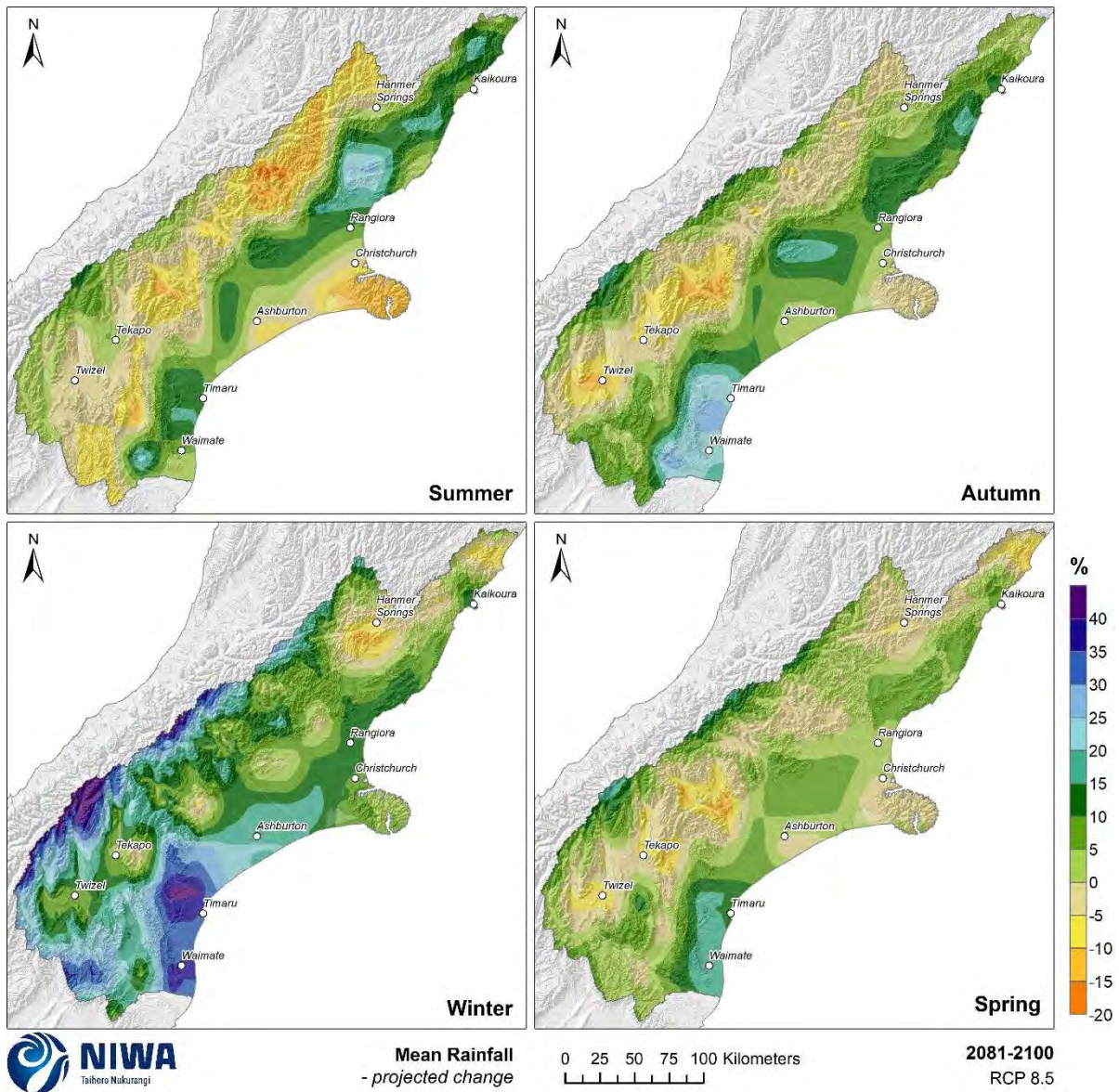


Figure 5-7: Projected seasonal mean rainfall changes by 2090 for RCP8.5. Relative to 1986-2005 average, based on the average of six global climate models. Results are based on dynamical downscaled projections using NIWA's Regional Climate Model. Resolution of projection is 5km x 5km.

5.1.1 Model confidence

Key message

- The complete range of model projections (as shown in this section) demonstrate the difference with season and RCP, allowing interpretation of the range of model uncertainty.
- The direction of change for rainfall is less certain than for temperature, owing to models projecting both increases and decreases of rainfall within the same scenario.

The climate change projections in other sections this report show the average of six dynamically downscaled climate models. This is useful as the average is the ‘best estimate’ of future conditions, but these results taken alone do not allow for communication of uncertainty or range in potential future outcomes within the different scenarios and time periods. This section presents the full range of model results for rainfall, to help the reader understand that there is no ‘single answer’ in terms of future projections.

Projected changes in seasonal and annual rainfall are shown for Christchurch, Hanmer and Tekapo in Table 5-1. Note that data in this table was derived from additional IPCC Fifth Assessment Report models than are presented in the maps in this report (the maps are the average of six dynamically downscaled models, whereas the data here are from ~40 statistically downscaled models), in order to enable an assessment of the range of rainfall change for Christchurch, Hanmer and Tekapo by 2040 and 2090 under RCP4.5 and RCP8.5. The difference between dynamical and statistical downscaling is explained in Appendix A.

Figure 5-8 and Figure 5-9 illustrate the seasonal and annual rainfall projections for each RCP, for the two time periods of 2040 and 2090, respectively. The projections for Christchurch are shown in this example. The coloured vertical bars, and inset stars, show all the individual models, so the complete range is displayed (unlike Table 5-1 where the 5th to 95th percentile range has been calculated). These figures are an excellent way of not only demonstrating the difference between models for each season and RCP, but also the range of model sensitivity (i.e. how the different models predict future conditions under the same scenarios/greenhouse gas concentrations). The closer together the model outcomes are, it can be inferred that these projections have more certainty. The black stars within each vertical bar represent the results of the six RCM simulations selected for presentation in this report.

For 2040 projections (Figure 5-8 and Table 5-1), there is a range of model results, as seen by the size of the coloured bars and the numbers inside the parentheses in the table. The average of all the models generally project an increase in rainfall, as indicated in the table and the horizontal black line on each bar in the figure. However, this doesn’t apply to all seasons at each location (e.g. on average, a decrease in winter rainfall of 4% is projected for Christchurch by 2040 under RCP8.5). Overall the direction of change is less certain than, say, for temperature (Section 4.1.1) where all models project warming.

For 2090 projections (Figure 5-9 and Table 5-1), the range of model results within the scenarios is similar to those at 2040. Most models are clustered within $\pm 15\%$ change, but some individual models project up to a 49% increase (winter at 2090 under RCP8.5 in Tekapo) and a 29% decrease (winter at 2090 under RCP8.5 at Christchurch).

Table 5-1: Projected changes in seasonal and annual rainfall (%) between 1986-2005 and two climate change scenarios (RCP4.5 and RCP8.5) at two future time periods. Time periods: mid-century (2031-2050; “2040”) and end-century (2081-2100; “2090”). The values in each column represent the ensemble average, taken over 41 models (RCP8.5) and 37 models (RCP4.5). Bracketed values represent the range (5th percentile to 95th percentile) over all models within that ensemble. [Source: MFE 2018].

		Summer	Autumn	Winter	Spring	Annual
2040	Christchurch					
	RCP8.5	1 (-5, 9)	3 (-8, 14)	-4 (-19, 6)	1 (-7, 10)	0 (-7, 6)
	RCP4.5	2 (-8, 11)	2 (-9, 14)	-3 (-14, 14)	2 (-8, 10)	0 (-5, 7)
	Hanmer					
	RCP8.5	1 (-8, 9)	1 (-7, 8)	-3 (-15, 6)	1 (-6, 7)	0 (-5, 5)
	RCP4.5	1 (-7, 11)	1 (-8, 9)	-2 (-14, 13)	2 (-3, 9)	0 (-3, 6)
	Tekapo					
	RCP8.5	2 (-6, 11)	0 (-6, 8)	11 (-1, 26)	6 (-6, 19)	6 (-6, 19)
RCP4.5	2 (-6, 13)	-1 (-10, 7)	9 (-8, 20)	4 (-9, 19)	4 (-9, 19)	
2090	Christchurch					
	RCP8.5	8 (-2, 23)	8 (-4, 21)	-12 (-29, 8)	1 (-9, 13)	0 (-9, 11)
	RCP4.5	3 (-4, 13)	3 (-9, 13)	-4 (-21, 10)	2 (-6, 11)	1 (-7, 7)
	Hanmer					
	RCP8.5	9 (-1, 26)	2 (-7, 12)	-10 (-24, 7)	1 (-9, 12)	0 (-8, 8)
	RCP4.5	3 (-7, 12)	1 (-8, 9)	-3 (-17, 10)	2 (-6, 9)	1 (-5, 6)
	Tekapo					
	RCP8.5	5 (-12, 17)	-2 (-10, 8)	28 (4, 49)	13 (-4, 29)	11 (2, 22)
RCP4.5	3 (-8, 16)	0 (-8, 10)	14 (-7, 31)	7 (-4, 21)	6 (-1, 15)	

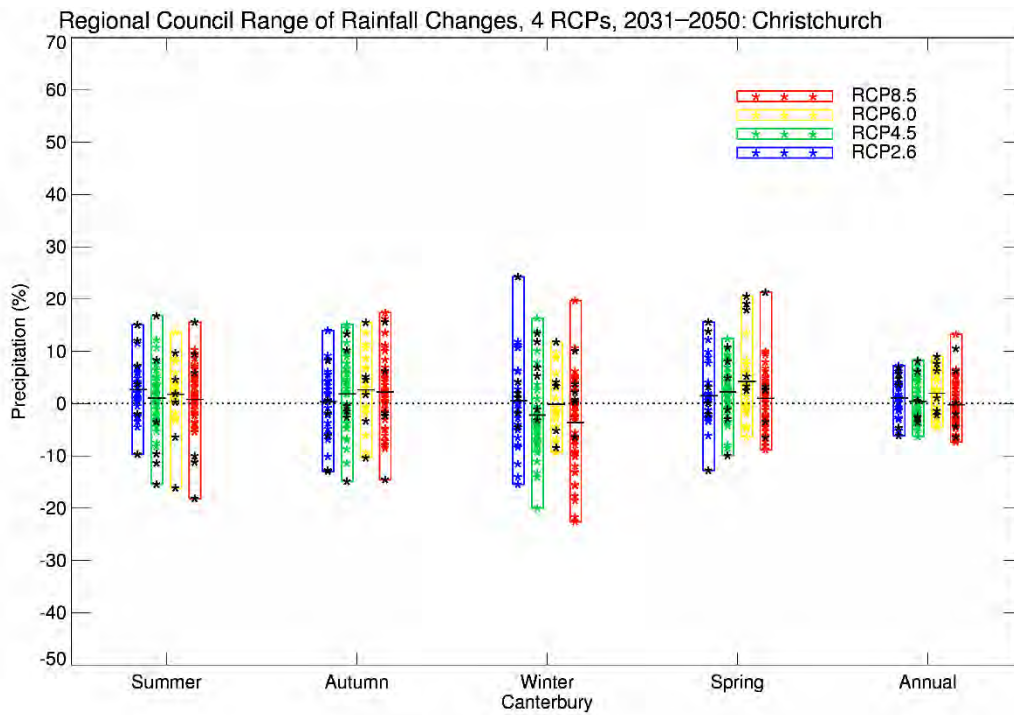


Figure 5-8: Projected seasonal and annual rainfall change for Christchurch by 2040 (2031-2050). Coloured stars represent all models as derived by statistical downscaling. Black stars correspond to the six-model RCM-downscaling, and the horizontal bars are the average over all downscaled results (statistical and RCM).

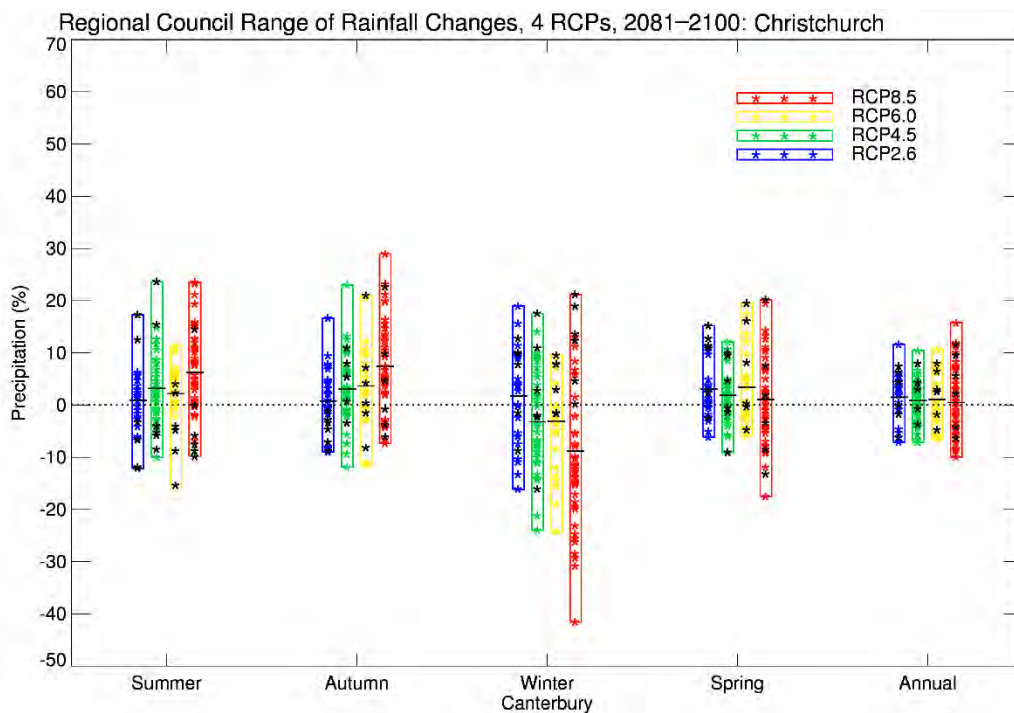


Figure 5-9: Projected seasonal and annual rainfall change for Christchurch by 2090 (2081-2100). Coloured stars represent all models as derived by statistical downscaling. Black stars correspond to the six-model RCM-downscaling, and the horizontal bars are the average over all downscaled results (statistical and RCM).

5.2 Dry days

Key messages

- By 2040 under RCP4.5 the number of dry days per year decreases near the coast and around the Canterbury Plains (1-5 fewer dry days per year), with increases of 1-5 more annual dry days for most remaining parts of Canterbury.
- By 2090 under RCP8.5, decreases in annual dry days of 1-15 days are projected for many eastern parts of Canterbury, with increases of 1-15 more dry days per year for most remaining parts of the region.
- Seasonally, the largest changes are projected by 2090 under RCP8.5: e.g. 4-10 more *spring* and *summer* dry days projected for many western parts of Canterbury, with 2-6 fewer *summer* and *autumn* dry days projected for many eastern parts of Canterbury.

A dry day considered here is when < 1 mm of rainfall is recorded over a 24-hour period. Historic (average over 1986-2005) and future (average over 2031-2050 and 2081-2100) maps for dry days are shown in this section. The historic maps show annual and seasonal average numbers of dry days and the future projection maps show the change in the number of dry days compared with the historic period. Note that the historic maps are on a different colour scale to the future projection maps.

Historically, the largest annual number of dry days is experienced in eastern parts of Canterbury and about the Mackenzie Basin (250-300 days per year; Figure 5-10). Many remaining areas of Canterbury average around 200-250 dry days per year. Westernmost areas of the region experience the fewest annual dry days for the region, averaging 100-150 dry days per year. The seasonal distribution of dry days in Canterbury is relatively even, although there tends to be more dry days winter and fewer dry days in summer (Figure 5-12).

By 2040 under RCP4.5 (Figure 5-11), the number of dry days per year generally decreases near the east coast and around the Canterbury Plains (1-5 fewer dry days per year), with increases of 1-5 more annual dry days for most remaining parts of Canterbury. By 2090 under RCP8.5, a similar geographic pattern of change is projected. Decreases in annual dry days are projected for many eastern parts of Canterbury (1-15 fewer dry days per year), with increases of 1-15 more dry days per year for most remaining parts of Canterbury.

Seasonal projections of change in dry days are shown for RCP4.5 by 2040 (Figure 5-13) and 2090 (Figure 5-15), and RCP8.5 by 2040 (Figure 5-14) and 2090 (Figure 5-16). The largest changes are projected by 2090 under RCP8.5. For example, 4-10 more spring and summer dry days are projected for many western parts of Canterbury by 2090 under RCP8.5. In contrast, 2-6 fewer summer and autumn dry days are projected for many eastern parts of Canterbury by 2090 under RCP8.5.

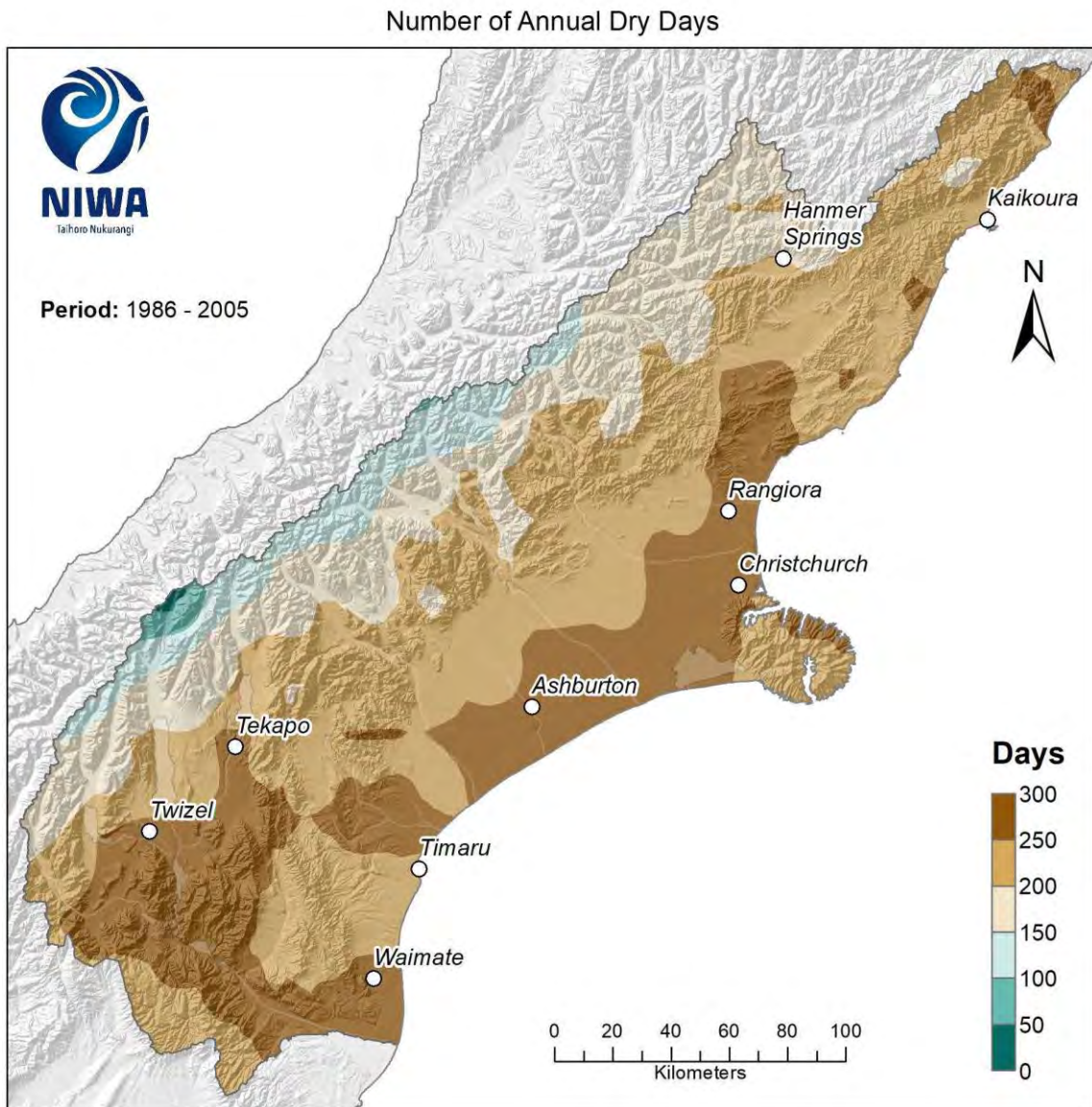


Figure 5-10: Modelled annual number of dry days (daily rainfall <1mm), average over 1986-2005. Results are based on dynamical downscaled projections using NIWA's Regional Climate Model. Resolution of projection is 5km x 5km.

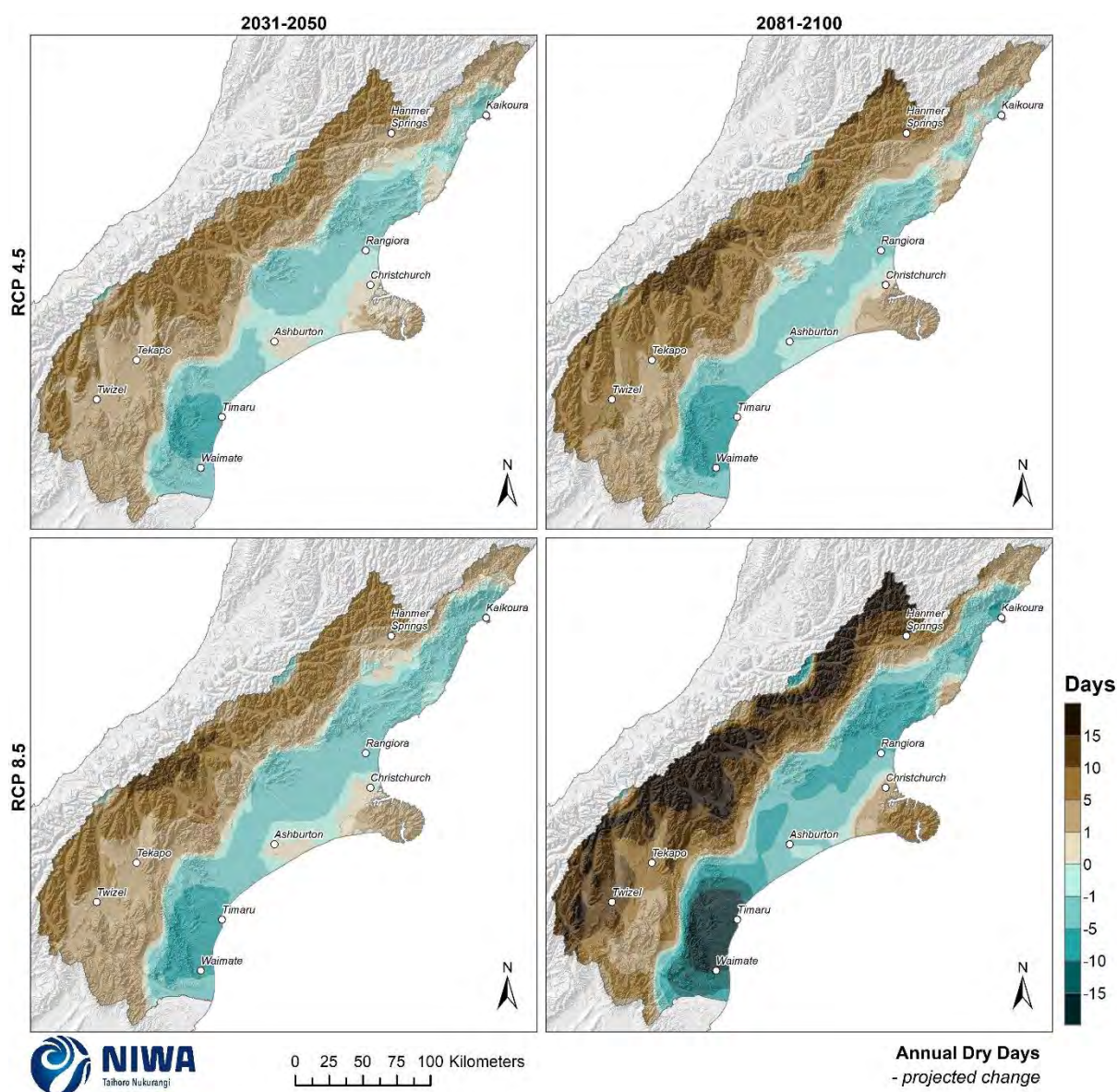


Figure 5-11: Projected annual number of dry day (daily rainfall <1mm) changes by 2040 and 2090, under RCP4.5 and RCP8.5. Climate change scenarios: RCP4.5 (top panels) and RCP8.5 (bottom panels). Time periods: mid-century (2031-2050; “2040” – panels on left) and end-century (2081-2100; “2090” – panels on right). Changes relative to 1986-2005 average, based on the average of six global climate models. Results are based on dynamical downscaled projections using NIWA’s Regional Climate Model. Resolution of projection is 5km x 5km.

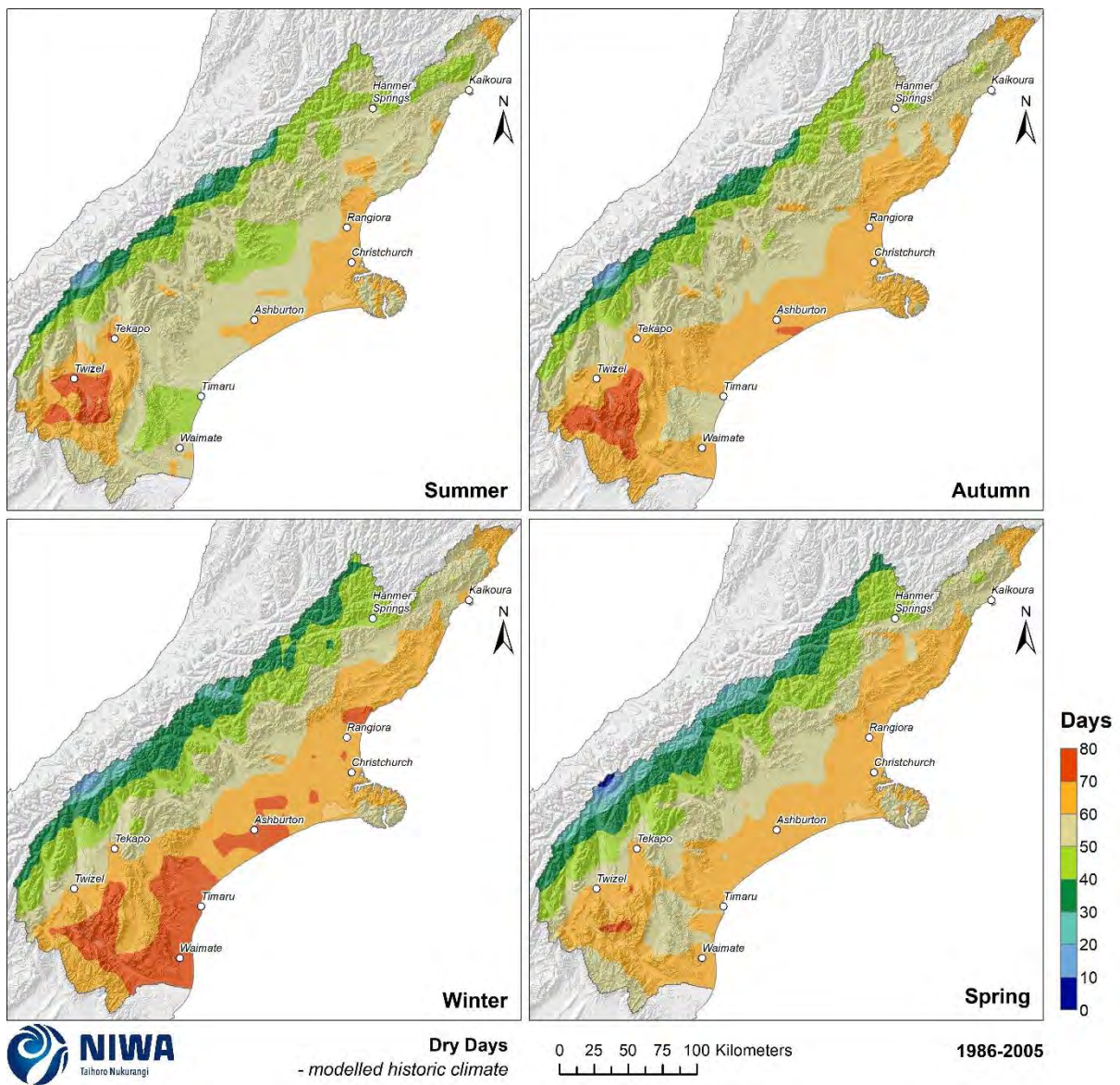


Figure 5-12: Modelled seasonal number of dry days (daily rainfall <1mm), average over 1986-2005. Results are based on dynamical downscaled projections using NIWA's Regional Climate Model. Resolution of projection is 5km x 5km.

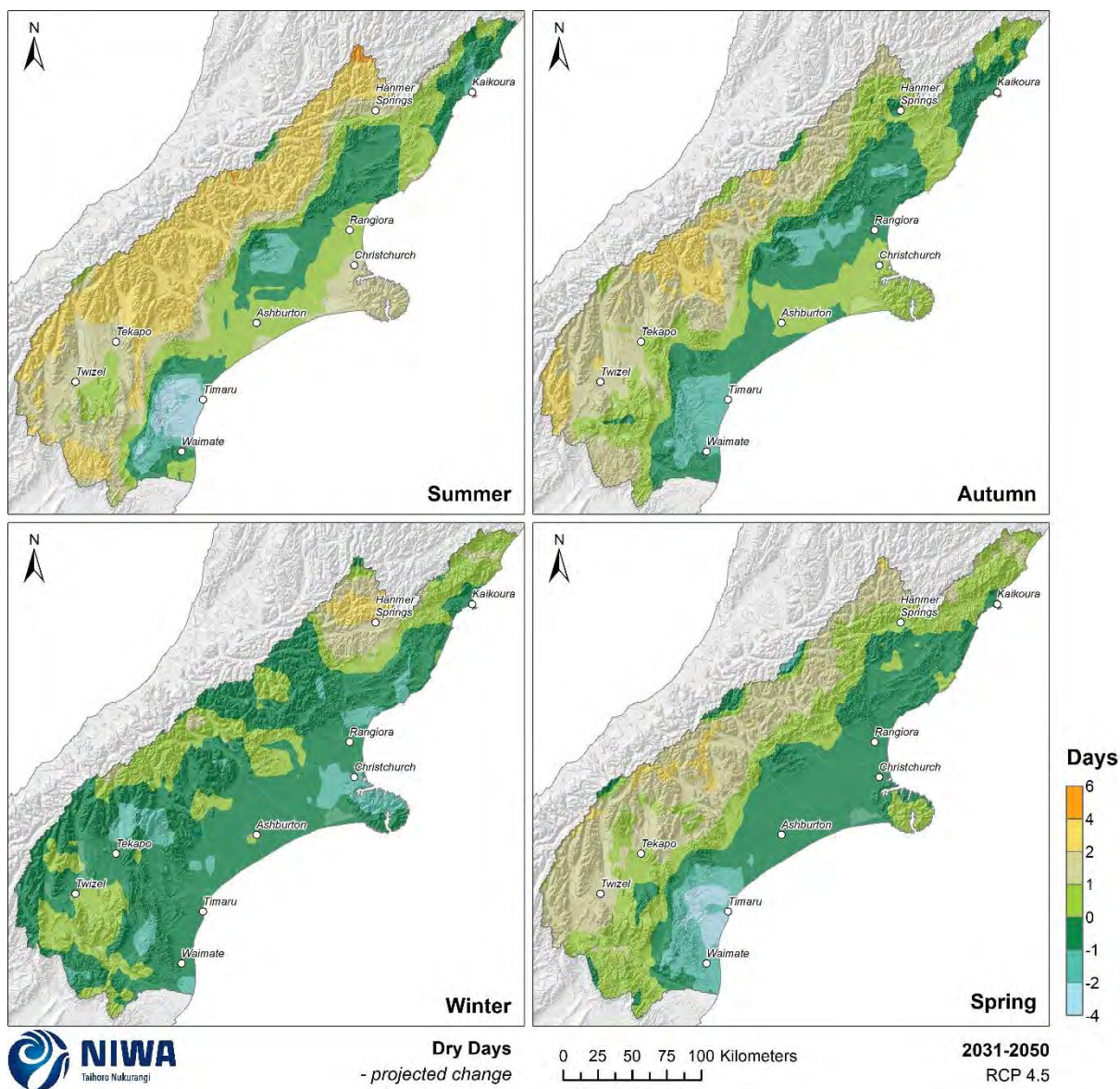


Figure 5-13: Projected seasonal number of dry day (daily rainfall <1mm) changes by 2040 for RCP4.5. Relative to 1986-2005 average, based on the average of six global climate models. Results are based on dynamical downscaled projections using NIWA's Regional Climate Model. Resolution of projection is 5km x 5km.

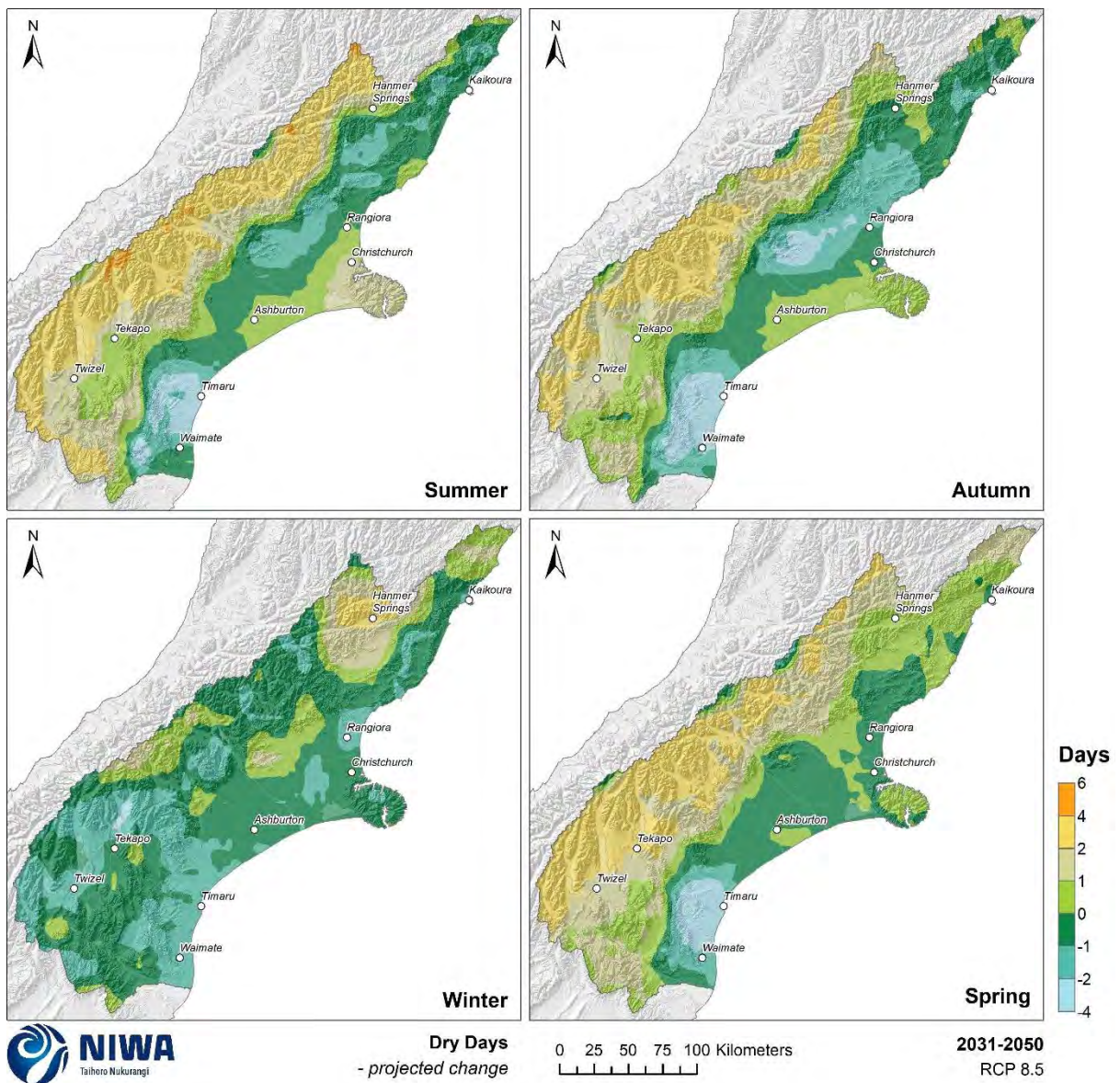


Figure 5-14: Projected seasonal number of dry day (daily rainfall <1mm) changes by 2040 for RCP8.5. Relative to 1986-2005 average, based on the average of six global climate models. Results are based on dynamical downscaled projections using NIWA's Regional Climate Model. Resolution of projection is 5km x 5km.

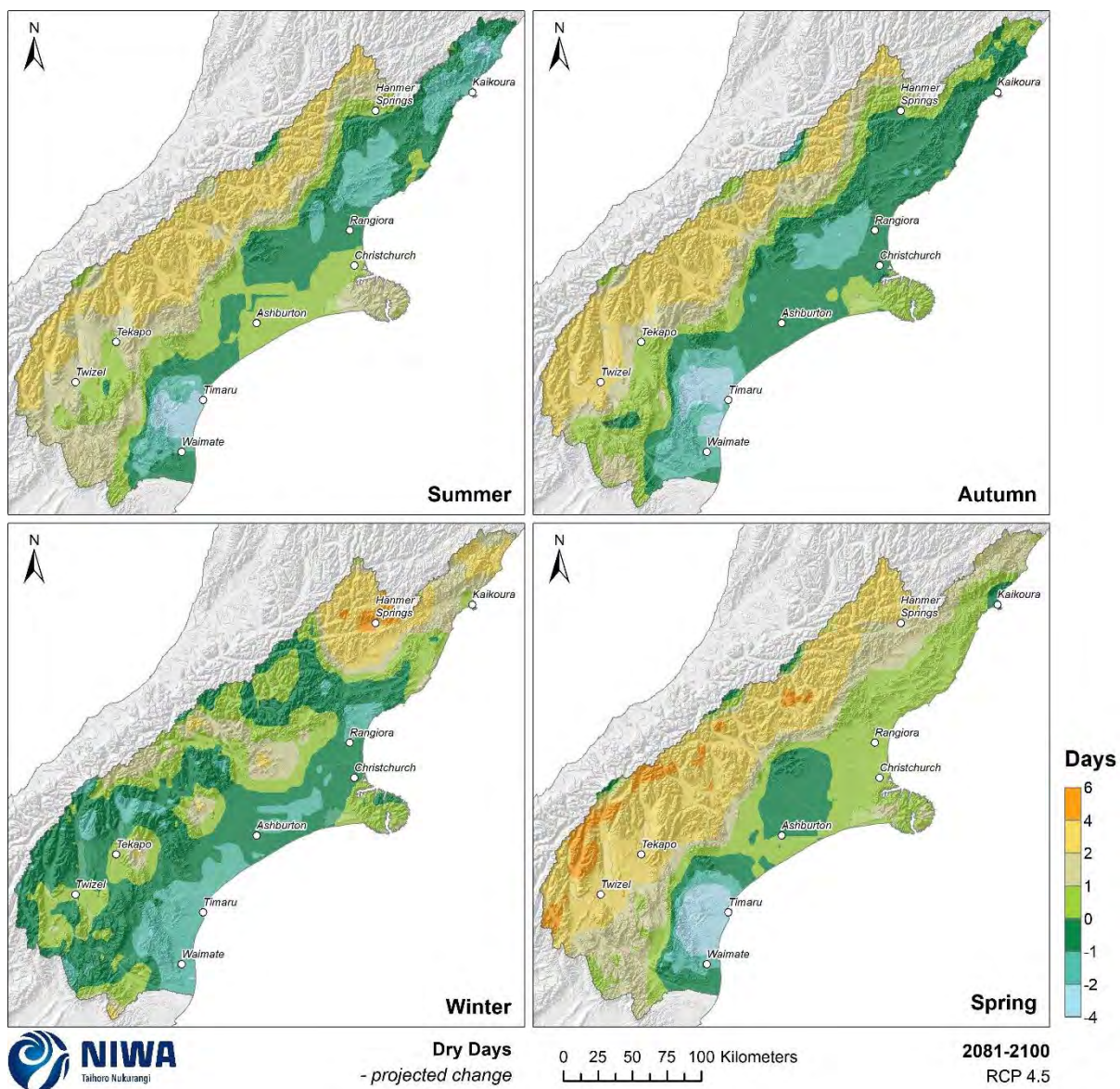


Figure 5-15: Projected seasonal number of dry day (daily rainfall <1mm) changes by 2090 for RCP4.5. Relative to 1986-2005 average, based on the average of six global climate models. Results are based on dynamical downscaled projections using NIWA's Regional Climate Model. Resolution of projection is 5km x 5km.

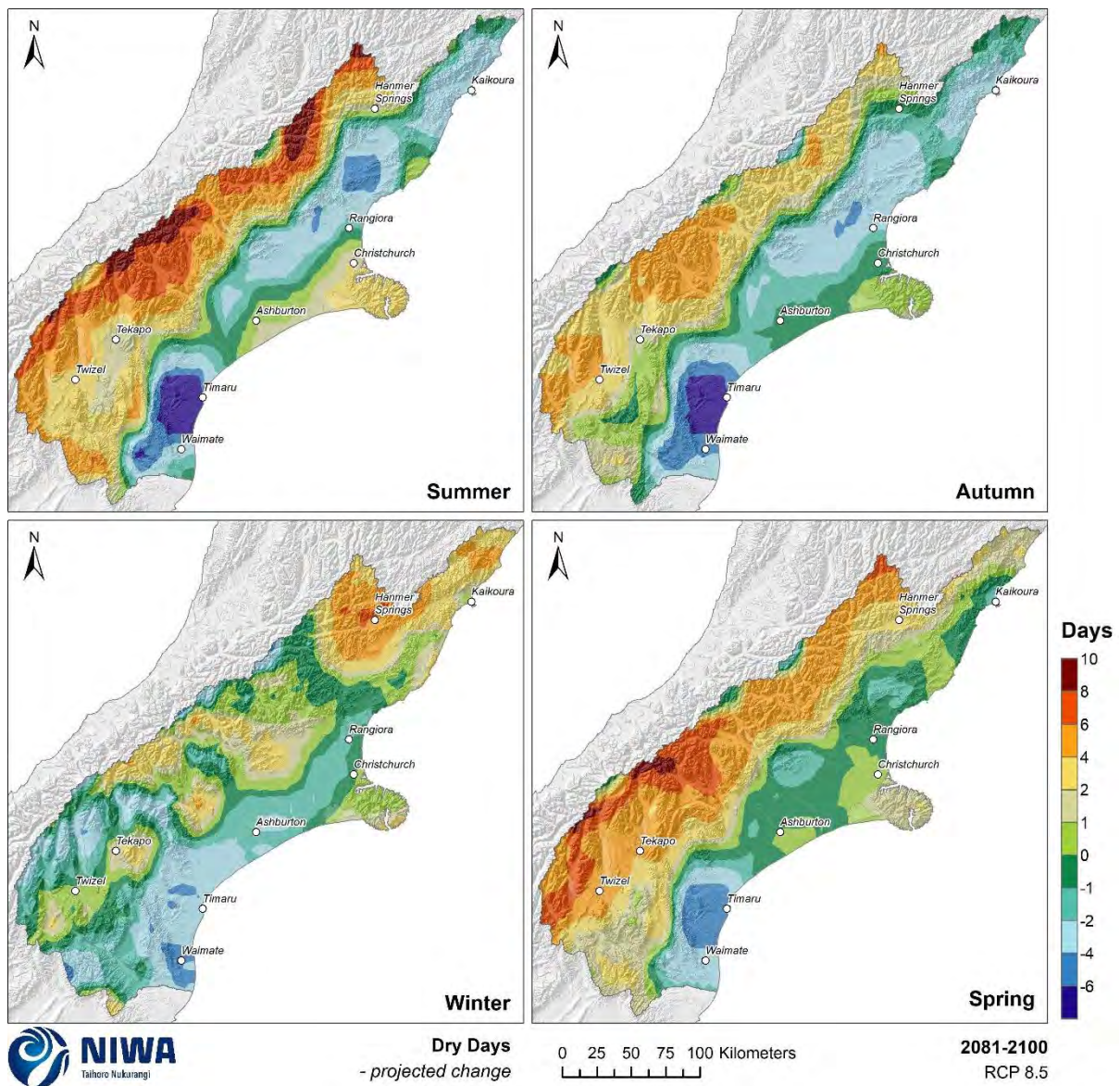


Figure 5-16: Projected seasonal number of dry day (daily rainfall <1mm) changes by 2090 for RCP8.5. Relative to 1986-2005 average, based on the average of six global climate models. Results are based on dynamical downscaled projections using NIWA's Regional Climate Model. Resolution of projection is 5km x 5km.

5.3 Snow days

Key message

- The number of snow days reduces everywhere, with the largest reduction in the coldest mountainous areas where there are a relatively large number of snow days in the baseline climate.

Snow days were estimated by counting precipitation days where the mean temperature was below freezing point. As such, it is a crude measure of snow days. It is likely the modelled number of historic (1986-2005) snow days (Figure 5-17) is underestimated, particularly for low elevation locations where snowfall often occurs when the ambient air temperature is at or above 0°C. Nevertheless, this measure provides a reference to which future changes can be compared. The modelled historic conditions suggest that 0-1 snow days per year occur for low elevation eastern areas, and 1-10 days per year for the Mackenzie Basin and other inland areas. 25-100 snow days per year occur in higher elevation alpine regions. In the future, the number of snow days reduces everywhere, with the largest reduction (typically 10-25 days) in the coldest mountainous areas where there are a relatively large number of snow days in the historic climate (Figure 5-18).

A factor needing further analysis is the potential change in snow amounts. In general, climate simulations show a reduction in snow days. It is possible snow amount could increase with rising temperatures in certain circumstances; a warmer atmosphere can hold more moisture, and on a day where temperatures are higher but still cool enough to snow, there is potential for increased heavy snowfalls. No analysis of snow extremes has been carried out at this point, however.

Number of Annual Snow Days

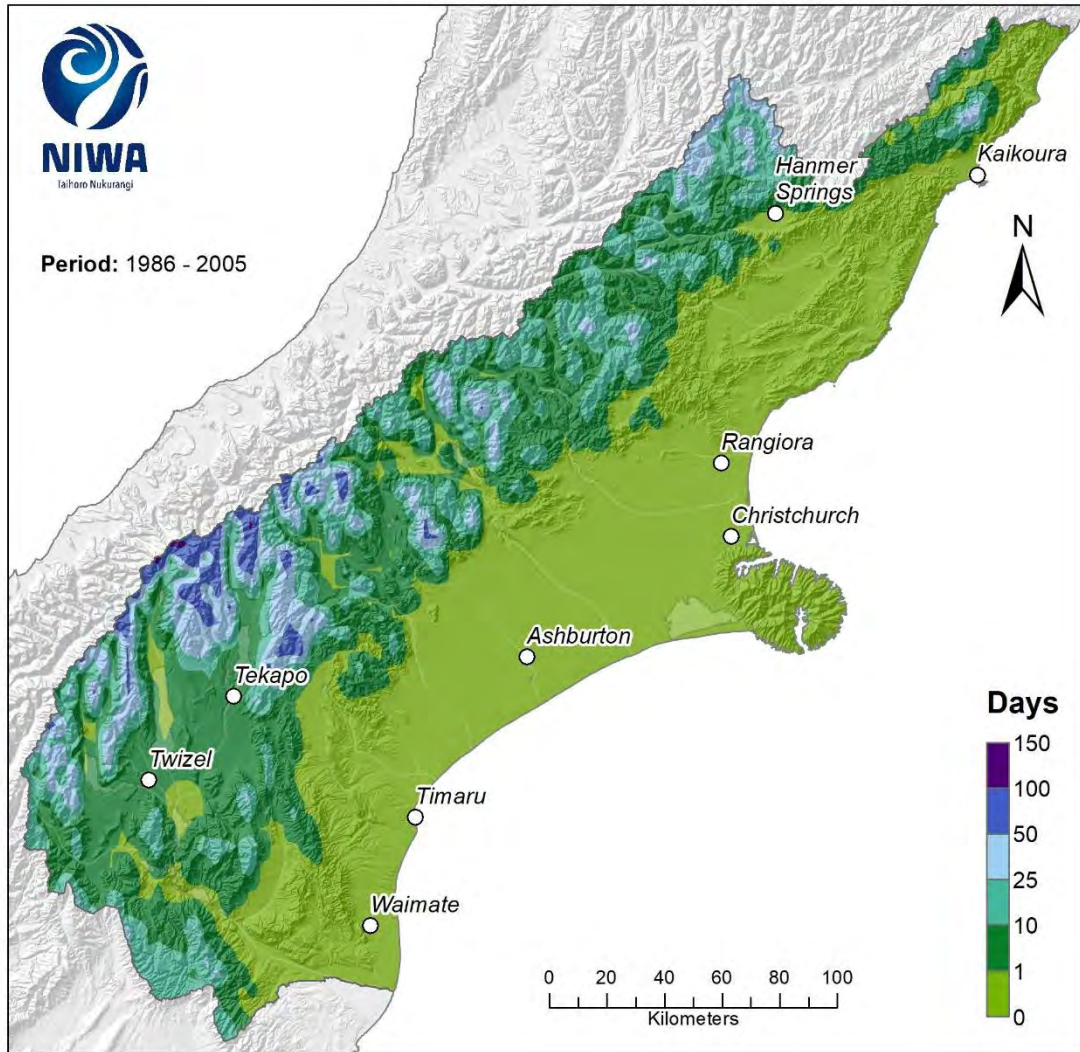


Figure 5-17: Modelled annual number of snow days, average over 1986-2005. Results are based on dynamical downscaled projections using NIWA's Regional Climate Model. Resolution of projection is 5km x 5km.

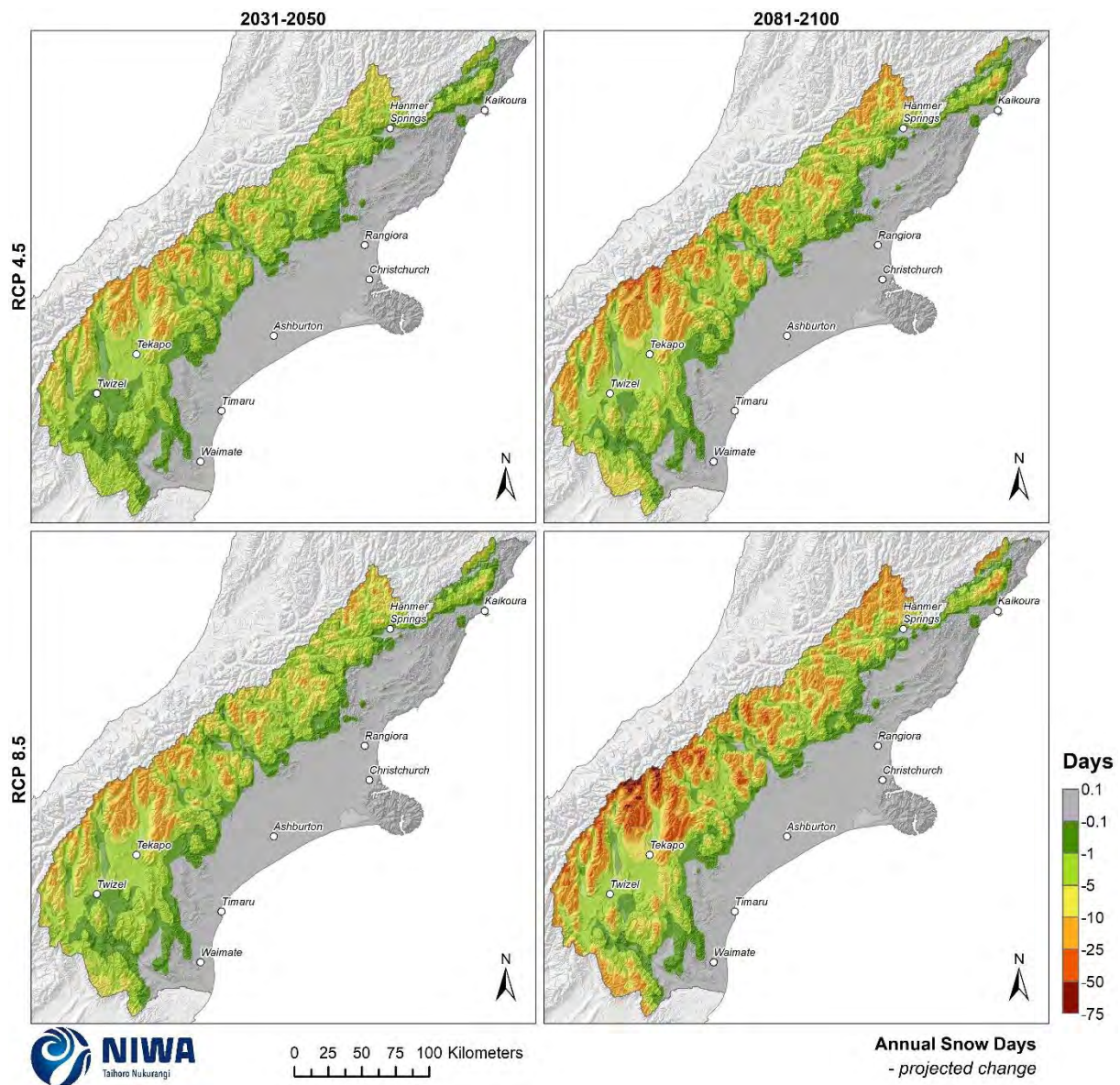


Figure 5-18: Projected change in the number of annual snow days by 2040 and 2090, under RCP4.5 and RCP8.5. Climate change scenarios: RCP4.5 (top panels) and RCP8.5 (bottom panels). Time periods: mid-century (2031-2050; “2040” – panels on left) and end-century (2081-2100; “2090” – panels on right). Changes relative to 1986-2005 average, based on the average of six global climate models. Results are based on dynamical downscaled projections using NIWA’s Regional Climate Model. Resolution of projection is 5km x 5km.

5.4 Potential evapotranspiration deficit

Key messages

- The future amount of accumulated PED is projected to increase across most of Canterbury, therefore drought potential is projected to increase.
- By 2040 under both RCPs, an increase in accumulated PED of 50-100 mm per year projected for most eastern parts of Canterbury.
- By 2090 under RCP8.5, an increase in accumulated PED of 100-200 mm per year projected for many inland areas of Canterbury and about Christchurch.

The measure of meteorological drought² that is used in this section is 'potential evapotranspiration deficit' (PED). Evapotranspiration is the process where water held in the soil is gradually released to the atmosphere through a combination of direct evaporation and transpiration from plants. As the growing season advances, the amount of water lost from the soil through evapotranspiration typically exceeds rainfall, giving rise to an increase in soil moisture deficit. As soil moisture decreases, pasture production becomes moisture-constrained and evapotranspiration can no longer meet atmospheric demand.

The difference between this demand (evapotranspiration deficit) and the actual evapotranspiration is defined as the 'potential evapotranspiration deficit' (PED). In practice, PED represents the total amount of water required by irrigation, or that needs to be replenished by rainfall, to maintain plant growth at levels unconstrained by water shortage. As such, PED estimates provide a robust measure of drought intensity and duration. Days when water demand is not met, and pasture growth is reduced, are often referred to as days of potential evapotranspiration deficit.

PED is calculated as the difference between potential evapotranspiration (PET) and rainfall, for days of soil moisture under half of available water capacity (AWC), where an AWC of 150mm for silty-loamy soils is consistent with estimates in previous studies (e.g. Mullan et al., 2005). PED, in units of mm, can be thought of as the amount of missing rainfall needed in order to keep pastures growing at optimum levels. Higher PED totals indicate drier soils. An increase in PED of 30 mm or more corresponds to an extra week of reduced grass growth. Accumulations of PED greater than 300 mm indicate very dry conditions.

Historic (average over 1986-2005) and future (average over 2031-2050 and 2081-2100) maps for PED are shown in this section. The historic maps show annual accumulated PED in units of mm and the future projection maps show the change in the annual accumulated PED compared with the historic period, in units of mm. Note that the historic maps are on a different colour scale to the future projection maps.

For the historic period, the highest PED accumulation is experienced about the Mackenzie Country (500-700 mm per year, on average) (Figure 5-19). Low-elevation eastern areas of Canterbury and the westernmost alpine areas generally experience between 0-300 mm of PED per year. Higher elevation areas in central parts of Canterbury generally experience 200-400 mm of PED per year.

² Meteorological drought happens when dry weather patterns dominate an area and resulting rainfall is low. Hydrological drought occurs when low water supply becomes evident, especially in streams, reservoirs, and groundwater levels, usually after an extended period of meteorological drought.

In the future, the amount of accumulated PED is projected to increase across most of the Canterbury region (Figure 5-20), therefore drought potential is projected to increase. The increase in PED is greatest by 2090 under RCP8.5. By 2040 under both RCPs, most eastern parts of the region are projected to experience an increase in PED of 50-100 mm per year. Some inland areas are projected to experience an additional 100-150 mm of PED per year. By 2090 under RCP8.5, PED is projected to increase by 100-200 mm per year for many inland parts of Canterbury as well as about Christchurch. In the southeast of Canterbury near Timaru, a small area is projected to observe a small decrease of between 0-25 mm of PED per year, however this decrease is not significant. This reflects the increase in annual rainfall that is projected for this area under the 2090 RCP8.5 scenario.

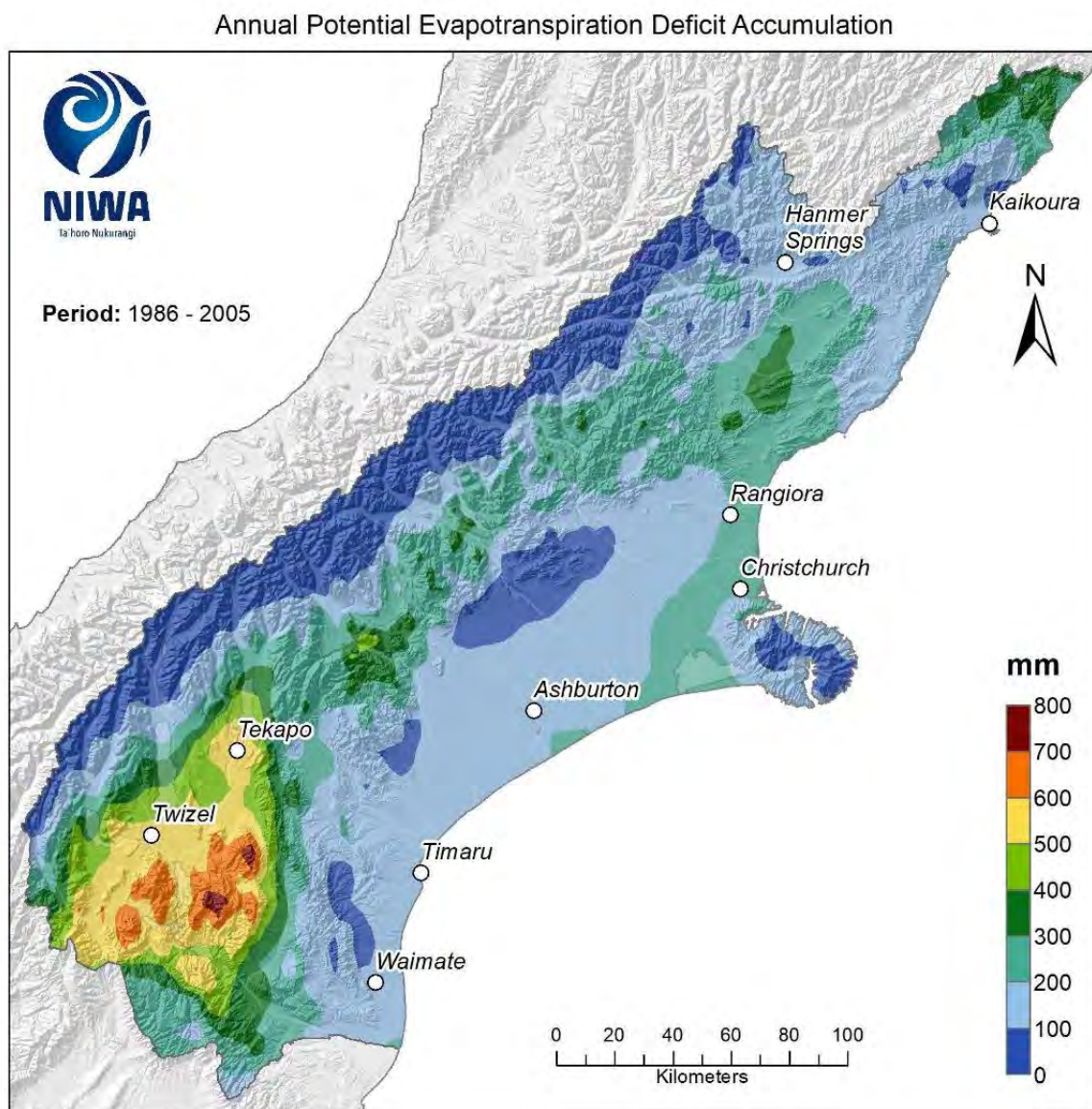


Figure 5-19: Modelled annual potential evapotranspiration deficit accumulation (mm), average over 1986-2005. Results are based on dynamical downscaled projections using NIWA's Regional Climate Model. Resolution of projection is 5km x 5km.

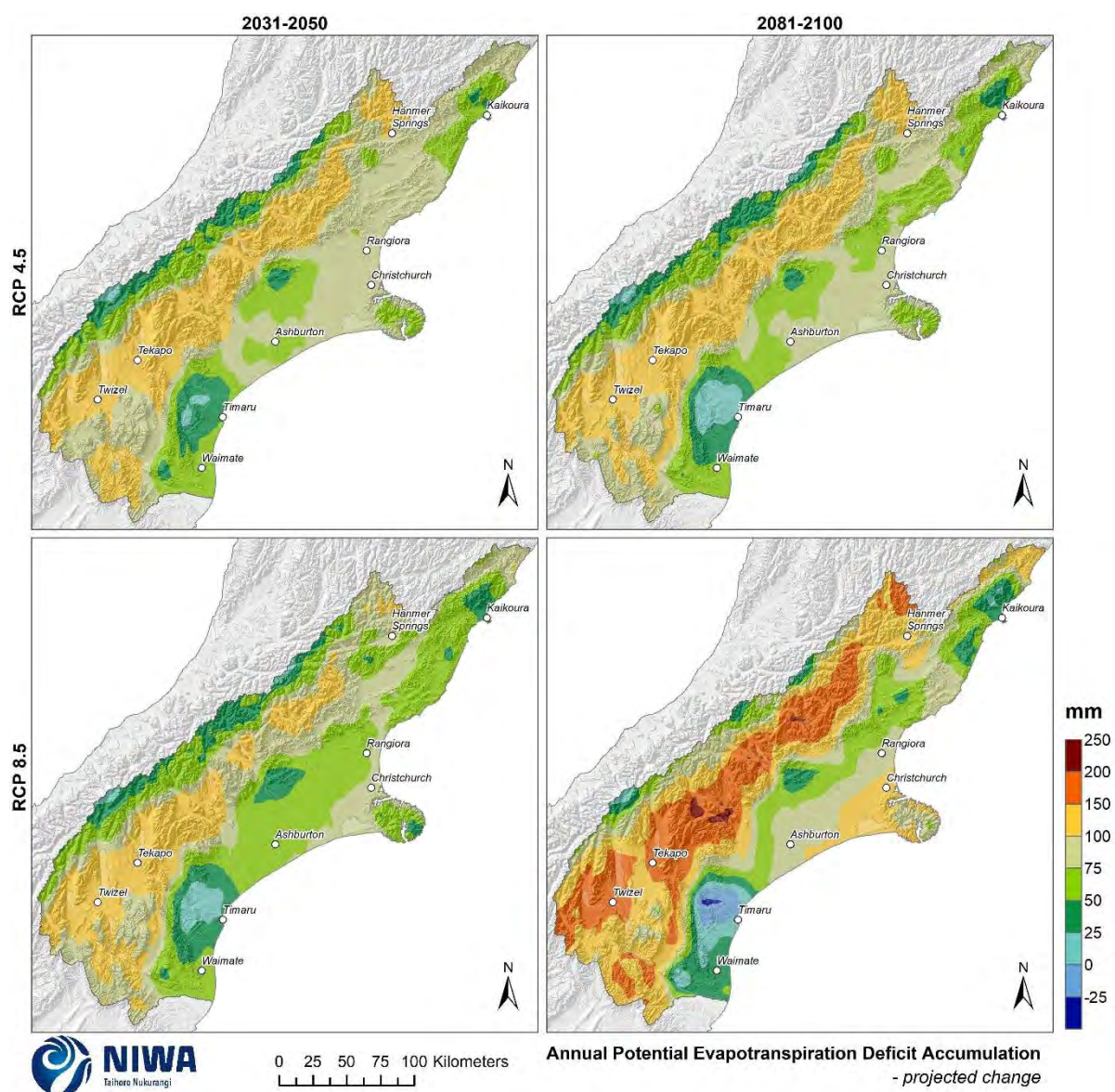


Figure 5-20: Projected annual potential evapotranspiration deficit (PED) accumulation changes for RCP4.5 and RCP8.5, by 2040 and 2090. Relative to 1986-2005 average, based on the average of six global climate models. Results are based on dynamical downscaled projections using NIWA's Regional Climate Model. Resolution of projection is 5km x 5km.

5.5 Soil moisture deficit

Key messages

- By 2040 under RCP4.5 the number of SMD days per year decreases for many eastern parts of Canterbury (3-10 fewer SMD days per year), with increases of 5-10 annual SMD days for some western parts of the region.
- By 2090 under RCP8.5, decreases in annual SMD days of 5-30 days are projected for many southern parts of Canterbury, with increases of 5-20 SMD days per year for many inland parts of the region.
- Seasonally, the largest changes are projected for winter by 2090 under RCP8.5: e.g. 15-30 fewer *winter* SMD days projected for much of eastern South Canterbury.

Soil moisture deficit (SMD) is calculated based on incoming daily rainfall (mm), outgoing daily potential evapotranspiration (PET), and a fixed available water capacity of 150 mm (the amount of water in the soil 'reservoir' that plants can use). In the calculation, evapotranspiration continues at its potential rate until about half of the water available to plants is used up (75 mm out of the total 150 mm available). Subsequently, the rate of evapotranspiration decreases, in the absence of rain, as further water extraction takes place. Evapotranspiration is assumed to cease if all the available water is used up (i.e. all 150 mm).

A day of SMD is considered in this report to be when soil moisture is below 75 mm of available soil water capacity. The timing of changes in the days of soil moisture deficit projections indicates how droughts may change in timing throughout the year. Soil moisture deficit and PED are similar measures of dryness, but in this report SMD is measured in days and PED is measured in mm of accumulation, so PED is a more sensitive measure of drought intensity than SMD.

Historic (average over 1986-2005) and future (average over 2031-2050 and 2081-2100) maps for days of SMD are shown in this section. The historic maps show the annual and seasonal number of days of SMD and the future projection maps show the change in the number of days of SMD compared with the historic period. Note that the historic maps are on a different colour scale to the future projection maps.

Historically, the largest annual number of SMD days is experienced in southern parts of Canterbury (300-350 days per year; Figure 5-21). Areas around Ashburton, Christchurch and Rangiora average around 250-300 SMD days per year. Annual number of SMD days are fewest along the western border of the region, averaging <150 SMD days in these parts. Summer is typically the season with the largest number of SMD days, with 80-90 dry days for much of the region (Figure 5-23).

By 2040 under RCP4.5 (Figure 5-22), the number of SMD days per year decreases for many eastern parts of Canterbury (3-10 fewer SMD days per year), with increases of 5-10 annual SMD days for some western parts of the region. By 2090 under RCP8.5, decreases in annual SMD days are projected for many southern parts of Canterbury (5-30 fewer SMD days per year), with increases of 5-20 SMD days per year for many inland parts of the region. This spatial pattern resembles that observed for the corresponding scenarios of rainfall (Section 5.1; Figure 5-2) and PED (Section 5.4; Figure 5-19).

Seasonal projections of change in SMD days are shown for RCP4.5 by 2040 (Figure 5-24) and 2090 (Figure 5-26), and RCP8.5 by 2040 (Figure 5-25) and 2090 (Figure 5-27). By 2040 under RCP4.5, summer increases of 3-10 SMD days are projected for most of Canterbury. The largest seasonal changes are projected for winter by 2090 under RCP8.5. For example, 15-30 fewer winter SMD days are projected for much of eastern South Canterbury by 2090 under RCP8.5.

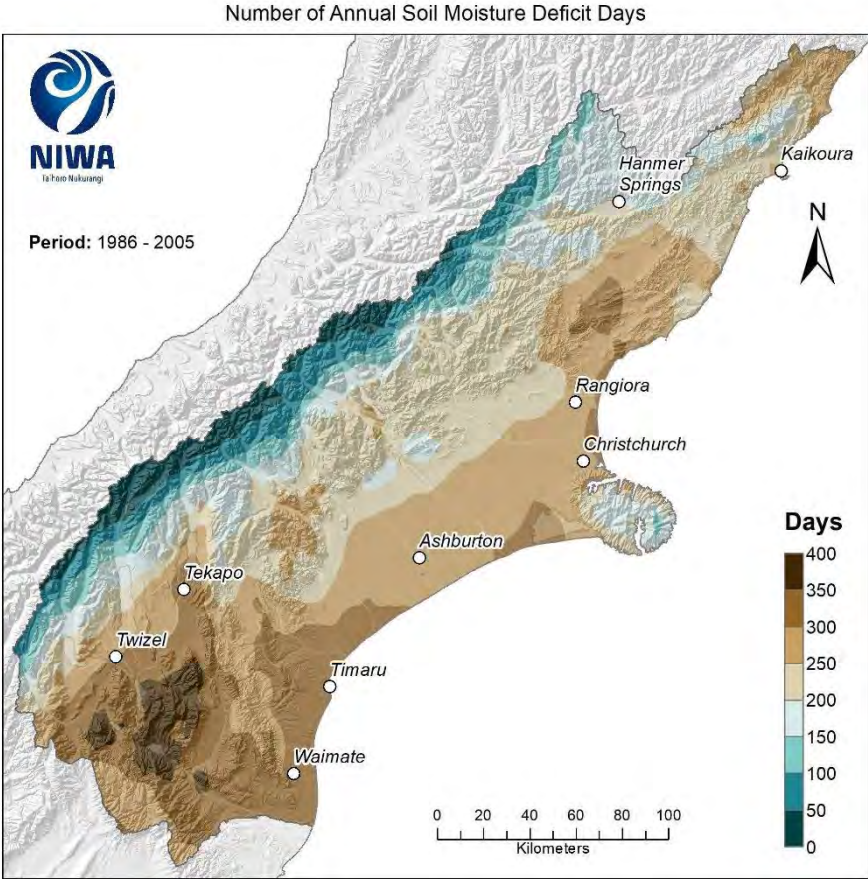


Figure 5-21: Modelled annual number of days of soil moisture deficit, average over 1986-2005. Results are based on dynamical downscaled projections using NIWA's Regional Climate Model. Resolution of projection is 5km x 5km.

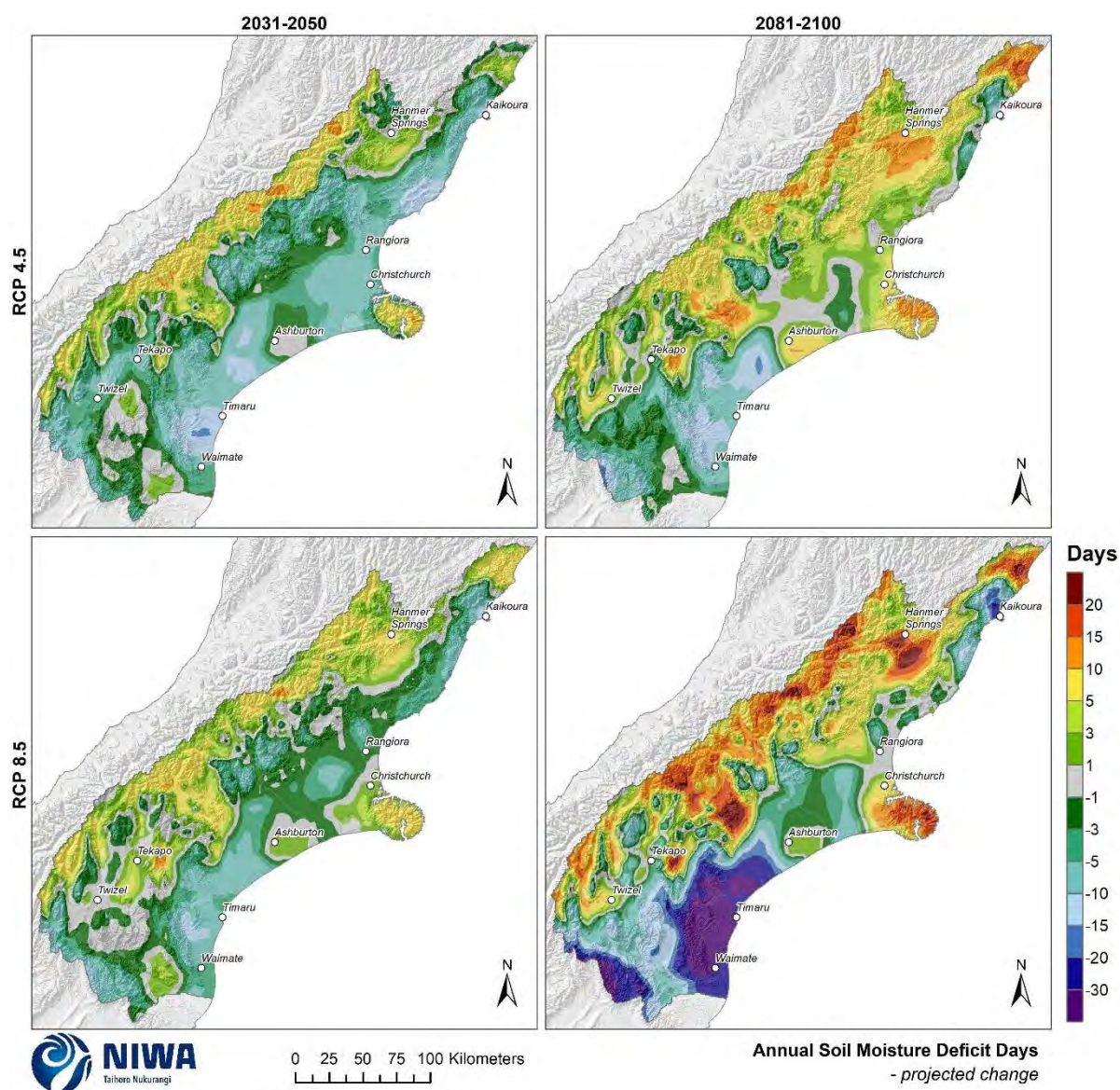


Figure 5-22: Projected change in the annual number of soil moisture deficit days by 2040 and 2090, under RCP4.5 and RCP8.5. Climate change scenarios: RCP4.5 (top panels) and RCP8.5 (bottom panels). Time periods: mid-century (2031-2050; “2040” – panels on left) and end-century (2081-2100; “2090” – panels on right). Changes relative to 1986-2005 average, based on the average of six global climate models. Results are based on dynamical downscaled projections using NIWA’s Regional Climate Model. Resolution of projection is 5km x 5km.

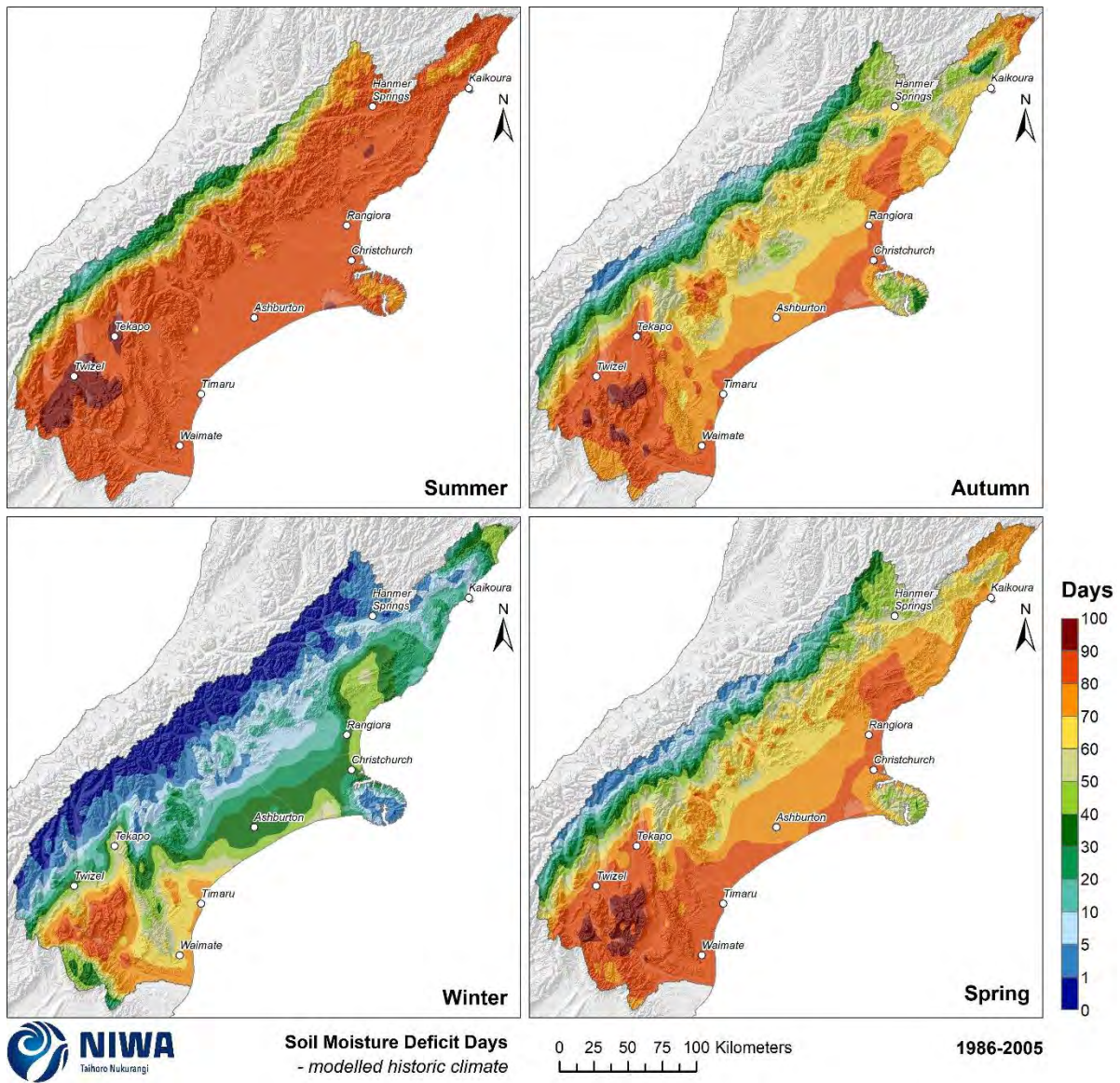


Figure 5-23: Modelled seasonal number of days of soil moisture deficit, average over 1986-2005. Results are based on dynamical downscaled projections using NIWA's Regional Climate Model. Resolution of projection is 5km x 5km.

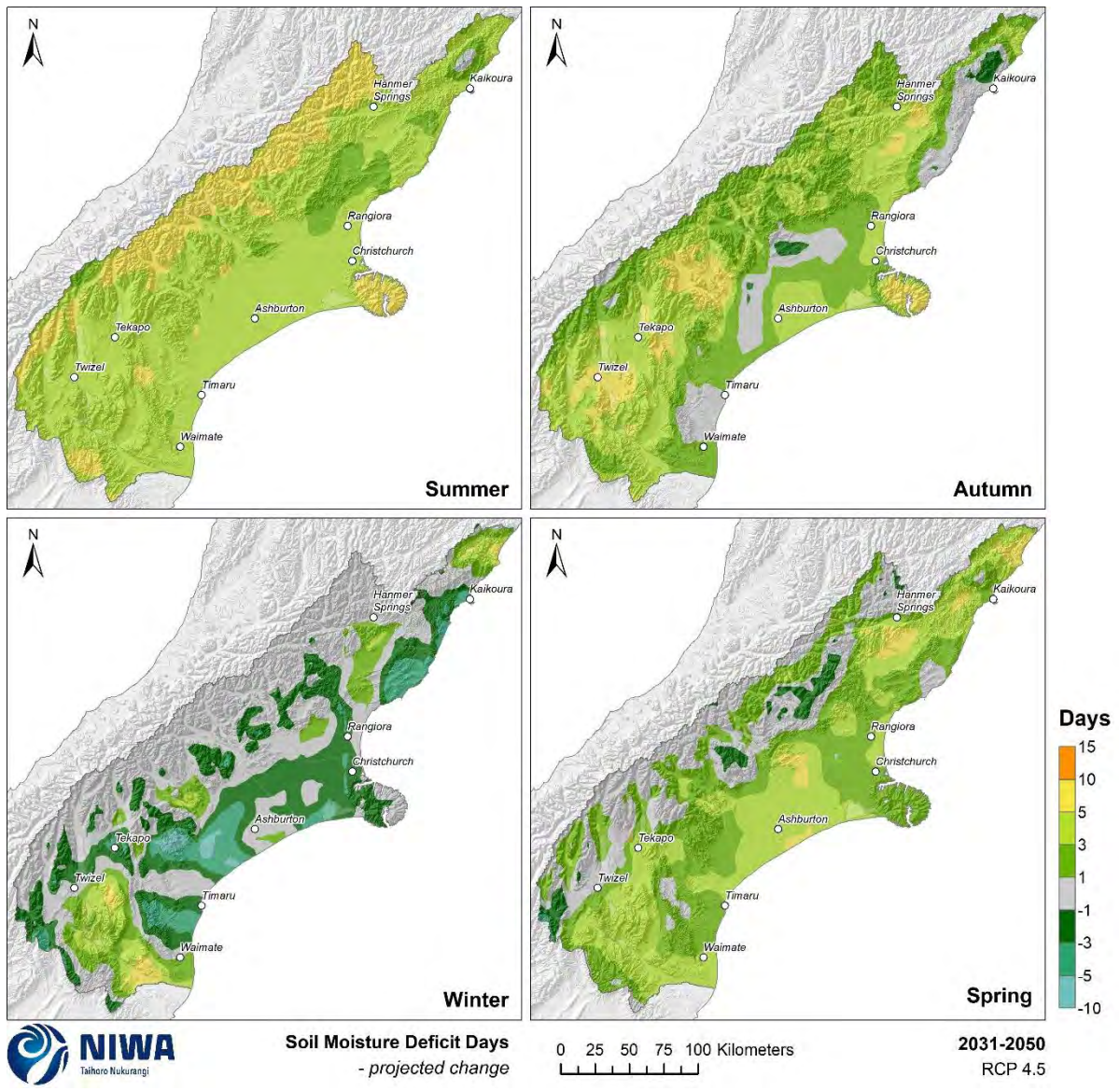


Figure 5-24: Projected change in the number of seasonal soil moisture deficit days by 2040 for RCP4.5. Relative to 1986-2005 average, based on the average of six global climate models. Results are based on dynamical downscaled projections using NIWA's Regional Climate Model. Resolution of projection is 5km x 5km.

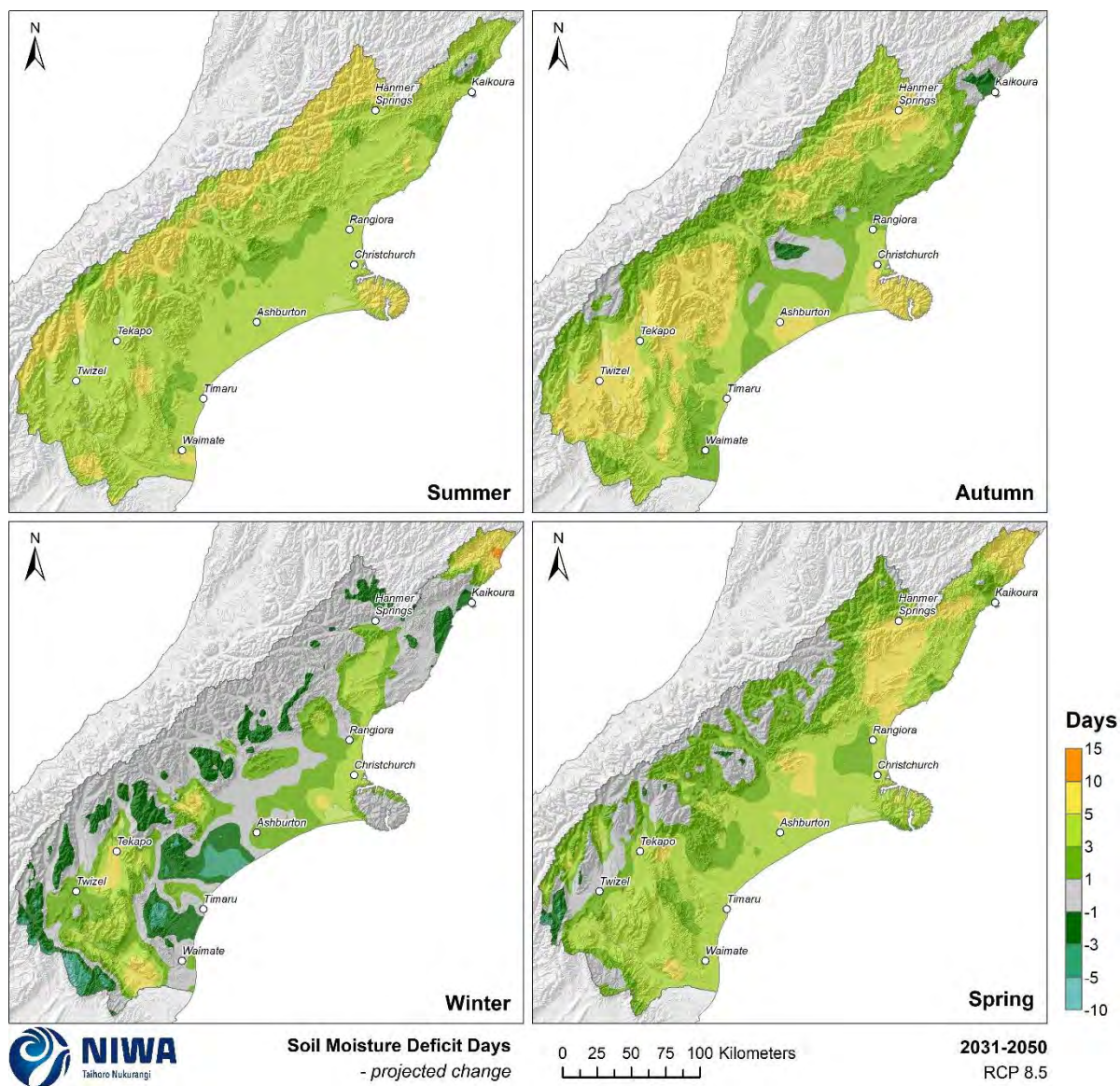


Figure 5-25: Projected change in the number of seasonal soil moisture deficit days by 2040 for RCP8.5. Relative to 1986-2005 average, based on the average of six global climate models. Results are based on dynamical downscaled projections using NIWA's Regional Climate Model. Resolution of projection is 5km x 5km.

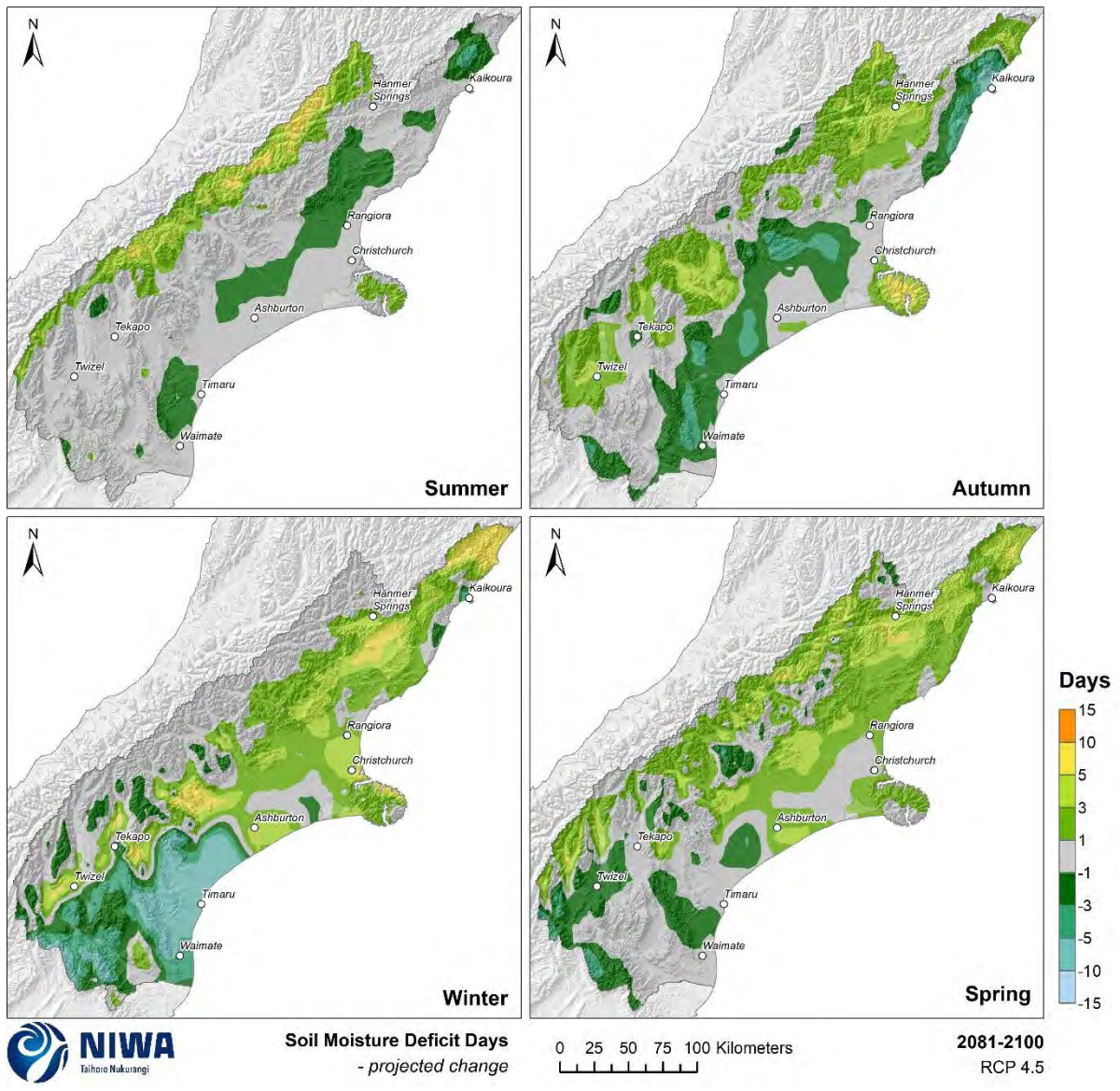


Figure 5-26: Projected change in the number of seasonal soil moisture deficit days by 2090 for RCP4.5. Relative to 1986-2005 average, based on the average of six global climate models. Results are based on dynamical downscaled projections using NIWA's Regional Climate Model. Resolution of projection is 5km x 5km.

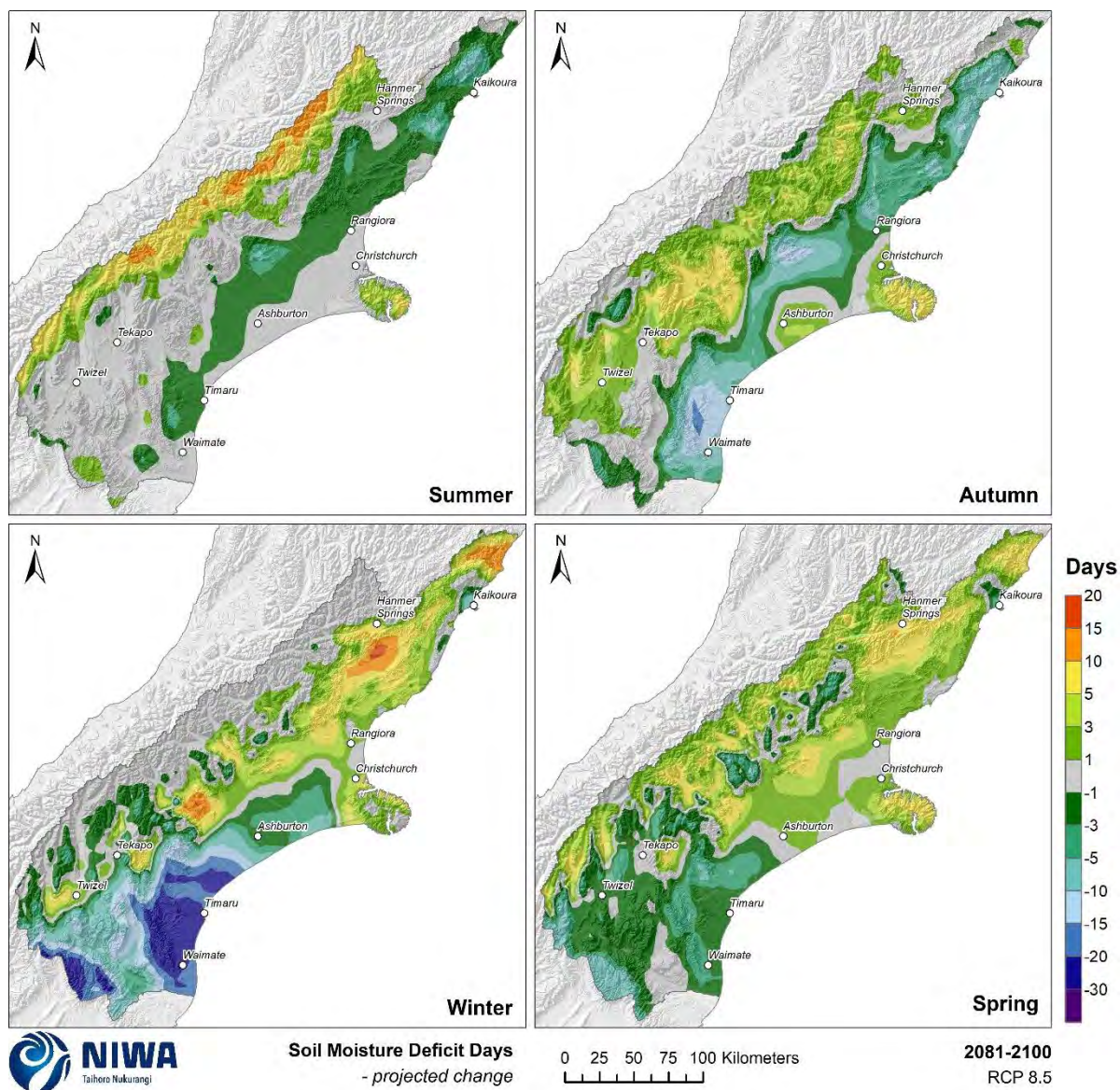


Figure 5-27: Projected change in the number of seasonal soil moisture deficit days by 2090 for RCP8.5. Relative to 1986-2005 average, based on the average of six global climate models. Results are based on dynamical downscaled projections using NIWA's Regional Climate Model. Resolution of projection is 5km x 5km.

6 Other climate variables

Modelled wind, surface solar radiation and relative humidity data have not had bias correction processes applied as has been carried out for temperature and rainfall. For this reason, only the future *relative changes* in these variables have been reported here using the modelled climate data. By doing this, the effect of biases in absolute values of these variables are minimised.

6.1 Mean wind speed

Key messages

- Increases in annual mean wind speed are typically projected for Canterbury; mostly ranging between 0-5%, but up to 10% by 2090 under RCP8.5.
- Seasonally, the largest changes are projected for winter and spring by 2090 under RCP8.5: e.g. 5-15% increase in mean wind speed projected for much of Canterbury, with 15-25% increases projected for inland areas north and west of Rangiora.

Future change (average over 2031-2050 and 2081-2100) maps for annual and seasonal mean wind speed are shown in this section.

In the future, annual mean wind speed is mostly projected to slightly increase in Canterbury (Figure 6-1). By 2040 under RCP4.5 and RCP8.5, small annual mean wind speed increases ranging between 0-5% are projected for most of Canterbury, with minimal change (between 0-2% reduction) projected for isolated inland and coastal areas. By 2090 under RCP4.5, small increases in annual mean wind speed of between 0-5% are projected for most of Canterbury. Isolated areas (mainly about Tekapo and Kaikoura) are projected to observe a minimal change in annual mean wind speed (between 0-2% reduction). The greatest annual change is projected by 2090 under RCP8.5. Under this scenario, much of Canterbury is projected to observe a 2-10% increase in annual mean wind speed.

Seasonal projections of change in mean wind speed are shown for RCP4.5 by 2040 (Figure 6-2) and 2090 (Figure 6-4), and RCP8.5 by 2040 (Figure 6-3) and 2090 (Figure 6-5). By 2040 under RCP4.5, summer, autumn and spring increases in mean wind speed between 0-5% are projected for most of Canterbury. During autumn, decreases in mean wind speed of 2-5% are projected about Tekapo. Winter mean wind speed is projected to decrease by 2-10% for some parts of the Southern Alps to the north of Tekapo. By 2040 under RCP8.5, projected changes to mean wind speed during summer and autumn range between -2% to +5% for most of Canterbury. Spring is generally projected to observe an increase in mean wind speed of 2-10%, with a small area of decreasing wind speed (between 0-5% reduction) projected about Tekapo. Winter mean wind speed increases of 5-10% are projected about and to the south of Hanmer Springs, with decreases of 2-10% projected in parts of the Southern Alps north of Tekapo.

By 2090 under RCP4.5, mean wind speed during summer and autumn is projected to increase between 0-5% for most of Canterbury. Winter mean wind speed increases of 5-10% are projected for many inland areas north and west of Rangiora. Spring mean wind speed decreases of 2-10% are projected about Tekapo. The largest seasonal changes are projected for winter and spring by 2090 under RCP8.5. During these seasons, mean wind speed increases of 5-15% are projected for many parts of Canterbury. Under this scenario, winter mean wind speed increases of 15-25% are projected for inland areas to the north and west of Rangiora.

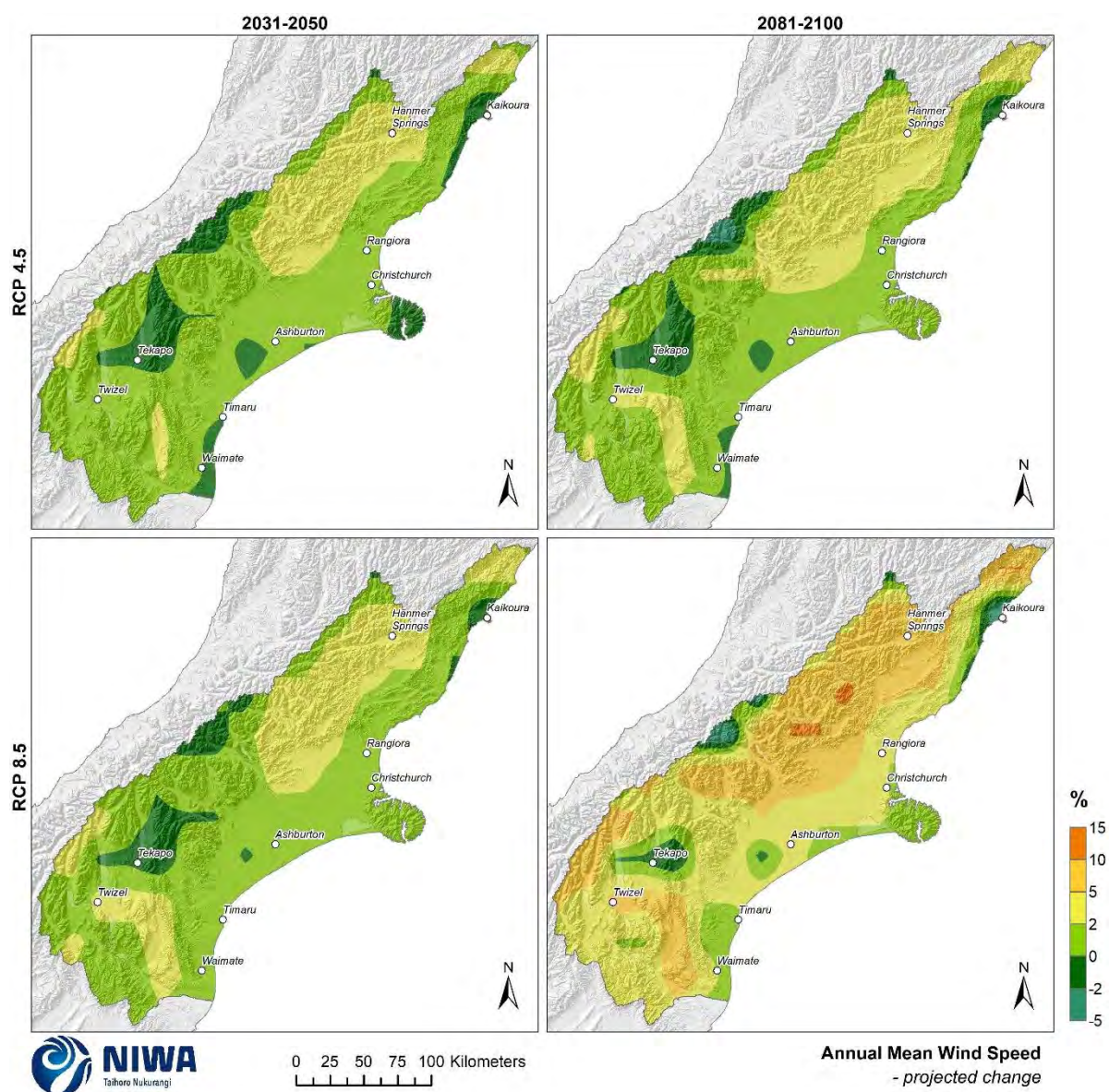


Figure 6-1: Projected annual mean wind speed changes by 2040 and 2090, under RCP4.5 and RCP8.5. Climate change scenarios: RCP4.5 (top panels) and RCP8.5 (bottom panels). Time periods: mid-century (2031-2050; “2040” – panels on left) and end-century (2081-2100; “2090” – panels on right). Changes relative to 1986-2005 average, based on the average of six global climate models. Results are based on dynamical downscaled projections using NIWA's Regional Climate Model. Resolution of projection is 5km x 5km.

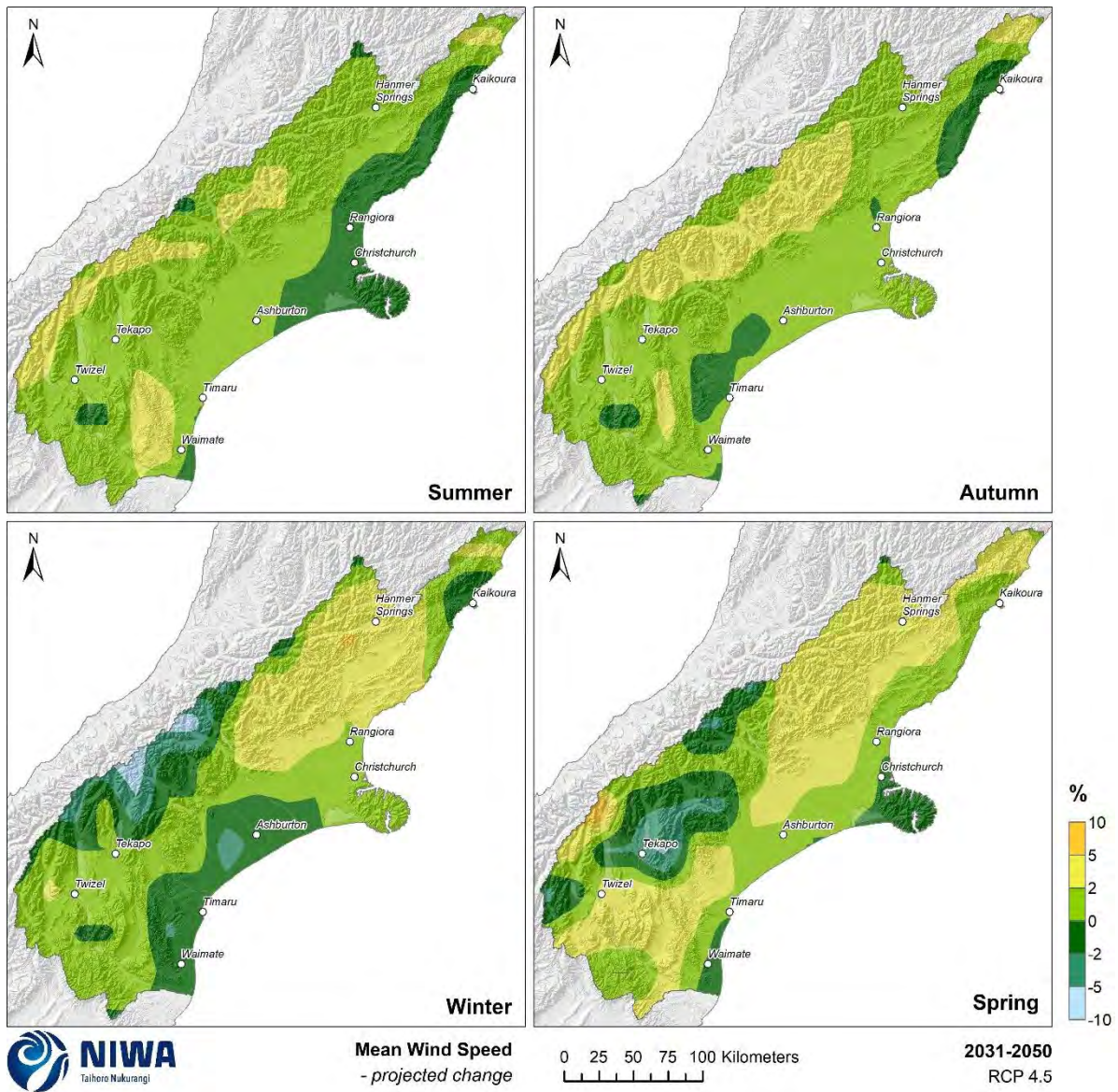


Figure 6-2: Projected seasonal mean wind speed changes by 2040 for RCP4.5. Relative to 1986-2005 average, based on the average of six global climate models. Results are based on dynamical downscaled projections using NIWA's Regional Climate Model. Resolution of projection is 5km x 5km.

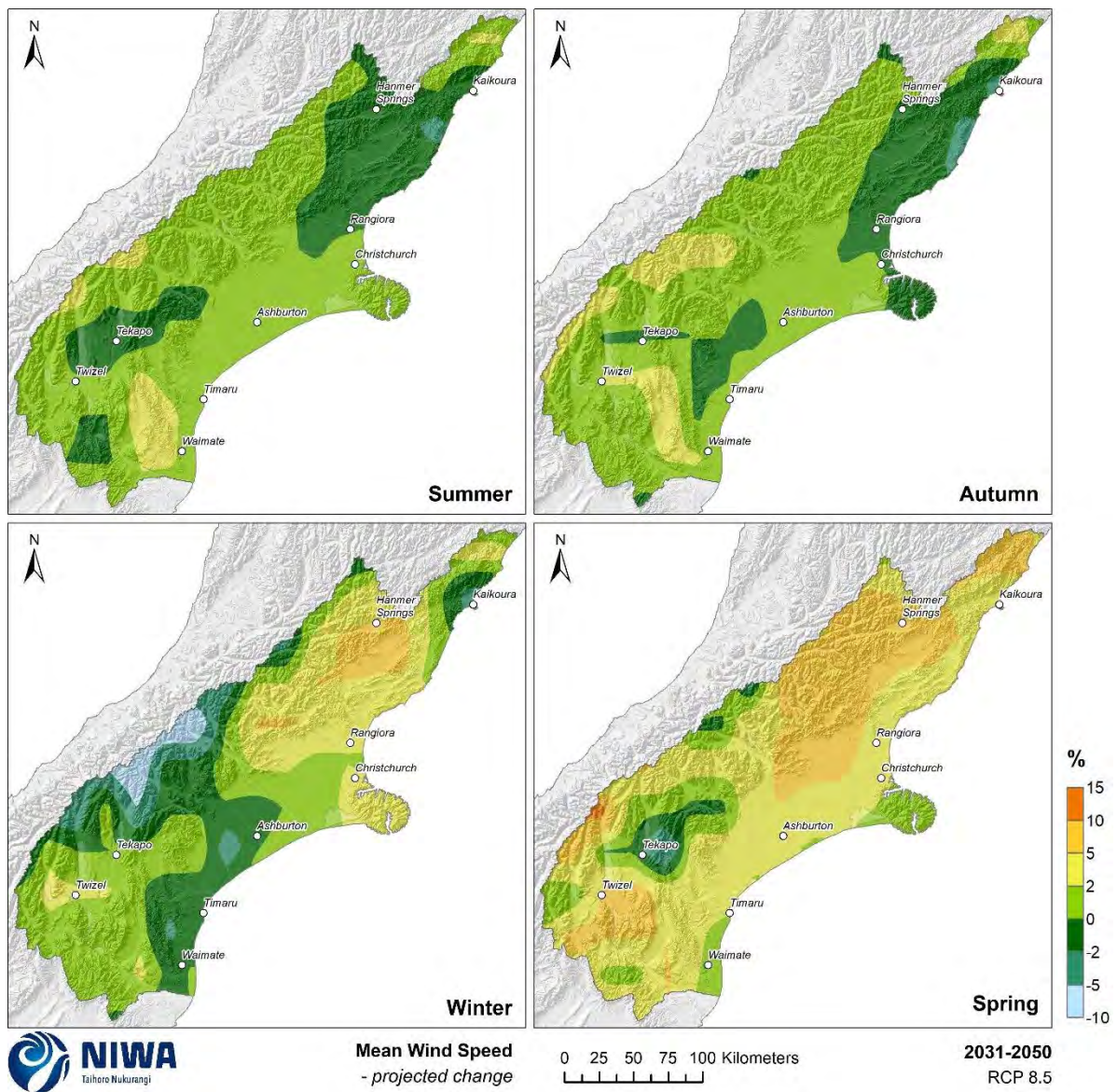


Figure 6-3: Projected seasonal mean wind speed changes by 2040 for RCP8.5. Relative to 1986-2005 average, based on the average of six global climate models. Results are based on dynamical downscaled projections using NIWA's Regional Climate Model. Resolution of projection is 5km x 5km.

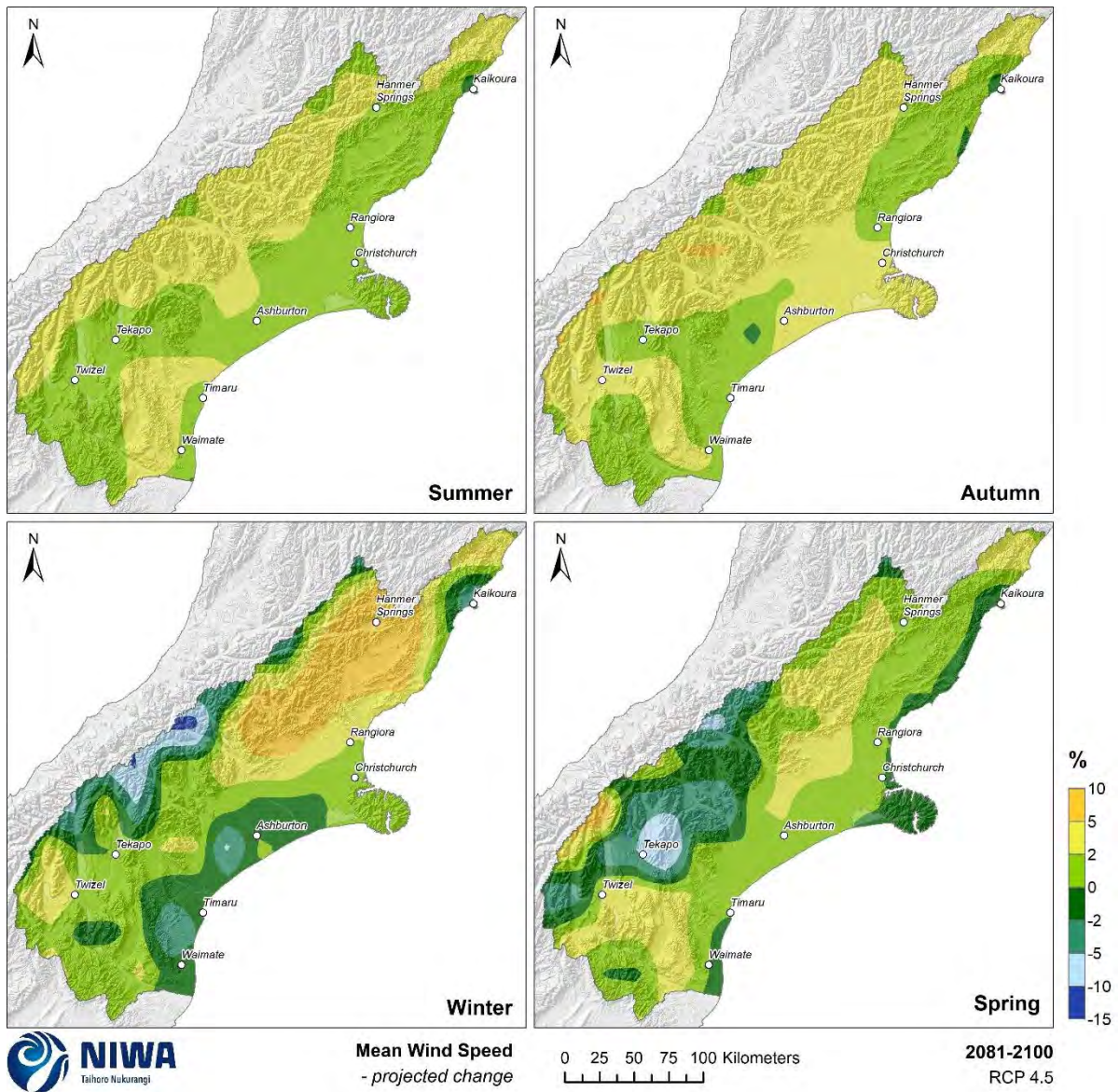


Figure 6-4: Projected seasonal mean wind speed changes by 2090 for RCP4.5. Relative to 1986-2005 average, based on the average of six global climate models. Results are based on dynamical downscaled projections using NIWA's Regional Climate Model. Resolution of projection is 5km x 5km.

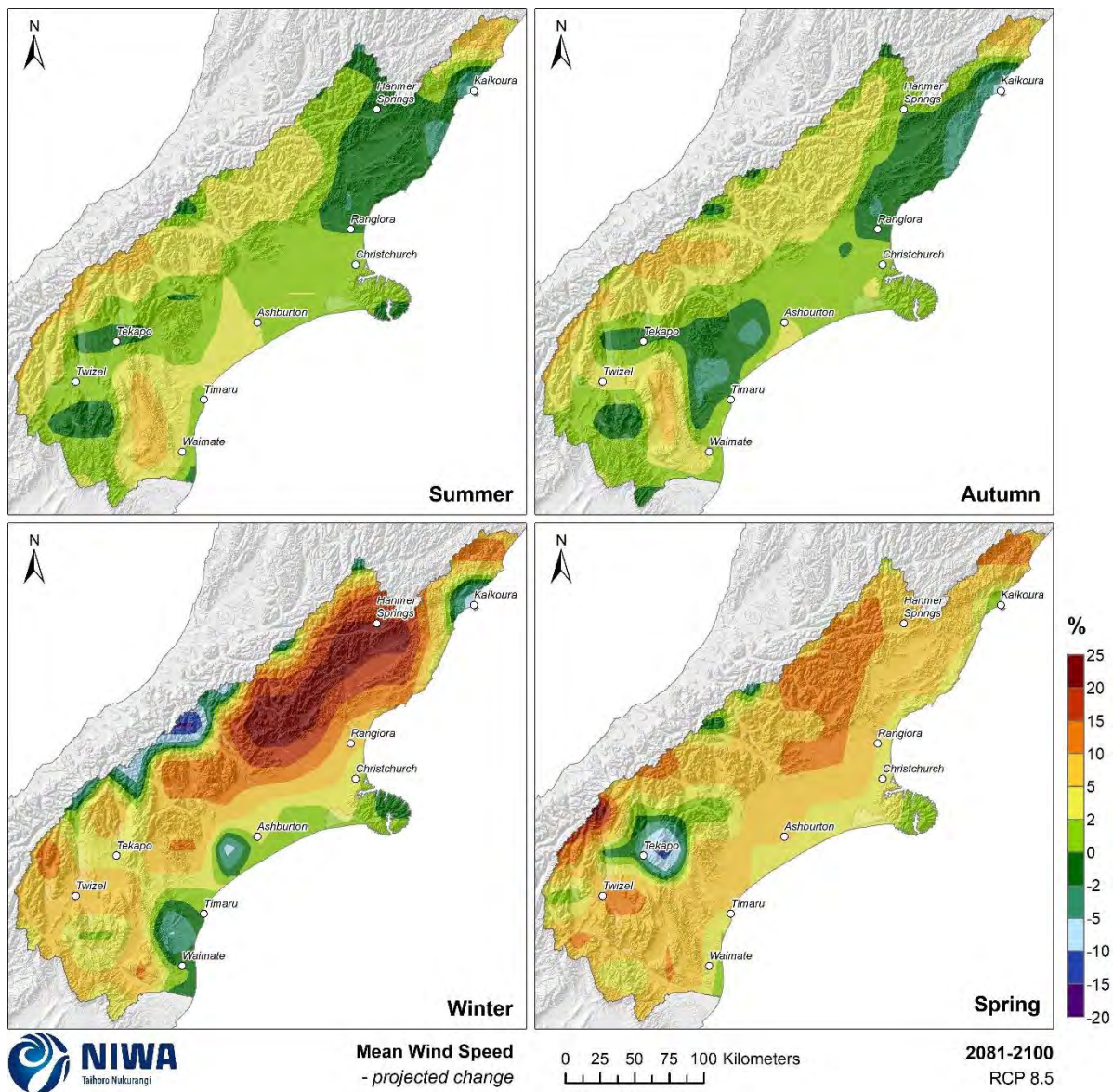


Figure 6-5: Projected seasonal mean wind speed changes by 2090 for RCP8.5. Relative to 1986-2005 average, based on the average of six global climate models. Results are based on dynamical downscaled projections using NIWA's Regional Climate Model. Resolution of projection is 5km x 5km.

6.2 Surface solar radiation

Key messages

- Annual changes to surface solar radiation in Canterbury are generally projected to be ± 2.5 W/m^2 . Reductions of $2.5\text{-}10$ W/m^2 are projected for eastern parts of the region by 2090 under RCP8.5.
- Seasonally, the largest changes to surface solar radiation are projected for summer by 2090 under RCP8.5; increases of $5\text{-}15$ W/m^2 are projected for western parts of Canterbury, with decreases of $5\text{-}10$ W/m^2 for eastern parts of the region.

This section contains maps showing the future projected change in surface solar radiation (solar radiation received at the land surface). Surface solar radiation is affected by cloud cover, so can be thought of as a proxy for changes in sunshine. Future change (average over 2031-2050 and 2081-2100) maps of annual and seasonal surface solar radiation are shown in this section, and the units are watts per square metre.

Annual changes to surface solar radiation in Canterbury are generally projected to be ± 2.5 W/m^2 (Figure 6-6). The exception is eastern parts of the region by 2090 under RCP8.5, where surface solar radiation reductions of $2.5\text{-}10$ W/m^2 are projected. This corroborates with increased rainfall projected in this area (particularly about Timaru) under the corresponding future climate scenario.

Seasonal projections of change in surface solar radiation are shown for RCP4.5 by 2040 (Figure 6-7) and 2090 (Figure 6-9), and RCP8.5 by 2040 (Figure 6-8) and 2090 (Figure 6-10). By 2040 under RCP4.5, autumn and spring changes to surface solar radiation in Canterbury are generally projected to be ± 2.5 W/m^2 . During winter, a reduction of $2.5\text{-}5$ W/m^2 is projected for western parts of Canterbury, with a reduction of $0\text{-}2.5$ W/m^2 projected for remaining parts of the region. Summer surface solar radiation is projected to increase by $2.5\text{-}10$ W/m^2 for western parts of Canterbury. By 2040 under RCP8.5, projected changes surface solar radiation in Canterbury are comparable to those projected under RCP4.5. The notable difference is during summer, with decreases of $2.5\text{-}10$ W/m^2 projected for much of eastern Canterbury.

By 2090 under RCP4.5, seasonal changes to surface solar radiation in Canterbury are generally projected to be ± 5 W/m^2 . A reduction of $5\text{-}10$ W/m^2 is projected for parts of western Canterbury in winter. The largest seasonal changes are projected for summer by 2090 under RCP8.5. During this season, surface solar radiation increases of $5\text{-}15$ W/m^2 are projected for western parts of Canterbury, with decreases of $5\text{-}10$ W/m^2 for eastern parts of the region.

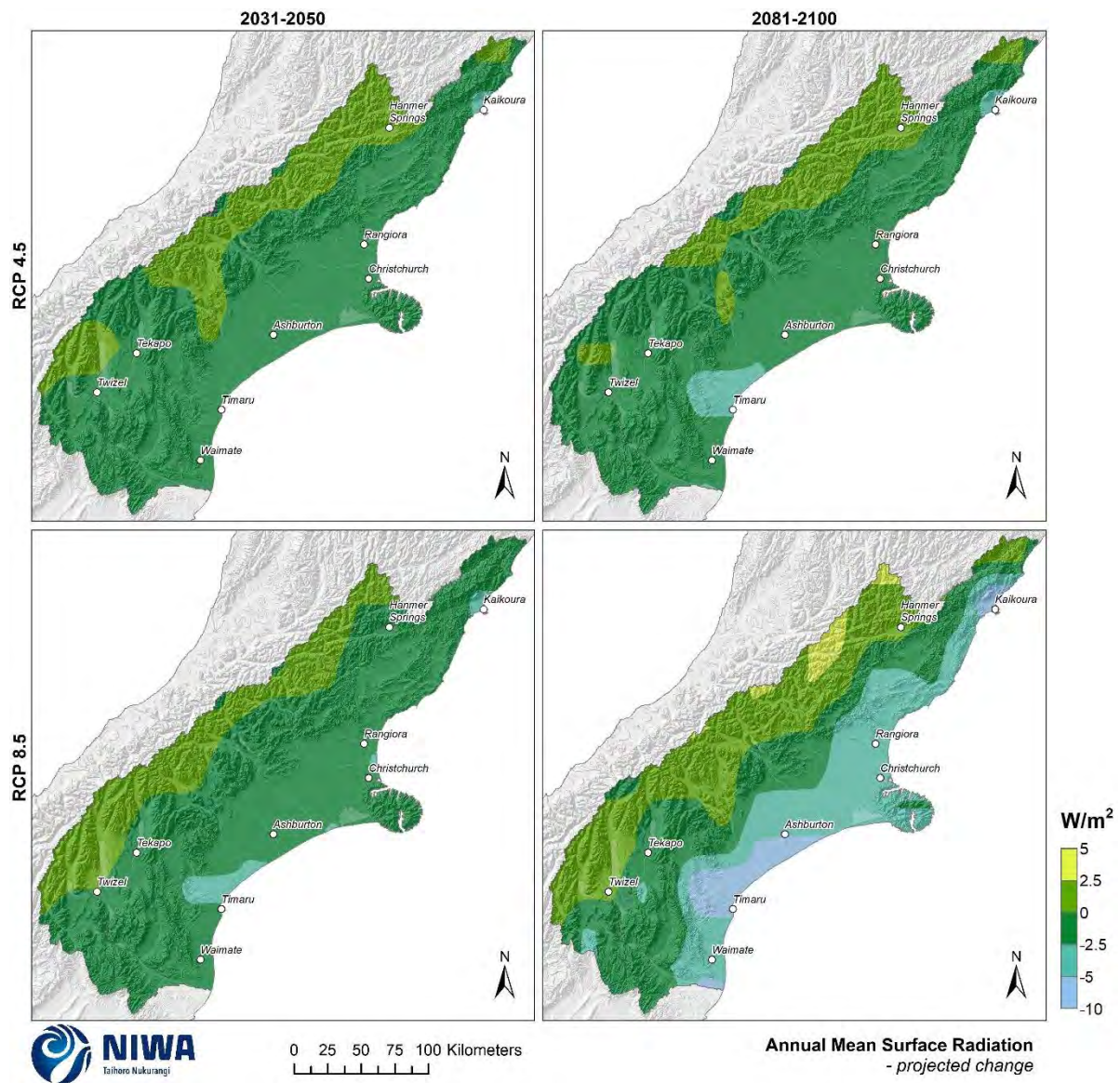


Figure 6-6: Projected annual mean surface solar radiation changes by 2040 and 2090, under RCP4.5 and RCP8.5. Climate change scenarios: RCP4.5 (top panels) and RCP8.5 (bottom panels). Time periods: mid-century (2031-2050; “2040” – panels on left) and end-century (2081-2100; “2090” – panels on right). Changes relative to 1986-2005 average, based on the average of six global climate models. Results are based on dynamical downscaled projections using NIWA’s Regional Climate Model. Resolution of projection is 5km x 5km.

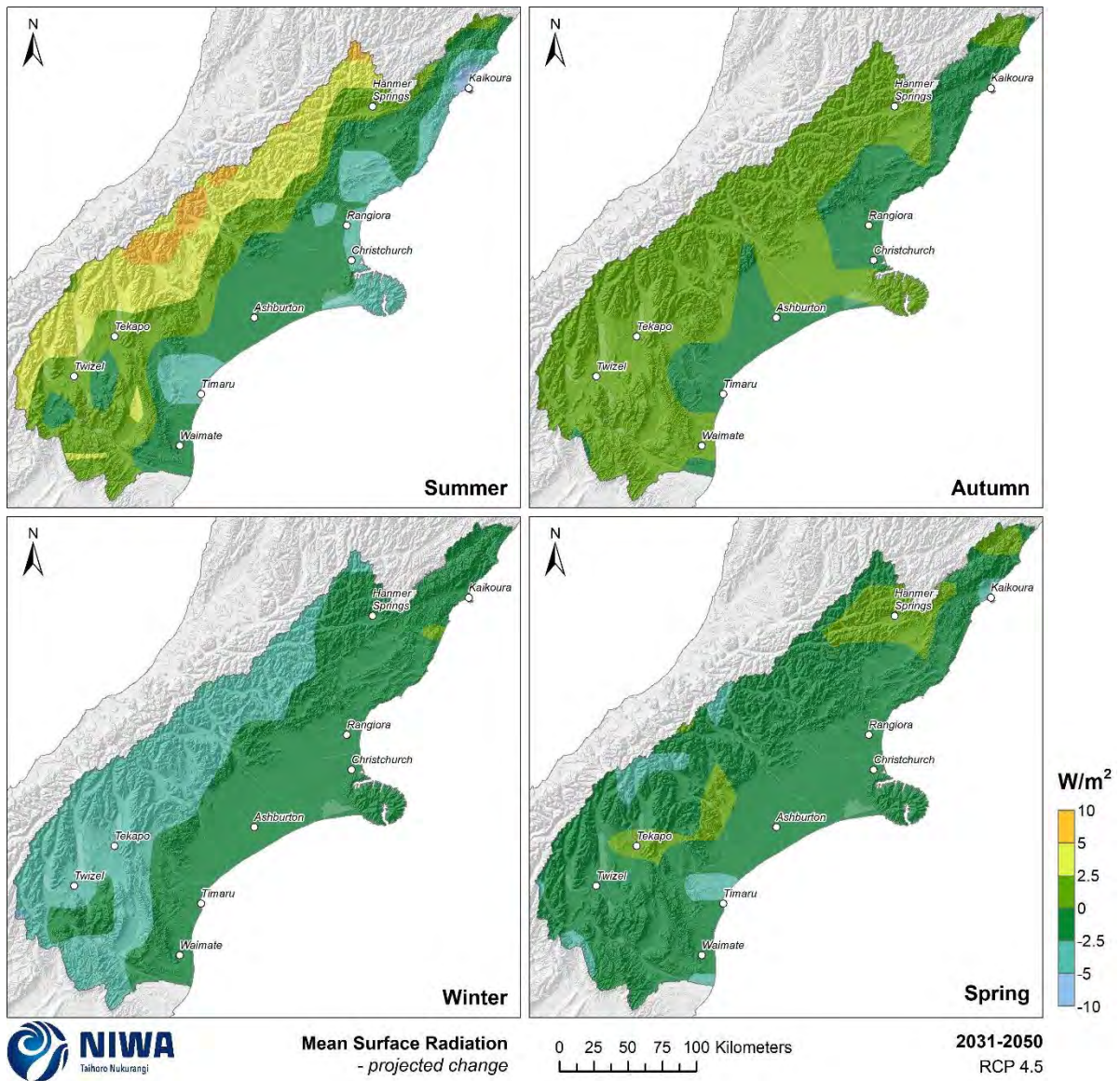


Figure 6-7: Projected seasonal mean surface solar radiation changes by 2040 for RCP4.5. Relative to 1986-2005 average, based on the average of six global climate models. Results are based on dynamical downscaled projections using NIWA's Regional Climate Model. Resolution of projection is 5km x 5km.

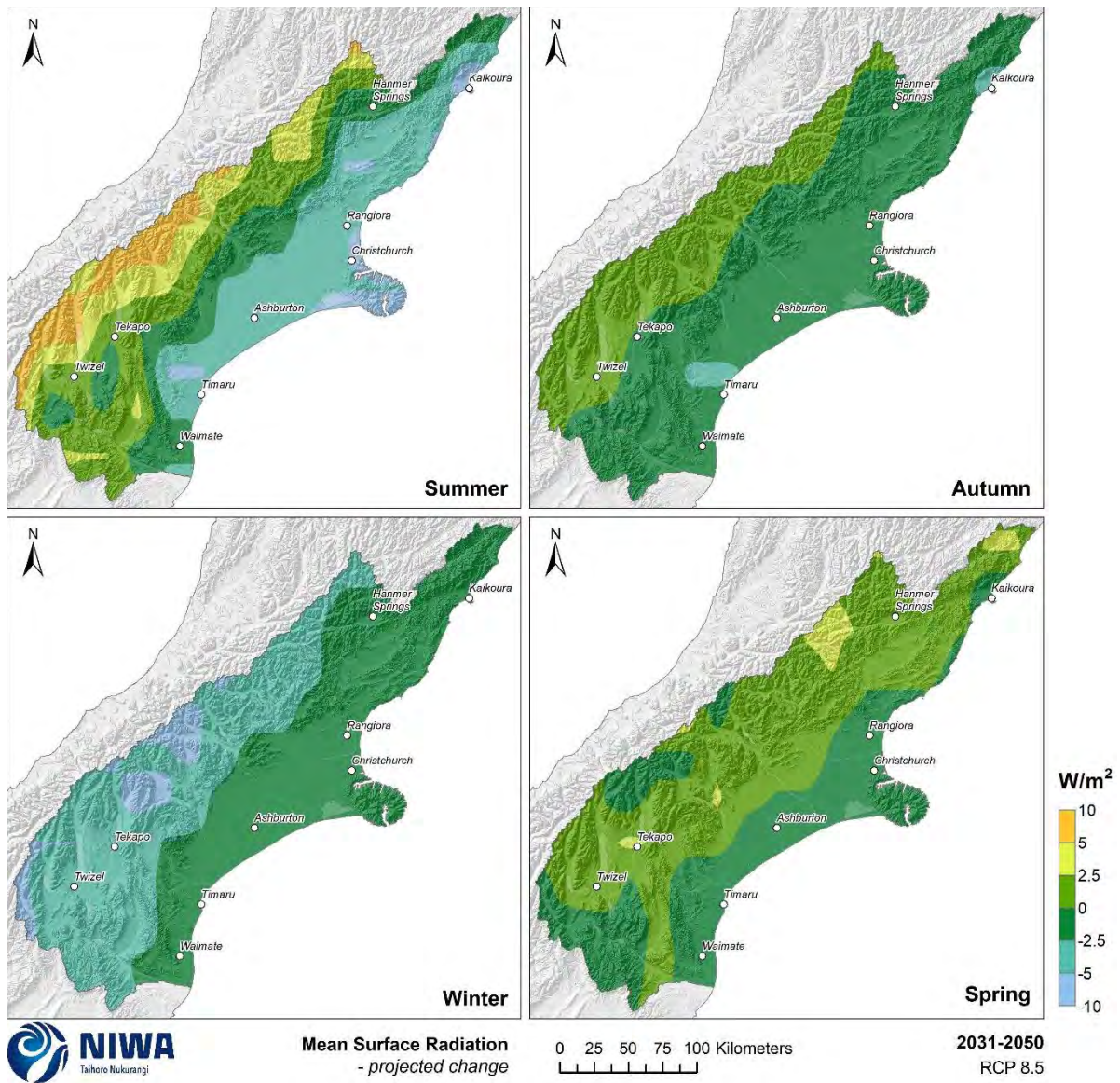


Figure 6-8: Projected seasonal mean surface solar radiation changes by 2040 for RCP8.5. Relative to 1986-2005 average, based on the average of six global climate models. Results are based on dynamical downscaled projections using NIWA's Regional Climate Model. Resolution of projection is 5km x 5km.

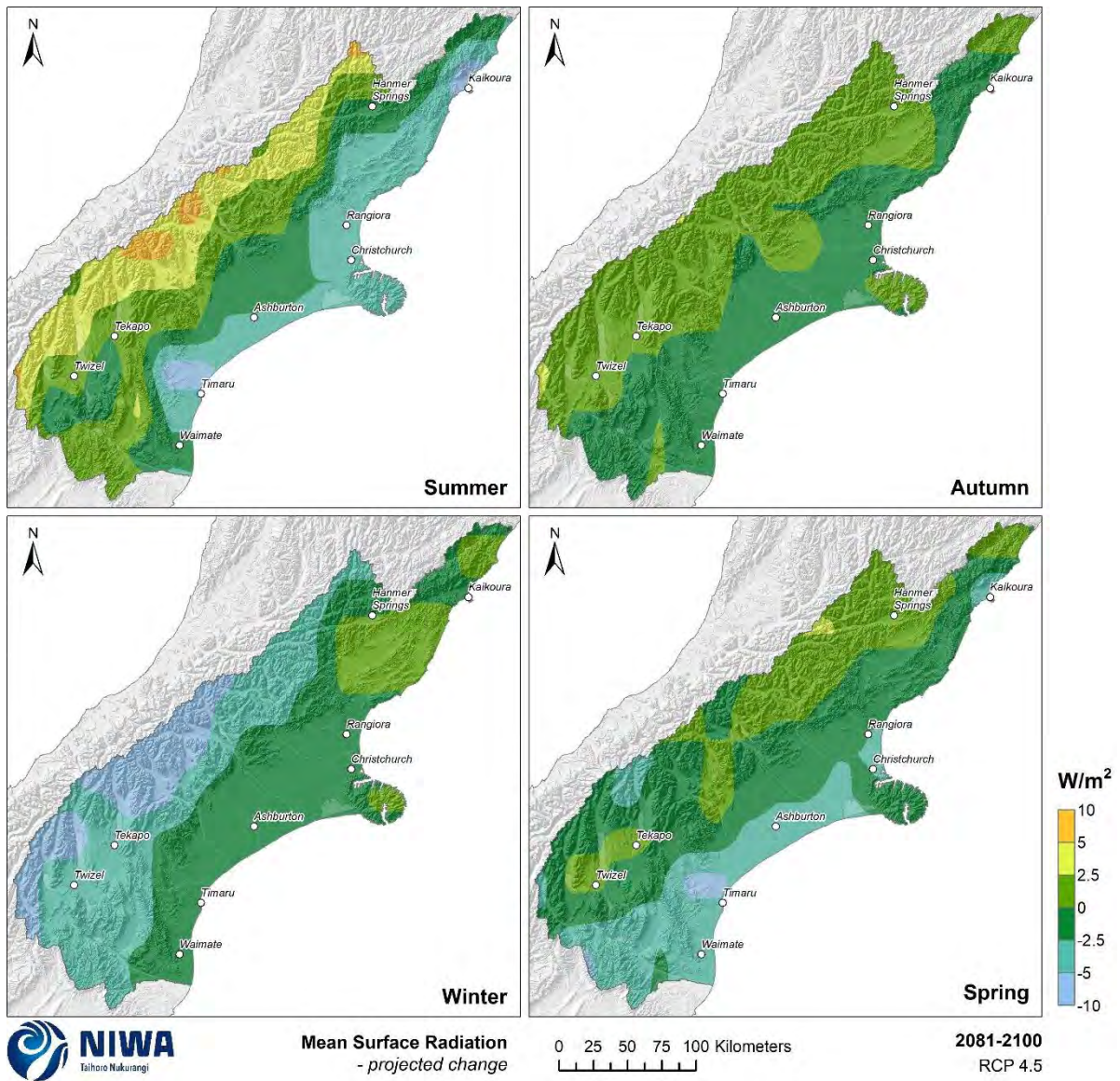


Figure 6-9: Projected seasonal mean surface solar radiation changes by 2090 for RCP4.5. Relative to 1986-2005 average, based on the average of six global climate models. Results are based on dynamical downscaled projections using NIWA's Regional Climate Model. Resolution of projection is 5km x 5km.

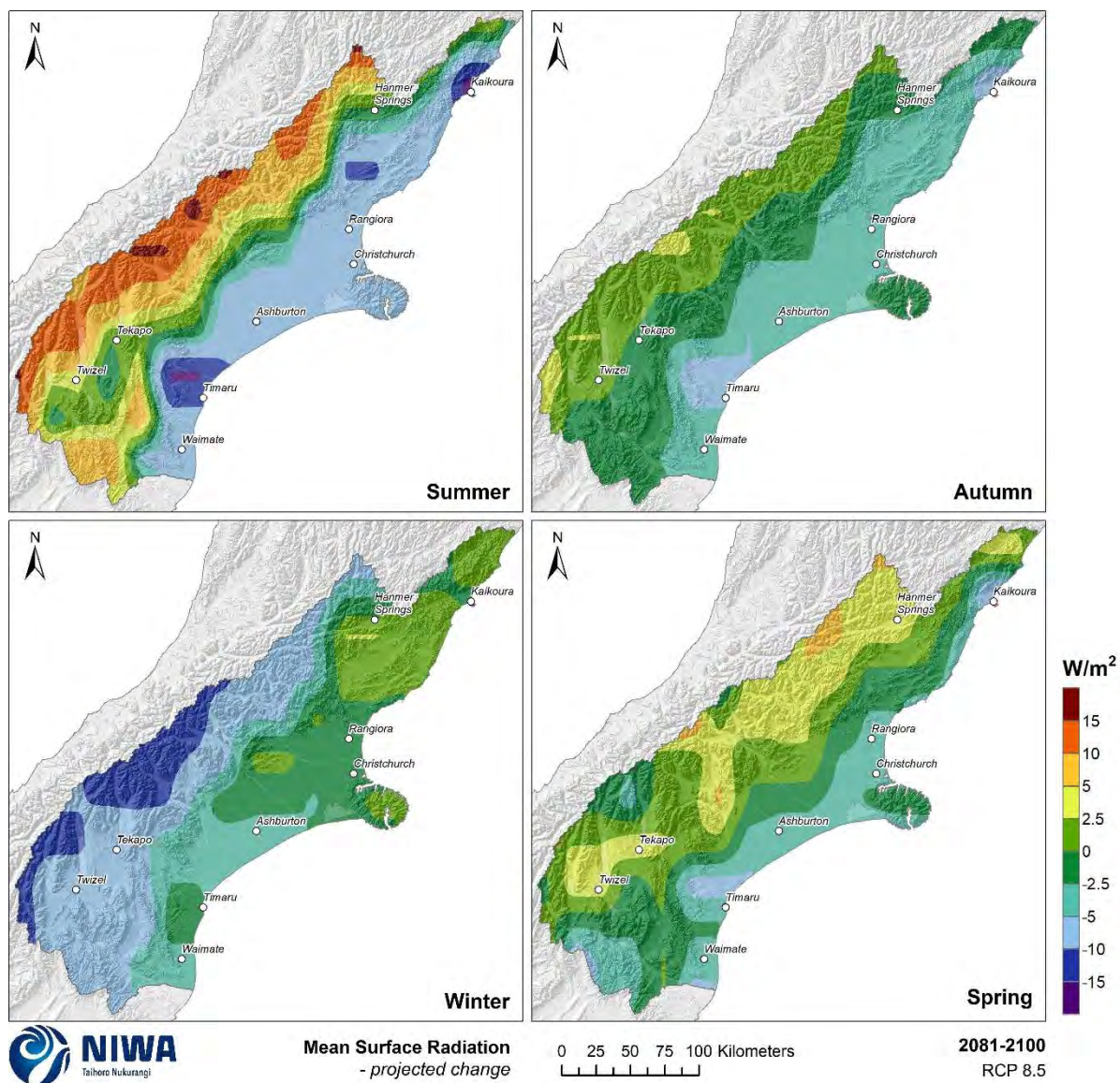


Figure 6-10: Projected seasonal mean surface solar radiation changes by 2090 for RCP8.5. Relative to 1986-2005 average, based on the average of six global climate models. Results are based on dynamical downscaled projections using NIWA's Regional Climate Model. Resolution of projection is 5km x 5km.

6.3 Relative humidity

Key messages

- Minimal change to annual mean relative humidity in Canterbury is generally projected (0-2% decline). By 2090, reductions of 2-3% are projected for western areas under RCP4.5, with reductions of 3-10% projected for western areas under RCP8.5.
- Seasonally, the largest changes to mean relative humidity are projected for spring by 2090 under RCP8.5; decreases of 3-10% are projected for most parts of Canterbury.

Future change (average over 2031-2050 and 2081-2100) maps of annual and seasonal relative humidity are shown in this section.

In the future, annual mean relative humidity is generally expected to decline in Canterbury (Figure 6-11). Higher reductions are projected for western parts of Canterbury compared to eastern parts of the region. By 2040 under RCP4.5 and RCP8.5, minimal changes (reductions of 0-2%) are expected for most of Canterbury. By 2090, reductions of 2-3% are projected for western areas under RCP4.5, with reductions of 3-10% projected for these areas under RCP8.5.

Seasonal projections of change in mean relative humidity are shown for RCP4.5 by 2040 (Figure 6-12) and 2090 (Figure 6-14), and RCP8.5 by 2040 (Figure 6-13) and 2090 (Figure 6-15). By 2040 under RCP4.5 and RCP8.5, minimal changes to mean relative humidity in Canterbury are generally projected (0-2% reductions). Decreases of 2-5% are projected for some western parts during spring. Minimal change is projected for isolated coastal areas about Timaru and Kaikoura during summer, autumn and winter.

By 2090 under RCP4.5, seasonal changes to mean relative humidity are generally projected to be minimal for eastern parts of Canterbury (0-2% reductions), with reductions of 2-5% projected for western parts of the region in spring. The largest seasonal changes to mean relative humidity are projected for spring by 2090 under RCP8.5. During this season, mean relative humidity decreases of 3-10% are projected for most parts of Canterbury.

A note about relative humidity compared to specific humidity: Projected decreases in relative humidity are a consequence of the higher temperatures. The absolute water content of the air, as measured by specific humidity, increases with time, but the temperature effect is larger; the rate of decrease in relative humidity over New Zealand is mostly 1–2% per degree increase in mean temperature. This is in line with evidence in the recent observations (Simmons et al., 2010) in reanalysis and station data over low and mid latitudes.

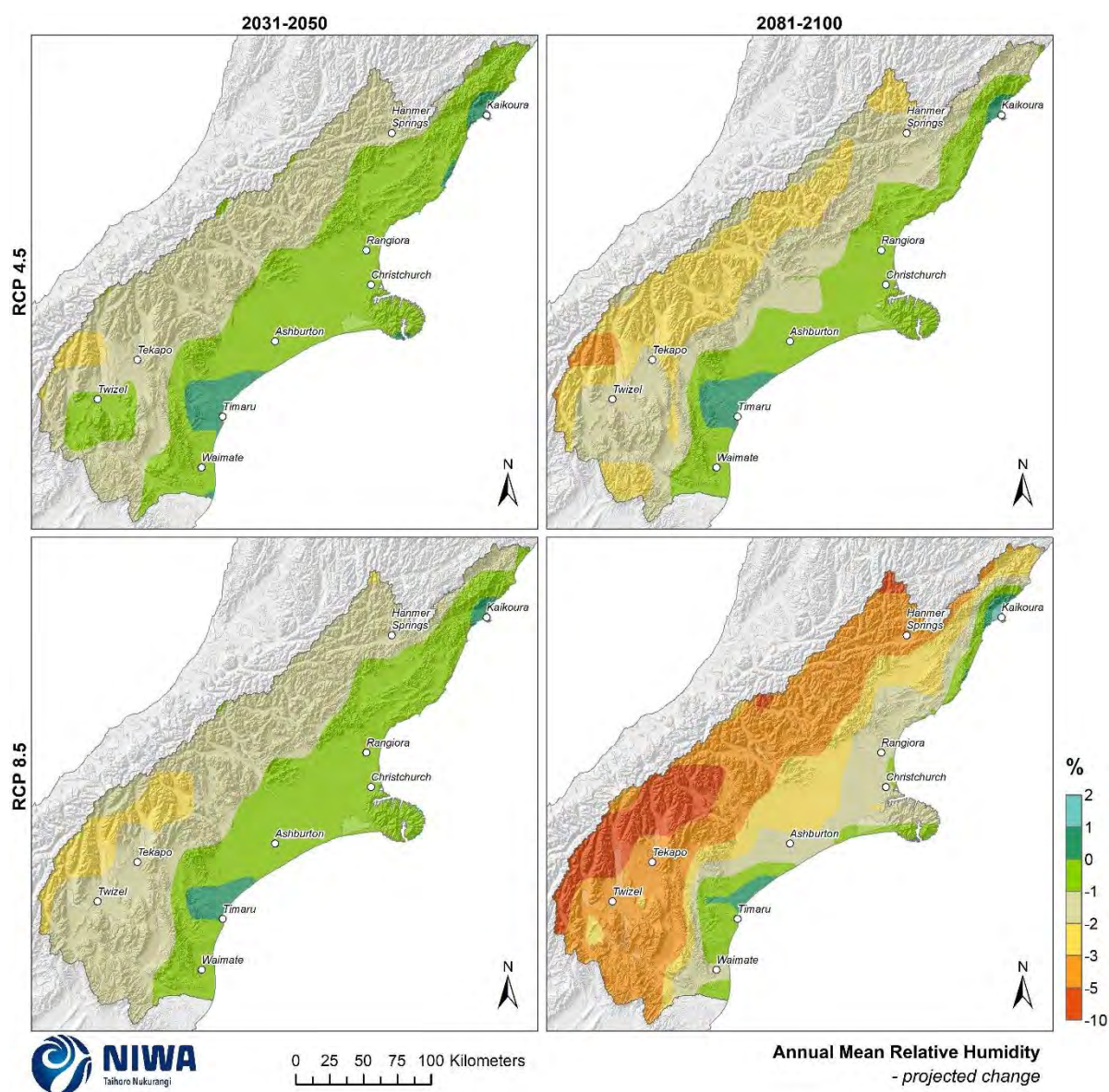


Figure 6-11: Projected annual mean relative humidity changes by 2040 and 2090, under RCP4.5 and RCP8.5. Climate change scenarios: RCP4.5 (top panels) and RCP8.5 (bottom panels). Time periods: mid-century (2031-2050; “2040” – panels on left) and end-century (2081-2100; “2090” – panels on right). Changes relative to 1986-2005 average, based on the average of six global climate models. Results are based on dynamical downscaled projections using NIWA's Regional Climate Model. Resolution of projection is 5km x 5km.

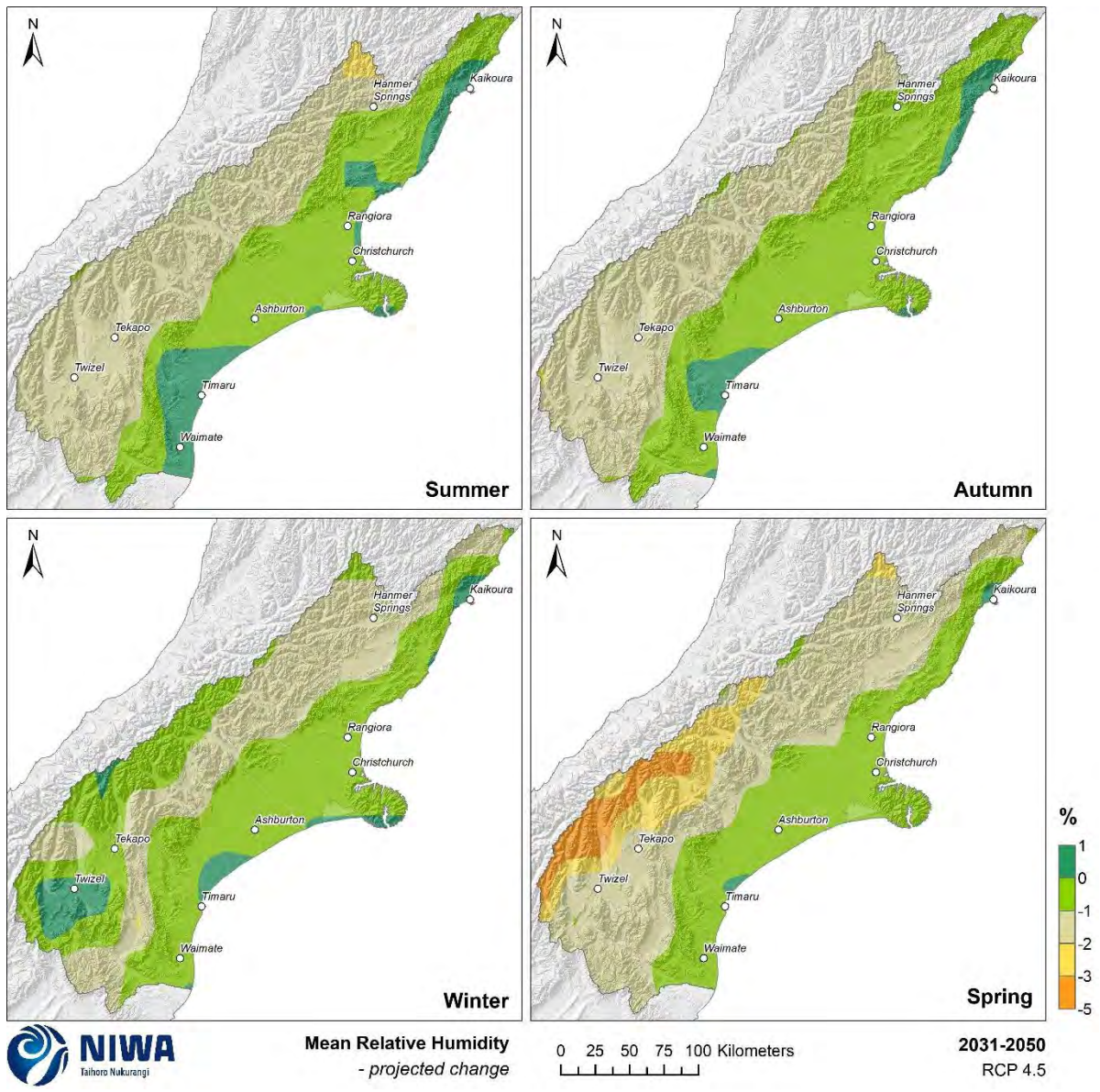


Figure 6-12: Projected seasonal mean relative humidity changes by 2040 for RCP4.5. Relative to 1986-2005 average, based on the average of six global climate models. Results are based on dynamical downscaled projections using NIWA's Regional Climate Model. Resolution of projection is 5km x 5km.

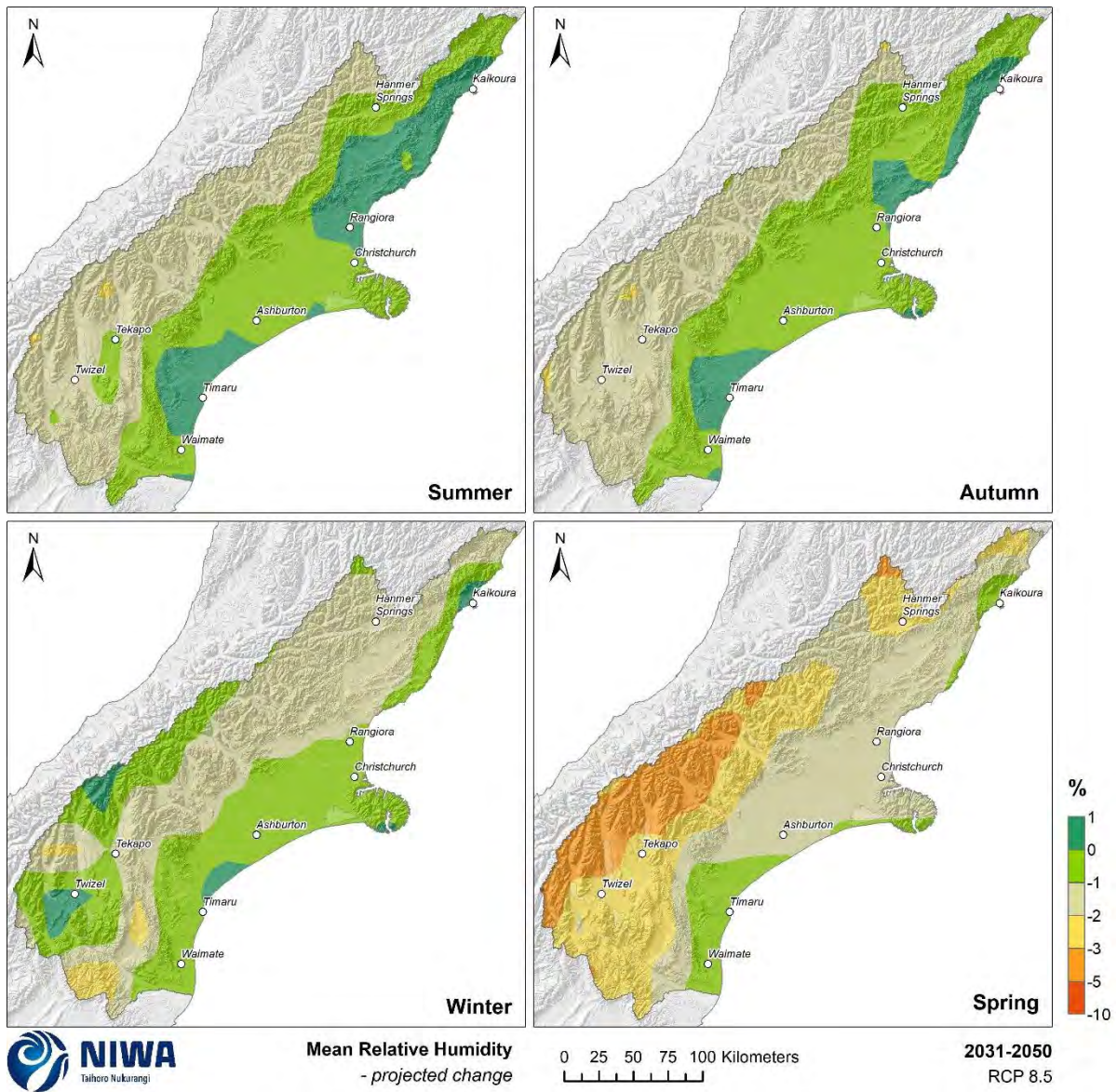


Figure 6-13: Projected seasonal mean relative humidity changes by 2040 for RCP8.5. Relative to 1986-2005 average, based on the average of six global climate models. Results are based on dynamical downscaled projections using NIWA's Regional Climate Model. Resolution of projection is 5km x 5km.

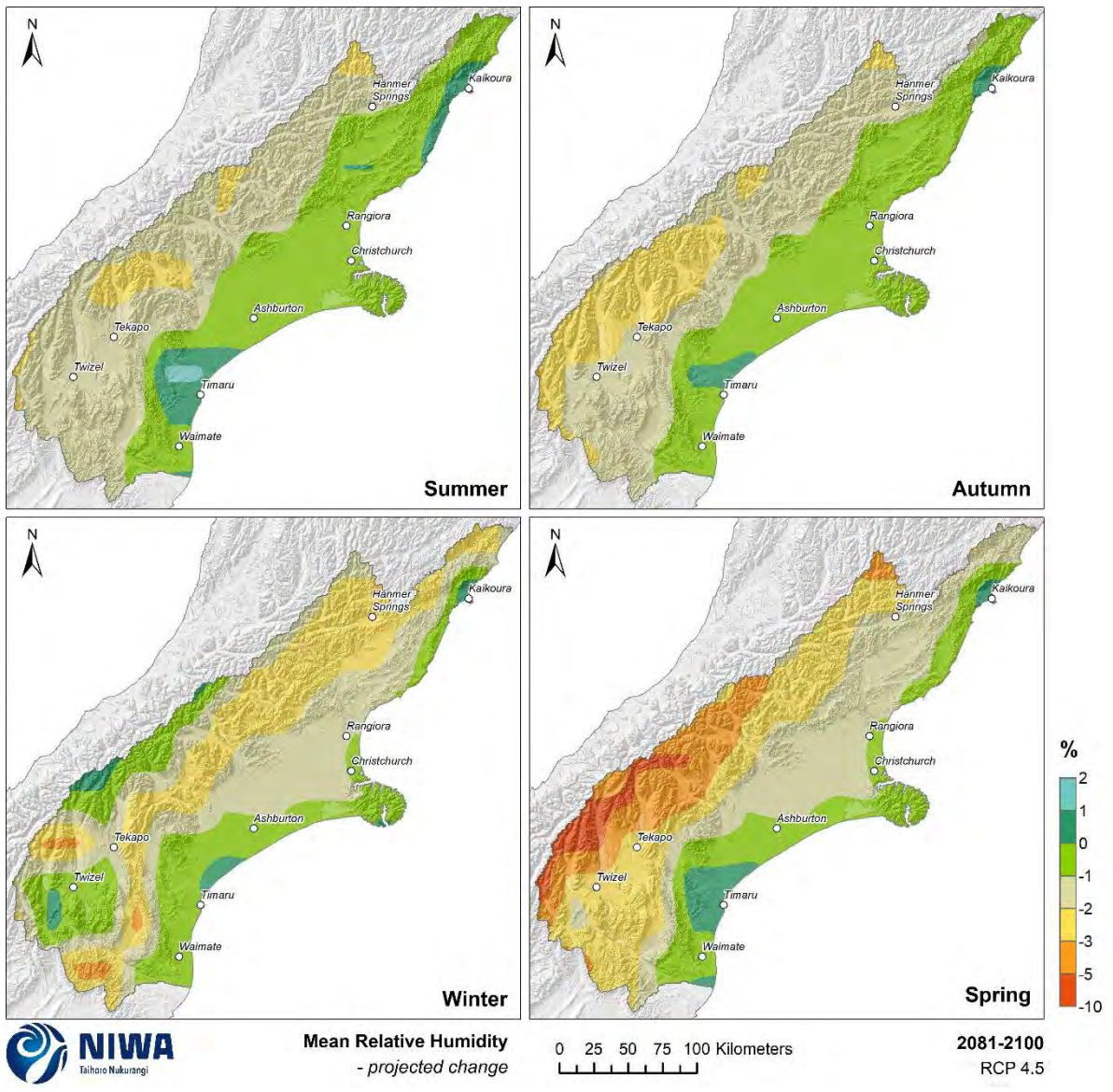


Figure 6-14: Projected seasonal mean relative humidity changes by 2090 for RCP4.5. Relative to 1986-2005 average, based on the average of six global climate models. Results are based on dynamical downscaled projections using NIWA's Regional Climate Model. Resolution of projection is 5km x 5km.

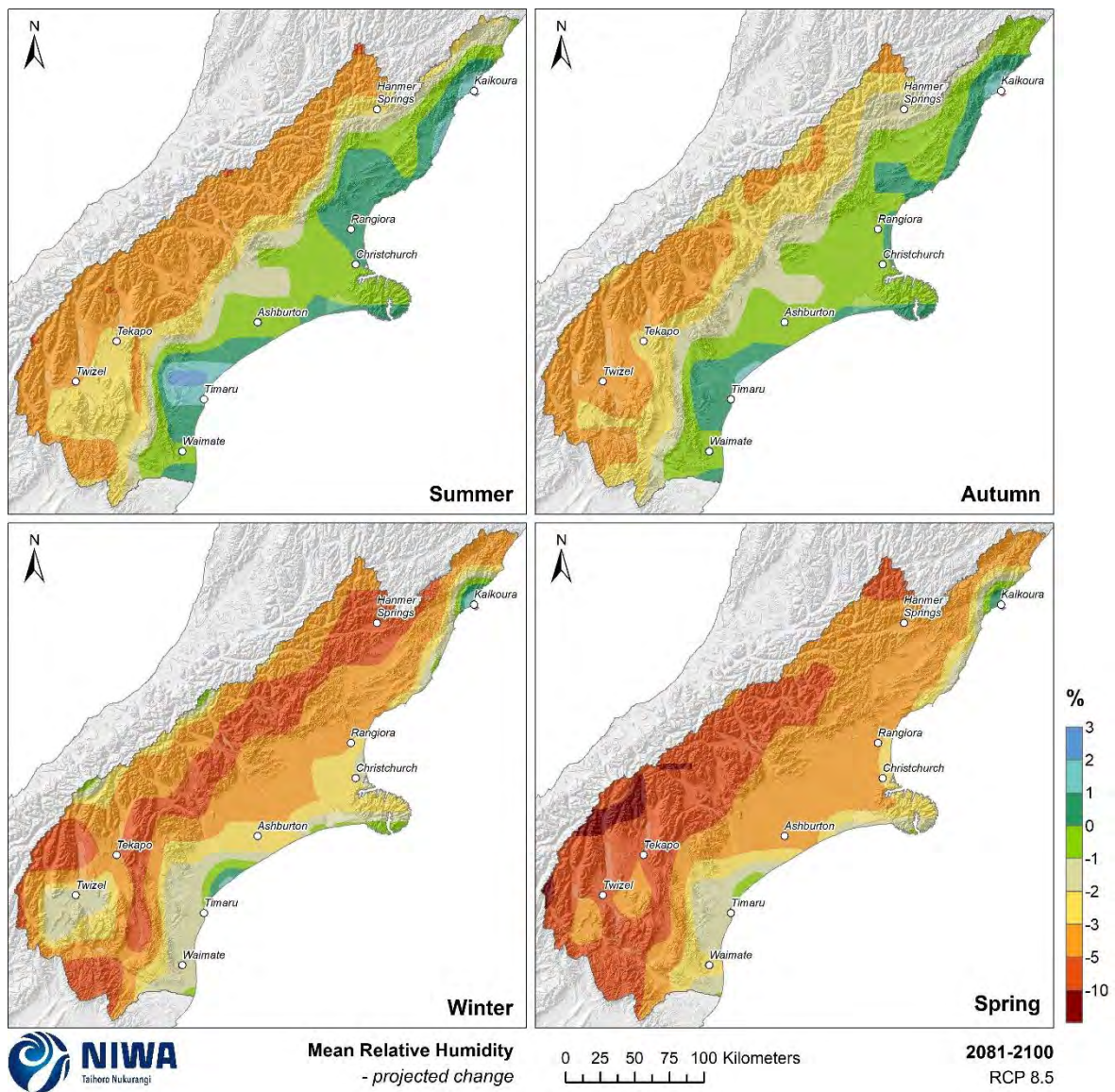


Figure 6-15: Projected seasonal mean relative humidity changes by 2090 for RCP8.5. Relative to 1986-2005 average, based on the average of six global climate models. Results are based on dynamical downscaled projections using NIWA's Regional Climate Model. Resolution of projection is 5km x 5km.

6.4 Air pressure

Key messages

- Mean sea level pressure (MSLP) is projected to increase in summer, causing more north easterly airflow and more anticyclonic patterns (high pressure systems).
- MSLP tends to decrease in model simulations during winter, especially over and south of the South Island, resulting in stronger westerly winds over central New Zealand.

Mean sea level pressure (MSLP) varies over New Zealand from day to day as different weather systems pass over the country. Figure 6-16 shows average seasonal MSLP over the Southwest Pacific, including New Zealand. Westerly or south westerly wind flows dominate over most of the South Island throughout the year. However, east to northeasterly winds are common in coastal areas of Canterbury, particularly during summer when daytime heating establishes a sea-breeze.

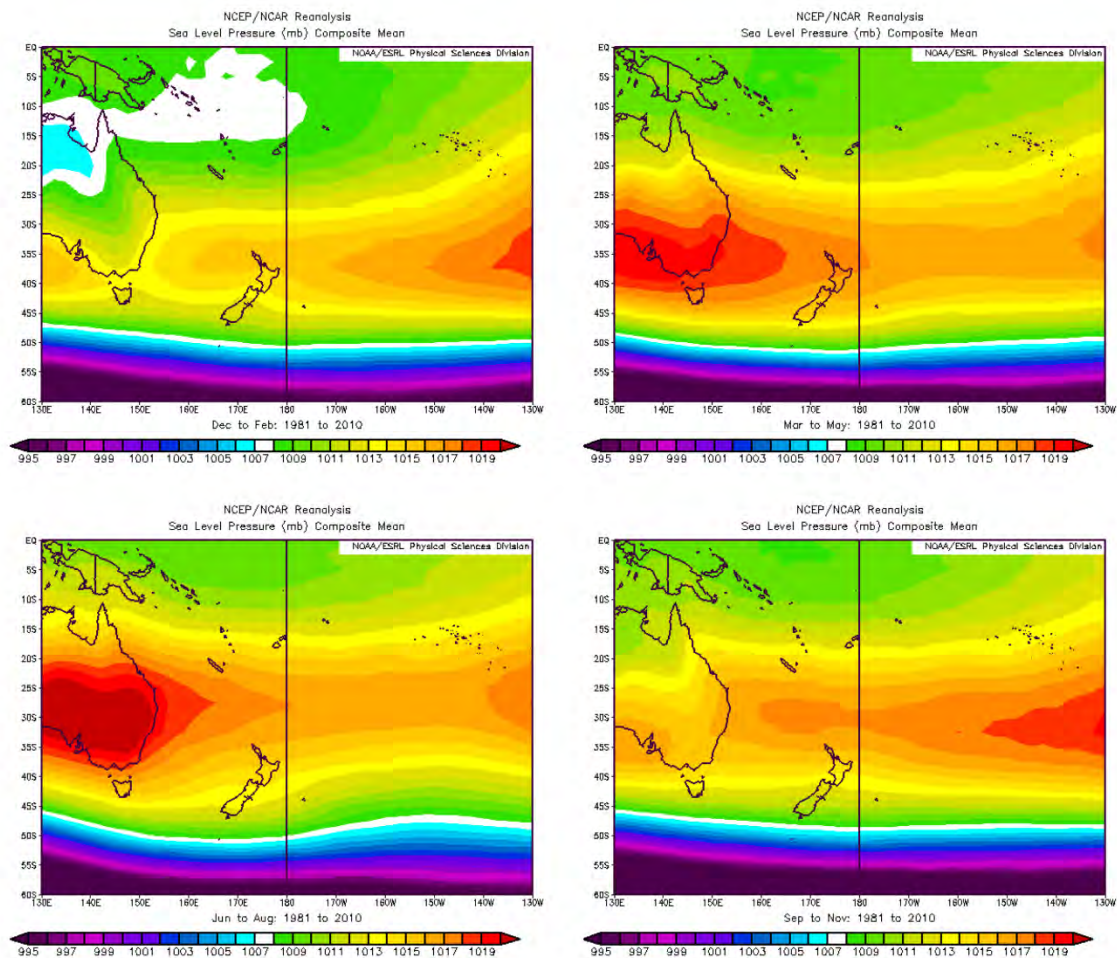


Figure 6-16: Average seasonal mean sea level pressure over the Southwest Pacific, 1981-2010. Top left: summer, top right: autumn, bottom left: winter, bottom right: spring. Sourced from: <https://www.esrl.noaa.gov/psd/cgi-bin/data/composites/printpage.pl>.

Future mean sea-level pressure projections have been derived from the Regional Climate Model (RCM) simulations. The key projected changes in mean sea-level pressure (MSLP) and mean winds are as follows (for more detail see Mullan et al., 2016; MFE, 2018):

- MSLP tends to increase in summer (December–February), especially to the south-east of New Zealand. In other words, the airflow becomes more north easterly, and at the same time more anticyclonic (high pressure systems).
- MSLP tends to decrease in winter (June–August), especially over and south of the South Island, resulting in stronger westerlies over central New Zealand.
- In the other seasons (autumn and spring), the pattern of MSLP change is less consistent with increasing time and increasing emissions. There is, however, still general agreement for autumn changes to be like those of summer (i.e., more anticyclonic), and for spring changes to be like those of winter (lower pressures south of the South Island, and stronger mean westerly winds over southern parts of the country).

7 Hydrological impacts of climate change

Key messages

- Mean annual discharge generally decreases by mid-century across Canterbury. By late century, mean discharge tends to increase along eastern areas of Canterbury (particularly under RCP8.5), with decreases to mean discharge projected for some inland areas.
- Mean annual low flow generally decreases by late century, with decreases exceeding 20% in many areas of the region.
- High flow (expressed as Q5% flow) changes are expected to be variable across the region, with both increases and decreases projected throughout Canterbury.
- Floods (characterised by the Mean Annual Flood) are expected to become larger for many parts of Canterbury, with some increases exceeding 100%. However, there are some pockets of little change or decreasing Mean Annual Flood.

This section covers the projected differences in several hydrological statistics between the baseline period (1986-2005) and two future periods. These are mid-century (2036-2056) and late-century (2086-2099), and are slightly different from the corresponding time slices of the atmospheric modelling because the modelling was done before this project was initiated. We do not expect that the conclusions drawn would be substantively different if the periods were aligned. The hydrological modelling analyses presented here were extracted from a national scale assessment (Collins & Zammit, 2016; Collins et al., 2018). The statistics included in this report are:

- Mean annual discharge;
- Mean annual low flow;
- The Q5% flow³; and
- The mean annual flood⁴ (MAF).

7.1 Mean annual discharge

The projected future differences in the annual discharge for RCP4.5 and RCP8.5 at two time periods are presented in Figure 7-1. At the annual scale, mean discharge matches the annual pattern in change in precipitation (Figure 5-2) and generally decrease by mid-century across Canterbury. By late century, mean discharge tends to increase along eastern areas of Canterbury (particularly under RCP8.5). In contrast, decreases to mean discharge are projected for inland areas (although increases are projected for many headwaters of the hydro lakes under RCP8.5) reflecting a potential change in phase of the precipitation under higher RCPs.

³ Q5: Flow that is exceeded 5 percent of the time.

⁴ The mean of the series of each year's highest daily mean flow (m³/s).

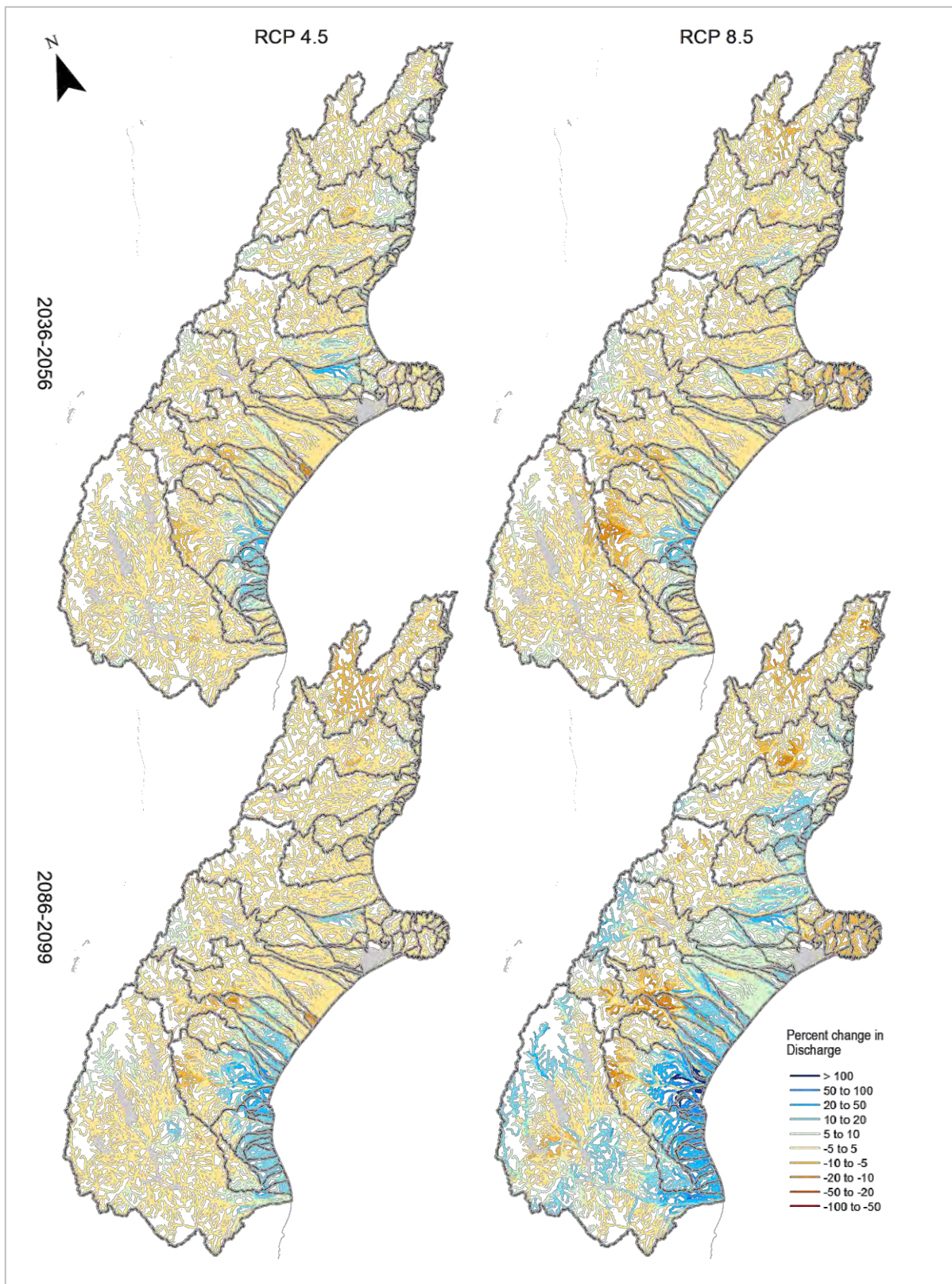


Figure 7-1: Percent changes in multi-model median of the mean discharge across Canterbury for mid (top) and late-century (bottom). Climate change scenarios: RCP4.5 (left panels) and RCP8.5 (right panels). Time periods: mid-century (2036-2056) and end-century (2086-2099).

7.2 Mean annual low flow

Mean annual low flow (MALF) is defined as the mean of the lowest 7-day average flows in each year of a projection period. Median changes in the MALF are presented for RCP4.5 and RCP8.5 at two time periods in Figure 7-2. At the annual scale, MALF generally decreases by mid-century across Canterbury, although increases are projected for some eastern areas (particularly south of Christchurch under RCP8.5). By late century, MALF tends to decrease for most of Canterbury, with decreases exceeding 20% in many areas of the region. Comparison of change in MALF across the region and changes in seasonal precipitation (Figure 5-4 to Figure 5-7) indicate that projected changes in MALF in Canterbury high country areas is not as expected. At present, MALF in high country catchments currently typically occurs in winter. Notably, it is the winter season when precipitation is projected to increase the most. As a result, MALF would be expected to increase in those catchments. This discrepancy is currently under investigation and is thought to be linked to: i) potential shift in the timing/season when MALF occurs (e.g. winter to spring or autumn MALF), and ii) potential impact of the number of no rain days between rainfall events.

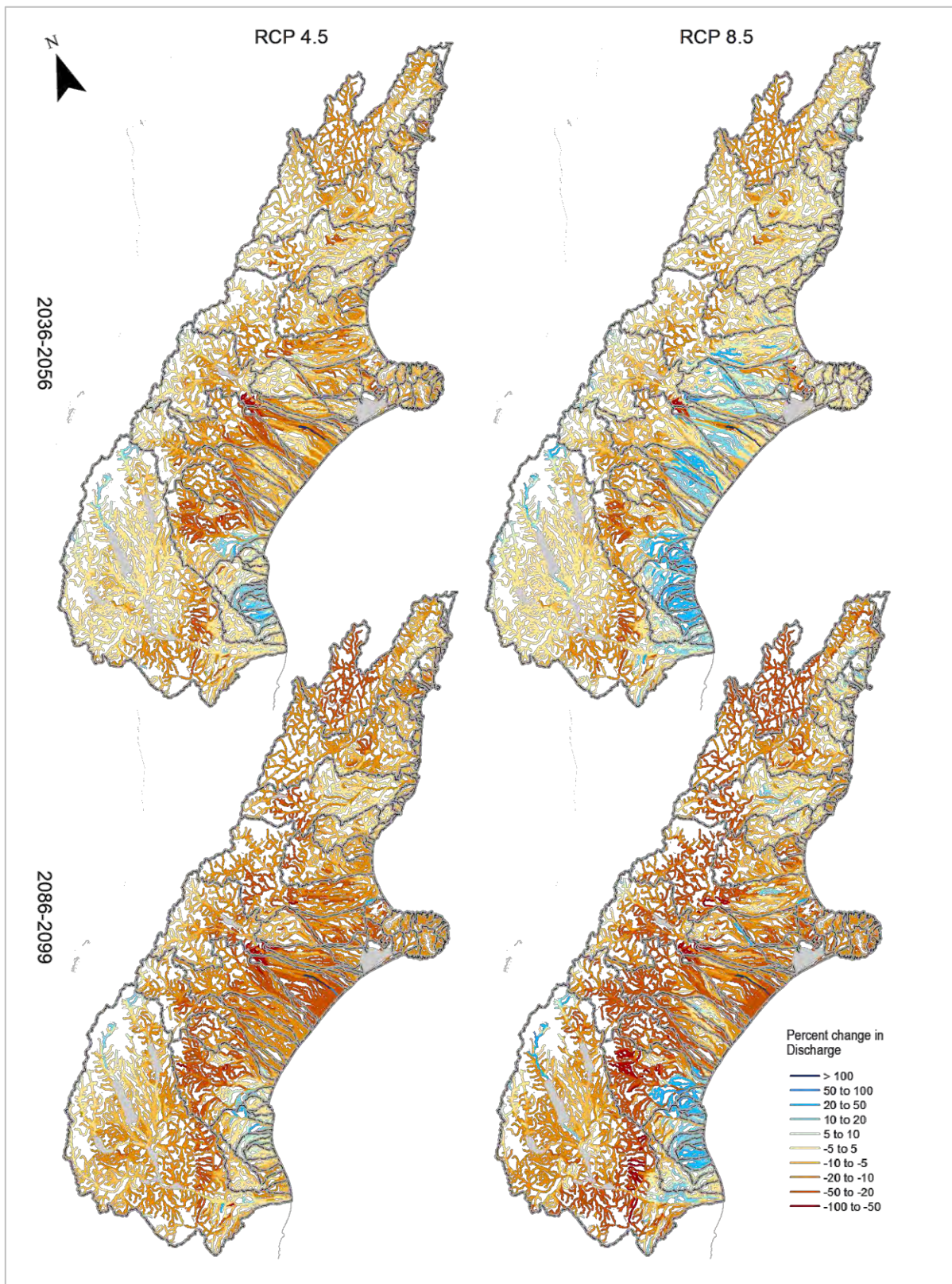


Figure 7-2: Percent changes in multi-model median of the mean annual low flow across Canterbury for mid-century (top) and late-century (bottom). Climate change scenarios: RCP4.5 (left panels) and RCP8.5 (right panels). Time periods: mid-century (2036-2056) and end-century (2086-2099).

7.3 High flow

The projected future differences in the Q5% flows (flow that is exceeded 5 percent of the time) for RCP4.5 and RCP8.5 at two time periods are presented in Figure 7-3. There are both increases and decreases projected throughout Canterbury, with the more pronounced differences generally manifesting themselves during the late-century period and under higher RCP. Increases in Q5% are more tangible and consistent in eastern areas under RCP8.5 (increasing by 50% or more). Decreases are modelled throughout Canterbury, but consistently for inland areas east of the Main Divide, decreasing by 20% or more. The apparent counter-intuitive changes in Q5% over the hill country is thought to be associated with a change in the duration of the events generating high flows. Under climate change it is expected that the intensity of large rainfall events (which generate high flows) is increasing, while the duration of those events is decreasing. As a result, it is expected that the duration of the high flow events is decreasing, generating a decrease in the Q5% hydrological characteristics. This is currently under investigation through NIWA SSIF funding and as part of Deep South National Science Challenge.

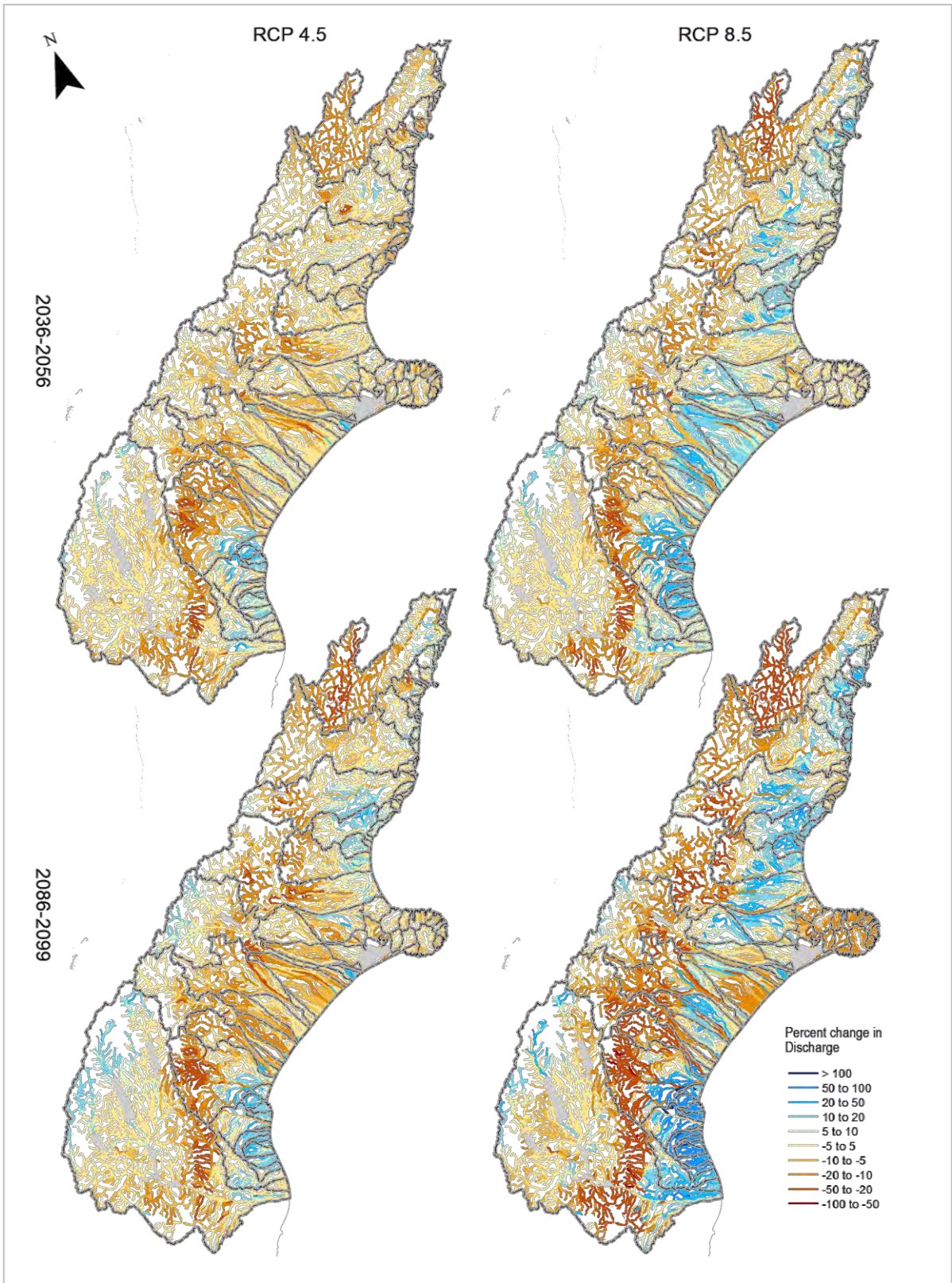


Figure 7-3: Percent changes in multi-model median Q5% across Canterbury for mid (top) and end of century (bottom). Climate change scenarios: RCP4.5 (left panels) and RCP8.5 (right panels). Time periods: mid-century (2036-2056) and end-century (2086-2099).

7.4 Mean annual flood

The projected future differences in the mean annual flood (MAF; the mean of the series of each year's highest daily mean flow) for RCP4.5 and RCP8.5 at two time periods are presented in Figure 7-4. While there are some pockets of little change or decreasing MAF, in general Canterbury is projected to experience an increase in MAF, with some increases exceeding 100% (by late-century under RCP8.5). There is little difference among the RCPs during the mid-century period, but by late-century, the increases in MAF become larger and more extensive progressively from RCP4.5 to RCP8.5.

The increase in MAF is a change that is largely consistent with the changes to rainfall presented in Ministry for the Environment (2018), especially regarding the 99th percentile of daily rainfall. Analysis of flow records indicates that MAF has a strong correspondence with observed mean annual rainfall (Henderson et al., 2018). It is noteworthy that flood design standards for significant infrastructure are usually made based on events with annual exceedance probabilities much smaller than that represented by MAF. Analysis of RCM rainfall projections undertaken for the High Intensity Rainfall Design project (Carey-Smith et al., 2018), has shown that events with small annual exceedance probability are projected to increase ubiquitously across the country in a way that scales with increasing temperatures. As such, MAF should not be considered a comprehensive metric for the possible impact of climate change on New Zealand flooding.

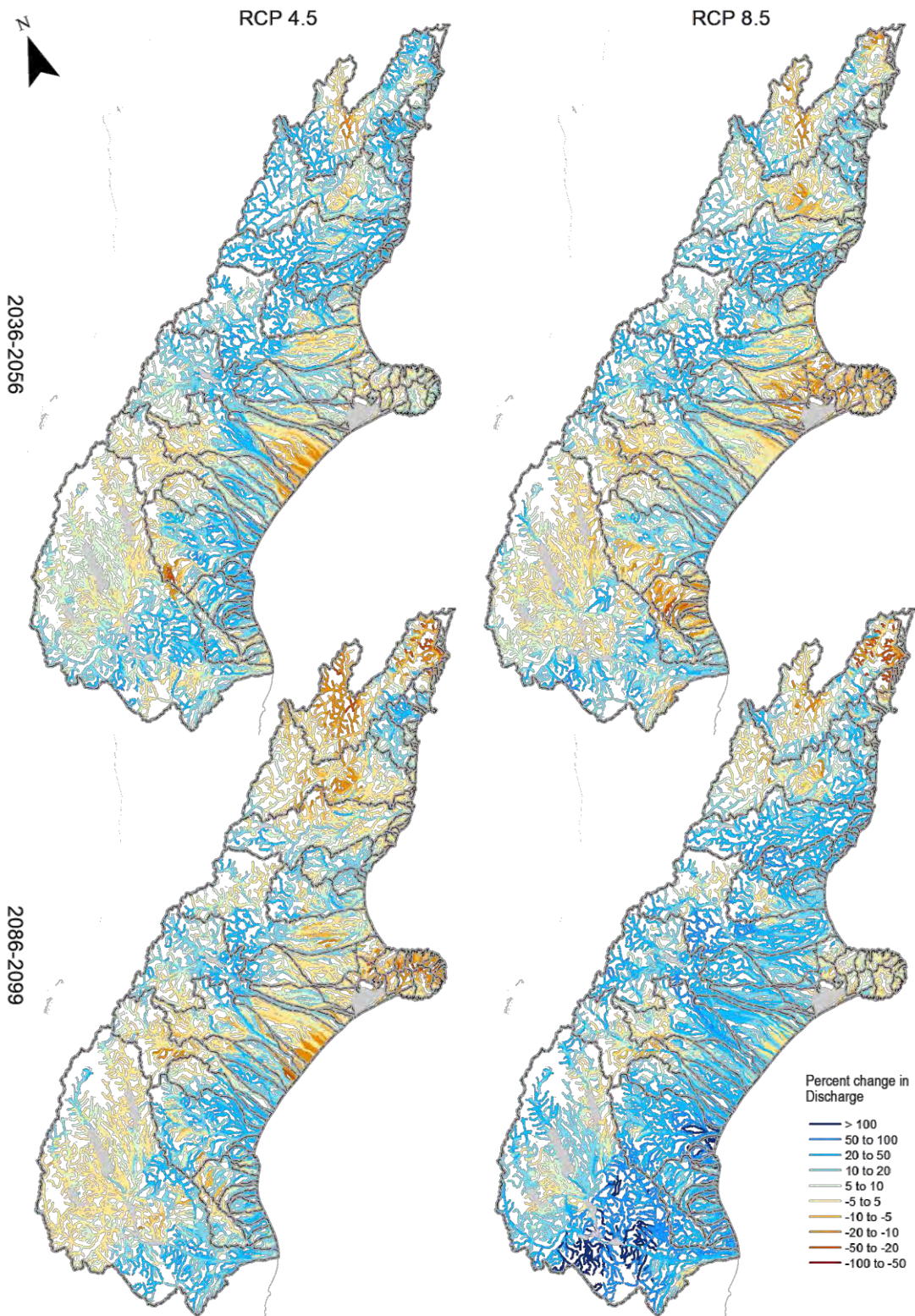


Figure 7-4: Percent changes in multi-model median of MAF across Canterbury for mid (top) and end of century (bottom). Climate change scenarios: RCP2.6 (left panels) and RCP4.5 (right panels). Time periods: mid-century (2036-2056) and end-century (2086-2099).

8 Sea-level rise and coastal impacts

8.1 Impacts of sea-level rise

One of the major and most certain (and so foreseeable) consequences of increasing concentrations of carbon dioxide⁵ and associated warming, is the rising sea level (Parliamentary Commissioner for the Environment, 2015). IPCC (2013) found that warming of the climate system is unequivocal, and many of the changes observed since the 1950s are unprecedented over timescales of decades to millennia. The atmosphere and ocean have warmed, and the amounts of snow and ice globally have diminished, causing sea level to rise.

Rising sea level in past decades is already affecting human activities and infrastructure in coastal areas in New Zealand, with a higher base mean sea level contributing to increased vulnerability to storms and tsunamis. Key impacts of an ongoing rise in sea level are:

- gradual inundation of low-lying marsh and adjoining dry land on spring high tides;
- escalation in the frequency of nuisance and damaging coastal flooding events (which has been evident in several low-lying coastal margins of New Zealand);
- exacerbated erosion of sand/gravel shorelines and unconsolidated cliffs (unless sediment supply increases);
- increased incursion of saltwater in lowland rivers and nearby groundwater aquifers, raising water tables in tidally-influenced groundwater systems.

These impacts will have increasing implications for existing development in coastal areas, along with environmental, societal and cultural effects. Infrastructure and its levels of service or performance will also be increasingly affected, such as wastewater treatment plants, potable water supplies, and particularly capacity and performance issues with stormwater and overland drainage systems (particularly gravity-driven networks). Transport infrastructure (roads, ports, airports) in the coastal margin will also be affected, both by increased nuisance shallow flooding of saltwater (e.g., vehicle corrosion) and more disruptive flooding and damage from elevated storm-tides and wave overtopping.

There are three types of SLR in relation to observations and projections:

- absolute (or eustatic) rise in ocean levels, measured relative to the centre of the Earth, and usually expressed as a global mean (which is used in most sea-level projections e.g., IPCC);
- offsets (or departures) from the global mean absolute SLR for a regional sea, e.g., the sea around New Zealand, which will experience slightly higher rises (5–10%) than the global average rate. There can be significant variation in the response to warming and wind patterns between different regional seas around the Earth;
- relative sea-level rise (RSLR), which is the net rise in sea level experienced on coastal margins from absolute, regional-sea offsets and local vertical land movement (measured relative to the local landmass). Local or regional adaptation to SLR needs to focus on RSLR, particularly if the coastal margin is subsiding.

⁵ Global average now above 400 ppm.

The first two types of SLR are measured directly by satellites, using radar altimeters, or by coalescing many tide-gauge records globally (after adjusting for local vertical land movement and ongoing re-adjustments in the Earth's crust following ice loading during the last Ice Age⁶).

RSLR is measured directly by tide gauges. One advantage of knowing the RSLR from gauge measurements is that this directly tracks the SLR that needs to be adapted to locally, or over the wider region represented by the gauge. If, for instance, the local landmass is subsiding, then the RSLR will be larger than the absolute rise in the adjacent ocean level acting alone.

8.2 Projections for New Zealand sea-level rise

A synthesis of the historic and future projections of SLR, both globally and for New Zealand, is available in the Ministry for the Environment (MfE) guidance for local government: *Coastal Hazards and Climate Change* (MfE 2017) and an accompanying Summary⁷ and set of Fact Sheets.⁸

Chapter 5 of the Coastal Guidance provides four specific New-Zealand based SLR scenarios to use when assessing and planning adaptation to coastal climate change in New Zealand (Figure 8-1). The SLR scenarios in the Coastal Guidance largely follow the synthesis of the IPCC Fifth Assessment Report (IPCC, 2013; Church et al., 2013), but are extended from 2100 to 2150, utilising the longer-range probabilistic projections of Kopp et al. (2014). Further, an adjustment has been made for ocean waters around New Zealand, where climate-ocean models have shown that SLR in our Pacific region will be somewhat higher than the global average rise – with IPCC projections couched in terms of the global average. The adjustment built into the New Zealand scenarios, for the regional ocean around New Zealand, is up to 0.05 m by 2100 for the higher RCP scenarios. A lesser pro-rata increment applies for the lower-emission RCPs.

The Coastal Guidance also listed a table of the time periods for which particular increments of SLR (relative to the 1986-2005 baseline) could be reached for the four different scenarios (Table 8-1). This information on time brackets can be applied to low-lying coastal areas, once the adaptation threshold SLR is known and agreed on from hazard and risk assessments, beyond which outcomes are not tolerable. All the details on developing firstly, hazard and risk assessments, then adaptation plans using the SLR scenarios, are available in the Coastal Guidance and Appendices (MfE 2017).

Table E-1, Appendices of MfE (2017) lists local values of sea level to use around New Zealand for the baseline (generally the 1986-2005 average MSL), to which the SLR projections are added. Based on the Port of Lyttelton, the baseline MSL of 0.12 m LVD-37 should be used for Canterbury when adding future SLR projections from Table 8-1 or Figure 8-1.

⁶ Scientific term is glacial isostatic adjustment (GIA)

⁷ <http://www.mfe.govt.nz/publications/climate-change/preparing-coastal-change-summary-of-coastal-hazards-and-climate-change>

⁸ <http://www.mfe.govt.nz/publications/climate-change/preparing-coastal-change-fact-sheet-series>

Table 8-1: Approximate years, from possible earliest to latest, when specific sea-level rise increments (metres above 1986–2005 baseline) could be reached for various projection scenarios of SLR for the wider New Zealand region. The earliest year listed is based on the RCP8.5 (83rd percentile) or H⁺ projection and the next three columns are based on the New Zealand median scenarios, with the latest possible year assumed to be from a scenario following RCP2.6 (median), which approximates the fully globally-implemented Paris Agreement. [Source: Table 11 in; MfE 2017]. **Note:** year for achieving the SLR is listed to the nearest five-year value.

Approximate year for the relevant New Zealand-wide SLR percentile scenario to reach increments of SLR (relative to baseline of 1986–2005)				
	Year achieved for RCP8.5 H ⁺ (83%ile)	Year achieved for RCP8.5 (median)	Year achieved for RCP4.5 (median)	Year achieved for RCP2.6 (median)
SLR (m)				
0.3	2045	2050	2060	2070
0.4	2055	2065	2075	2090
0.5	2060	2075	2090	2110
0.6	2070	2085	2110	2130
0.7	2075	2090	2125	2155
0.8	2085	2100	2140	2175
0.9	2090	2110	2155	2200
1.0	2100	2115	2170	>2200
1.2	2110	2130	2200	>2200
1.5	2130	2160	>2200	>2200
1.8	2145	2180	>2200	>2200
1.9	2150	2195	>2200	>2200

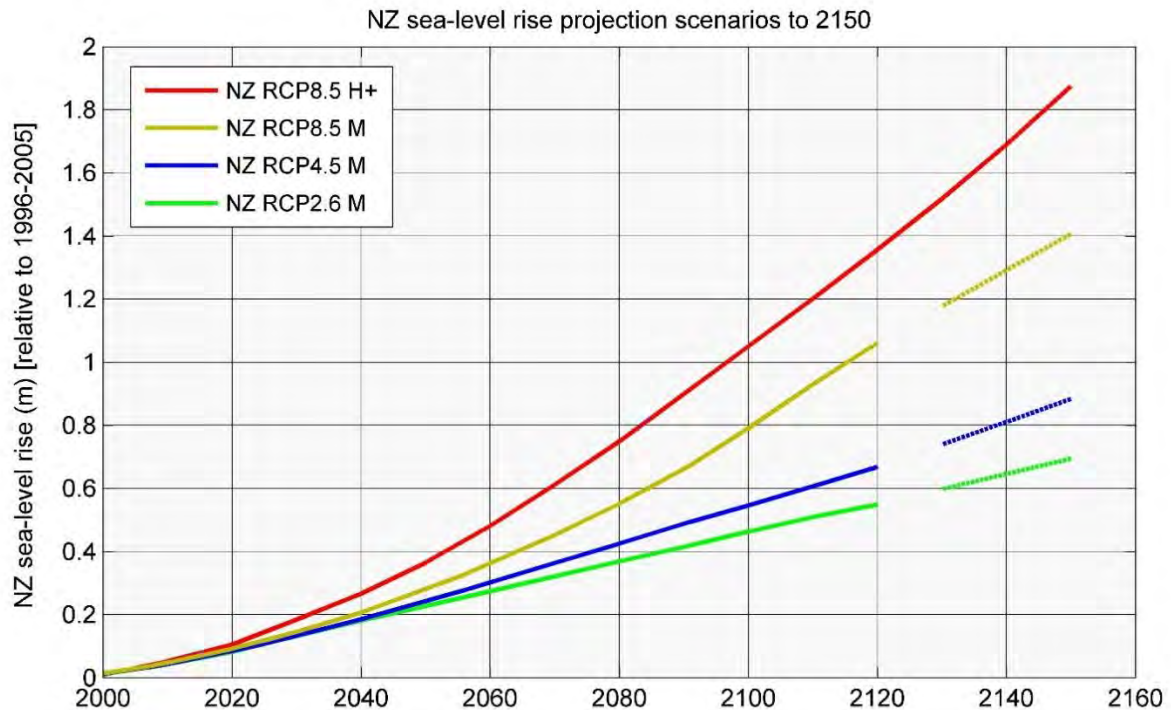


Figure 8-1: Four scenarios of New Zealand-wide regional SLR projections for use with this guidance, with extensions to 2150 based on Kopp et al. (2014)–K14. New Zealand scenario trajectories are out to 2120 (covering a minimum planning timeframe of at least 100 years), and the NZ H+ scenario trajectory is out to 2150 from K14. No further extrapolation of the IPCC-based scenarios beyond 2120 was possible, hence the rate of rise for K14 median projections for RCP2.6, RCP4.5 and RCP8.5 are shown as dashed lines from 2130, to provide an indication of the extension of projections to 2150. Note: All scenarios include a small SLR offset from the global mean SLR for the regional sea around New Zealand. [Source: Figure 27 MfE 2017].

8.3 Tides and the effect of rising sea level

8.3.1 Mean Spring tide levels

The present-day high tide marks are updated regularly by LINZ on web site:

<https://www.linz.govt.nz/data/geodetic-system/datums-projections-and-heights/vertical-datums/tidal-level-information-for-surveyors>

At the Port of Lyttelton, the Mean High Water Spring (MHWS) mark is 2.49 m CD with a Mean Low Water Spring (MLWS) mark of 0.27 m CD, with a mean spring-tide range of 2.22 m. The tide marks are based on averages of all spring tides in the 19-year period (1 January 2000 - 31 December 2018) using a set of tidal harmonic constituents extracted from the Lyttelton data record. The equivalent levels in Lyttelton Vertical Datum are MHWS= 1.25 m LVD-37 and MLWS= -0.97 m LVD-37. These tide marks are based on a MSL of 1.35 m CD or 0.12 m LVD-37, averaged over the period 1986–2005.

8.3.2 High-tide exceedances and effect of SLR

The full range of possible high tides (excluding weather, climate and SLR influences) was predicted over 100 years, covering all possible tidal combinations, based on tides extracted from the Lyttelton record. The resulting high-tide distribution curve is shown in Figure 8-2 (lower curve), in the form of a cumulative frequency of occurrence of high waters (also known as a high-tide exceedance nomograph) and with levels relative to mean sea level.

At Lyttelton, high tides cover a range of 0.87 m from the Highest Astronomical Tide (HAT)⁹ of 1.58 m, to the lowest neap high tide (Min HW) of 0.71 m. Other high-tide marks shown in Figure 8-2 include the Mean High Water Perigean Spring (MHWPS)¹⁰ and the Mean High Water Spring 10 percentile (MHWS-10). Measuring 1.30 m, the MHWS-10 is the high tide above which only 10% of all predicted high tides exceed it for the present-day situation. MHWS-10, which can be consistently defined around the New Zealand coast, was used in the recent national coastal risk exposure study for the Parliamentary Commissioner for the Environment (PCE) in 2015 (Bell et al., 2015; PCE, 2015). As a comparison, the LINZ-defined MHW level from the previous sub-section (8.3.1) for Lyttelton is exceeded by approximately 15% of all high tides.

Putting aside storm events, SLR will continually lift the base MSL, on which the tide rides, which means there will be an increasing percentage of normal high tides which exceed a given present-day elevation e.g., street level, berm or stopbank crest or present MHWS-10. Figure 8-2 shows the effect of changing high-tide inundation using two example SLR values of 0.65 m and 1.0 m SLR (Table 8-1 indicates that 0.65 m SLR would arise between 2070-2155, while the latter between 2100 to >2200). Based on the example of the present-day MHWS-10 level, which is exceeded by only 10% of all high tides (tide-only), a 0.65 m SLR will mean that same ground or tidal elevation would be exceeded by every high tide. In addition, the present-day HAT would be exceeded by approximately 82% of all high tides. These results exclude the influence of weather and storm surges on water level and assume the tidal characteristics for Lyttelton do not change substantially – rather they focus just on normal upper tidal inundation levels as seas rise.

⁹ Sometimes called the Maximum High Water (Max HW)

¹⁰ Perigean spring tides, also called “king” tides, occur around full or new moon, when the moon is closest in its monthly orbit around Earth (at its perigee). Small to moderate storm surge or waves can combine with these higher perigean spring tides to cause coastal flooding.

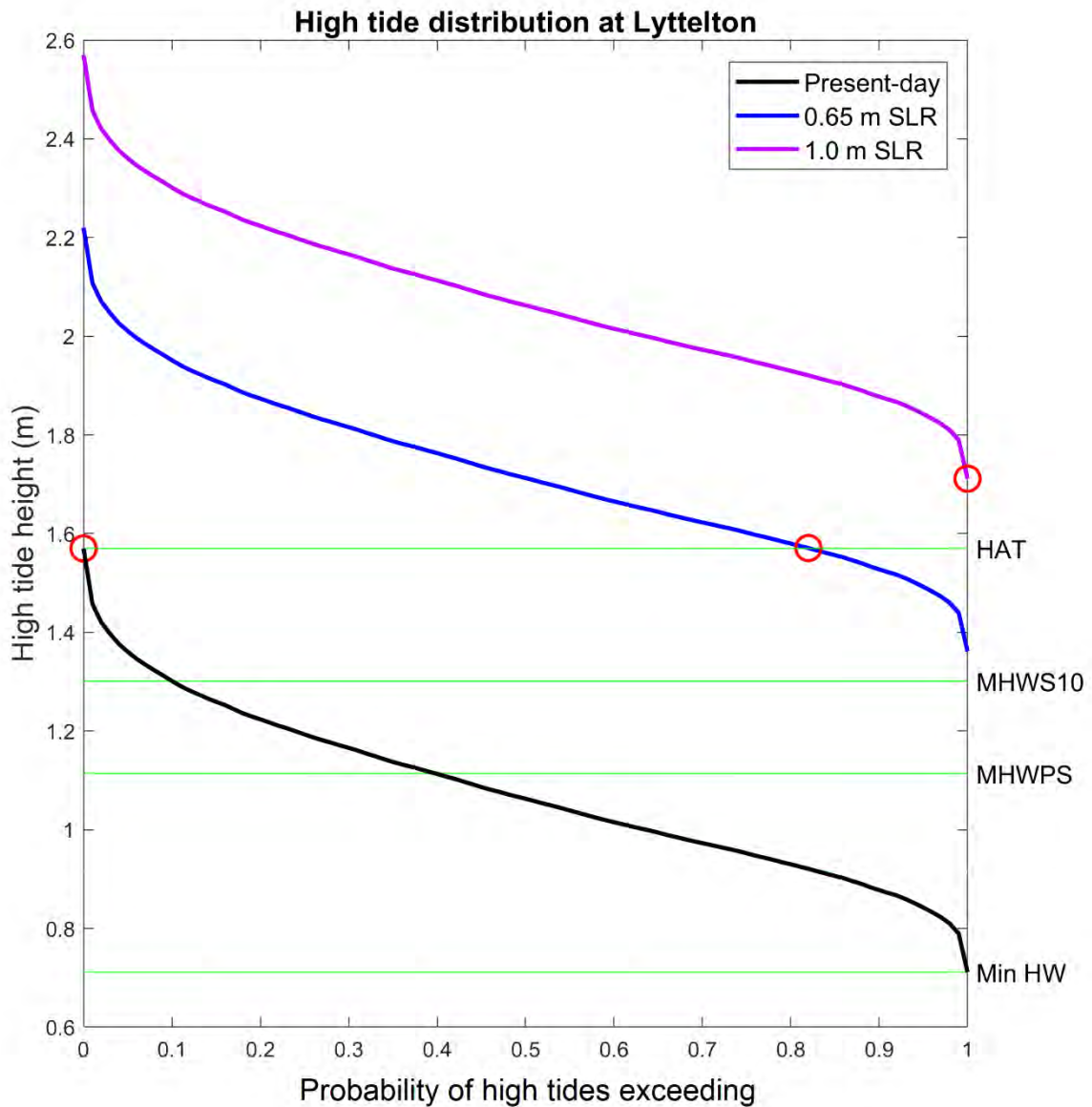


Figure 8-2: High-tide exceedance curve for all predicted high tides at Lyttelton (excluding effects of weather, climate and SLR). Datum is based on the on tidal constituents extracted from the Lyttelton gauge dataset by LINZ, relative to mean sea level, and processed by NIWA to predict all high tides over a 100-year period (excluding SLR for the heavy black line).

9 Summary and conclusions

This report presents climate change projections for Canterbury. Historic climatic conditions are presented to provide a context for future changes. The future changes discussed in this report consider differences between the historical period 1986-2005 and two future time-slices, 2031-2050 and 2081-2100. Note, the modelled differences between two time periods should not be attributed solely to climate change, as natural climate variability is also present and may add to or subtract from the climate change effect. The effect of natural variability has been reduced by averaging results from six GCM simulations, but it will still be present.

It is internationally accepted that further climate changes will result from increasing amounts of anthropogenically produced greenhouse gases in the atmosphere. The influence from anthropogenic greenhouse gas contributions to the global atmosphere is the dominant driver of climate change conditions, and it will continue to become more dominant if there is no slowdown in emissions, according to the IPCC. In addition, the climate will vary from year to year and decade to decade owing to natural variability.

Notably, future climate changes depend on the pathway taken by the global community (i.e. through mitigation of greenhouse gas emissions or a 'business as usual' approach). The global climate system will respond differently to future pathways of greenhouse gas concentrations. The representative concentration pathway approach taken here reflects this variability through the consideration of multiple scenarios (i.e. RCP4.5, the mid-range scenario, and RCP8.5, the business-as-usual scenario). The six climate models used to project New Zealand's future climate were chosen by NIWA because they produced the most accurate results when compared to historical climate and circulation patterns in the New Zealand and southwest Pacific region. They were as varied as possible to span the likely range of model sensitivity. The average of outputs from all six models (known as the 'ensemble average'), is presented in the climate change projection maps in this report. The ensemble-average was presented as this usually performs better in climate simulations than any individual model (the errors in different models are compensated).

Changes to Canterbury's future climate are likely to be significant. An increase in temperature and drought potential are among the main impacts. The following list summarises the projections of different climate variables in Canterbury:

1. The projected Canterbury temperature changes increase with time and greenhouse gas concentrations. Future annual average warming spans a wide range: 0.5-1.5°C by 2040, and 0.5-3.5°C by 2090. Diurnal temperature range (i.e., difference between minimum and maximum temperature of a given day) is expected to increase with time and emission scenarios.
2. Changes in extreme temperatures reflect the changes in the average annual signal. The average number of hot days is expected to increase with time and scenario. Annual hot days in some inland areas of Canterbury (particularly the southern Mackenzie Basin) are projected to increase by 60-85 days by 2090 under RCP8.5. As expected, the number of frost days is expected to decrease throughout the region. Largest decreases are expected in inland areas; 10-30 fewer frost days per year by 2040, and 20-50 fewer frost days per year by 2090.

3. Projected changes in rainfall show variability across the Canterbury region. Changes to annual rainfall of $\pm 5\%$ are projected for most of the region by 2040 and 2090. Seasonally the largest increases are projected during winter, with 15-40% more rainfall projected in many eastern, western and southern parts (by 2090 under RCP8.5).
4. The annual number of dry days (i.e., days where the total precipitation is less than 1 mm) is generally projected to decrease for many eastern parts of Canterbury, and increase about inland areas. By 2090 under RCP8.5, decreases in annual dry days of 1-15 days are projected for many eastern parts of Canterbury, with increases of 1-15 more dry days per year for most remaining parts of the region.
5. The number of snow days reduces everywhere, with the largest reduction in the high alpine areas where there are a relatively large number of snow days in the baseline climate.
6. The future amount of accumulated PED is projected to increase across most of Canterbury, therefore drought potential is projected to increase.
7. Both increases and decreases in days of soil moisture deficit are projected. By 2090 under RCP8.5, decreases in annual SMD days of 5-30 days are projected for many southern parts of Canterbury, with increases of 5-20 SMD days per year for many inland parts of the region.
8. Annual mean wind speeds are typically projected to increase; increases mostly range between 0-5%, but up to 10% higher wind speed projected for some areas by 2090 under RCP8.5.
9. Annual changes to surface solar radiation are generally projected to be $\pm 2.5 \text{ W/m}^2$.
10. Annual mean relative humidity is generally projected to decline by 0-2%.
11. Mean sea level pressure (MSLP) tends to increase in summer, especially to the south-east of New Zealand, resulting in the airflow becoming more north easterly, and at the same time more anticyclonic (high pressure systems). MSLP tends to decrease in winter, especially over and south of the South Island, resulting in stronger westerlies over central New Zealand.
12. The effects of climate change on hydrological characteristics were examined by driving NIWA's national hydrological model with downscaled Global Climate Model (GCM) outputs from 1971-2099 under different global warming scenarios. Using a combination of six GCMs and four warming scenarios allows us to consider a plausible range of future trajectories of greenhouse gas emissions and climatic responses. The changing climate over this century is projected to lead to the following hydrological effects:
 - Mean annual discharge generally decreases by mid-century across Canterbury. By late century, mean discharge tends to increase along eastern areas of Canterbury (particularly under RCP8.5), with decreases to mean discharge projected for some inland areas.

- Mean annual low flow generally decreases by late century, with decreases exceeding 20% in many areas of the region.
 - High flow (expressed as Q5% flow) changes are expected to be variable across the region, with both increases and decreases projected throughout Canterbury. More pronounced differences generally manifest during the late-century period and under higher RCPs.
 - Floods (characterised by the Mean Annual Flood) are expected to become larger for many parts of Canterbury, with some increases exceeding 100%. However, there are some pockets of little change or decreasing MAF.
13. Sea level rise (SLR) will continually lift the base mean sea level on which the tide rides, which means there will be an increasing percentage of normal high tides which exceed a given present-day elevation e.g., street level, berm or stopbank crest. Based on the example of the present-day MHWS-10 level, which is exceeded by only 10% of all high tides (tide-only), a 0.65 m SLR will mean that same ground or tidal elevation would be exceeded by every high tide. In addition, the present-day Highest Astronomical Tide would be exceeded by approximately 82% of all high tides given 0.65 m SLR.

10 Glossary of abbreviations and terms

Adaptation	The process of adjustment to actual or expected climate and its effects. In human systems, adaptation seeks to moderate or avoid harm or exploit beneficial opportunities. In some natural systems, human intervention may facilitate adjustment to expected climate and its effects.
Anomaly	The deviation of a variable from its value averaged over a reference period.
Anthropogenic	Human-induced; man-made. Resulting from or produced by human activities.
Anthropogenic emissions	Emissions of greenhouse gases, greenhouse gas precursors, and aerosols caused by human activities. These activities include the burning of fossil fuels, deforestation, land use changes, livestock production, fertilization, waste management, and industrial processes.
AOGCM	Atmosphere-ocean global climate model – a comprehensive climate model containing equations representing the behaviour of the atmosphere, ocean and sea ice and their interactions.
AR5	5th Assessment Report of IPCC – published in 2013/14 covering three Working Group Reports and a Synthesis Report.
Atmosphere	The gaseous envelope surrounding the Earth. The dry atmosphere consists almost entirely of nitrogen (78.1% volume mixing ratio) and oxygen (20.9% volume mixing ratio), together with a number of trace gases, such as argon (0.93% volume mixing ratio), helium and radiatively active greenhouse gases such as carbon dioxide (0.035% volume mixing ratio) and ozone. In addition, the atmosphere contains the greenhouse gas water vapour, whose amounts are highly variable but typically around 1% volume mixing ratio. The atmosphere also contains clouds and aerosols.
Available Water Capacity (AWC)	The amount of water in the soil 'reservoir' that plants can use.
Baseline/reference	The baseline (or reference) is the state against which change is measured. A baseline period is the period relative to which anomalies are computed.
BCC-CSM1.1	The Beijing Climate Centre Climate System Model version 1.1. A fully coupled global climate-carbon model. Part of CMIP5.
Bias correction	Procedures designed to remove systematic climate model errors.
Business as Usual (BAU)	Business as usual projections assume that operating practices and policies remain as they are at present. Although baseline scenarios could incorporate some specific features of BAU scenarios (e.g., a ban on a specific technology), BAU scenarios imply that no practices or policies other than the current ones are in place. RCP8.5 is known as the 'business as usual' climate change scenario.

Carbon dioxide (CO ₂)	A naturally occurring gas, also a by-product of burning fossil fuels from fossil carbon deposits, such as oil, gas and coal of burning biomass, of land use changes and of industrial processes (e.g., cement production). It is the principal anthropogenic greenhouse gas that affects the Earth's radiative balance. It is the reference gas against which other greenhouse gases are measured and therefore has a Global Warming Potential of 1.
CESM1-CAM5	The Community Earth System Model, version 5 of the Community Atmosphere Model primarily developed at the National Center for Atmospheric Research in the USA. Part of CMIP5.
Climate	Climate in a narrow sense is usually defined as the average weather, or more rigorously, as the statistical description in terms of the mean and variability of relevant quantities over a period ranging from months to thousands or millions of years. The classical period for averaging these variables is 30 years, as defined by the World Meteorological Organization. The relevant quantities are most often surface variables such as temperature, rainfall and wind. Climate in a wider sense is the state, including a statistical description, of the climate system.
Climate change	Climate change refers to a change in the state of the climate that can be identified (e.g., by using statistical tests) by changes in the mean and/or the variability of its properties, and that persists for an extended period, typically decades or longer. Climate change may be due to natural internal processes or external forcings such as modulations of the solar cycles, volcanic eruptions and persistent anthropogenic changes in the composition of the atmosphere or in land use.
Climate change scenario	A plausible and often simplified representation of the future climate, based on an internally consistent set of climatological relationships that has been constructed for explicit use in investigating the potential consequences of anthropogenic climate change, often serving as input to impact models. Climate projections often serve as the raw material for constructing climate scenarios, but climate scenarios usually require additional information such as the observed current climate. A climate change scenario is the difference between a climate scenario and the current climate.

Climate model	A numerical representation of the climate system based on the physical, chemical and biological properties of its components, their interactions and feedback processes, and accounting for some of its known properties. The climate system can be represented by models of varying complexity, that is, for any one component or combination of components a spectrum or hierarchy of models can be identified, differing in such aspects as the number of spatial dimensions, the extent to which physical, chemical or biological processes are explicitly represented or the level at which empirical parametrizations are involved. Coupled Atmosphere–Ocean General Circulation Models (AOGCMs) provide a representation of the climate system that is near or at the most comprehensive end of the spectrum currently available. There is an evolution towards more complex models with interactive chemistry and biology. Climate models are applied as a research tool to study and simulate the climate, and for operational purposes, including monthly, seasonal and inter-annual climate predictions.
Climate projection	A climate projection is the simulated response of the climate system to a scenario of future emission or concentration of greenhouse gases and aerosols, generally derived using climate models. Climate projections are distinguished from climate predictions by their dependence on the emission/concentration/ radiative forcing scenario used, which is in turn based on assumptions concerning, for example, future socioeconomic and technological developments that may or may not be realized.
Climate system	The climate system is the highly complex system consisting of five major components: the atmosphere, the hydrosphere, the cryosphere, the lithosphere and the biosphere, and the interactions between them. The climate system evolves in time under the influence of its own internal dynamics and because of external forcings such as volcanic eruptions, solar variations and anthropogenic forcings such as the changing composition of the atmosphere and land use change.
Climate variability	Climate variability refers to variations in the mean state and other statistics (such as standard deviations, the occurrence of extremes, etc.) of the climate on all spatial and temporal scales beyond that of individual weather events. Variability may be due to natural internal processes within the climate system (internal variability), or to variations in natural or anthropogenic external forcing (external variability).
Climate variable	An element of the climate that is liable to vary or change e.g. temperature, rainfall.

CMIP5	Coupled Model Inter-comparison Project, Phase 5, which involved coordinating and archiving climate model simulations based on shared model inputs by modelling groups from around the world. This project involved many experiments with coupled atmosphere-ocean global climate models, most of which were reported on in the IPCC Fifth Assessment Report, Working Group I. The CMIP5 dataset includes projections using the Representative Concentration Pathways.
Confidence	The validity of a finding based on the type, amount, quality, and consistency of evidence (e.g., mechanistic understanding, theory, data, models, expert judgment) and on the degree of agreement. Confidence is expressed qualitatively.
DEM	Digital elevation model.
Diurnal temperature range	The difference between the maximum and minimum temperature during a 24-hour period.
Downscaling (statistical, dynamical)	Deriving local climate information (at the 5 kilometre grid-scale in this report) from larger-scale model or observational data. Two main methods exist – statistical and dynamical. Statistical methods develop statistical relationships between large-scale atmospheric variables (e.g., circulation and moisture variations) and local climate variables (e.g., rainfall variations). Dynamical methods use the output of a regional climate/weather model driven by a larger-scale global model.
Drought (meteorological, hydrologic)	A period of abnormally dry weather long enough to cause a serious hydrological imbalance. Drought is a relative term; therefore, any discussion in terms of rainfall deficit must refer to the rainfall-related activity that is under discussion. For example, shortage of rainfall during the growing season impinges on crop production or ecosystem function in general (due to soil moisture drought, also termed agricultural drought), and during the runoff and percolation season primarily affects water supplies (hydrological drought). Storage changes in soil moisture and groundwater are also affected by increases in actual evapotranspiration in addition to reductions in rainfall. A period with an abnormal rainfall deficit is defined as a meteorological drought. A megadrought is a very lengthy and pervasive drought, lasting much longer than normal, usually a decade or more.
Emission scenario	A plausible representation of the future development of emissions of substances that act as radiative forcing factors (e.g., greenhouse gases, aerosols) based on a coherent and internally consistent set of assumptions about driving forces (such as demographic and socioeconomic development, technological change) and their key relationships.

Ensemble	A collection of model simulations characterizing a climate prediction or projection. Differences in initial conditions and model formulation result in different evolutions of the modelled system and may give information on uncertainty associated with model error and error in initial conditions in the case of climate forecasts and on uncertainty associated with model error and with internally generated climate variability in the case of climate projections.
ENSO	El Niño-Southern Oscillation. A natural global climate phenomenon involving the interaction between the tropical Pacific and the atmosphere, but has far-reaching effects on the global climate, especially for countries in the Pacific rim. ENSO is the strongest climate signal on time scales of one to several years, characteristically oscillating on a 3-7-year timescale. The quasi-periodic cycle oscillates between El Niño (unusually warm ocean waters along the tropical South American coast and west-central equatorial Pacific) and La Niña (colder-than-normal ocean waters off South America and along the central-east equatorial Pacific).
Eustatic sea-level rise	Absolute level of sea-level rise, measured relative to the centre of the earth. In contrast to relative sea-level rise which is measured relative to the land nearby.
Evapotranspiration	The combined process of evaporation from the Earth's surface and transpiration from vegetation.
Flood	The overflowing of the normal confines of a stream or other body of water, or the accumulation of water over areas not normally submerged. Floods include river (fluvial) floods, flash floods, urban floods, pluvial floods, sewer floods, coastal floods, and glacial lake outburst floods.
GCM	Global climate model. These days almost all GCMs are AOGCMs (atmosphere-ocean global climate models). See also climate model.
GFDL-CM3	The Coupled physical model version 3, developed by the Geophysics Fluid Dynamics Laboratory at NOAA in the USA. Part of CMIP5.
GISS-E2-R	The E2-R climate model developed by NASA Goddard Institute for Space Studies in the USA. Part of CMIP5.

Greenhouse effect	The radiative effect of all infrared-absorbing constituents in the atmosphere. Greenhouse gases, clouds, and (to a small extent) aerosols absorb terrestrial radiation emitted by the Earth's surface and elsewhere in the atmosphere. These substances emit infrared radiation in all directions, but, everything else being equal, the net amount emitted to space is normally less than would have been emitted in the absence of these absorbers. This is because of the decline of temperature with altitude in the troposphere and the consequent weakening of emission. An increase in the concentration of greenhouse gases increases the magnitude of this effect; the difference is sometimes called the enhanced greenhouse effect. The change in a greenhouse gas concentration because of anthropogenic emissions contributes to an instantaneous radiative forcing. Surface temperature and troposphere warm in response to this forcing, gradually restoring the radiative balance at the top of the atmosphere.
Greenhouse gas (GHG)	Greenhouse gases are those gaseous constituents of the atmosphere, both natural and anthropogenic, that absorb and emit radiation at specific wavelengths within the spectrum of terrestrial radiation emitted by the Earth's surface, the atmosphere itself, and by clouds. This property causes the greenhouse effect. Water vapour (H ₂ O), carbon dioxide (CO ₂), nitrous oxide (N ₂ O), methane (CH ₄) and ozone (O ₃) are the primary greenhouse gases in the Earth's atmosphere. Moreover, there are many entirely human-made greenhouse gases in the atmosphere, such as the halocarbons and other chlorine- and bromine-containing substances, dealt with under the Montreal Protocol. Beside CO ₂ , N ₂ O and CH ₄ , the Kyoto Protocol deals with the greenhouse gases sulphur hexafluoride (SF ₆), hydrofluorocarbons (HFCs) and perfluorocarbons (PFCs).
HadGEM2-ES	Climate model developed by the UK Met Office Hadley Centre, from the UK Unified Model. Part of CMIP5.
HAT	Highest Astronomical Tide. The highest tidal level which can be predicted to occur under average meteorological conditions over 18 years. Sometimes called the maximum high water.
Humidity	<i>Specific</i> humidity is the ratio of the mass of water vapour to the total mass of the system (water plus air) in a parcel of moist air. <i>Relative</i> humidity is the ratio of the vapour pressure to the saturation vapour pressure (the latter having a strong dependence on temperature).
Hydrologic drought	Hydrologic drought occurs when low water supply becomes evident, especially in streams, reservoirs, and groundwater levels, usually after an extended period of meteorological drought.

Industrial Revolution	A period of rapid industrial growth with far reaching social and economic consequences, beginning in Britain during the second half of the 18th century and spreading to Europe and later to other countries including the United States. The invention of the steam engine was an important trigger of this development. The industrial revolution marks the beginning of a strong increase in the use of fossil fuels and emission of, in particular, fossil carbon dioxide.
IPCC	Intergovernmental Panel on Climate Change. This body was established in 1988 by the World Meteorological Organisation (WMO) and the United Nations Environment Programme (UNEP) to objectively assess scientific, technical and socioeconomic information relevant to understanding the scientific basis of risk of human induced climate change, its potential impacts and options for adaptation and mitigation. Its latest reports (the Fifth Assessment) were published in 2013/14 (see www.ipcc.ch/).
IPO	Interdecadal Pacific Oscillation – a long timescale oscillation in the ocean–atmosphere system that shifts climate in the Pacific region every one to three decades.
Mean annual flood (MAF)	The mean of the series of each year’s highest daily mean flow.
Mean annual low flow (MALF)	The mean of the lowest 7-day average flows in each year of a projection period.
Mean discharge	The average annual streamflow or discharge of a river.
Mean sea level (MSL)	The surface level of the ocean at a point averaged over an extended period such as a month or year, or the average level which would exist in the absence of tides. Mean sea level is often used as a national datum to which heights on land are referred. Mean sea level changes with the averaging period used, due to climate variability and long-term sea-level rise.
MFE	Ministry for the Environment.
Mitigation (of climate change)	A human intervention to reduce the sources or enhance the sinks of greenhouse gases.
Model spread	The range or spread in results from climate models, such as those assembled for Coupled Model Intercomparison Project Phase 5 (CMIP5). Does not necessarily provide an exhaustive and formal estimate of the uncertainty in feedbacks, forcing or projections even when expressed numerically, for example, by computing a standard deviation of the models’ responses. To quantify uncertainty, information from observations, physical constraints and expert judgement must be combined, using a statistical framework.
NIWA	National Institute of Water and Atmospheric Research Ltd.
NorESM1-M	The Norwegian Earth System Model. Part of CMIP5.

Ozone	Ozone, the triatomic form of oxygen (O ₃), is a gaseous atmospheric constituent. In the troposphere, it is created both naturally and by photochemical reactions involving gases resulting from human activities (smog). Tropospheric ozone acts as a greenhouse gas. In the stratosphere, it is created by the interaction between solar ultraviolet radiation and molecular oxygen (O ₂). Stratospheric ozone plays a dominant role in the stratospheric radiative balance. Its concentration is highest in the ozone layer.
Paris agreement	The Paris Agreement aims to respond to the global climate change threat by keeping a global temperature rise this century well below 2°C above pre-industrial levels and to pursue efforts to limit the temperature increase even further to 1.5°C.
PED	Potential evapotranspiration deficit. PED can be thought of as the amount of water needed to be added as irrigation, or replenished by rainfall, to keep pastures growing at levels that are not constrained by a shortage of water.
Percentiles	The set of partition values which divides the total population of a distribution into 100 equal parts, the 50th percentile corresponding to the median of the population.
PET	Potential evapotranspiration. The amount of evaporation that would occur if a sufficient water source were available.
Precipitation	Describes all forms of moisture that falls from clouds (rain, sleet, hail, snow, etc). 'Rainfall' describes just the liquid component of precipitation.
Pre-industrial	Conditions at or before 1750. See also Industrial revolution.
Projection	A numerical simulation (representation) of future conditions. Differs from a forecast; whereas a forecast aims to predict the exact time-dependent conditions in the immediate future, such as a weather forecast a future cast aims to simulate a time-series of conditions that would be typical of the future (from which statistical properties can be calculated) but does not predict future individual events.
Radiative forcing	A measure of the energy absorbed and retained in the lower atmosphere. More technically, radiative forcing is the change in the net (downward minus upward) irradiance (expressed in W/m ² , and including both short-wave energy from the sun, and long-wave energy from greenhouse gases) at the tropopause, due to a change in an external driver of climate change, such as, for example, a change in the concentration of carbon dioxide or the output of the sun.

Regional Climate Model (RCM)	A numerical climate prediction model run over a limited geographic domain (here around New Zealand), and driven along its lateral atmospheric boundary and oceanic boundary with conditions simulated by a global climate model (GCM). The RCM thus downscales the coarse resolution GCM, accounting for higher resolution topographical data, land-sea contrasts, and surface characteristics. RCMs can cater for relatively small-scale features such as New Zealand’s Southern Alps.
Relative sea-level rise (RSLR)	A tide gauge records a combined signal of the vertical change (positive or negative) in the level of both the sea and the land to which the gauge is affixed; or relative sea level change, which is typically referred to as relative sea-level rise.
Representative Concentration Pathways (RCPs)	Representative concentration pathways. They describe four possible climate futures, all of which are considered possible depending on how much greenhouse gases are emitted in the years to come. The four RCPs, RCP2.6, RCP4.5, RCP6, and RCP8.5, are named after a possible range of radiative forcing values in the year 2100 relative to pre-industrial values (+2.6, +4.5, +6.0, and +8.5 W/m ² , respectively)
Resolution	In climate models, this term refers to the physical distance (metres or degrees) between each point on the grid used to compute the equations. Temporal resolution refers to the time step or time elapsed between each model computation of the equations.
SAM	Southern Annular Mode. Represents the variability of circumpolar atmospheric jets that encircle the Southern Hemisphere that extend out to the latitudes of New Zealand. Positive phases of SAM are associated with relatively settled weather in New Zealand, whereas negative phases are associated with unsettled weather over the country.
Scenario	In common English parlance, a ‘scenario’ is an imagined sequence of future events. The IPCC Fifth Assessment describes a ‘climate scenario’ as: A plausible and often simplified representation of the future climate, based on an internally consistent set of climatological relationships that has been constructed for explicit use in investigating the potential consequences of anthropogenic climate change, often serving as input to impact models. The word ‘scenario’ is often given other qualifications, such as ‘emission scenario’ or ‘socio-economic scenario’. For the purpose of forcing a global climate model, the primary information needed is the time variation of greenhouse gas and aerosol concentrations in the atmosphere.
Sea surface temperature (SST)	The sea surface temperature is the subsurface bulk temperature in the top few metres of the ocean, measured by ships, buoys and drifters.
Seven-station series	This refers to seven long-term temperature records used to assess New Zealand’s warming on the century time-scale. The sites are located in Auckland, Wellington, Masterton, Nelson, Hokitika, Lincoln, and Dunedin.

Simulation	Simulation is the imitation of the operation of a real-world process or system over time. The act of simulating something first requires that a model be developed; this model represents the key characteristics, behaviours and functions of the selected physical or abstract system or process. The model represents the system itself, whereas the simulation represents the operation of the system over time.
SLR	Sea-level rise.
SOI	Southern Oscillation Index, representing seesaws of atmospheric pressure in the tropical Pacific, one pole being at Tahiti and the other at Darwin, Australia. Extreme states of this index are indicative of El Niño or La Niña events in the equatorial Pacific. Typically, El Niño events produce more south-westerly flow than usual over New Zealand and associated cooler conditions, with more rainfall in western parts and frequently drought conditions in the east. La Niña events produce more high pressures over the South Island and warmer north-easterly airflow over the North Island, sometimes with drought conditions in the South Island.
Soil moisture deficit (SMD)	A day of soil moisture deficit is considered in this report to be when soil moisture is below 75 mm of available soil water capacity. SMD is calculated based on incoming daily rainfall (mm), outgoing daily potential evapotranspiration (PET, mm), and a fixed available water capacity (the amount of water in the soil 'reservoir' that plants can use) of 150 mm. Evapotranspiration (ET) is assumed to continue at its potential rate until about half of the water available to plants is used up, whereupon it decreases, in the absence of rain, as further water extraction takes place. ET is assumed to cease if all the available water is used up.
Solar radiation	Electromagnetic radiation emitted by the Sun with a spectrum close to the one of a black body with a temperature of 5770 K. The radiation peaks in visible wavelengths. When compared to the terrestrial radiation it is often referred to as shortwave radiation.
Spatial and temporal scales	Climate may vary on a large range of spatial and temporal scales. Spatial scales may range from local (less than 100,000 km ²), through regional (100,000 to 10 million km ²) to continental (10 to 100 million km ²). Temporal scales may range from seasonal to geological (up to hundreds of millions of years).
TopNet	A semi-distributed hydrological model for simulating catchment water balance and river flow, developed by NIWA.
Trend	In this report, the word trend designates a change, generally monotonic in time, in the value of a variable.

Uncertainty	A state of incomplete knowledge that can result from a lack of information or from disagreement about what is known or even knowable. It may have many types of sources, from imprecision in the data to ambiguously defined concepts or terminology, or uncertain projections of human behaviour. Uncertainty can therefore be represented by quantitative measures (e.g., a probability density function) or by qualitative statements (e.g., reflecting the judgment of a team of experts).
VCSN	Virtual Climate Station Network. Made up of observational datasets of a range of climate variables: maximum and minimum temperature, rainfall, relative humidity, solar radiation, and wind. Daily data are interpolated onto a 0.05° longitude by 0.05° latitude grid (approximately 4 kilometres longitude by 5 kilometres latitude), covering all New Zealand (11,491 points). Primary reference to the spline interpolation methodology is Tait et al (2006).

Appendix A Climate modelling methodology

Key messages

- Climate model simulation data from the IPCC Fifth Assessment has been used to produce climate projections for New Zealand.
- Six climate models were chosen by NIWA for dynamical downscaling. These models were chosen because they produced the most accurate results when compared to historical climate and circulation patterns in the New Zealand and southwest Pacific region.
- Downscaled climate change projections are at a 5 km x 5 km resolution over New Zealand.
- Climate projection and historic baseline maps and tables present the average of the six downscaled models.
- Climate projections are presented as a 20-year average for two future periods: 2031-2050 (termed '2040') and 2081-2100 (termed '2090'). All maps show changes relative to the baseline climate of 1986-2005 (termed '1995').

NIWA has used climate model simulation data from the IPCC Fifth Assessment to update climate change scenarios for New Zealand through both regional climate model (dynamical) and statistical downscaling processes. The downscaling processes are described in detail in a climate guidance manual prepared for the Ministry for the Environment (2018), but a short explanation is provided below. Dynamical downscaling results are presented for all variables in this report.

Global climate models (GCMs) are used to make future climate change projections for each future scenario, and results from these models are available through the Fifth Coupled Model Inter-comparison Project (CMIP5) archive (Taylor et al., 2012). Six GCMs were selected by NIWA for dynamical downscaling, and the sea surface temperatures (SSTs) from these six CMIP5 models used to drive an atmospheric global model, which in turn drives a higher resolution regional climate model (RCM) nested over New Zealand. These CMIP5 models were chosen because they produced the most accurate results when compared to historical climate and circulation patterns in the New Zealand and southwest Pacific region. In addition, they were chosen because they were as varied as possible in the parent global model to span the likely range of model sensitivity. For climate simulations, dynamical downscaling utilises a high-resolution climate model to obtain finer scale detail over a limited area based on a coarser global model simulation.

The six GCMs chosen for dynamical downscaling were BCC-CSM1.1, CESM1-CAM5, GFDL-CM3, GISS-E2-R, HadGEM2-ES and NorESM1-M. The NIWA downscaling (GCM then RCM) produced simulations that contained hourly precipitation results from 1970 through to 2100. The native resolution of the regional climate model is 27 km and there are known biases in the precipitation fields derived from this model. The daily precipitation projections, as well as daily maximum and minimum temperatures, have been bias-corrected so that their statistical distributions from the RCM matches those from the Virtual Climate Station Network (VCSN) when the RCM is driven by the observed sequence of weather patterns across New Zealand (known as ‘re-analysis’ data). A detailed description of this bias-correction method is provided by Sood (2014). When the RCM is driven from the free-running GCM, forced only by CMIP5 SSTs, there can be an additional bias in the distribution of weather patterns affecting New Zealand, and the RCM output data for the historical climate will therefore not match the observed distributions exactly.

The RCM output is then downscaled statistically (by interpolation from the model 27 km grid) to a ~5 km x ~5 km resolution with a daily time-step. The ~5 km grid corresponds to the VCSN grid¹¹. Figure 10-1 shows a schematic for the dynamical downscaling method used in this report.

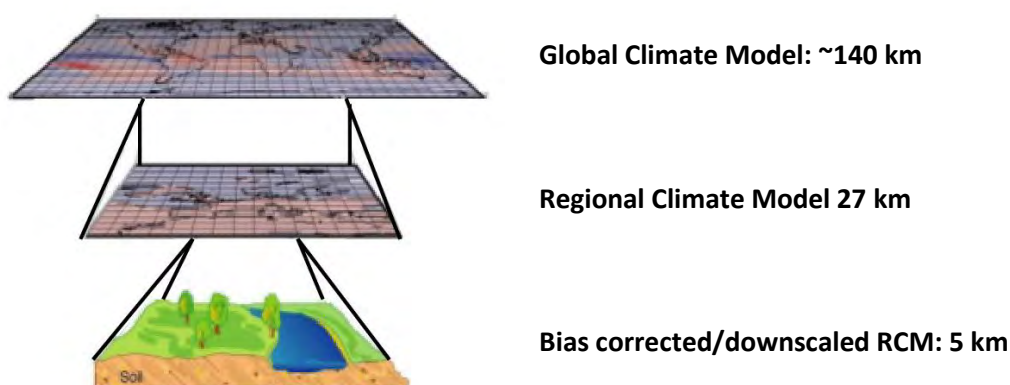


Figure 10-1: Schematic showing dynamical downscaling method used in this report.

The climate change projections from each of the six dynamical models are averaged together, creating what is called an ensemble-average. The ensemble-average is mapped in this report, because the models were chosen to cover a wide range of potential future climate conditions. The ensemble-average was presented as this usually performs better in climate simulations than any individual model (the errors in different models are compensated).

Climate projections are presented as a 20-year average for two future periods: 2031-2050 (termed ‘2040’) and 2081-2100 (termed ‘2090’). All maps show changes relative to the baseline climate of 1986-2005 (termed ‘1995’), as used by IPCC. Hence the projected changes by 2040 and 2090 should be thought of as 45-year and 95-year projected trends. Note that the projected changes use 20-year averages, which will not entirely remove effects of natural variability. The baseline maps (1986-2005) show modelled historic climate conditions from the same six models as the future climate change projection maps.

¹¹ Virtual Climate Station Network, a set of New Zealand climate data based on a 5 km by 5 km grid across the country. Data have been interpolated from ‘real’ climate station records (TAIT, A., HENDERSON, R., TURNER, R. & ZHENG, X. G. 2006. Thin plate smoothing spline interpolation of daily rainfall for New Zealand using a climatological rainfall surface. *International Journal of Climatology*, 26, 2097-2115.)

Appendix B Hydrological modelling methodology

Key messages

- NIWA's TopNet model was used in this study. TopNet is a spatially semi-distributed, time-stepping model of water balance. The model is driven by time-series of precipitation and temperature, and additional weather elements where available.
- TopNet was run continuously from 1971 to 2100, with the spin-up period 1971 excluded from the analysis. The climate inputs were stochastically disaggregated from daily to hourly time steps.
- The simulation results comprise time-series of modelled river flow for each computational sub-catchment, and for each of the six GCMs and two RCPs considered.
- Hydrological projections are presented as the average for two future periods: 2036-2056 (termed 'mid-century') and 2086-2099 (termed 'late-century'). All maps show changes relative to the baseline climate (1986-2005 average).

To assess the potential impacts of climate change on agricultural water resources and flooding, a hydrological model is required that can simulate soil moisture and river flows continuously and under a range of different climatic conditions, both historical and future. Ideally the model would also simulate complex groundwater fluxes but there is no national hydrological model capable of this at present. Because climate change implies that environmental conditions are shifting from what has been observed historically, it is advantageous to use a physically based hydrological model over one that is more empirical, with the assumption that a better representation of the biophysical processes will allow the model to perform better outside the range of conditions under which it is calibrated.

The hydrological model used in this study is NIWA's TopNet model (Clark et al., 2008), which is routinely used for surface water hydrological modelling applications in New Zealand. It is a spatially semi-distributed, time-stepping model of water balance. It is driven by time-series of precipitation and temperature, and of additional weather elements where available. TopNet simulates water storage in the snowpack, plant canopy, rooting zone, shallow subsurface, lakes and rivers. It produces time-series of modelled river flow (without consideration of water abstraction, impoundments or discharges) throughout the modelled river network, as well as evapotranspiration, and does not consider irrigation. TopNet has two major components, namely a basin module and a flow routing module.

The model combines TOPMODEL hydrological model concepts (Beven et al., 1995) with a kinematic wave channel routing algorithm (Goring 1994) and a simple temperature based empirical snow model (Clark et al., 2008). As a result, TopNet can be applied across a range of temporal and spatial scales over large watersheds using smaller sub-basins as model elements (Ibbitt and Woods, 2002; Bandaragoda et al., 2004). Considerable effort has been made during the development of TopNet to ensure that the model has a strong physical basis and that the dominant rainfall-runoff dynamics are adequately represented in the model (McMillan et al., 2010). TopNet model equations and information requirements are provided by Clark et al. (2008) and McMillan et al. (2013).

For the development of the national version of TopNet used here, spatial information in TopNet was provided by national datasets as follows:

- Catchment topography based on a nationally available 30 m Digital Elevation Model (DEM).
- Physiographical data based on the Land Cover Database version two and Land Resource Inventory (Newsome et al., 2012).
- Soil data based on the Fundamental Soil Layer information (Newsome et al., 2012).
- Hydrological properties (based on the River Environment Classification version one (REC1) (Snelder and Biggs, 2002)¹²).

The method for deriving TopNet's parameters based on GIS data sources in New Zealand is given in Table 1 of Clark et al. (2008). Due to the paucity of some spatial information at national/regional scales, some soil parameters are set uniformly across New Zealand.

To carry out the simulations required for this study, TopNet was run continuously from 1971 to 2100, with the spin-up period 1971 excluded from the analysis. The climate inputs were stochastically disaggregated from daily to hourly time steps. As the GCM simulations are "free-running" (based only on initial conditions, not updated with observations), comparisons between present and future hydrological conditions can be made directly (as each GCM is characterised by specific physical assumptions and parameterisation), but this also means that simulated hydrological hindcasts do not track observational records.

Hydrological simulations are based on the REC 1 network aggregated up to Strahler¹³ catchment order three (approximate average catchment area of 7 km²) used within previous national and regional scale assessments (Pearce et al., 2017a; 2017b); residual coastal catchments of smaller stream orders remain included. The simulation results comprise hourly time-series of various hydrological variables for each computational sub-catchment, and for each of the six GCMs and two RCPs considered. To manage the volume of output data, only river flows information was preserved; all the other state variables and fluxes can be regenerated on demand.

Because of TopNet assumptions, soil and land use characteristics within each computational sub-catchment are homogenised. Essentially this means that the soil characteristics and physical properties of different land uses, such as pasture and forest, will be spatially averaged, and the hydrological model outputs will approximate conditions across land uses.

¹² Due to time constraints associated with this project, it is not possible to assess the potential impact of climate change on the Digital River Network 3 available for the Canterbury region.

¹³ Strahler order describes river size based on tributary hierarchy. Headwater streams with no tributaries are order 1; 2nd order streams develop at the confluence of two 1st order tributaries; stream order increases by 1 where two tributaries of the same order converge.

11 References

- BANDARAGODA, C., TARBOTON, D.G., WOODS, R.A. 2004. Application of TOPNET in the distributed model intercomparison project. *J. Hydrol.*, 298:178–201.
- BELL, R.G., PAULIK, R., WADHWA, S. (2015) *National and regional risk exposure in low-lying coastal areas: areal extent, population, buildings and infrastructure*. Report prepared for the Parliamentary Commissioner for the Environment by NIWA. Wellington: Parliamentary Commissioner for the Environment. Retrieved from www.pce.parliament.nz/media/1384/national-and-regional-risk-exposure-in-low-lying-coastal-areas-niwa-2015.pdf
- BEVEN, K.J., LAMB, R., QUINN, P., ROMANOWICZ, R., FREER, J. 1995. TOPMODEL, in: Computer Models of Catchment Hydrology, edited by: Singh, V. P., *Water Resour. Publ.*, Highlands Ranch, Colorado, 627–668, 1995.
- CAREY-SMITH, T., HENDERSON, R., SINGH, S. 2018. High intensity rainfall design system: version 4. *NIWA Client Report*, 2018022CH (ELF16250 for Envirolink): 71.
- CHURCH, J.A., CLARK, P.U., CAZENAVE, A., GREGORY, J.M., JEVREJEVA, S., LEVERMANN, A., MERRIFIELD, M.A., MILNE, G.A., NEREM, R.S., NUNN, P.D., PAYNE, A.J., PFEFFER, W.T., STAMMER, D., UNNIKRISHNAN, A.S. (2013) Sea level change. In: T.F. STOCKER, D. QIN, G.-K. PLATNERS et al. (Eds). *Climate change 2013: The physical science basis*. Cambridge University Press, Cambridge, United Kingdom and New York, NY, USA.
- CLARK, M. P., RUPP, D. E., WOODS, R. A., ZHENG, X., IBBITT, R. P., SLATER, A. G., SCHMIDT, J. & UDDSTROM, M. J. 2008. Hydrological data assimilation with the ensemble Kalman filter: Use of streamflow observations to update states in a distributed hydrological model, *Adv. Water Resour.*, 31, 1309-1324, doi:10.1016/j.advwatres.2008.06.005.
- COLLINS, D., ZAMMIT, C. 2016. Climate change impacts on agricultural water resources and flooding. Client report for Ministry for Primary Industries. 2016114CH. 72.
- COLLINS, D., MONTGOMERY, K., ZAMMIT, C. 2018. Hydrological projections for New Zealand rivers under climate change. Client report prepared for Ministry for the Environment. 2018193CH. 107.
- DEAN, S., ROSIER, S., CAREY-SMITH, T. & STOTT, P. A. 2013. The role of climate change in the two-day extreme rainfall in Golden Bay, New Zealand, December 2011. *Bulletin of the American Meteorological Society*, 94, 561-563.
- GORING, D.G. 1994. Kinematic shocks and monoclinal waves in the Waimakariri, a steep, braided, gravel-bed river, *Proceedings of the International Symposium on Waves: Physical and Numerical Modelling*, University of British Columbia, Vancouver, Canada, 21–24 August, 1994, pp. 336–345.
- HENDERSON, R.D., COLLINS, D.B.G., DOYLE, M., WATSON, J. 2018. Regional Flood Estimation Tool for New Zealand Final Report Part 2. *NIWA Client Report*, 2018177CH for Envirolink Tools (MBIE): 44.
- IBBITT, R.P., WOODS, R. 2002. Towards rainfall-runoff models that do not need calibration to flow data, in: *Friend 2002 – Regional Hydrology: Bridging the Gap Between Research and Practice*, edited by: van Lanen, H.A.J., Demuth, S., IAHS Publ., 274, 189–196.
- IPCC (ed.) 2013. *Climate Change 2013: The Physical Science Basis. Contribution of Working Group I to the Fifth Assessment Report of the Intergovernmental Panel on Climate Change*, Cambridge, United Kingdom and New York, NY, USA: Cambridge University Press.
- IPCC (ed.) 2014a. *Climate Change 2014: Impacts, Adaptation, and Vulnerability. Part A: Global and Sectoral Aspects. Contribution of Working Group II to the Fifth Assessment Report of the Intergovernmental Panel on Climate Change*, Cambridge, United Kingdom and New York, USA: Cambridge University Press.

- IPCC (ed.) 2014b. *Climate Change 2014: Impacts, Adaptation, and Vulnerability. Part B: Regional Aspects. Contribution of Working Group II to the Fifth Assessment Report of the Intergovernmental Panel on Climate Change*, Cambridge, United Kingdom and New York, USA: Cambridge University Press.
- IPCC 2014c. Climate change 2014: Mitigation of climate change. Contribution of Working Group III to the Fifth Assessment Report of the Intergovernmental Panel on Climate Change. In: EDENHOFER, O., PICHES-MADRUGA, R., SOKONA, Y., FARAHANI, E., KADNER, S., SEYBOTH, K., ADLER, A., BAUM, I., BRUNNER, S., EICKEMEIER, P., KRIEMANN, B., SAVOLAINEN, J., SCHLÖMER, S., VON STECHOW, C., ZWICKEL, T. & MINX, J. C. (eds.). Cambridge University Press.
- IPCC 2018. Global warming of 1.5C: An IPCC Special Report on the impacts of global warming of 1.5C above pre-industrial levels and related global greenhouse gas emission pathways, in the context of strengthening the global response to the threat of climate change, sustainable development, and efforts to eradicate poverty, Accessed on 8/10/2018 from <http://ipcc.ch>.
- KOPP, R.E., HORTON, R.M., LITTLE, C.M., MITROVICA, J.X., OPPENHEIMER, M., RASMUSSEN, D.J., STRAUSS, B.H., TEBALDI, C. (2014) Probabilistic 21st and 22nd century sea-level projections at a global network of tide-gauge sites. *Earth's Future* 2(8): 383–406. Retrieved from <http://dx.doi.org/10.1002/2014EF000239>.
- LINDSEY, R. 2019. Climate Change: Global Sea Level. National Oceanic and Atmospheric Administration (NOAA) Climate.gov. <https://www.climate.gov/news-features/understanding-climate/climate-change-global-sea-level> Accessed 4/02/2020.
- MACARA, G. R. 2016. The climate and weather of Canterbury. 2nd edition. NIWA Science and Technology Series, Number 68. 41p. Accessed at: <https://niwa.co.nz/our-science/climate/publications/regional-climatologies/canterbury>
- MCMILLAN, H., FREER, J., PAPPENBERGER, F., KRUEGER, T., CLARK, M. 2010. Impacts of uncertain river flow data on rainfall-runoff model calibration and discharge predictions. *Hydrol. Processes* 24(10): DOI: 10.1002/hyp.7587: 1270-1284.
- MCMILLAN, H.K., HREINSSON, E.O., CLARK, M.P., SINGH, S.K., ZAMMIT, C., UDDSTROM, M.J. 2013. Operational hydrological data assimilation with the recursive ensemble Kalman Filter. *Hydrol. Earth Syst. Sci.*, 17, 21-38.
- MINISTRY FOR THE ENVIRONMENT 2008. Climate Change Effects and Impacts Assessment. A Guidance Manual for Local Government in New Zealand. In: MULLAN, B., WRATT, D., DEAN, S., HOLLIS, M., ALLAN, S., WILLIAMS, T., KENNY, G. & MFE (eds.). Wellington: Ministry for the Environment.
- MINISTRY FOR THE ENVIRONMENT 2016. Climate change projections for New Zealand. Atmospheric projections based on simulations undertaken for the IPCC fifth Assessment. Wellington: Ministry for the Environment.
- MINISTRY FOR THE ENVIRONMENT 2017. Coastal hazards and climate change: Guidance for local government. Lead authors: BELL, R., LAWRENCE, J., ALLAN, S., BLACKETT, P., & STEPHENS, S. Ministry for the Environment Publication ME-1292.
- MINISTRY FOR THE ENVIRONMENT 2018. Climate change projections for New Zealand: atmospheric projections based on simulations undertaken for the IPCC 5th Assessment, 2nd edition. Accessed at: <https://www.mfe.govt.nz/node/21990>.
- MULLAN, A. B., PORTEOUS, A., WRATT, D. & HOLLIS, M. 2005. Changes in drought risk with climate change. NIWA report WLG2005-23 for Ministry for the Environment and Ministry of Agriculture and Fisheries, Wellington.
- MULLAN, A. B., SOOD, A. & STUART, S. 2016. Climate Change Projections for New Zealand based on simulations undertaken for the IPCC 5th Assessment. Part A: Atmosphere Changes. NIWA Client Report for Ministry for the Environment, WLG2015-31. June 2016.

- NASA/GISS. 2019. Global Temperature: Global Land-Ocean Temperature Index. *Global Climate Change: Vital Signs of the Planet*. <https://climate.nasa.gov/vital-signs/global-temperature/> Accessed 4/02/2020.
- NEWSOME, P.F.J., WILDE, R.H., WILLOUGHBY, E.J. 2012. *Land Resource Information System Spatial Data Layers*, Technical Report, Palmerston North, Landcare Research NZ Ltd., New Zealand, 2000, Updated in 2012.
- NIWA 2020. Southern Annular Mode. *Climate: Information and resources*. <https://niwa.co.nz/climate/information-and-resources/southern-annular-mode> Date accessed: 30/01/2020.
- PARLIAMENTARY COMMISSIONER FOR THE ENVIRONMENT 2015. Preparing New Zealand for rising seas: certainty and uncertainty. Wellington: Parliamentary Commissioner for the Environment. Retrieved from: www.pce.parliament.nz/publications/preparing-new-zealand-for-rising-seas-certainty-and-uncertainty.
- PEARCE, P., FEDAEFF, N., MULLAN, B., SOOD, A., BELL, R., TAIT, A., COLLINS, D., ZAMMIT, C. 2017a. Climate change and variability - Wellington Region. Prepared for Greater Wellington Regional council, Report 2017066AK.
- PEARCE, P., BELL, R., BOSTOCK, H., CAREY-SMITH, T., COLLINS, D., FEDAEFF, N., KACHHARA, A., MACARA, G., MULLAN, B., PAULIK, R., SOMERVELL, E., SOOD, A., TAIT, A., WADHWA, S., WOLLEY, J.-M. 2017b. Auckland Region climate change projections and impacts. Prepared for Auckland Council, Council Controlled Organisations, and District Heath Boards. Revised Report 2018021AK.
- REISINGER, A., KITCHING, R. L., CHIEW, F., HUGHES, L., NEWTON, P. C. D., SCHUSTER, S. S., TAIT, A. & WHETTON, P. 2014. Australasia. In: BARROS, V. R., FIELD, C. B., DOKKEN, D. J., MASTRANDREA, M. D., MACH, K. J., BILIR, T. E., CHATTERJEE, M., EBI, K. L., ESTRADA, Y. O., GENOVA, R. C., GIRMA, B., KISSEL, E. S., LEVY, A. N., MACCRACKEN, S., MASTRANDREA, P. R. & WHITE, L. L. (eds.) *Climate Change 2014: Impacts, Adaptation, and Vulnerability. Part B: Regional Aspects. Contribution of Working Group II to the Fifth Assessment Report of the Intergovernmental Panel on Climate Change*. Cambridge, UK, and New York, NY, USA: Cambridge University Press.
- RENWICK, J. A. & THOMPSON, D. 2006. The Southern Annular Mode and New Zealand climate. *Water & Atmosphere*, 14, 24-25.
- ROYAL SOCIETY OF NEW ZEALAND 2016. Climate change implications for New Zealand, 72 pp. Available from: <http://www.royalsociety.org.nz/expert-advice/papers/yr2016/climate-change-implications-for-new-zealand/>.
- SALINGER, M. J. & MULLAN, A. B. 1999. New Zealand climate: temperature and precipitation variations and their links with atmospheric circulation 1930–1994. *International Journal of Climatology*, 19, 1049-1071.
- SALINGER, M. J., RENWICK, J. A. & MULLAN, A. B. 2001. Interdecadal Pacific Oscillation and South Pacific climate. *International Journal of Climatology*, 21, 1705-1721.
- SIMMONS, A. J., WILLETT, K. M., JONES, P. D., THORNE, P. W. & DEE, D. P. 2010. Low-frequency variations in surface atmospheric humidity, temperature, and precipitation: Inferences from reanalyses and monthly gridded observational data sets. *Journal of Geophysical Research: Atmospheres*, 115.
- SNELDER, T.H., BIGGS, B.J.F. 2002. Multiscale River Environment Classification for water resources management, *J. Am. Water Resour. Assoc.*, 38, 1225–1239, doi:10.1111/j.1752-1688.2002.tb04344.x.
- SOOD, A. 2014. Improved Bias Corrected and Downscaled Regional Climate Model Data for Climate Impact Studies: Validation and Assessment for New Zealand. *ResearchGate Article*. https://www.researchgate.net/publication/265510643_Improved_Bias_Corrected_and_Downscaled_Regional_Climate_Model_Data_for_Climate_Impact_Studies_Validation_and_Assessment_for_New_Zealand Date accessed: 31/02/2020.

STATS NZ 2020. Interdecadal Pacific Oscillation. *New Zealand's Environmental Reporting Series: Environmental Indicators*.

http://archive.stats.govt.nz/browse_for_stats/environment/environmental-reporting-series/environmental-indicators/Home/Atmosphere-and-climate/interdecadal-pacific-oscillations.aspx Date accessed: 30/01/2020.

TAIT, A., HENDERSON, R., TURNER, R. & ZHENG, X. G. 2006. Thin plate smoothing spline interpolation of daily rainfall for New Zealand using a climatological rainfall surface. *International Journal of Climatology*, 26, 2097-2115.

TAYLOR, K. E., STOUFFER, R. J. & MEEHL, G. A. 2012. An Overview of CMIP5 and the Experiment Design. *Bulletin of the American Meteorological Society*, 93, 485-498.

WILLEIT, M., GANOPOLSKI, A., CALOV, R. & BROVKIN, V. 2019. Mid-Pleistocene transition in glacial cycles explained by declining CO₂ and regolith removal. *Science Advances*, 5, eaav7337.